Cell size homeostasis in animal cells

Clotilde Cadart

NNT : 2017SACLS103

THÈSE DE DOCTORAT
DE L'UNIVERSITÉ PARIS-SACLAY

Préparée à l'Université Paris-Sud au sein de l'Institut Curie

Spécialité : Sciences de la vie et de la santé

Ecole doctorale n° 577 Structure et Dynamique des Systèmes Vivants

Présentée et soutenue à Paris le 3 mai 2017 par

Clotilde CADART

Cell size homeostasis in animal cells

Jury :

Président :	
Pr. Bernard Mignotte	Professeur, Université Versailles St-Quentin
Rapporteurs :	
Dr. Silvia Santos	D.R., MRC Imperial College London
Dr. Damien Coudreuse	D.R., CNRS UMR 6290
Examinateurs :	
Dr. Marco Cosentino-Lagomarsino	D.R., CNRS UMR 7238
Dr. Ariel Lindner	D.R., INSERM U1001
Dr. Lydia Robert	C.R., CNRS UMR 8237
Directeur de thèse :	
Dr. Matthieu Piel	D.R., CNRS UMR 144

Acknowledgments

I would like thank to the members of my thesis comittee who accepted to evaluate my work, especially Silvia Santos and Damien Coudreuse who reviewed this manuscript. Thanks also to Buzz Baum and Nicolas Minc for their advices during the yearly thesis advisory meetings.

Many thanks to Matthieu Piel who hosted me in his lab. Under his supervision, I discovered a way of doing science that is innovative, interdisciplinary, rigorous, always very creative and independent. Coming from médecine, I still remember my first amazement when I started experiments in his lab and I feel very lucky for the variety of things I could learn in the unique scientific environment he creates. I am very grateful that he let me choose the project I was passionate about and that he gave me so much independence to conduct my research while providing excellent scientific support.

A huge thank to my collaborators Marco, Sylvain, Olivier and Victor. In addition to significantly improving various aspects of the project, these collaborations were always a great source of fun and support and an opportunity to learn a lot. They helped me gaining confidence in what I was doing and I greatly enjoyed working with each of them.

I also have to thank all the members of the Piel lab; the passion they put in their work and their scientific excellence were inspiring examples. Thanks to the past members: Hawa, Paolo, Ewa, Maël, Julie, Franzi, Emmanuel, Sylvain, Matthew, YanJun, Olivier; the present members: Rafaele, Guilherme, Damien, Nico, Nishit, Pablo Saez and Pablo Vargas, Lucie, Alexis, Larisa, Gaurav, Juanma; the kind visitors: Louis, Bianca; and the great interns who participated to my project: Charlotte Pirot and Camille Balekely.

I also found a lot of support and scientific advices in the Baum lab, especially from Helen, Andrea, Tom, Nélio and Nunu, the cell culture room companions from the Perez lab, especially Gaëlle, Lou, Sandrine, Séverine, Emilie and José; and of course the Viovy and the Vignjevic labs who are always there to give you spirit and offer you a piece of cake, especially Youmna, Fabien, Jorge, Dennis, Céline, Marine, Ayako, Catherine and Stéphanie.

Thanks to all the Institut Curie and the IPGG members who make it a great place to work both for the stimulating scientific environment and the friendly parties. I also was very happy to share these PhD years with my friends from the Master: Olivier, Andreas, Orso, Fabien, Charlène and Annaëlle.

I am incredibly grateful to my dear friends Nico, Lucie, Madda, Youmna, Diana, Tom, Andrea, Hawa and Coralie. Their presence on my side and their example were essential to persevere during these past years. I am very lucky to have such kind and fun friends.

Enfin, un grand merci à Laurence pour sa générosité et son soutien indispensables. Merci à Anne pour tous les séjours passés ensemble. Merci à mes parents, leur générosité, leur courage et leur sens de l'humour sont un exemple quotidien, leur soutien et leur admiration quoique j'entreprenne une grande chance. Merci également à mes trois soeurs chéries Irène, Elisabeth et Marthe. Elles savent toute l'admiration que j'ai pour elles et la joie que j'ai à passer du temps avec chacune.

Abstract

The way proliferating mammalian cells maintain a constant size through generations is still unknown. This question is however central because size homeostasis is thought to occur through the coordination of growth and cell cycle progression. In the yeast S. pombe for example, the trigger for cell division is the reach of a target size Fantes (1977). This mechanism is referred to as sizer. The homeostatic behavior of bacteria and daughter cells of the yeast S. cerevisiae on the contrary was recently characterized as an adder where all cells grow by the same absolute amount of volume at each cell cycle. This leads to a passive regression towards the mean generation after generation Campos et al. (2014); Soifer et al. (2016); Taheri-Araghi et al. (2015). These findings were made possible by the development of new technologies enabling direct and dynamic measurement of volume over full cell cycle trajectories. Such measurement is extremely challenging in mammalian cells whose shape constantly fluctuate over time and cycle over 20 hours long periods. Studies therefore privileged indirect approaches Kafri et al. (2013); Sung et al. (2013); Tzur et al. (2009) or indirect measurement of cell mass rather than cell volume Mir et al. (2014); Son et al. (2012). These studies showed that cells overall grew exponentially and challenged the classical view that cell cycle duration was adapted to size and instead proposed a role for growth rate regulation. To date however, no clear model was reached. In fact, the nature and even the existence of the size homeostasis behavior of mammalian cells is still debated Lloyd (2013).

In order to characterize the homeostatic process of mammalian cells, we developed a technique that enable measuring, for the first time, single cell volume over full cell cycle trajectories Cadart et al. (2017); Zlotek-Zlotkiewicz et al. (2015). We found that several cell types, HT29, HeLa and MDCK cells behaved in an adder-like manner. To further test the existence of homeostasis, we artificially induced asymmetrical divisions through confinement in micro-channels. We observed that asymmetries of sizes were reduced within the following cell cycle through an adder-like behavior. To then understand how growth and cell cycle progression were coordinated in a way that generates the adder, we combined our volume measurement method with cell cycle tracking. We showed that G1 phase duration is negatively correlated with initial size. This adaptation is however limited by a minimum duration of G1, unraveled by the study of artificially-induced very large cells. Nevertheless, the adder behavior is maintained even in the absence of time modulation, thus suggesting a complementary growth regulatory mechanism. Finally, we propose a method to estimate theoretically the relative contribution of growth and timing modulation in the overall size control and use this framework to compare our results with that of bacteria.

Overall, our work provides the first evidence that proliferating mammalian cells behave in an adder-like manner and suggests that both growth and cell cycle duration are involved in size control.

List of abbreviations

4EBP	eukaryotic initiation factor E4 binding protein
ADP	adenosine diphosphate
AMP	adenosine monophosphate
AMPK	AMP-activated protein kinase
ATP	adenosine triphosphate
CDK	cyclin-dependent kinase
CV	coefficient of variation
DMEM	Dubelcco's Modified Eagle Medium
EDTA	ethylenediaminettraacetic acid
EGF	Epidermal Growth Factor
eIF2α	eukaryotic initiation factor 2 α
ER	endoplasmic reticulum
ERK	extracellular signal-regulated kinase
FXm	Fluorescence exclusion measurement
IGF-1	insulin like growth factor-1
IGFR	insulin growth factor receptor
IRS	insuline receptor substrate
MAPK	mitogen activated protein kinase
MEK	mitogen activated protein kinase kinase
MCT	membrane domain containg mTORC2
mRNA	messenger ribonucleic acid
mTORC1	mechanistic target of rapalycin complex 1
mTORC2	mechanistic target of rapalycin complex 2
MLS	mitochondria localizing signal
Myo19	Myosin 19
NA	numerical aperture
NETO	New end take-off
PDMS	polydimthylsiloxane
PI3K	phosphoinositide 3-kinase
PIP2	phosphatidylinositol (4,5)-diphosphate
PIP3	phosphatidylinositol (3,4,5)-diphosphate
PKA	protein kinase A
PLL	Poly-L-lysine

PEG	Poly-ethylene-glycol
PSF	Point Spread Function
R	Restriction point
Ras	rat sarcoma protein
Rb	retinoblastoma protein
RCP	Rate changing point
Rheb	Ras-homolog enriched in brain protein
RNA	ribonucleic acid
ROI	region of interest
rRNA	ribosomal ribonucleic acid
RTK	receptor tyrosine kinase
S6K	S6 kinase
SA	surface area
siRNA	silencing ribonucleic acid
SREBP	sterol regulatory element-binding protein
TAZ	transcriptional co-activator with PDZ-binding motif
TSC1/2	tuberus sclerosis complex 1 or 2
YAP	Yes-associated protein

Contents

Acknowledgments i

Abstract iii

List of abbreviations v

1 The question of cell size regulation 9

1.1 Defining cell size . . . 9

1.1.1 Cell mass and cell volume . . . 9

1.1.2 Cell size in proliferating cells: coordination between growth and cell cycle progression . . . 10

1.2 Cell size homeostasis in metazoan cells . . . 11

1.2.1 Cell size vs. Organ size . . . 11

1.2.2 Intrinsic vs. extrinsic regulation of cell size . . . 12

1.2.2.1 Flexibility upon environmental changes . . . 12

1.2.2.2 Coupling of cell growth and cell cycle progression? . . . 13

1.2.3 Proliferating cells in multicellular organisms. . . . 13

1.2.4 Evolutionary point of view on the requirement of growth regulation in unicellular and multicellular organisms . . . 15

1.3 Conclusion . . . 16

2 Size homeostasis study: question, challenges and concepts step by step 17

2.1 Sizer, timer & adder . . . 18

2.2 Coordination of cell cycle progression to growth . . . 19

2.3 Models of size-sensing mechanism . . . 23

2.3.1 Geometric measurement of absolute length . . . 23

2.3.2 Volume measurement through titration-based mechanism . . . 23
2.3.3 Surface area measurement . . . 25
2.3.4 Conclusion: the importance of cell volume . . . 26
2.4 An emergent role for growth regulation in size control . . . 28
2.4.1 The regulation of growth . . . 28
2.4.1.1 Growth in volume. . . . 28
2.4.1.2 Growth in mass. . . . 28
2.4.1.3 Growth and metabolism. . . . 29
2.4.1.4 Density throughout the cell cycle . . . 29
2.4.1.5 Conclusion . . . 30
2.4.2 Measuring cell growth at the single-cell level . . . 30
2.4.2.1 New techniques enabling single-cell measurement. . . . 30
2.4.2.2 From population-level studies to single-cell measurement. . . . 30
2.5 Combination of processes? . . . 31
2.5.1 Independent control in each cell cycle phase. . . . 31
2.5.2 One overarching mechanism . . . 31
2.5.3 Parallel and concurrent processes . . . 31
2.6 Robustness and flexibility of size control . . . 32
2.6.1 Apparent flexibility of size thresholds . . . 32
2.6.2 What we can learn from studying cells in different growth environments . . . 32
2.7 Conclusion . . . 34

3 Current understanding of size homeostasis in yeast and bacteria 37

3.1 Cell size homeostasis in bacteria . . . 37
3.1.1 Brief description of the cell cycle of bacteria . . . 37
3.1.2 Phenomenological description and recent emergence of the adder model . . . 37
3.1.3 Beyond the adder observation, current mechanisms debated . . . 41
3.1.3.1 Control in each sub-periods . . . 41
3.1.3.2 Molecular players . . . 41
3.1.4 Trying to unify the different findings in the field of bacteria . . . 42
3.1.4.1 How do these controls combine to generate an adder? . . . 42

3.1.4.2 Lessons from model-free approaches. 42
3.2 Cell size homeostasis in yeast 42
3.2.1 Size control in *S. pombe* 42
3.2.1.1 *S. pombe*, cell cycle and size-checkpoints. 42
3.2.1.2 *S. pombe* is the classical example of a sizer in wild-type cells. 43
3.2.1.3 *S. pombe*. grows in a bilinear fashion. 43
3.2.1.4 In search for the mechanism generating geometric sensing of size. . . 43
3.2.2 Size control in *S. cerevisiae* 46
3.2.2.1 *S. cerevisiae*, cell cycle and checkpoints 46
3.2.2.2 Lack of consensus about the growth behaviour of *S. cerevisiae*. . . . 46
3.2.2.3 Daughter cell of *S. cerevisiae* behave in an adder-like manner. . . . 46
3.2.2.4 Whi5 and the inhibitor-dilution size sensor model for G1/S transition 47
3.3 Lessons from yeast and bacteria 48

4 Cell size homeostasis in metazoan cells 49

4.1 Growth and cell cycle pathways in mammalian cells 49
4.1.1 Pathways regulating the growth rate 49
4.1.1.1 The mTOR pathway 50
4.1.1.2 Other pathways 51
4.1.1.3 Conclusion. 53
4.1.2 Cell cycle regulation 53
4.1.2.1 Brief overview of the mammalian cell cycle 53
4.1.2.2 Commitment to a new the cell cycle: checkpoint(s) for growth during G0 and G1 54
4.2 Population-level studies and evidence of size control in early work 54
4.2.1 Evidence of size-sensing in G1 54
4.2.2 Results challenging the idea of size control in metazoan cells. 56
4.3 The challenging problem of characterizing cell growth in metazoan cells 56
4.4 Current views on the homeostatic process in metazoan cells 57
4.4.1 Cells grow exponentially or super-linearly 57
4.4.2 No clear role for time modulation, possible existence of a growth-rate modulation 58

4.5 Conclusion . . . 58

5 General conclusion and aims of this study **61**

5.1 General conclusion . . . 61

5.2 Aims of this study . . . 62

6 Methods **65**

6.1 Long time-lapse acquisition in animal cells to characterize growth: state of the art and challenges . . . 65

6.2 Fluorescence-exclusion based volume measurement . . . 67

6.2.1 Volume measurement method: principle and validation . . . 67

6.2.1.1 Method principle . . . 67

6.2.1.2 Theoretical validation . . . 67

6.2.1.3 Experimental validation . . . 68

6.2.2 Image analysis optimization . . . 68

6.2.3 Protocol optimization for long time-lapse acquisition . . . 70

6.2.3.1 Improve nutrient access . . . 70

6.2.3.2 Standardized cell culture protocol to try reduce variability . . . 70

6.2.3.3 Analytical validation of the quality of growth in the experiments . . . 74

6.2.3.4 Improving the fluorescent probes . . . 77

6.3 Cell growth analysis: clonal & single-cell curves, cell cycle transitions . . . 77

6.3.1 Single-cell curves . . . 77

6.3.1.1 Careful control of the sources of volume curves fluctuations . . . 77

6.3.1.2 Semi-automated analysis of hundreds of single-growth curves . . . 78

6.3.2 Clonal growth curves . . . 80

6.3.3 Cell cycle transitions keypoint analysis . . . 81

6.4 Developing tools to induce asymmetrical divisions . . . 84

6.4.1 Inducing asymmetrical divisions using micro-channels . . . 84

6.4.1.1 Micro-channels induce asymmetrical cell divisions and allow volume measurement . . . 84

6.4.1.2 Optimization of the micro-channels device to improve nutrient access 84

6.4.2 Asymmetrical patterns . . . 85

6.4.3 Drug-induced asymmetrical distribution of organelles . . . 85
6.5 Choice of cell types . . . 87
6.5.1 Description of the cell types used in this study . . . 87
6.5.2 Establishing new stable lineages . . . 88
6.6 Statistical analysis . . . 88

7 Results **93**

7.1 Summary . . . 93
7.2 Manuscript in preparation for submission . . . 95
7.3 Concluding remarks . . . 139
7.3.1 Analysis planed before the submission . . . 139
7.3.2 Important experiments needed to complete the work . . . 139

8 Discussion **143**

8.1 Single cell growth measurement in mammalian cells . . . 143
8.1.1 Single cell measurement of volume with the FXm . . . 143
8.1.1.1 FXm allows measurement of both suspended and adherent cells . . . 143
8.1.1.2 FXm allows measurement of cell volume . . . 144
8.1.1.3 Results from direct measurement of single cell growth might precise some of the previous findings . . . 144
8.1.1.4 FXm measurements provide a robust set of data for the study of size homeostasis . . . 144
8.1.2 Current limitations of the FXm . . . 145
8.1.2.1 Limitation to cells which do not internalize the probe . . . 145
8.1.2.2 FXm currently requires a device confining the cells . . . 145
8.2 Growth and time modulation . . . 146
8.2.1 Time modulation . . . 146
8.2.1.1 G1 duration is correlated with volume in HT29 and HeLa cells and gated by a minimum duration . . . 146
8.2.1.2 S and G2 phases . . . 147
8.2.1.3 Conclusion on the role of time adaptation . . . 150
8.2.2 Growth modulation . . . 151
8.2.2.1 Experimental evidence . . . 151

8.2.2.2 Growth regulation and cellular homeostasis . . . 151
8.2.2.3 Conclusions on the role of growth modulation . . . 153
8.2.3 Conclusion on the respective contribution of time and growth modulation in size control . . . 156
8.2.3.1 Classification of the results into three types of combinations of growth and time modulation . . . 156
8.2.3.2 Identification of three distinct rate-limiting processes for cell cycle and cell growth . . . 157
8.3 Is there a unique mechanism or several processes resulting in the adder? . . . 157
8.3.1 Generality of the adder, from bacteria to mammalian cells . . . 157
8.3.1.1 Generality of the adder in our results . . . 157
8.3.1.2 Generality of the adder in the litterature . . . 157
8.3.2 Is there enough evidence to conclude that size homeostasis is an adder in mammalian cells? . . . 158
8.3.2.1 Statistical resolution is currently lacking to confirm the adder in any organism. . . . 158
8.3.2.2 Testing the adder . . . 158
8.3.3 Size homeostasis is a flexible process . . . 158
8.3.3.1 Bacteria and *S. cerevisiae*: not always an adder . . . 159
8.3.3.2 Why flexibility is important when trying to build a model for size homeostasis . . . 159
8.3.3.3 Conclusion: phenomenological adder and molecular adder . . . 159
8.3.4 Several scenarios can explain the apparent adder in mammalian cells . . . 160
8.4 Perspectives: a combination of processes, both single and tissue-level determined? . . . 162

9 Conclusion **165**

Bibliography **167**

A Appendix 1: Review **187**

B Appendix B: Protocol article **189**

C Appendix C: résumé en français **191**

INTRODUCTION

Chapter 1

The question of cell size regulation

1.1 Defining cell size 9
1.1.1 Cell mass and cell volume 9
1.1.2 Cell size in proliferating cells: coordination between growth and cell cycle progression 10
1.2 Cell size homeostasis in metazoan cells 11
1.2.1 Cell size vs. Organ size 11
1.2.2 Intrinsic vs. extrinsic regulation of cell size 12
1.2.3 Proliferating cells in multicellular organisms. 13
1.2.4 Evolutionary point of view on the requirement of growth regulation in unicellular and multicellular organisms 15
1.3 Conclusion 16

When observing cells within a tissue, two important observations can be made: different cell types have different cell sizes, and there is little variability of sizes within cell types. These two observations define the two main questions of cell size regulation: (i) what sets the absolute value of cell size (or the mean value in a population of the same type), (ii) what defines the spread of cell sizes in a population of cells (the variance of the distribution) (figure 1.1). One complexity when trying to answer these questions lies in the fact that size can be defined in various ways. Another source of complexity is added when addressing the question in cells coming from multicellular organisms (figure 1.2). In these cases, cells also answer to rules edited at the tissue level, and the role of intrinsic cell size regulation in these organisms is very controversial. In this section, we will address these two complexities in order to define clearly the frame of our study.

1.1 Defining cell size

1.1.1 Cell mass and cell volume

In many studies focusing on cell growth, cell mass is chosen as a surrogate size parameter. Growth is indeed often defined as mass production Roberts and Lloyd (2012); Goranov and Amon (2010). In line with this, many studies on cell growth also quantified the amount of newly synthesized proteins or elements of the biosynthetic machinery such as RNA amount to assess growth rate (reviewed in Mitchison (2003)). The recent finding in some studies in mammalian cells that growth rate could be the key parameter to reach a target size Kafri et al. (2013); Ginzberg et al. (2015) suggests even more

that regulation of the biosynthetic machinery, perhaps through the mTOR pathway as hypothesized by the authors Ginzberg et al. (2015) might be important. Until this point, our work has focused on cell volume. It is commonly accepted that density or volume can be good parameters to study growth Mitchison (2003) but more recent techniques will be useful to rigorously assess the quality of these two parameters as proxies for cell growth. Choosing cell volume as a surrogate size parameter raises various interesting questions. Cell size can indeed be defined as a volume where chemical reactions take place and there are examples where dilution or concentrations of proteins in the cytoplasm are key in defining cell cycle transitions Schmoller and Skotheim (2015). Cell volume combined with cell shape are also critical for many events happening at mitosis (reviewed in Cadart et al. (2014)). Recent work reporting that cell volume increases for a short period of time during mitosis Zlotek-Zlotkiewicz et al. (2015) shows that cells can actively change their volume and raises interesting hypothesis about the roles of these changes. It is possible that cells use these changes of volume and shape to probe or alter their mechanical environment in very packed tissue such as epithelia. Finally, the factors that determine the homeostatic volume for a given cell is a current topic of interest theoretically. One interesting question related to how homeostatic volume is set is the role of the nucleus compartment: the nucleus-to-cytoplasmic ratio is known since a long time to be a conserved characteristic of each cell type Jorgensen and Tyers (2004). Another observation is that to increase above a certain amount of mass, a strategy broadly used by cells is to increase the number of nuclei (reviewed in Edgar et al. (2014)). Overall, the relation between nucleus size and either cell mass or cell volume is still very poorly understood but it could perhaps help understanding what defines the absolute size of a given cell type.

1.1.2 Cell size in proliferating cells: coordination between growth and cell cycle progression

For cells that proliferate, at each generation, the final size reached before division Sf, is the result of how fast the cell grew and how long it grew. Maintaining a constant size through generation requires that the rate of division and the rate of size doubling are equal.

There are many reasons to think that growth is a fluctuating process through time and thus, that a concerted progression of cell cycle and growth is needed. First, cell growth can depend on the amount of synthetic machinery or surface area for nutrient uptake, thus are likely to show exponential properties (reviewed in Mitchison (2003)). Theoretical work showed that in the case of exponentially growing cells, a size checkpoint is needed to avoid propagation and expansion of differences of sizes in the population across time (Sveiczer et al. (2004), also reviewed in Mitchison (2003)). Second, cell growth can be affected by local fluctuations in the environment, such as nutrient concentration. Third, intrinsic cell-to-cell variability, leading to non-homogeneous growth or cycling Kiviet et al. (2014); Newman et al. (2006); Kempe et al. (2015); Raj et al. (2006); Atay and Skotheim (2014) and response to the external environment in a given population of cells is a source of noise that homeostasis needs to compensate so that variability is not amplified through time. A fourth argument, unrelated to growth, is the symmetry of division: any asymmetry will generate unequal volumes in daughter cells that will need to converge to the same average final volume to maintain a constant mean size distribution through time. The budding yeast for example systematically divides into a large mother cell and a smaller budding daughter cell and a mechanism is required to allow small budded cells to grow more than large mother cells (reviewed in Jorgensen and Tyers (2004)). In mammalian cells that normally divide symmetrically, the segregation error of division has recently been estimated to $7-10\%$ depending on the cell type when measuring dry mass Sung et al. (2013) or volume Tzur et al. (2009) (figure 1.3).

All these reasons strongly suggest that, in order to maintain a constant distribution of sizes, regulatory mechanisms that link cell cycle progression to cell growth must exist to compensate for extrinsic and

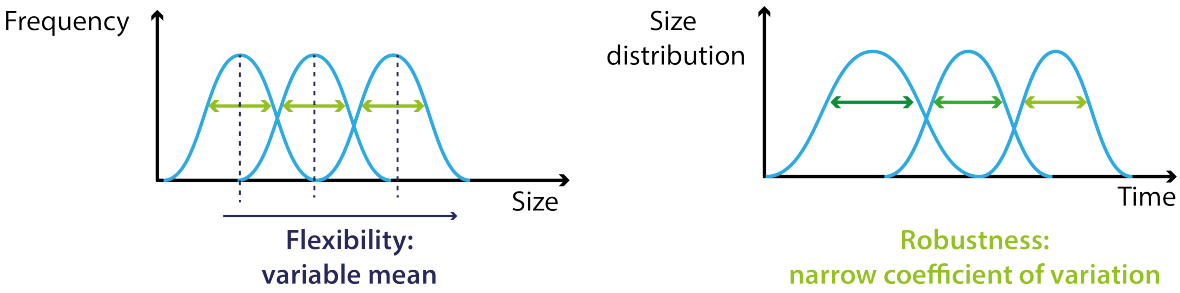

Figure 1.1: Robustness and flexibility of size homeostasis. A size homeostasis mechanism typically shows two distinct properties. **(i) Robustness** explains how cell size is homogeneous in a population of cells of the same cell type at a given time. If a perturbation induces abnormal sizes and leads to a spreading of sizes in the population, the homeostasis mechanism will correct these abnormal sizes and the distribution of sizes will progressively goes back to its initial spreading. This property of the size homeostasis mechanism is therefore reflected by the coefficient of variation (CV) of sizes in the population. **(ii) Flexibility** describes the fact that the average mean size of a cell population varies upon environmental conditions: if nutrients are in excess, cells will typically grow fast and reach larger sizes than if nutrients are in limiting amounts.

intrinsic sources of growth variability. The outcome of a good coordination of these two processes leads to size homeostasis in the population with a constant and narrow distribution of sizes through time (figure 1.1). In fact, historically research in genetic determinants of cell size and shape in *S. pombe* led to the seminal discovery of cell cycle mutants Nurse (1975). Although there is strong evidence that unicellular organisms such as bacteria or yeast actively coordinate their growth to their cell cycle progression (discussed in chapter 3 of this introduction), this is currently debated in metazoans. In the next section we briefly discuss the different controversies related to this question in animal cells.

1.2 Cell size homeostasis in metazoan cells

The question of cell size homeostasis in metazoan cells is very controversial, with many biologists arguing that coordination of cell growth and cell cycle progression in order to actively regulate size do not exist in these organisms Grewal and Edgar (2003); Conlon and Raff (2003); Echave et al. (2007); Lloyd (2013), a debate that has been very well summarized in Jorgensen and Tyers (2004) (figure 1.2). Sophisticated methods to accurately measure cell growth and cell cycle progression in single animal cells recently renewed the field Kafri et al. (2013); Son et al. (2012); Sung et al. (2013); Tzur et al. (2009) (discussed in detail in section 4.3). One review recently discussed these recent works Ginzberg et al. (2015). However, there is currently a lack in the literature of work that would bridge the gap between these recent works on single animal cells and the previous findings in multicellular organisms such as *Drosophila* that led part of the community to doubt that cell size regulation at the single-cell level exists in multicellular organisms. We want to discuss the main questions of this debate, hoping that it will help us to define a convincing frame for our own work.

1.2.1 Cell size vs. Organ size

Famous studies in *Drosophila* imaginal disc have been able to show that cell size and cell number adapt reciprocally in order to maintain constant disc size: when cell division is inactivated cells grow bigger in order to compensate for a lower cell number, conversely, when the cell number is increased by overexpressing cycle regulators, cell size decreases (reviewed in Su and O'Farrell (1998); Edgar (2006). This result and others led to the strong opinion in the field that in metazoans, developmental

control of organ size and growth often takes precedence over cell size. However, there are also examples of organs where cell size is highly conserved in order to preserve cell function. In *Drosophila* brain for example, there is no adaptation of cell size to altered cell number and reduced or increased cell proliferation lead to micro or macrocephaly respectively (reviewed Homem et al. (2015)).

Thus, for some cell types, cell function is highly dependent on cell size and cell size must be actively maintained. When studying metazoan cells, one might keep in mind that cell size homeostasis behaviors may differ between cell types.

1.2.2 Intrinsic vs. extrinsic regulation of cell size

1.2.2.1 Flexibility upon environmental changes

Varying external conditions can induce variations of cell size for a given cell type. Depending upon nutritional conditions, it has been shown for example that epithelial gut cell size in *Drosophila* can vary dramatically (reviewed in Edgar (2006)). For some observers, these sorts of experiments demonstrate that absolute size is not intrinsically regulated at the cellular level, and that cell size is simply the fluctuating and passive result of extracellular signals affecting growth or proliferation Echave et al. (2007). In other words, a cell does not know which size it must have, it passively adapts to the environment. A first argument against this perhaps too simplistic view is that even though a given cell type may adopt a wide range of size depending on external conditions, limitations as to the extent of this range of possible sizes still exist. Minimal size exists and there are examples *in vivo* of small cells that enter the next cycle only when they have grown again. Recently, Homem et al. for example showed that cell cycle exit of neuroblasts cells from *Drosophila pupas* was linked to a metabolic transition from glycolytic to mitochondrial oxidative respiration Homem et al. (2014). This switch of metabolism induces a lengthening of cell cycling that cannot compensate for a slower growth rate, size progressively decreases until cells finally terminate proliferations and differentiate. A similar observation *in vitro* is that hematopoietic cells that reached very small sizes after growth factor and mitogen starvation take several days to re-enter the cell cycle after stimulation with their growth factor and mitogen interleukin-3 Lum et al. (2005)

More importantly, a size homeostasis mechanism needs to be both robust and flexible. In other words, it should allow an adaptation of the mean size of the population to external chemical or mechanical constraints while preventing a dispersion of sizes (figure 1.1). Thus, the observation that the mean cell size in the population can adopt a wide range of possible sizes does not rule out the need of a mechanism to ensure that the variance of sizes will be constant. Remarkably, this flexibility is well-characterized in unicellular organisms such as yeast or bacteria that tend to grow larger when cultured in nutrient rich environment compared to nutrient poor conditions. As we explain in the next chapter, when studying size homeostasis mechanism in any cell type, keeping in mind that the mechanism we are looking for should explain both robustness and flexibility of the process is helpful to interpret the experimental results and progress (section 2.6).

In our study, we are focusing on the robustness of size homeostasis. A population of cells in a given culturing condition *in vitro* (*i.e.* nutrient availability, temperature, cell density) has a given homeostatic size and our question is how variation around this homeostatic size is maintained constant. The most common hypothesis in unicellular organisms is that variation of sizes in a population is maintained through a coupling between growth and cell cycle progression. This hypothesis is however hotly debated in the field of metazoan cells.

1.2.2.2 Coupling of cell growth and cell cycle progression?

Another argument often opposed to size regulation at the single cell level is that cell growth and cell cycle progression are not coordinated in metazoan cells because they respond to two distinct and independent pathways Lloyd (2013). Examples where growth phases are clearly separated in time from proliferation phases are rife through development O'Farrell (2004); Saucedo and Edgar (2002), and they allow, for example, proliferation and morphogenesis in small embryos that cannot import nutrients yet. In addition to examples in development, models of metazoan cell types where growth can be uncoupled from cell cycle progression exist. In Schwann cells for example, glial growth factor promote cell growth without promoting cell division whereas mitogens drive cell division independently of cell growth Roberts and Lloyd (2012); Conlon and Raff (2003); Echave et al. (2007).

However, there are also multiple evidence of interplay between cell growth and cell cycle progression. A first aspect of this interplay that is not entirely answered yet is how metazoan cells make the decision to enter a new cell cycle depending on the extracellular environment. It has been proposed that in metazoan cells *in vitro* two checkpoints in G1 that condition the decision of entering a new cycle of growth and division can be distinguished Foster et al. (2010). The first one is growth-factor dependent and is based on the Ras/Raf/MAPK/Cyclin D pathway. The second checkpoint, later in G1, checks nutrient availability through the well-known mTOR/AkT/Myc/Cyclin E pathway. The second evidence of interplay between the two pathways are the several studies that point at a size-dependent or growth-rate dependent G1 phase duration in metazoan cells (reviewed in Ginzberg et al. (2015) and discussed in details in chapter 4 of this introduction).

Moreover, although it is clear that tissue-level regulatory signals impact the average size in the population, there is no proof that these signals are sufficient to explain how cells maintain an homogeneous size distribution. All the arguments supporting the idea that coordination between growth and cell cycle progression is important to maintain size homeostasis in proliferating unicellular organisms (section 1.1.2) are still valid for cells that proliferate in multicellular organisms. Understanding how mutliple tissue or body-level signals are integrated at the single cell level in order to generate a uniform response despite all possible extrinsic and intrinsic sources of variability is at the heart of the question of size homeostasis in metazoan cells and poorly understood to date (figure 1.3). In this context, reductionist approaches and studies of how growth and cell cycle progression are coordinated at the single cells remain important.

1.2.3 Proliferating cells in multicellular organisms.

Studying cell-size regulation at the single-cell level usually requires the use of immortalized cells, and most of the time cancer-derived cells, which proliferate indefinitely through time. As remarked by some, such examples of cells are rare *in vivo* Lloyd (2013). An interesting question that has been poorly addressed is the regulation of cell mass for cells that do not proliferate anymore. In that case, cell mass is the result of the proper balance between growth (mass production) and degradation. Since our work is focusing on proliferating cells, we will not discuss any further this question that has been reviewed in-depth elsewhere (reviewed in Lloyd (2013)).

What is important however for the context of our study is that the choice of cell type for single cell studies will have important consequences on the direct relevance of the findings. It is for example simpler to understand the direct relevance of single-cell studies performed on suspended cell types such as lymphoblasts Son et al. (2012); Tzur et al. (2009). Such cells are perhaps less prone to be under paracrine influence and have to proliferate very fast while generating a homogeneous clone upon immune activation. Hence, a mechanism actively regulating cell size might be important in these cells and single-cell experimental set-ups are more likely to study cells in conditions that still

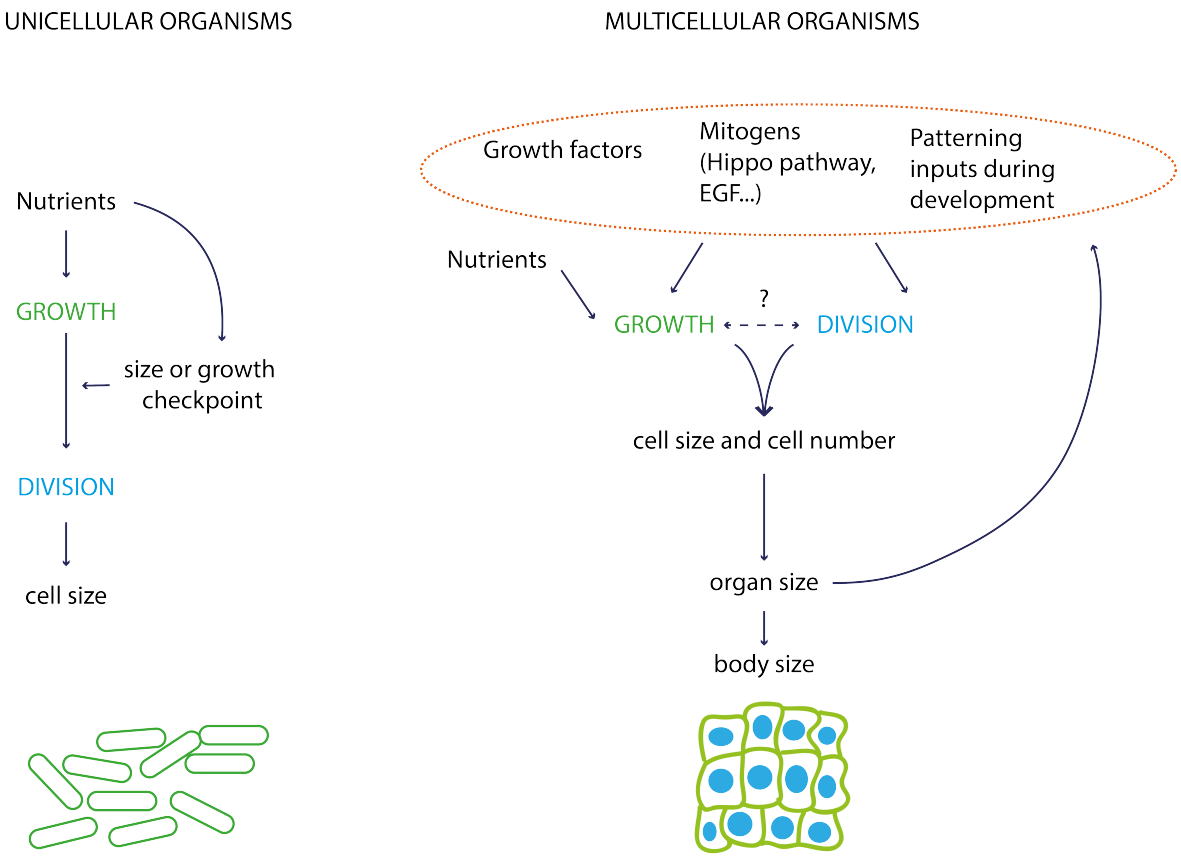

Figure 1.2: Growth and division in multicellular vs. unicellular organisms. How growth and cell cycle progression are regulated is a different question in unicellular and multicellular organisms. **In unicellular organisms**, the view is that cells grow with the only restriction that nutrients are in sufficient amounts in the extracellular environment. A mechanism coordinating cell cycle progression with cell growth ensures that cell divides at the right size. This coordination is typically thought to occur through a checkpoint sensitive to either size or growth (checkpoints and size sensing mechanisms are discussed in section 2.3 and 2.2). Importantly, the average size in the population varies upon environmental change therefore suggesting that this checkpoint might be tuned by the environment in some cases. **In multicellular organisms**, an additional layer of complexity arises from the fact that growth is determined not only by nutrient amounts but also several tissue-level regulatory signals such as growth factors. This is also true for the division rate which depends on mitogens such as EGF or mechano-sensitive pathways such as the Hippo pathway which regulates cell number in an organ. Moreover patterning inputs during development precisely define proliferation in time and space. The classical view is therefore that growth and division are regulated at the organ or body level by distinct pathways and do not necessarily need to be coordinated.

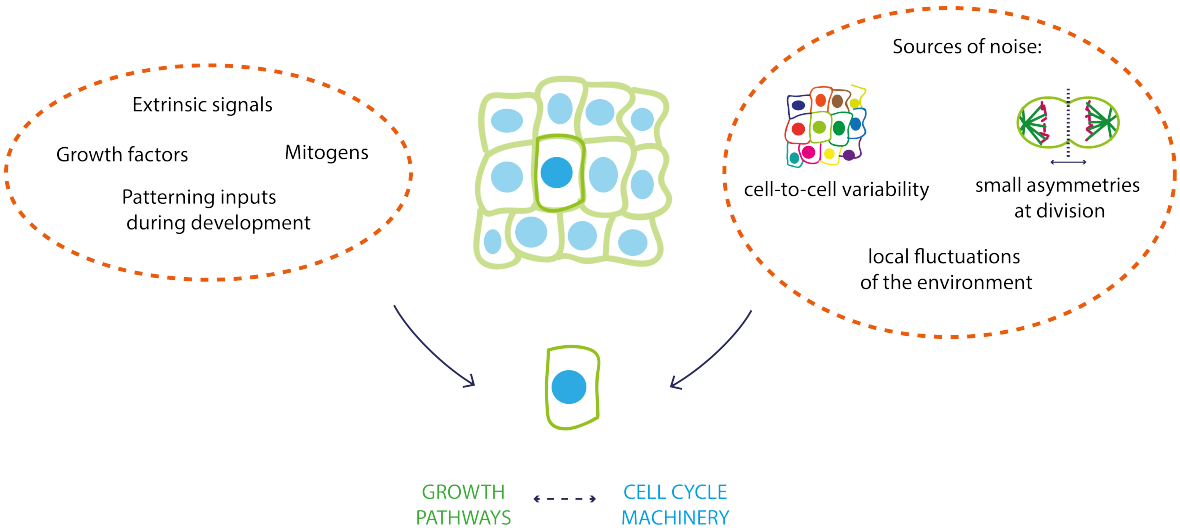

Figure 1.3: How do single cell integrate extrinsic regulatory signals? In a tissue, cells must integrate extrinsic regulatory signals such as growth factors, mitogens or patterning inputs during development. However, during this process one can identify several sources of noise: (i) local fluctuations of the chemical or mechanical environment might induce fluctuations in the signals delivered to the cell or in the environment directly 'sensed' by the cell; (ii) cell-to-cell variability due to noise in gene expression for example results in difference in the response of several cells to the same input; (iii) finally, small asymmetries at division lead to fluctuations of size that must be corrected to maintain a homogeneous size distribution in the population. These fluctuations add up on top of the tissue-level growth and division regulatory signals and might need to be compensated for by an active regulation of growth and cell cycle progression at the single cell level.

seem relevant *in vivo* Lloyd (2013); Jorgensen and Tyers (2004). This does not mean however that studies performed on single cells originating from packed tissues such as epithelia where paracrine and organ-level regulation exist are irrelevant. Proliferation occurs in many situations at the adult stage: liver regeneration and rapid gut epithelia turnover, for example. Second, on an evolutionary point of view, there is no reason to think that multicellularity means that intrinsic cell size regulation is lost.

1.2.4 Evolutionary point of view on the requirement of growth regulation in unicellular and multicellular organisms

Bringing the question of cell size homeostasis from unicellular organisms to multicellular involves moving the question from a context where cells proliferate as long as external nutrients are available to a context where cells grow and proliferate in response to defined developmental patterns or tissue homeostasis rules. The most well-known regulatory pathway that senses tissue homeostasis and tunes proliferation and cell growth in order to maintain homeostasis is the Hippo pathway (reviewed in Yu et al. (2015)). The fact that multicellularity requires proliferation and growth rules defined at the tissue level does not exclude an intrinsic regulation of cell growth and cell cycle proliferation. This point of view is almost like assuming that the acquisition of multicellularity and the gain of ways to define rules at the tissue level through evolution were necessarily accompanied by a loss of rules defined at the single-cell level. However, there is no evidence for that at all. The pathways regulating cell growth Laplante and Sabatini (2012); Caron et al. (2015) (section 4.1) and cell cycle progression Cross et al. (2011); Malumbres (2014) (section 4.1.2) are highly conserved among eukaryotes and if there are molecular links between these two pathways, it is possible that some of these links were already present in the common ancestor to eukaryotes.

Furthermore, suspicions against the interest of studying cell size homeostasis in cancerous cells at the single cell level rather than primary cells or cells in tissues are often raised. Yet, this is not considering the fact that these cells actually behave in a very close way to proliferating unicellular organisms for some aspects: they proliferate regardless of tissue-level rules, as long as nutrients and oxygen are available. If coordination between cell cycle progression and cell growth is found in these cells, it means that the underlying mechanisms were conserved despite gaining multicellularity and tissue-level rules orchestrating growth and cell cycle progression. In some cases, it may be argued that tissue-level rules override cellular-level rules, but there must be some cases where the latter remain important for evolution to have conserved them.

1.3 Conclusion

Overall, we highlighted the main challenges of studying cell size regulation in metazoan cells compared to unicellular organisms. In proliferating unicellular organisms, cell size homeostasis is ultimately the result of a coordination between cell growth and cell cycle progression. To study cell size regulation in these cells: (i) the chosen size parameter should be accurately measured and its relevance assessed; and (ii) mathematical approaches to characterize growth and model different size-homeostasis mechanisms may illustrate differences between modes of cell size regulation.

Bringing the question to cells coming from multicellular organisms, several additional questions must be considered when a single-cell approach was chosen: (i) homeostatic behaviors may vary depending on the cell type; (ii) designing robust single cell experiments where extracellular factors such as nutrients availability and cell-to-cell signaling are controlled and understood is crucial to guarantee reproducibility; then finally (iii) designing future experiments that will translate findings in single cell studies to tissue-level homeostasis studies is the next challenge.

Chapter 2

Size homeostasis study: question, challenges and concepts step by step

2.1 Sizer, timer & adder . . . 18
2.2 Coordination of cell cycle progression to growth . . . 19
2.3 Models of size-sensing mechanism . . . 23
2.3.1 Geometric measurement of absolute length . . . 23
2.3.2 Volume measurement through titration-based mechanism . . . 23
2.3.3 Surface area measurement . . . 25
2.3.4 Conclusion: the importance of cell volume . . . 26
2.4 An emergent role for growth regulation in size control . . . 28
2.4.1 The regulation of growth . . . 28
2.4.2 Measuring cell growth at the single-cell level . . . 30
2.5 Combination of processes? . . . 31
2.5.1 Independent control in each cell cycle phase. . . . 31
2.5.2 One overarching mechanism . . . 31
2.5.3 Parallel and concurrent processes . . . 31
2.6 Robustness and flexibility of size control . . . 32
2.6.1 Apparent flexibility of size thresholds . . . 32
2.6.2 What we can learn from studying cells in different growth environments . . . 32
2.7 Conclusion . . . 34

When studying cell size control in proliferating single cells, we can define six distinct steps. (i) First, at the very basic phenomenological level, the question of size homeostasis is the question of how size added at each cell cycle is adapted to initial size in order to correct abnormal sizes and prevent size dispersion. This can be classified into distinct phenomenological models. Following on from this, one will want to understand how the coordination of cell cycle and growth leads to the observed homeostatic behaviour. The adaptation of cell cycle progression to cell size is thought to be the key player of size control (ii) and acts through size-sensing mechanisms that relate size or growh with cell cycle transitions (iii). However, an emerging hypothesis is that growth itself plays an active role in size control (iv). Therefore several processes might play a role in overall size control and various possibilities as to how they combine can be envisioned (v). Finally, a common property to all size homeostatic behaviours is that they are flexible to environmental changes. Although this is another

side of the question of size homeostasis, keeping it in mind can prove extremely useful guide in the interpretation of the results obtained even at steady growth conditions (vi).

Here, we will describe each of these six steps that pave the way to the study of cell size control in single proliferating cells. We try to assimilate the concepts established from studies in bacteria, yeast and metazoan cells. An overview of the current understanding of size control in each of these organisms will be discussed, cell type by cell type in the following chapter 3

2.1 Sizer, timer & adder

Sizer and adder Cell size homeostasis in proliferating cells is achieved through adapting the amount of growth produced in the cell cycle to the initial size: large cells grow less while small cells grow more. The strength of this correction varies. Size homeostatic behaviours are usually sorted into three main categories: the sizer, the adder and the timer. In this section, we use size as a generic term for any size parameter such as mass, volume or surface area. The relevance and significance of each of these parameters varies upon the cell type and will be discussed later.

Historically, the most famous model for size homeostasis is that of the sizer where a size threshold (S_T) restricts the transition to the next event of the cell cycle. This ensures that the entry into the next phase of the cell cycle is not triggered until the size threshold is reached at one stage of the cell cycle:

$$S_f = S_T$$

Where S_f is the final size. The classical example of a sizer behaviour is that of the yeast *S. pombe* Fantes (1977) and is described in 3.2.1.

Alternatively, the adder mechanism relies a constant addition of size at each cell cycle, independently of initial size (S_i) Amir (2014); Voorn and Koppes (1998):

$$S_f = S_i + \Delta S \tag{2.1}$$

where $\Delta S = C$, a constant.Therefore, the cell at the generation $(n+1)$ is:

$$S_{f,n+1} = \frac{S_{f,n}}{\sigma} + \Delta S \tag{2.2}$$

where σ is the symmetry of division. In the case of cells dividing symmetrically ($\sigma = 2$), we can calculate the difference from the mean size $\langle S_f \rangle$ for a given cell of size $S_{f,0}$:

$$\begin{cases} E_0 = S_{f,0} - \langle S_f \rangle \\ E_n = S_{f,n} - \langle S_f \rangle \end{cases} \tag{2.3}$$

Using equation 2.2, we have:

$$E_{n+1} = \tfrac{1}{2} S_{f,n} + \Delta S - \langle S_f \rangle \tag{2.4}$$

In the case of an adder, $\Delta S \approx 1/2 \cdot \langle S_f \rangle$, therefore:

$$E(n) = E_0 \times \left(\frac{1}{2}\right)^n \tag{2.5}$$

This shows that the difference with the mean size is reduced division after division.

Size convergence rate. Importantly, the size convergence principle described above does not require a perfect adder or symmetry of division. In an imperfect adder, size added (ΔS) is described

as the sum of a size-dependent term ($a.Si$) and a constant term (ΔS_C). In Jun and Taheri-Araghi (2015), authors show that, as long as $-1 < a < 1$, size still converges towards:

$$S_i \rightarrow \frac{\Delta S}{(1-a)} \tag{2.6}$$

This point stresses the fact that a phenomenological description of the size homeostatic processes using the terminology of sizer, adder or imperfect adder only defines the rate of size convergence in a population of proliferating cells. The observation of an adder for example does not necessarily imply the existence of an underlying molecular mechanism directly controlling size added. How the combination of distinct process can lead to an effective adder is discussed in section 2.5.

The size-growth plot. To characterize the homeostatic behaviour of a given cell type, a commonly used approach is to look at the correlation between size added and initial size. When growth is exponential, final size (S_f) is related to initial size (S_i) as:

$$S_f = S_i e^{\gamma\tau} \tag{2.7}$$

where γ is the growth rate and τ the cell cycle duration. The relationship between growth and initial size is:

$$\gamma\tau = log(S_f) - log(S_i) \tag{2.8}$$

From equation 2.8 the folowing relationship is derived:

$$\gamma\tau = \langle\gamma\tau\rangle - \lambda(log(S_i) - \langle log(S_i)\rangle) \tag{2.9}$$

This relationship is that of the famous 'size-growth plot', first used in the yeast *S.cerevisiae*, as a way to distinguish between sizer and adder behaviour Di Talia et al. (2007). The slope λ of this plot indicates the strength of size control and is 1 in the case of a sizer, 0 in the case of a timer and 0.5 in the case of an adder. This relationship and its linear version are described in 2.1.

Growth control in exponentially and linearly growing cells. In the case where cells grow linearly, the adder mechanism can simply be achieved by 'counting' time: if all cells grow for the same time (timer), they add the same amount of size. On the contrary, if cells grow exponentially, the timer rapidly leads to a divergence of size in the population Mitchison (2003),(see figure 2.1). To control size in this case, two mechanisms can be envisioned: (i) an adaptation of cell cycle duration to size or growth where small cells will be delayed in the cell cycle in order to have enough time to grow as much (adder) or more (sizer) than large cells (figure 2.2) or (ii) an adaptation of growth to cell cycle progression so that small cells will boost their growth speed while large cells will slow down their growth speed so that they produce an equal (adder) or higher(sizer) amount of net growth during the same time.

Adaptation of cell cycle progression to growth has long thought to be central in the process of size control Turner et al. (2012); Jorgensen and Tyers (2004); Conlon and Raff (1999). However, more recently, the alternative hypothesis that growth was adapted to cell cycle was raised Ginzberg (2015); Goranov and Amon (2010). Finally, we recall that the existence of any coordination between these two processes at the single cell level is debated in animal cells Lloyd (2013), (see also section 1.2.2.2). We will now describe the evidence supporting that cell cycle is coordinated to cell growth.

2.2 Coordination of cell cycle progression to growth

Strong evidence supporting the importance of time modulation in size control Three types of observations strongly support the importance of coordination of cell cycle progression to growth.

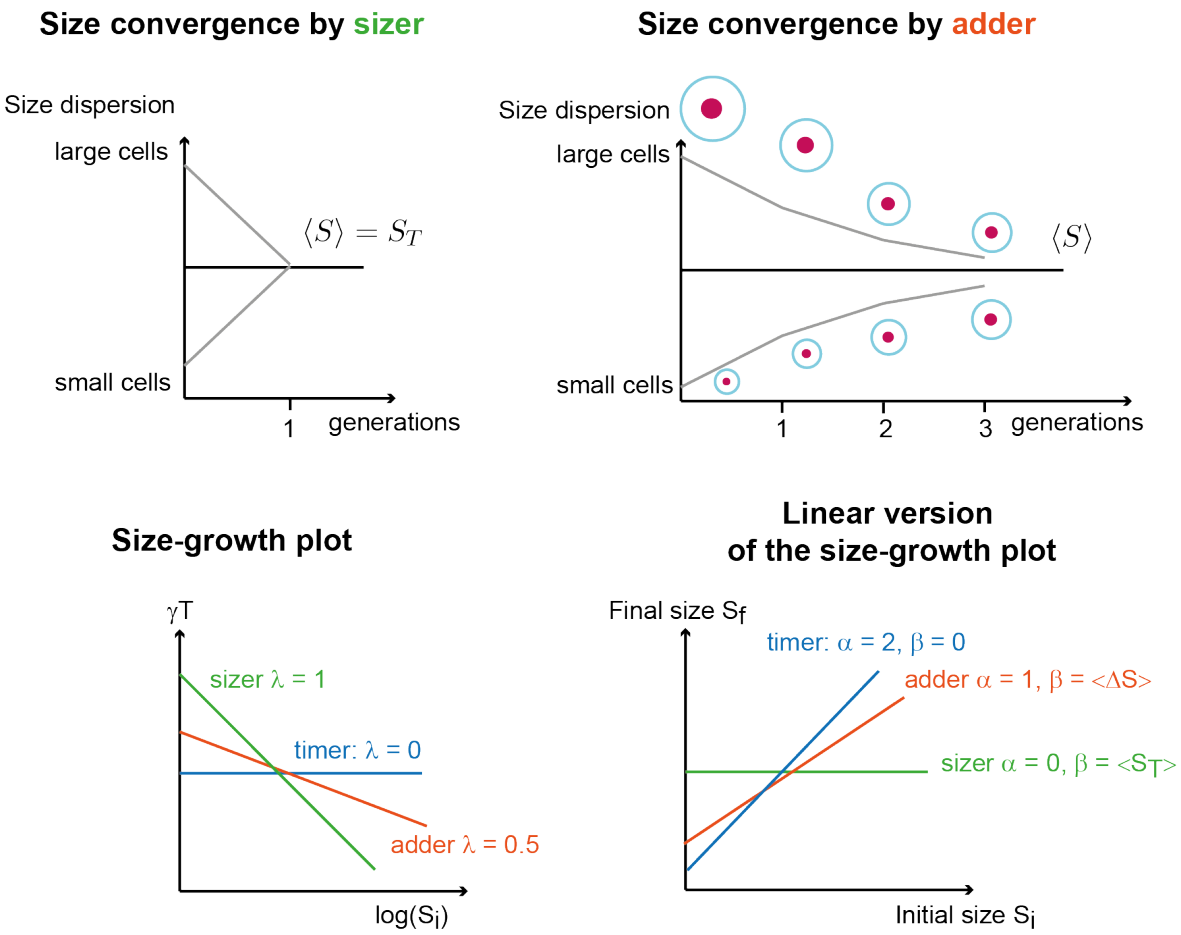

Figure 2.1: Sizer and adder. Top: in case of a sizer, size converge within one generation since size at division $S_f = S_T$ the target size in the population, independently of the initial size. Alternatively, in the adder model, sizes converge towards the mean size ($\langle S \rangle$) division by division. Bottom: to characterize the homeostatic behaviour from data acquired on single-cell, two types of plots are usually used: the size-growth plot in the case of exponential growth (left) and the S_f *vs.* S_i plot in the case of linear growth (right). **For the size-growth plot**: the relationship tested is: $\gamma\tau = \langle \gamma\tau \rangle - \lambda(log(V_i) - \langle log(V_i) \rangle)$. The slope λ is equal to 1 in the case of a sizer, 1/2 in the case of an adder and 0 in the case of a timer. **For the S_f *vs.* S_i plot**, the relationship tested is: $S_f = \alpha S_i + \beta$. In the case of a sizer, $S_f = S_T$, so $\alpha = 0$ and $\beta = S_T$, in the case of an adder, $S_f = S_i + \Delta S$, so $\alpha = 1$ and $\beta = \Delta S = Cst.$ and for a timer, $S_f = 2S_i$ thus $\alpha = 2$ and $\beta = 0$.

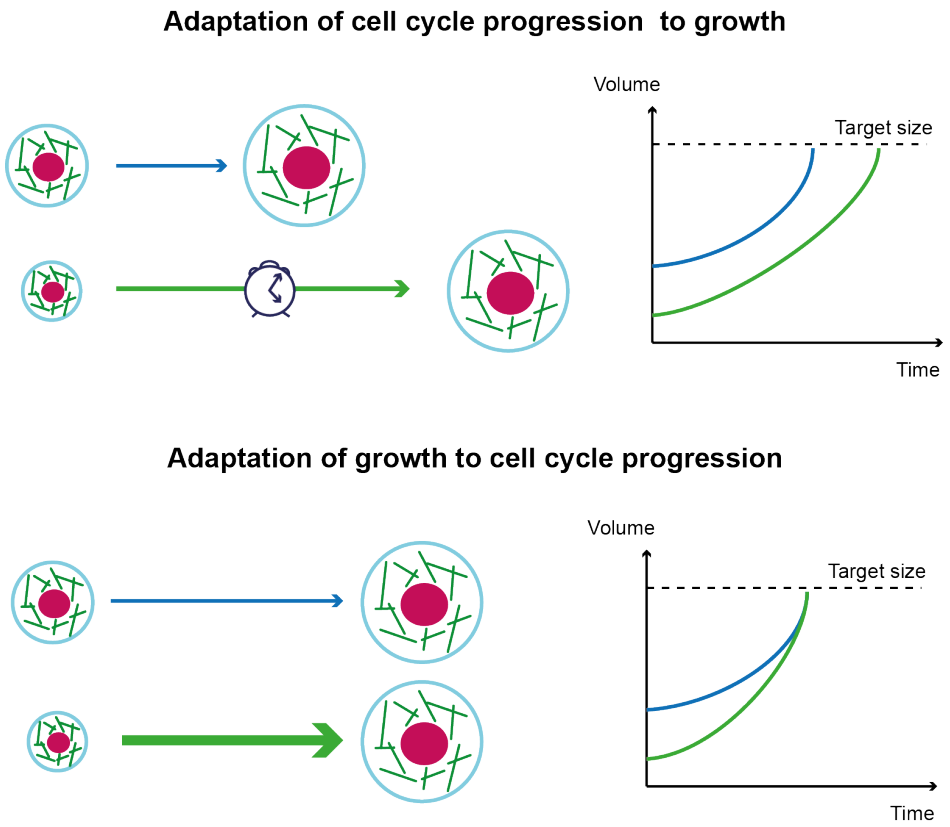

Figure 2.2: Time or growth modulation to control size. Size control requires adaptation of growth added to initial size. In the case where cells do not grow linearly, a mechanism must coordinate cell growth and cell cycle progression, this could theoretically be achieved through either (i) adaptation of cell cycle progression to growth: small cells that grow slower under exponential growth, are delayed to have more time to grow than large cells; or (ii) adaptation of growth to cell cycle progression: small and large cells grow for the same amount of time but small cells grow faster than large cells.

First, many genetic screenings for mutants affecting size control highlighted the role of proteins involved in the cell cycle machinery Soifer and Barkai (2014); Jorgensen (2002). Second, in proliferating cells, commitment to a new round of division is under the influence of nutrient sensing to ensure that the environment can sustain another cycle of growth. Third, the observation of negative correlation between cell cycle duration and cell size is well-documented in many cell types.

These three observations support the idea that checkpoints controlling size, growth or ability to grow (nutrient sensing) exists throughout the cell cycle. We describe here the principles of theses checkpoints. Current understanding of how time is coordinated to size in each specific specie is detailed in the following chapter (chapter 3).

Cell cycle progression is controlled by cyclines-Cdk networks that define irreversible transitions. How the cell cycle clock is set by the timely production and degradation of cyclins is a entire field of research that is beyond the scope of this work. For the question of size control, we only define a few concepts. Briefly, the cell cycle is generally described as successive phases gated by checkpoints. In eukaryotes, transitions through these checkpoints are regulated by the orderly expression, activation and degradation of cyclin and cyclin-dependent kinases (Cdk) (reviewed in Malumbres (2014); Fisher et al. (2012); Malumbres and Barbacid (2009); Santos and Ferrell (2008)). These proteins interact in networks whose structure ultimately generates bistable switches. Such bistable switches are characterized by two stable states separated by an unstable state and ensure that transitions are fast and irreversible so that the sequence of cell cycle phases: G1/S/G2/M is always respected Tyson and Novák (2015); Novak et al. (2010); Verdugo et al. (2013); Fisher et al. (2012). Checkpoints typically verify that all the processes initiated during the phase were achieved and/or that all the material needed for the next phase is available. During S phase, cells duplicate their genome and the passage from S to G2 is gated by a checkpoint verifying that a new complete and identical copy of DNA was synthesized. During M phase, cells partition the genome into two identical copies. Mitosis checkpoints verify that potential mis-segregation of DNA are corrected before completing mitosis. Finally, much evidence supports the idea that G1/S and G2/M transitions are gated by checkpoints sensitive to size or growth-related events (size, growth or nutrient amounts) Turner et al. (2012); Jorgensen and Tyers (2004), (see figure 2.3).

Restriction point verifies that nutrient availability is sufficient for another round of division Examples of checkpoints that are conditionned by growth or nutrient amounts are rife in eukaryotes. In the yeast *S. cerevisiae*, the restriction point Start occurs in late G1 and is nutrient-dependent: in the case of nutrient starvation cells are blocked in G1. Conversely, once the restriction point is passed, cells will complete the cell cycle even if nutrients are removed from the culture media Jorgensen and Tyers (2004). In metazoan cells, growth factors or nutrient deprivation blocks cell growth and results in cell cycle arrests in G1. This led to the definition of a nutrient-dependent restriction point Pardee (1974). It has been proposed that two checkpoints in G1 condition the decision of entering a new cycle of growth and division Foster et al. (2010). The first one is growth-factor dependent and is based on the Ras/Raf/MAPK/Cyclin D pathway. The second checkpoint, later in G1, checks nutrient availability through the well-known mTOR/AkT/Myc/Cyclin E pathway (the checkpoints for mammalian cells are discussed in more details in section 4.1.2.2).

Size threshold-dependent checkpoints The simplest way to control cell size is by setting a thresholding size gating passage through the next cell cycle phase. Evidence that cell cycle duration is negatively correlated with initial size have long been provided in the yeasts *S. pombe* Fantes (1977); Nurse (1975); Sveiczer et al. (1996) and *S. cerevisiae* Hartwell and Unger (1977); Johnston (1977). In bacteria *E.coli*, this time-dependent size control has long been hypothesized Donachie

(1968); Donachie and Blakely (2003), although experimental validation at the single-cell level was only provided recently Osella et al. (2014); Robert et al. (2014). In metazoan cells, where size control study is a beginning field, this role is more debated (reviewed in Lloyd (2013); Ginzberg et al. (2015)) and direct experimental testing is still required.

From correlation to causality Filling the gap from observation of a correlation between time and size to causality is one of the most tricky aspects of size homeostasis studies. In yeast, temperature sensitive cyclines mutants allow blocking cell cycle progression while maintaining growth: the cell elongates and reaches unusual large sizes Fantes (1977). The advantage here is that once temperature is switched back to the normal value, the mutants can almost be considered as a normal wild-type cell (see figure 2.3). Cells that divide asymmetrically and generate one large and one small daughter cells are also an interesting way to study time adaptation to cell size through comparison of sister cell's progression through the next cell cycle. Artificial induction of asymmetrical division has in fact been used in *Amoeba proteus* in very early work Prescott (1956) to study time adaptation to size and this strategy could be extended to other cell types (figure 2.3).

2.3 Models of size-sensing mechanism

Coordination between cell cycle progression to cell growth is supposed to occur through size thresholds that translate a size measurement into an information for the cell-cycle machinery. When a critical size is attained, an irreversible cell-cycle transition is triggered. The sizing mechanism could rely either on an absolute size threshold (of mass or volume for example) or alternatively measure a dynamic parameter such as the biosynthetic status (i.e. growth rate, metabolic threshold) Jorgensen and Tyers (2004) (see figure 2.4).

2.3.1 Geometric measurement of absolute length

In cells that have a cylinder shape and grow length-wise such as *S. pombe* or *E. coli*, a gradient-diffusion based size-sensing mechanism has been proposed. This model is based on the production of an inhibitor at the poles of the cell, generating a gradient of diffusion from the pole to the center of the cell. This protein inhibits a phase-transition activator located at the center of the cell. As the cell elongates, the inhibitor is produced further from the center and its local concentration at the center of the cell decreases until it is no longer sufficient to inhibit the activator (see figure 2.4). In *S. pombe*, pom1 was proposed to localize in a gradient of diffusion and inhibit cdr2, a protein from the mitotic promoting factor Moseley et al. (2009); Martin (2009). In *E. coli* and *B. subtilis*, a similar function and localization of the complex MinCD that prevents formation of the cytokinesis ring through the inhibition of the polymerization of the tubulin-like protein FtsZ was proposed (reviewed in Robert (2015)).

However, this length-sensing model is not adapted to cells of more complex shapes such as the spherical *S. cerevisiae* or metazoan cells which have constantly fluctuating shapes.

2.3.2 Volume measurement through titration-based mechanism

Most models of size sensing rely on a molecule whose copy number scales with overall cell size and is titrated against a component of the cell that has a constant size (*i.e.* DNA copy number). Theoretically, this titration method can allow measurement of either absolute or added size. The

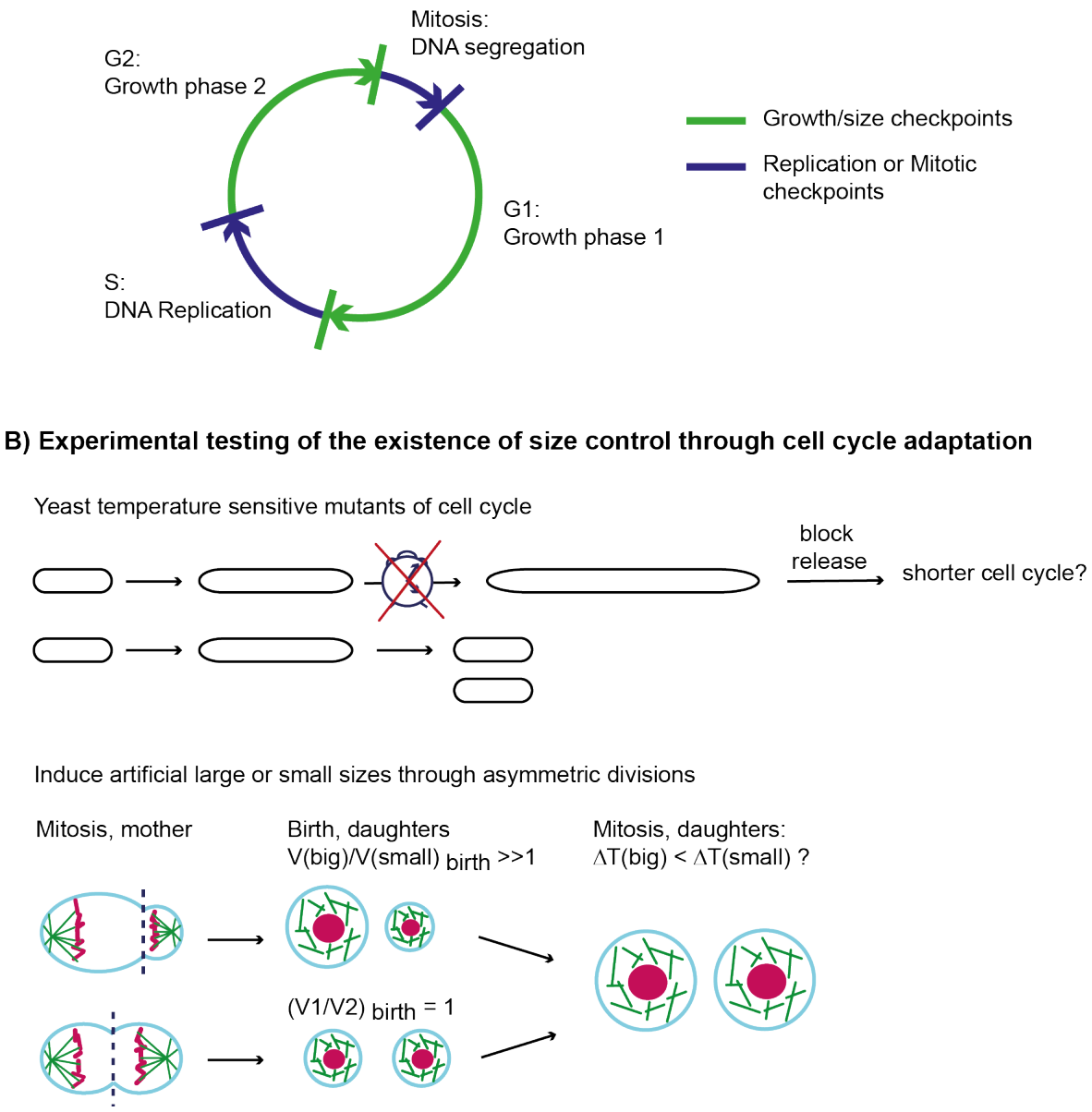

Figure 2.3: Coordination of cell cycle progression to growth through checkpoints. A) In eukaryotes, cell cycle is gated by checkpoints. A very basic description of the cell cycle is that of a succession of phases dedicated to specific tasks. G1 and G2 are the growth phases where size or growth checkpoints are thought to occur. **B) Experimental tricks to test the existence of coordination between cell cycle progression and cell growth.** In *S. pombe*, temperature sensitive cyclines mutants are a great tool to transiently block cell cycle progression while maintaining cell growth: the cell elongates and reaches very large size. Once the block is release, the rate at which size correction is achieved and the adaption of cell cycle duration to abnormal sizes can be studied. Asymmetric divisions are another way to obtain size dispersion. Physiological examples exist such as the asymmetric division of *S. cerevisiae* but developing tools to artificially induce asymmetrical divisions could be of great interest for the study of size homeostasis Cadart et al. (2014).

titration models always assume that cell density (mass over volume ratio) is constant and that the amount of proteins (mass) thus the relationship between protein copy number and protein concentration is fixed.

Accumulation of an initiator protein: added volume The first model for a molecular mechanism generating an adder behaviour was the initiator accumulation model Sompayrac and Maaloe (1973) (figure 2.4). In this case, two proteins, one auto-repressor (AR) and one initiator (I) are coded on the same operon. The Auto-repressor inhibits its own transcription in a concentration-dependent manner so that it is present at constant concentration: $dN_{AR}/dV = C$. Therefore, the initiator which is transcribed at a rate dependent of the auto-repressor is accumulated proportionately to cell volume and independently of cell growth rate. The initiator locates at the origin of replication and activates replication when reaching a threshold number. Replication initiation triggers the degradation of the initiator to reset the system. A key aspect of this model is that measurement of absolute growth (volume added) is made independently of growth rate. If growth rate rather than growth added was sensed, one can easily imagine that very slow growth conditions would lead to cells being larger than at fast growth conditions because of the time needed to reach the threshold growth rate. This would be in contradiction with the great amount of experimental evidences showing that cells tend to reduce in size when grown in nutrient poor conditions Turner et al. (2012).

The initiator accumulation model was recently discussed again in the light of the recent findings of an adder mechanism in bacteria Soifer et al. (2016); Ho and Amir (2015); Robert (2015) : a potential candidate for the auto-repressor could be the DNA helicase DnaA that accumulates at the oriC and triggers replication initiation in a dose-dependent manner (more details in 3.1.3). Alternatively for *E. coli*, it was also proposed that the accumulation of surface area material needed to achieve cytokinesis matched the characteristics of the initiator since its production was proportionate to cell volume and its amount was fully used (reset to zero) during septation Harris and Theriot (2016).

Dilution of an inhibitor: absolute volume A variation of the initiator model proposes that titration is compared against a fixed amount of protein rather than a fixed number of DNA loci (figure 2.4). This dilution-based model was hypothesized in *S. cerevisiae* where the inhibitory molecule Whi5 was found to be of constant amount, thus decreasing concentration, during G1 when size control is thought to occur Schmoller et al. (2015). In this model, similarly to the previous one, the copy number of initiator protein increases proportionately to cell volume ($dN_I/dV = C$) while the inhibitor (repressor) protein remains at a fixed number of molecules ($N_R = C$). As the cell increases in volume, the ratio N_R/N_A decreases up to a threshold value where inhibition is released and transition triggered. Note that unlike the accumulation of initiator protein model, absolute volume rather than volume added is measured here. This model is interesting because it could be a very general way for a cell to measure its volume as it simply requires one protein whose synthesis rate does not scale with volume.

2.3.3 Surface area measurement

In *S. pombe*, an alternative mechanism to the gradient-based size sensing was proposed by Pan et al. (2014). This mechanism proposes that absolute surface area rather than length is measured. Similarly to the previously described titration models, here the activator protein cdr2 accumulates in a membrane region of constant area: the cortical nodes at the middle of the cell cortex. The difference with the previous model is that cdr2 accumulates proportionately to surface area, not volume (figure 2.4).

The surface area dependent accumulation of cdr2 at the cortical nodes requires 3 distinct compartments: the cytoplasm, the cortex and the cortical node which has a constant surface area. In the first compartment, the cytoplasm, cdr2 concentration is constant because it is synthesized proportionately to cell volume:

$$\rho_1 = \frac{N_1}{V_1} = C$$

Where N_1, V_1 and ρ_1 are the copy number of activator cdr2, the volume and the concentration in the first compartment. In the second compartment, the cell cortex, new cdr2 coming from the cytoplasm binds to the membrane at a rate: $k_{1\to2}$ while other cdr2 molecules leave the membrane either back to the cytoplasm ($k_{2\to1}$) or to the third compartment constituted by the cortical nodes ($k_{2\to3}$). The membrane surface area is SA_2 for the second compartment and SA_3 for the cortical nodes. At steady state:

$$\begin{cases} 0 = k_{1\to2} \cdot \frac{N_1}{V_1} \cdot SA_2 - k_{2\to1} \cdot N_2 - k_{2\to3} \cdot \frac{N_2}{SA_2} \cdot SA_3 \\ 0 = k_{2\to3} \frac{N_2}{SA_2} \cdot SA_3 - k_{3\to1} \cdot N_3 \end{cases} \tag{2.10}$$

Where ρ and N define the concentration and copy number of cdr2 in each compartment.The authors show that the solution to this system is:

$$\begin{cases} \rho_3 = \rho_1 \cdot \frac{k_{1\to2}}{k_{3\to1}} \cdot \left(\frac{k_{2\to1}}{k_{2\to3}} + \frac{SA_3}{SA_2} \right)^{-1} \\ \rho_2 = \rho_3 \cdot \frac{k_{3\to1}}{k_{2\to3}} \end{cases} \tag{2.11}$$

Several important observations about this model should be made. First, since $SA_3 = C$, ρ_3 the density of cdr2 at the cortical nodes increases proportionally to the surface area of the cortex SA_2 as long as the rate of accumulation of cdr2 at the cortical node ($k_{2\to3}$) is higher than the rate of dissociation from the cortical node to the cytoplasm ($k_{3\to1}$): $k_{2\to3}/k_{3\to1} \gg 1$. Like in any titration model, it is proposed that when this concentration reaches a specific threshold, cell-cycle transition is triggered. Second, surface area sensing is possible only if association and dissociation from the membrane occur at two separate compartments on the membrane in addition to the cytoplasmic compartment. In the second compartment association scales with surface area (cortex) and in the third one (the cortical node), surface area is constant and association scales with the surface area of the second compartment. Indeed, in the case where there are only two compartments, one cytoplasmic and one at the membrane, we find: $\rho_2 = (k_{1\to2}/k_{2\to1}) \cdot \rho_1 = C$, assuming that the cytoplasmic concentration remains constant. In the case where $k_{2\to1} = 0$ and molecules accumulate at the membrane proportionally to cell volume, $\rho_2 = k_{1\to2} \cdot \rho_1$ and we fall back to a volume titration mechanism.

2.3.4 Conclusion: the importance of cell volume

An important remark here is that size-sensing mechanisms in cells that have more complex shapes than that of a cylinder will most likely rely on cell volume measurement. Theoretically, it is easier to conceive a sensing mechanism based on the titration of a molecule agaisnt a growing volume than against an increasing amount of mass. Experimental testing of the relevance of a given size parameter requires finding conditions where it can be decoupled from other size parameters. Work in bacteria for example showed that replication is initiated at a fixed volume per origin and that this was robust to various perturbations of cell shape while other potential size sensors such as length or surface area were not Si et al. (2016); Zheng et al. (2016). An interesting experiment in organisms where volume-dependent size control is assumed would be to decouple mass from volume (modify cell density) but this is to date rarely explored, mostly because cell density is a parameter difficult to measure.

Overall, volume appears as the central parameter for size-sensing. This observation is important because most of the studies on metazoan cell size were performed by measuring cell mass Park et al. (2010); Sung et al. (2013); Mir et al. (2011); Son et al. (2012); Godin et al. (2010) rather than volume which is more difficult to measure in these cells (see results in metazoan cells section 4.3) .

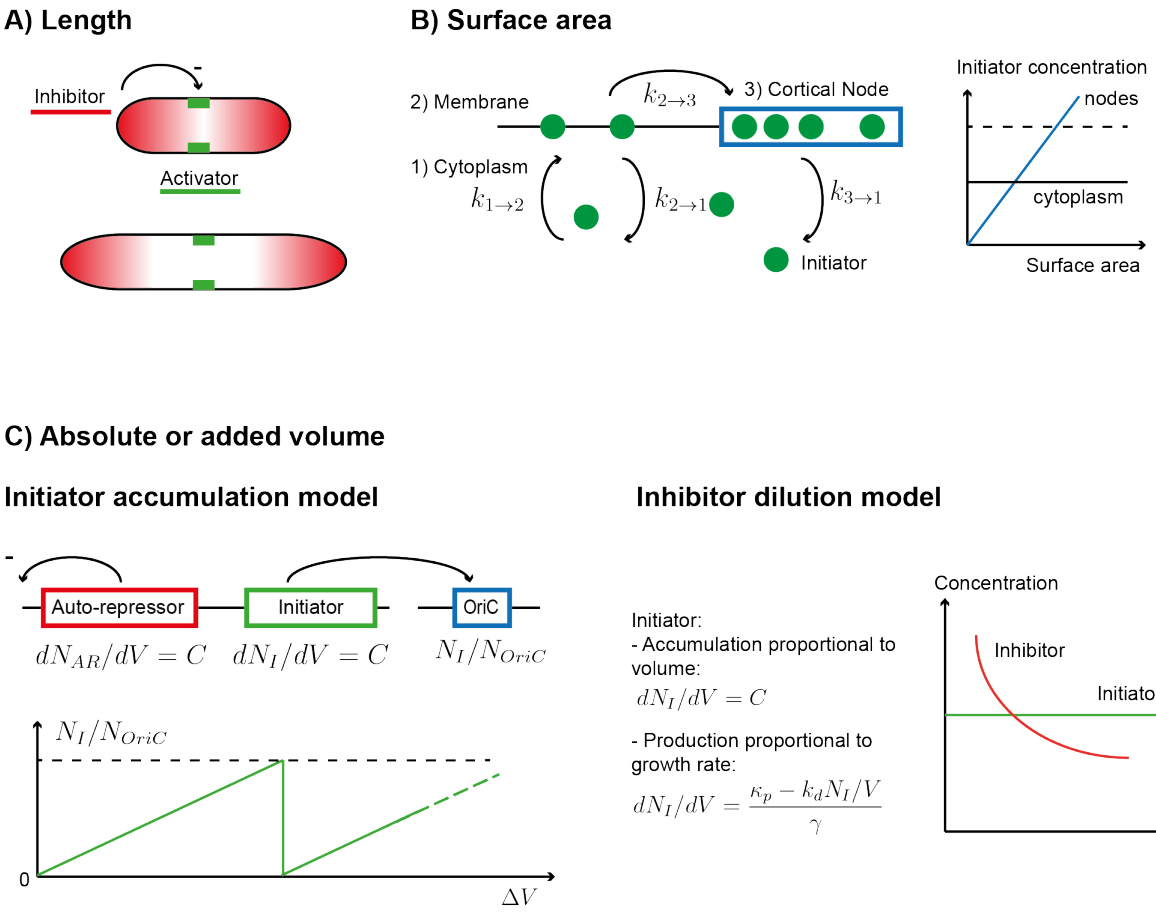

Figure 2.4: Molecular mechanisms of size sensing. This figure illustrates the mechanism described in details in the main text. **A) Cell length** can be measured through the establishment of gradient of diffusion of an inhibitor which acts in a concentration-dependent manner on an activator located at the minimum of the gradient. **B) Surface area** can be sensed when an activator (green circles) accumulates proportionately to surface area at a specific region of the cortex of constant area (cortical nodes). **C) Volume** can be sensed in cells that have complex shapes through either: (left) accumulation of an initiator proportionately to cell volume that is titrated against a fixed number of DNA origins or (right) dilution of an inhibitor that is titrated against a fixed amount of activator.

Parallel to the recent improvements in the characterization of molecular mechanism linking size sensing to cell cycle events, several works suggested that modulation of growth rather than cell cycle was key in size control.

2.4 An emergent role for growth regulation in size control

For a long time, the hypothesis that growth could be coordinated to the cell cycle was neglected Jorgensen and Tyers (2004). This was probably because of both the amount of evidence supporting a time-dependent size control and the number of experiments showing that blocking cell cycle progression did not block cell growth Jorgensen and Tyers (2004); Lloyd (2013). Recently however, several works have hinted that growth regulation might be an important aspect of size control.

2.4.1 The regulation of growth

What pathways are involved in cell growth is a very broad question. Here we only gather a few recent pieces of evidence suggesting a role for growth regulation in cell size control.

2.4.1.1 Growth in volume.

Budding yeast has been reported in several studies to show phase-dependent rate of volume growth Goranov et al. (2009); Leitao et al. (2016). In these cells that have a cell wall, growth in volume is limited by the addition of membrane. Membrane extension is driven by the fusion of lipid vesicles that are transported to the fusion sites on actin cables. Polarization of these actin cables is regulated by cell cycle proteins. Thus in *S. cerevisiae*, volume growth and its localization are directly under the influence of cell-cycle progression Goranov et al. (2009); Goranov and Amon (2010). Membrane addition in *E.coli* has also recently been proposed as the core mechanism of cell size control Harris and Theriot (2016). How membrane synthesis is regulated in metazoan cells that do not have a cell wall and how it impacts cell size homeostasis might be an important question and will require more investigation. Interestingly, the mevalonate pathway, more specifically the protein RAB11, has been identified as a key regulator of autophagy and endosomal recycling. Its inhibition induces an increase in both cell volume and density Miettinen and Bjo (2015).

2.4.1.2 Growth in mass.

The definition of mass as a size parameter is unclear. Indeed, although strictly speaking, a cell adds mass through importing more molecules, most of the studies measuring cell mass actually measure macromolecules content (proteins) Kafri et al. (2013); Sung et al. (2013); Mir et al. (2011), neglecting the contribution of smaller molecules such as amino acids, ions, nucleotides... This distinction is however important because nutrient accumulation and protein synthesis are not necessarily coupled Son et al. (2015b). Both parameters are of course important but might not relate the same way to to cell cycle. An interesting result in budding yeast showed that size increase was under the influence of external glucose sensing but not importing, while division rate increase was correlated with glucose influx Schmidt-Glenewinkel and Barkai (2014).

It is worth noting here that mass accumulation can be the result of either an increase in protein synthesis or a decrease in degradation or both. Protein degradation is likely to be important for cell growth via preventing accumulation of misfolded or effete proteins, and guaranteeing correct protein

turnover Roberts (2013). In exponentially growing mammalian cells, the half-life of most proteins have been estimated to range from a few minutes to a few hours Eden et al. (2011). This aspect is well illustrated by research in neuronal cells although no consensus has been reached yet: in some studies, proteasome degradation was shown to be required for cell growth Inoue et al. (2004); Kavakebi et al. (2005); Laser et al. (2003), while others showed that its inhibition increased cell growth Song et al. (2009). Therefore, the regulation of protein degradation might be an interesting research direction to understand how growth rate is regulated.

Nutrient import and protein synthesis are related yet distinct processes. For a long time, the common description of protein production used the ribosome-centered model that predicts exponential growth as long as ribosomes are in sufficient amounts. However, recent findings suggested that protein synthesis rate is in fact limited by other factors such as an increase in transcriptional demand Kafri et al. (2016b). Furthermore, mass addition through nutrient uptake and biosynthesis of new proteins is an energy-requiring process directly related with cell metabolic state.

2.4.1.3 Growth and metabolism.

In yeast, it is often observed that phases where cells grow are separated from phases where they accomplish energy-demanding processes such as DNA replication or segregation Goranov and Amon (2010) (see also figure 2.3). The observation that growth rate is phase-dependent was reported several time in both *S. pombe* and *S. cerevisiae* Goranov et al. (2009); Bryan et al. (2010); Sveiczer and Horváth (2016). In animal cells, growth is less well characterized but the two only studies that measured cell growth at the single-cell level over complete cell cycles reported a change in growth-rate at the G1/S transition Son et al. (2012); Mir et al. (2014). This decoupling has been hypothesized to be the result of evolutionary selection of processes enabling accumulation of resources prior to energy-demanding tasks Goranov and Amon (2010). Although the complex and bidirectional interplay between cell-cycle machinery and metabolic enzymes is well-documented Kaplon et al. (2015), the underlying molecular mechanism enabling active regulation of growth rate in a phase-dependent manner is mostly unknown.

A very interesting and new question related to how metabolism impacts cell growth is that of cellular allometry, namely the question of how cellular metabolism scales with cell size da Silva et al. (2006); Glazier (2014). Several models propose that surface area, resource transport or intracellular composition determine the relationship between metabolic rate and size (reviewed in Glazier (2014)). Often in these models, mitochondrial function and homeostasis appears as a key determinant of cell metabolic state. Interestingly, in mammalian cells, a recent study suggested that although mitochondrial content scales with cell size, its functionality is optimum at a given size Miettinen and Bjorklund (2016). Size-dependent growth rates observed in some population of animal cells Son et al. (2012) could be explained by this optimum size for fitness and mitochondrial function. Investigating the relation between organelle homeostasis and size homeostasis is probably an interesting research direction. A potential approach to this question could be the development of tools to decouple the symmetry of segregation of a specific organelle with respect to the cytoplasm Cadart et al. (2014).

2.4.1.4 Density throughout the cell cycle

The above listed observations underline the fact that mass and volume regulation are most often considered and studied separately. This is mainly because of the technical challenge of measuring both mass and volume at the same time in live cells. Yet, understanding how mass and volume evolve together and are co-regulated is probably an important question that might unravel important aspects of cell growth. The idea that organelle and protein content always scales with cell volume is widespread

Schmoller and Skotheim (2015). However, examples where cell density drops at specific points of the cell cycle have indeed been reported in various cell types such as *S. cerevisiae* Bryan et al. (2010); Hartwell (1970); Baldwin and Kubitschek (1984) or cancerous human cells Zlotek-Zlotkiewicz et al. (2015); Son et al. (2015a). The consequence of such regulated changes in density on cell's physiology are still mysterious.

2.4.1.5 Conclusion

The role of the regulation of growth in size control is a new and emergent idea only supported by scattered observations across organisms. It might however turn out to be one of the most promising directions for making further progress in understanding size homeostasis. Findings in this field could in fact relate to a separate important question of size regulation in multicellular organisms where many terminally differentiated cells do not divide but still actively regulate their growth and metabolism Lloyd (2013).

Until recently, one limiting aspect to the study of growth regulation was technical. Methods enabling direct measurement of mass, volume or density at the single-cell level are still fairly recent (reviewed in Popescu et al. (2014); Bryan et al. (2014)) and will likely continue to provide new insights into how growth and volume evolve dynamically. We discuss the importance of single-cell measurements of growth in the next section.

2.4.2 Measuring cell growth at the single-cell level

2.4.2.1 New techniques enabling single-cell measurement.

For a long time, most of the characterization of cell growth, from bacteria to eukaryote, was performed at the population level. Recent technical improvements enabled accurate characterization of cell growth at the single-cell level. For bacteria or yeast that have very regular shapes, the size parameter measured is almost systematically volume, through automated image analysis of cell outlines in phase-contrast. The main challenge was the development of platforms continuously supplying fresh medium and maintaining steady-growth conditions. Although early attempts were not always satisfying Mitchison (2005), progress in microfluidics recently solved the problem of precise environmental growth conditions control (reviewed in Duncombe et al. (2015); Okumus et al. (2014)). The famous mother machine allowed the first high-throughput study of bacteria cell growth Wang et al. (2010). This machine enables maintaining steady growth conditions and the number of cells in the device for hundreds of uninterrupted cell cycles. Other similar approaches were later developed, both for bacteria Ullman et al. (2013); Moffitt et al. (2012); Long et al. (2013); Si et al. (2016) and yeast Nobs and Maerkl (2014). It is worth noting that several works reported the use of resonating micro-mechanical structures to measure cell's mass of bacteria, yeast or mammalian cells Godin et al. (2010); Park et al. (2010); Son et al. (2012). These methods yield higher resolution in cell size measurement than that based on shape outline and their low throughput was recently solved Cermak et al. (2016).

2.4.2.2 From population-level studies to single-cell measurement.

As explained in the next chapter (section 4.3), single-cell growth studies in metazoan cells are lagging behind because of the several additional difficulties brought by these cell types (*i.e.* long cell cycles and fluctuating shapes). Nevertheless, single-cell studies in yeast and bacteria contradicted several results obtained on population studies and emphasize the importance of direct measurement. In

bacteria for example, recent single-cell studies Osella et al. (2014); Campos et al. (2014); Taheri-Araghi et al. (2015); Adiciptaningrum et al. (2015) challenged the long-standing hypothesis of a sizer acting at replication initiation that had been established on population-based studies Donachie (1968). Moreover, other studies showed that individual growth rate could not be inferred from population growth rate Lin and Amir (2016); Hashimoto et al. (2016) while others demonstrated that individual cells systematically deviate from the growth law defined at the population level Kennard et al. (2016); Taheri-Araghi et al. (2015). More fundamentally, one can argue that the reason why size control is needed is because it must compensate not only for extrinsic sources of variability affecting the whole population (*i.e.* fluctuating external chemical or mechanical signals) but also intrinsic sources of variability arising from noise in cell cycle gene expression for example Di Talia et al. (2007). How individual cells correct for these fluctuations can only be studied via the tracking of single-cell growth and cell cycle progression.

2.5 Combination of processes?

Different scenarios currently discuss how overall size control can be achieved (figure 2.5).

2.5.1 Independent control in each cell cycle phase.

The most classical view, inherited from the cell cycle studies in yeast, is that each phase acts independently and is gated by a single rate-limiting process. This gate controls either time (timer) or size (sizer) or anything in between (adder, near-adder). The sum of the strength of size control in each individual sub-period results in an effective size-control. Often, this description combines a phase where most of the growth occurs and a strong size control is exerted (*i.e.* G1 phase for *S. cerevisiae* Di Talia et al. (2007); Schmoller et al. (2015); Delarue et al. (2016) or B phase for *E. coli* Wallden et al. (2016); Adiciptaningrum et al. (2015)) with a timer phase dedicated to other processes such as replication. The overall result can be in that case an effective adder behaviour although the underlying mechanism does not actually 'count' added size.

2.5.2 One overarching mechanism

Alternatively, an adder behaviour can be the consequence of a unique rate-limiting process that controls a constant added size. In Harris and Theriot (2016), it is proposed that the maintenance of a constant surface-to-volume ratio exerts a constraint on cell growth that ultimately renders an adder over the complete cell cycle for *E. coli*. Another proposition is that of a molecular mechanism counting added volume between two consecutive initiation replication events, thus overlapping one cell cycle in both *E.coli* Ho and Amir (2015); Amir (2014); Zheng et al. (2016); Si et al. (2016) and *S.cerevisiae* Soifer et al. (2016) (see above section 2.3.2 for a description of the mechanisms).

2.5.3 Parallel and concurrent processes

Finally, it is possible to view the overall cell cycle as the combination of parallel and concurrent processes. This view gives a possible interpretation of the generality of the noisy adder behaviour across organisms, from yeast Soifer et al. (2016); Delarue et al. (2016) to bacteria Campos et al. (2014); Taheri-Araghi et al. (2015); Deforet et al. (2015); Soifer et al. (2016). Such a noisy homeostatic behaviour could indeed be a systems-level property resulting from the combination of several growth-dependent and time-dependent processes that evolved to maintain homeostasis

while preserving enough flexibility to external fluctuations. This corresponds to a more theoretical description of the cell cycle where no assumption is made about the nature of the homeostatic process or its underlying mechanism. In Osella et al. (2014), the description of the cell cycle progression as a function that depends both on size and time is close to this view (also discussed in Grilli et al. (2016); Kennard et al. (2016)). Another proposition along these lines is that of describing size convergence through generations as an autoregressive model with noise. The amplitude of the noise fluctuations depend on the growth environment and predict the effective strength of size control Tanouchi et al. (2015).

In fact, it is important to recall that a key characteristic of all size homeostatic behaviours observed is that they not only maintain a narrow distribution of sizes through generations but also show adaptation to fluctuating environments and growth conditions. Among the scenarios described here (shown in figure 2.5), the ones that explain both aspects are probably the more likely ones.

2.6 Robustness and flexibility of size control

2.6.1 Apparent flexibility of size thresholds

A classical example of the dependence of cell size on growth rate defined by the nutritional conditions is the famous 'growth law' in bacteria that states that the average cell size in a population scales with the growth rate, independently of the medium composition that generated this growth rate Schaechter et al. (1958):

$$\langle S(\gamma) \rangle = S_0 e^{(T \cdot \gamma)} \tag{2.12}$$

where T is a constant duration $T \approx 60min$, γ is the average exponential growth rate defined by $log2/\langle \tau \rangle$ (τ is the average doubling time) and S_0 is a constant with volume dimensions. This seminal work was further investigated and it is now commonly accepted that nutrient composition rather than growth rate itself sets the average cell size (reivewed in Vadia and Levin (2015). Examples of environmental control of cell size in yeast are also rife Turner et al. (2012); Davie and Petersen (2012). In these cells, the famous and well-conserved mTOR pathway is thought to be the key intermediate that links sensing of external nutrient conditions to fine-tuning of the cyclines thresholds required for cell cycle transitions Turner et al. (2012); Davie and Petersen (2012). It was for example shown in *S. pombe*, that the greatwall-endosulfine PP2A.B55 pathway links TORC1 activity to the mitosis promoting Cdk1-Cyclin B complex. This allows the triggering of division at smaller sizes in nitrogen poor medium compared with nitrogen rich medium Chica et al. (2016).

2.6.2 What we can learn from studying cells in different growth environments

Understanding the adaptation of size control to fluctuating environments is beyond the scope of our study. We simply mention this important property because it has proven to be key in understanding size control in yeast and bacteria. In both fission yeast and budding yeast, studying cell size in various growth conditions enabled the discovery of cryptic size-sensing and nutrient-sensing checkpoints that were hidden under the fast, optimal growth conditions typically used for cell culture (see section on yeast 3.2). This highlights the fact that size control in these cells is unlikely to be the result of a unique mechanism but is rather the result of several processes. In both *E.coli* Wallden et al. (2016) and *S.cerevisiae* Delarue et al. (2016) the strength of size control ranges from sizer-like to adder-like depending on the growth conditions. This further reinforces the idea that effective size control might be the result of rate-limiting processes that depend on growth rate and that studying varying growth

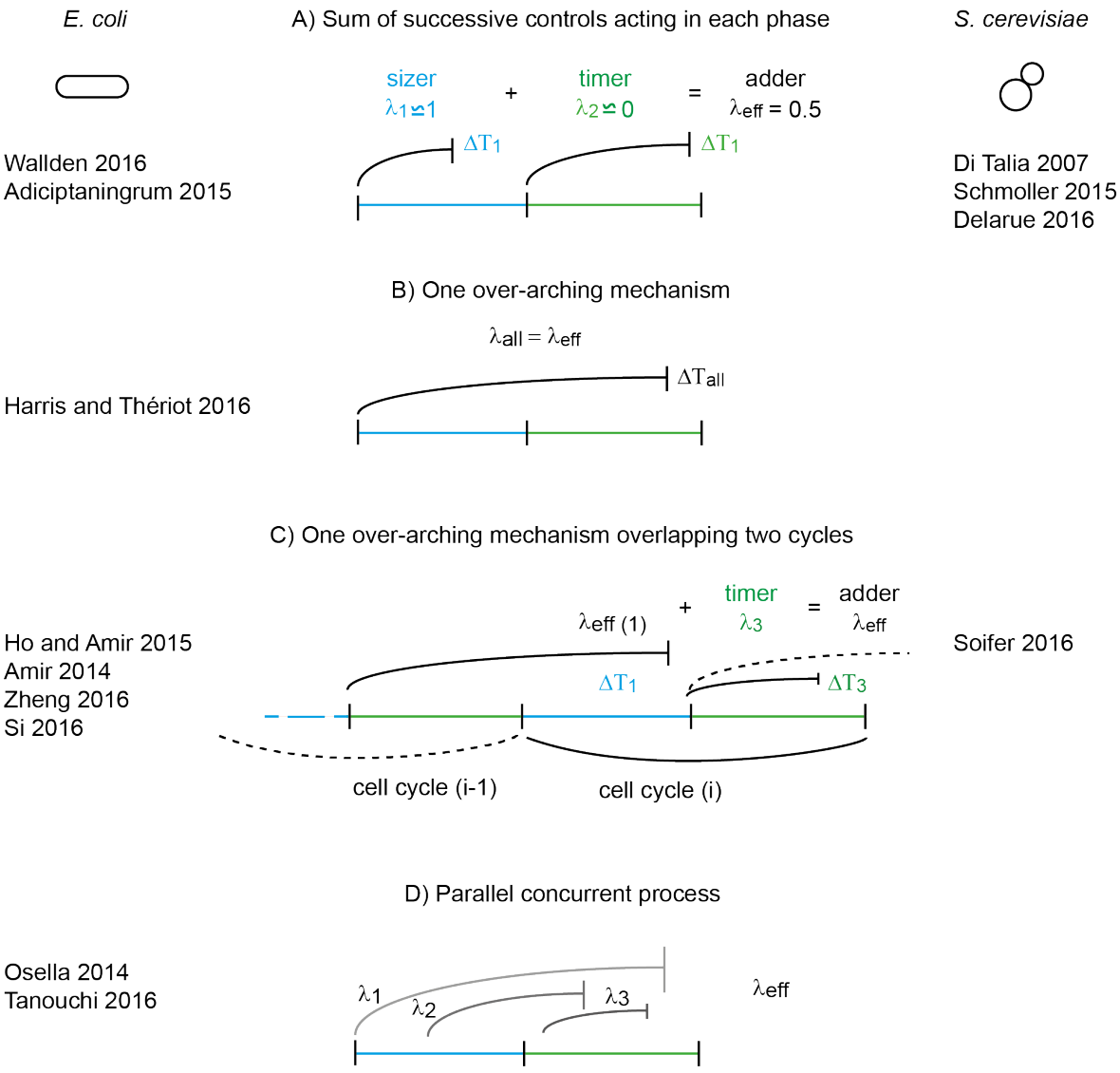

Figure 2.5: Size-control throughout the cell cycle phases. Different scenarios currently discuss how overall size control can be achieved: A) a combination of distinct controls in distinct phases that ad-up to give an effective size control; B) and C) One over-arching mechanism that can potentially act on overlapping cell cycles and D) parallel and concurrent processes that become rate-limiting depending on the conditions and ensure an adaptable homeostatic process. *(Scheme adapted from unpublished work by Marco Cosentino-Lagomarsino).*

conditions will inform us a lot on the nature of these rate-limiting processes. Several interpretations of the flexibility of size thresholds exist. It is proposed that this flexibility optimizes fitness in limited and fluctuating resources: in rich nutrient conditions, cells would grow bigger and 'stock' while in poor nutrient conditions, size thresholds would be set lower to minimize cell cycle duration Jorgensen and Tyers (2004). An alternative possibility raised in bacteria is that the dependence of size on growth rate is not an adaptative process but just the passive consequence of the mechanism that ensure size control: for *E. coli*, this would be a mechanism where a constant volume is added per origin while the number of origins per cell depends on growth rate Amir (2017).

Therefore, keeping in mind this concept is important when studying cell size, even in metazoan cells. In fact, one of the reasons why it is sometimes argued that cell size control is of limited interest in such cells is that they show flexibility upon environmental changes (see previous chapter 1.2.2.1). One of the lessons from single-cell organisms however is that they show the same flexibility and that this flexibility is indicative of the nature of the mechanism(s) driving size control.

2.7 Conclusion

In this chapter, we defined the key concepts for the study of cell size homeostasis in proliferating cells. At the phenomenological level, adder or sizer classification help defining a spectrum of strength of size control, with increasing efficiency as the behaviour is close to that of a sizer Amir (2014); Jun and Taheri-Araghi (2015); Voorn and Koppes (1998); Fantes (1977); Sveiczer et al. (1996). However the mechanism underlying a given behaviour is complex and possibly combines several processes Osella et al. (2017). The basis of size control is thought to be through an adaptation of cell cycle progression to size Turner et al. (2012); Jorgensen and Tyers (2004) but future work might unravel a contribution of growth regulation in size control Goranov and Amon (2010); Ginzberg et al. (2015). This last idea is to date mostly hypothetical but several observation suggest that it might be crucial to understand size control.

Three main hurdles currently make the study of cell size homeostasis a complex and exciting problem. The first challenge is to accurately and dynamically measure cell size at the single-cell level, since population-level studies can only partially describe the homeostatic process. This was recently addressed through great improvements of microfluidic tools that led to important discoveries in both bacteria Wang et al. (2010); Osella et al. (2014); Campos et al. (2014); Taheri-Araghi et al. (2015); Wallden et al. (2016) and yeast Soifer et al. (2016); Nobs and Maerkl (2014). Such measurement in metazoan cells remains, however, extremely rare and difficult with only two studies reporting direct measurement Son et al. (2012); Mir et al. (2014). An additional important direction of development is that of investigating how distinct size parameters such as volume and mass have different importance in overall size control Si et al. (2016); Zheng et al. (2016) and how they are co-regulated to maintain density Goranov et al. (2009); Bryan et al. (2014); Popescu et al. (2014).

The second challenge is to find ways to experimentally test the actual contribution of cell cycle progression or growth in size control. In yeast, a traditional strategy is the use cell-cycle mutants Fantes (1977) to decouple cell cycle progression from cell growth and artificially disperse cell size to test how size compensation occurs. An alternative approach, long explored in the bacteria field relies on studying the different rate-limiting processes under fast or slow growth conditions Wallden et al. (2016); Kennard et al. (2016). Finally, we propose that artificially modulating the symmetry of division of cell volume or organelles at mitosis could be an attractive tool Cadart et al. (2014), especially in metazoan cells where genetic mutations or study in various growth condition are more difficult to obtain.

The third challenge is to develop theoretical work to (i) unify the experimental data collected and

test whether they are sufficient or not to distinguish between different models Grilli et al. (2016); (ii) formalize the possible molecular mechanism underlying size control and ask whether it explains both size convergence (robustness) and adaptability to growth conditions (flexibility) Delarue et al. (2016); Soifer et al. (2016); Ho and Amir (2015); Si et al. (2016).

In the next chapter, we use the concepts explained above to describe the current understanding of size homeostasis in bacteria, yeast and finally metazoan cells.

Chapter 3

Current understanding of size homeostasis in yeast and bacteria

3.1 Cell size homeostasis in bacteria 37
3.1.1 Brief description of the cell cycle of bacteria 37
3.1.2 Phenomenological description and recent emergence of the adder model . . 37
3.1.3 Beyond the adder observation, current mechanisms debated 41
3.1.4 Trying to unify the different findings in the field of bacteria 42
3.2 Cell size homeostasis in yeast 42
3.2.1 Size control in *S. pombe* 42
3.2.2 Size control in *S. cerevisiae* 46
3.3 Lessons from yeast and bacteria 48

3.1 Cell size homeostasis in bacteria

3.1.1 Brief description of the cell cycle of bacteria

Before detailing the current results in the field of bacteria, it is important to briefly recall specific characteristics of its cell cycle. A typical aspect of *E. coli* and *B. subtilis* growth is that, at fast growth, chromosome replication takes more time than size doubling. To resolve this apparent paradox, Cooper and Helmstetter proposed that DNA replication is initiated during the previous cell cycle Cooper and Helmstetter (1968). This model only works if cells initiate replication on average only once per cell cycle and division only occurs when a round of chromosome replication is completed. To explain how replication initiation is regulated, it was then proposed that replication initiates at a fixed mass per DNA origin Donachie and Blakely (2003); Donachie (1968). A schematic of the bacteria cell cycle and the problem of overlapping rounds of replications is described in 3.1.

3.1.2 Phenomenological description and recent emergence of the adder model

Research in the field of bacteria size homeostasis made important progress in the past years with new microfluidic tools Wang et al. (2010); Long et al. (2013); Moffitt et al. (2012); Ullman et al. (2013)

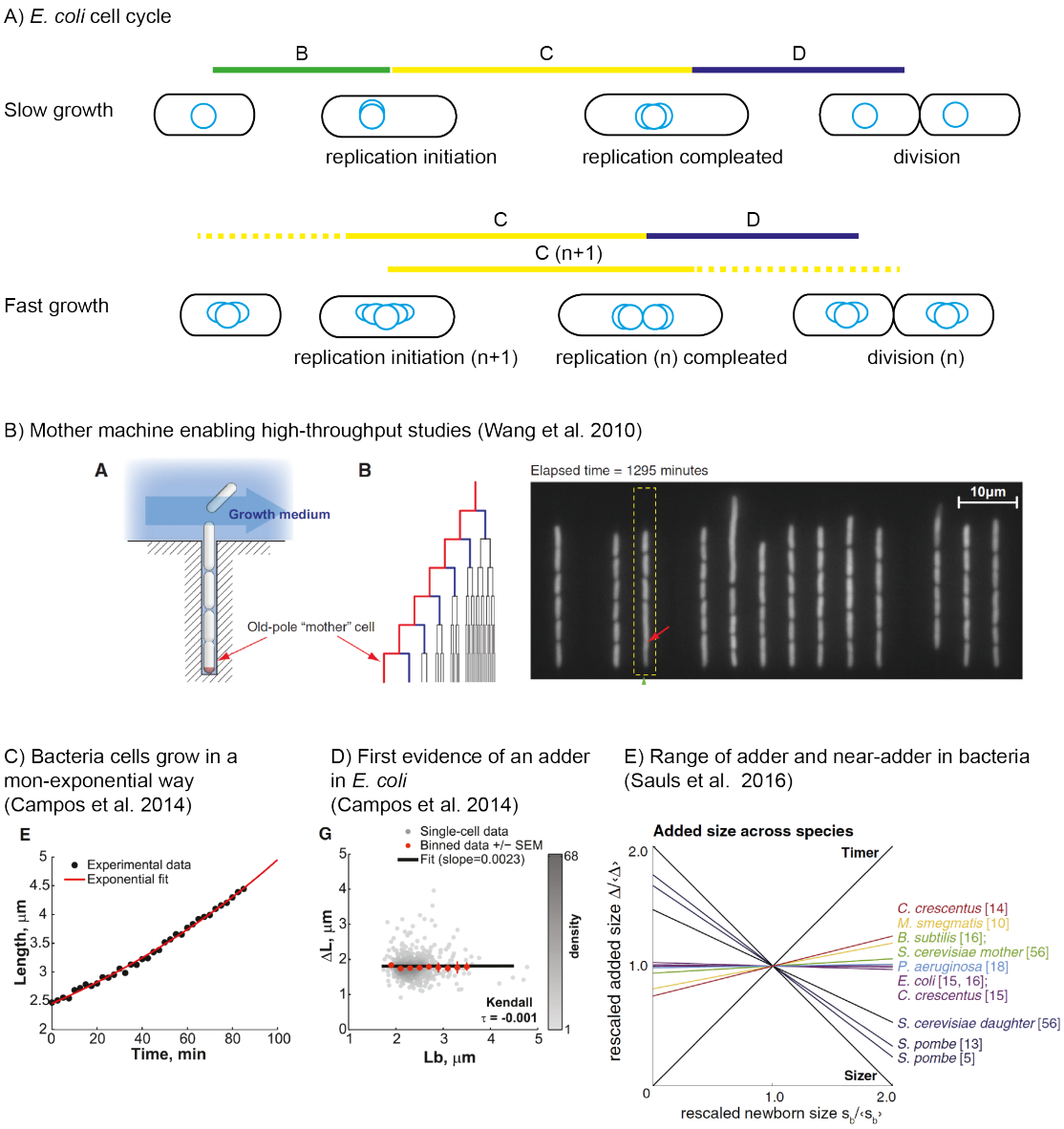

Figure 3.1: *E.coli*: cell cycle and size control. A) Cell cycle. Three distinct phases are identified: B period spans from birth (mother cell division) to chromosome replication initiation; C period is the period required for chromosome replication and D period is the period during which septation is achieved. At fast or intermediate growth, overlapping rounds of replication are observed where replication is initiated during the previous cell cycle. **B) High throughput measurement of cell size.** Here is an example of the mother machine developed in Wang et al. (2010): a 'mother' cell is trapped in a dead-end channel and continuous flow of growth medium enables (i) constant nutrient concentrations in the device and (ii) removal of cells excess cells to maintain a constant cell number. Hence this device enables maintaining steady growth conditions for hours and single-cell growth tracking of hundreds of successive generations. **C) Bacteria growth is well characterized by a mono-exponential curve**. *(Figure adapted from Campos et al. (2014)).* **D and E) The size homeostatic process in several bacteria types is close to an adder. D)** The first evidence was brought by Campos et al. (2014), in *E. coli* where ΔL, the added length was shown to be uncorrelated with length at birth Lb. In bacteria, length is a proxy for volume measurement since these cell only grow length-wise. *(Figure adapted from Campos et al. (2014)).* **E)** Later on, several studies reported the observation of an adder or near-adder in other bacteria cel types such as *C. crescentus* Campos et al. (2014); Iyer-Biswas et al. (2014), *P. aeruginosa* Deforet et al. (2015), *B. subtilis* Taheri-Araghi et al. (2015) and *M. segmatis* Santi et al. (2013). *(Figure gathering these results adapted from Sauls et al. (2016)).*

enabling high throughput single-cell measurement of size through successive cell cycles. These new measurements led to three main observations.

Bacteria cells grow exponentially. First, single-cell growth trajectories showed that cells grow exponentially with a constant growth rate throughout the cell cycle both in volume Osella et al. (2014); Iyer-Biswas et al. (2014); Wang et al. (2010) and mass Godin et al. (2010) (figure 3.1).

Evidence of an adder behaviour at fast growth Second, several works contributed to a phenomenological characterization of the homeostatic process in bacteria. The first studies ruled out the existence of a timer Robert et al. (2014) and showed that cell cycle progression in *E. coli* depends on both size and time Osella et al. (2014). Later, several independent studies reported the observation of an adder behaviour in *B. subtilis, P. aeruginosa, C. crescentus* and *E. coli*, Campos et al. (2014); Deforet et al. (2015); Taheri-Araghi et al. (2015); Soifer et al. (2016),(figure 3.1; for a review, see Sauls et al. (2016); Jun and Taheri-Araghi (2015)). In these studies, the adder is characterized by the absence of correlation between the amount of volume gained ΔV and the initial size Vi. This challenges the model from Donachie and colleagues where replication initiation is gated by a sizer Donachie (1968); Donachie and Blakely (2003) and volume gained is expected to be anti-correlated with initial size. The possibility of an adder-based homeostatic process in bacteria had previously been hypothesized in theory papers long ago Voorn and Koppes (1998) and more recently by Amir (2014).

However, the emphasis made on the generality of the adder behaviour should not lead to an over-simplified description of the size homeostasis process in these cells. Indeed, the initial analysis of the results in *C. crescentus* Iyer-Biswas et al. (2014) yielded evidence of a sloppy size control mechanism very close to that of a timer with a slope coefficient of the plot $V_f = \alpha V_i + \beta$ equal to 1.8 (see 2.1, for description of the plot). It is only when the data were re-analyzed by Jun *et al.* with the same methodology then that used for their own results in *E. coli* that the adder behaviour was found Jun and Taheri-Araghi (2015) with a slope coefficient close to 1.2. This observation is important as it indicates that the behaviour quantified here is noisy, unlikely to be generated by a direct and unique mechanism 'counting' added size since the latter would be expected to provide narrower distribution of ΔV and more homogeneous behaviour in the population. Later, it was also reported that the same strain of *E. coli* could shift from an adder behaviour to a sizer behaviour when grown under very slow growth conditions Wallden et al. (2016).

Therefore, although the observation of the adder behaviour delivers a simple and message and is helpful to characterize the rate of convergence of size for these cells Jun and Taheri-Araghi (2015); Sauls et al. (2016), corrections and refinements to this answer from previous Osella et al. (2014) and current Wallden et al. (2016) work are crucial to move forward in the characterization of the homeostatic process in bacteria.

Universal scaling law. Finally, a third intriguing observation was that the distribution of key variables such as size, cell cycle duration or elongation rate collapse when rescaled to their mean across conditions and species Osella et al. (2014); Taheri-Araghi et al. (2015); Soifer et al. (2016), suggesting the existence of more general and common constraints on growth Giometto et al. (2013) (figure 3.2).

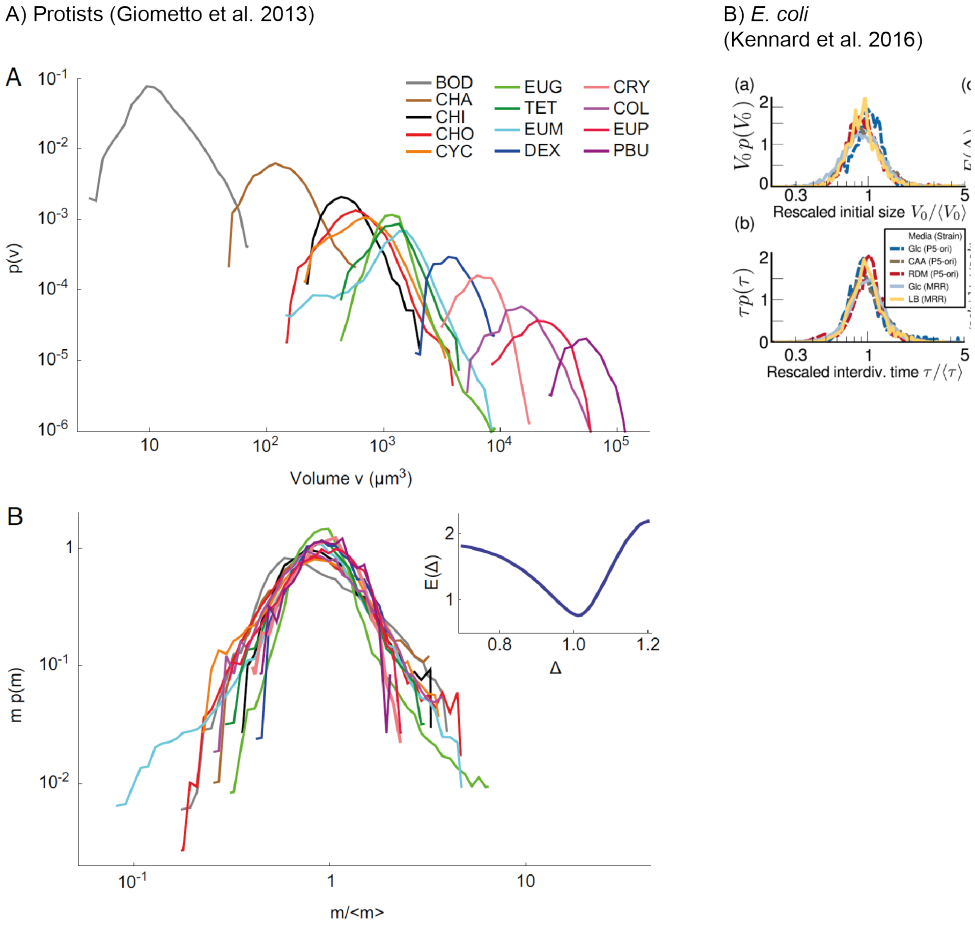

Figure 3.2: Size distributions collapse when rescaled to their mean across species. A) Rescaling in protists. Top: probability distribution of the volume of 13 protist species. Volume ranges from 10 to $10^5 \mu m^3$. Bottom: when rescaled to the mean size $\langle m \rangle$, the probability distribution all collapse. *(figure adapted from Giometto et al. (2013)).* **B) In bacteria,** both probability distribution of volume V_0 (top) and interdivision time τ (bottom) collapse when rescaled to the mean volume $\langle V \rangle$ and $\langle \tau \rangle$ respectively. *(figure adapted from Kennard et al. (2016)).*

3.1.3 Beyond the adder observation, current mechanisms debated

The mechanism underlying the observed adder is currently hotly debated (reviewed in Osella et al. (2017)).

3.1.3.1 Control in each sub-periods

In several works, cell cycle duration was reported to be correlated to initial size Osella et al. (2014); Campos et al. (2014); Robert et al. (2014); Soifer et al. (2016). These first observations were later refined by a systematic analysis of the correlations between size, growth rate and sub-period duration at the single-cell level in *E.coli* Adiciptaningrum et al. (2015); Wallden et al. (2016). The results of these two studies only match partially. Both studies show that B period duration is negatively correlated with initial size, suggesting the existence of size control during this phase. This is reminiscent of the population-level model from Donachie where a sizer gates the transition from B to C phase Donachie (1968). However the two studies did not agree on whether B period was a perfect sizer Wallden et al. (2016) or a more sloppy size control Adiciptaningrum et al. (2015). Indeed, in both cases, a positive correlation between initiation size and birth size was found at slow growth rate, thus contradicting the existence of a sizer. Yet the loss of this correlation at faster growth rate led Wallden *et al.* to hypothesize that the model of initiation at a constant volume was true even at slow growth rate. Moreover, both studies confirmed that C Adiciptaningrum et al. (2015) or C+D Wallden et al. (2016) durations were a timer and did not depend on initial size. However, in one of the two studies, D period was found to be little but significantly negatively correlated with growth rate Adiciptaningrum et al. (2015).

3.1.3.2 Molecular players

With the growing body of evidence that bacteria size homeostatic process is an adder, the initiator protein accumulation model long described by Sompayrac and Maaloe (1973) gained interest (see section 2.3.2). Several successive implementations were proposed to explain how it could be compatible with the observation of an adder Campos et al. (2014); Ho and Amir (2015); Soifer et al. (2016); Amir (2014, 2017); Robert (2015). In Ho and Amir (2015), the authors propose a model where the constant added volume is measured between two sets of replication initiation, thus overlapping two cell cycles rather than from birth to mitosis. The authors show that this model reconciliates a revisited version of Donachie's model Donachie (1968); Donachie and Blakely (2003) and the more recent works showing the adder. In that case, replication initiation occurs at a constant added volume per origin, (whereas Donachie's model stated that it occured at a constant volume per origin) and no correlation is observed between initial size and added volume, consistent with the conclusions from previous works Campos et al. (2014); Taheri-Araghi et al. (2015); Soifer et al. (2016). Importantly, this model also explains the adaptation of average size to growth condition, more specifically the fact that average size in the population scales with growth rate Soifer et al. (2016); Amir (2017); Si et al. (2016); Zheng et al. (2016); Ho and Amir (2015) (the growth law, also discussed in section 2.6). This model was further reinforced by two works showing that the addition of a constant volume per origin is robust to an extensive set of perturbations affecting either various general processes, from DNA replication to translation Si et al. (2016), or more specifically cell wall synthesis Si et al. (2016); Zheng et al. (2016).

In terms of molecular players, the favorite candidate for the initiator protein in *E. coli* is the molecule DnaA Donachie and Blakely (2003). This is because DnaA (i) is known to auto-repress, (ii) has an active ATP-bound form that binds to specific DNA sequences at replication origins OriC and (iii) initiates replication after reaching a threshold number of 20 copies. Upon replication initiation, all the ATP-bound DnaA is transformed into the inactive ADP-bound form (reviewed in Robert (2015)).

However, several other size-sensing mechanisms have been described in bacteria Robert (2015). Since volume appears to be the critical size parameter Zheng et al. (2016); Si et al. (2016), proteins involved in cell wall synthesis, more specifically the tubulin-like protein FtsZ central for septum synthesis and cytokinesis, and the actin homolog MreB (reviewed in Robert (2015)) might turn out to be critical for size control. In fact, an alternative model to the model of constant added volume per origin proposed that septum synthesis and volume-to-membrane growth rate ratio are at the heart of cell size control Harris and Theriot (2016).

3.1.4 Trying to unify the different findings in the field of bacteria

3.1.4.1 How do these controls combine to generate an adder?

How the sub-periods models, and the different rate-limiting processes described above add-up and result in an adder is far from being clear. Three distinct hypotheses are currently envisioned Osella et al. (2017): some works favor the possibility that one over-arching mechanism 'counts' added size Ho and Amir (2015); Harris and Theriot (2016); Amir (2014, 2017); Zheng et al. (2016); Si et al. (2016) while other studies describe the cell cycle as the combination of different controls that are rate-limiting in different conditions Wallden et al. (2016). A third possibility is that several control processes act in parallel on overlapping time scales. These alternatives are described in figure 2.5.

3.1.4.2 Lessons from model-free approaches.

Aspects of size control in bacteria are hotly debated to date. In this context, theoretical work is useful to put the results currently available in perspective. For instance, it can been shown analytically that the detectability threshold for a given size homeostasis mechanism (*i.e.* adder mechanism) depends on both the variability and the size of the sample and that the data currently available in bacteria do not reach this threshold yet Grilli et al. (2016). Therefore, formalisms that describe the cell cycle progression without making any *a priori* hypothesis about the nature of the size control mechanism are an interesting tool. These model-free approaches correspond to a description of cell cycle progression as a hazard division rate function that depends on dynamically measured parameters such as size, growth rate or time elapsed since birth Osella et al. (2014); Grilli et al. (2016); Kennard et al. (2016). The most common formalism on the contrary uses discrete-time equation (the unit is the cell cycle) and describes sizes across generations as an auto-regressive process Amir (2014); Soifer et al. (2016); Jun and Taheri-Araghi (2015); Sauls et al. (2016); Adiciptaningrum et al. (2015). Using such a model-free approach enabled showing that the deviation of individual cell behaviour with respect to the mean population is explained by a more general law than that of the 'adder': the collapse of size and interdivision time when rescaled to their means that is also observed in protists Giometto et al. (2013).

3.2 Cell size homeostasis in yeast

3.2.1 Size control in *S. pombe*

3.2.1.1 *S. pombe*, cell cycle and size-checkpoints.

S. pombe is probably the organism where size-control mechanisms have been best characterized (reviewed in : Turner et al. (2012); Jorgensen and Tyers (2004); Sveiczer and Horváth (2016)). Seminal

work from Fantes and Nurse established more than 40 years ago that fission yeast show evidence of a strong size-checkpoint in mid-G2 Nurse (1975); Fantes (1977); Sveiczer et al. (1996). An additional size-dependent checkpoint at G1/S that is revealed only in nutrient poor conditions also exists Turner et al. (2012). A scheme of *S. pombe* cell cycle and size checkpoints is shown in 3.3.

3.2.1.2 *S. pombe* is the classical example of a sizer in wild-type cells.

The size control exerted in mid-G2 is typical of a sizer that relies on time adaptation and yields almost perfect correction of size fluctuations within one cell cycle Fantes (1977). The use of temperature-sensitive loss-of-function mutants of *cdc* genes is probably one of the most robust experimental tool to characterize size control (see also figure 2.3). These mutants do not divide at the restrictive temperature but behave in a wild-type manner at the permissive temperature. It is therefore possible to generate abnormal large cells by maintaining them at the restrictive temperature and study whether and how cells go back to their normal cell length. This type of experiment showed that *cdc* mutants induced large cells cycled very rapidly in a minimum time until they returned to their normal cell length Fantes (1977); Sveiczer et al. (1996).

3.2.1.3 *S. pombe.* grows in a bilinear fashion.

It is accepted that *S. pombe* growth is on average well-characterized by a bi-linear function with a first slow linear growth separated from a second faster linear growth by a rate changing point (RCP) Sveiczer et al. (1996); Mitchison (2003); Nobs and Maerkl (2014). Fission yeast is cylindrical and extends only from the poles. At the beginning of the cell cycle, growth occurs only from the old pole; the new end take off (NETO) event characterizes the time when growth occurs through both poles. The increase of growth rate after the RCP is thought to correlate either with this NETO event or with S phase and doubling of DNA copy. Deviation from this bi-linear growth mode are discussed in Sveiczer and Horváth (2016); Cooper (2013). Importantly, the timing of RCP is negatively correlated with size at birth Mitchison and Nurse (1985), suggesting a size-dependent modulation of growth rate.

3.2.1.4 In search for the mechanism generating geometric sensing of size.

The evidence that a perfect sizer occurs in G2 in wild-type cells motivated studies looking for a geometric sensing enabling absolute size measurement in fission yeast. It was first proposed that a diffusion gradient of Pom1 along the long axis of the cell enabled cell length-sensing Martin (2009); Moseley et al. (2009): Pom1 is produced at the cell poles and diffuses to the center of the cell where it inhibits the mitotic promoting factor through inhibition of cdr2 in a concentration-dependent manner. When the cell reaches a critical length ($\approx 14\mu m$), the concentration of Pom1 is too weak to inhibit cdr2. Active cdr2 then inhibits Wee1 which releases the inhibition of Cdk1 and triggers mitotic entry (see also models of molecular mechanisms described in figure 2.4 and section 2.3). However, the diffusion-based effect of Pom1 was later contradicted Bhatia et al. (2014) and work even claimed that Pom1 was not the actual size-sensor in the cell Wood and Nurse (2013). More intriguingly, it was shown that cells engineered to cycle with a minimalistic monomolecular Cdk module lacking the regulatory proteins required in the Pom1 model still divided at a length close to that of the wild-type, although with an increased cell-to-cell variation of size Coudreuse and Nurse (2010). An alternative model currently proposes that surface area, not length, is measured. This model states that the mitosis activating kinase cdr2 increases at the cortical nodes in a manner that reflects absolute surface area Pan et al. (2014) (figure 2.4). Overall, although there is a consensus about the existence of a sizer in fission yeast its molecular basis is still debated.

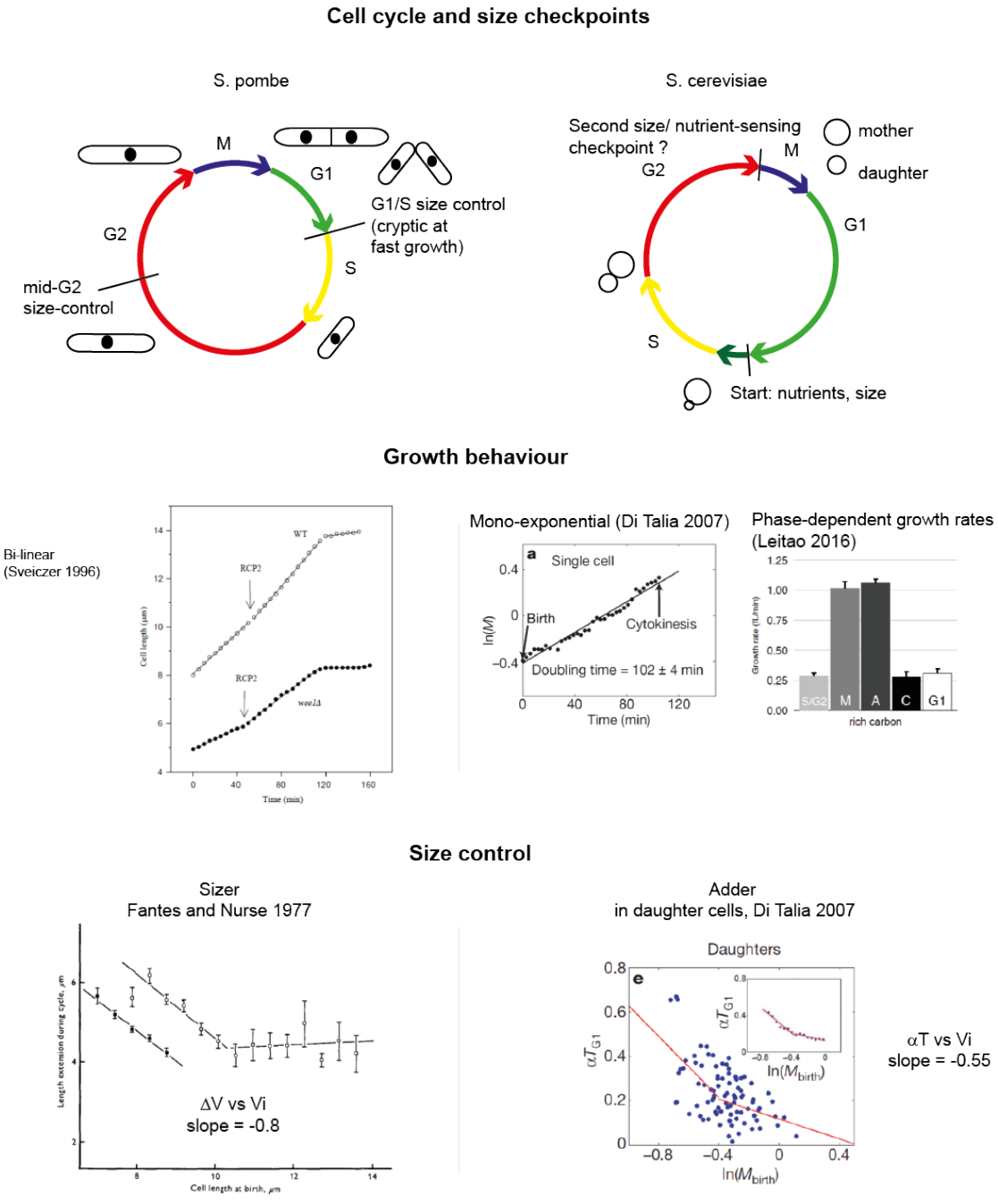

Figure 3.3: Cell cycle and size control in *S. cerevisiae* and *S. pombe* (continued next page)

Figure 3.3: Cell cycle and size control in *S. cerevisiae* and *S. pombe*. In the fission yeast *S. pombe*, nuclear (mitosis) and cytoplasm divisions (cytokinesis) are uncoupled: during mitosis, the two nuclei are separated and cytokinesis occurs in the following G1 phase after the septum formation. The main size control occurs in mid-G2 and was first discovered by Fantes (1977). A cryptic size checkpoint in G1 is observed in *wee1* mutants. Growth is most often described as a bilinear curve with a rate changing point (RCP) after which growth rate increases. The first evidence of a sizer was provided by Fantes (1977): the plot ΔV *vs.* Vi shows a strong negative correlation of slope close to 1 typical of a sizer mechanism. **In the budding yeast *S. cerevisiae*,** the most known checkpoint is at Start, an event in late G1. In S phase, budding occurs, in G2, most of the grotwth occurs in the budded cell, at cytokinesis, separation of the bud from the cell gives rise to a small daughter cell and a large mother cell. A second size-checkpoint in late G2 is currently debated. Whether growth of *S. cerevisaie* is a mono-exponential (left, Di Talia et al. (2007) or a phase-dependent linear growth (right, Leitao et al. (2016) is debated. Size control in budding yeast is a noisy size control, often characterized as an adder as shown by Di Talia et al. (2007): the slope coefficient of the elongation αT *vs.* $log(Vi)$ gives a slope coefficient close to 0.5, typical of an adder mechanism.

3.2.2 Size control in *S. cerevisiae*

3.2.2.1 *S. cerevisiae*, cell cycle and checkpoints

Budding yeast divide very asymmetrically into one large mother cell and one small daughter cell. Passage through Start, a short interval in late G1 phase is thought to be the period during which size control is achieved in order to correct this asymmetry of size Turner et al. (2012); Jorgensen and Tyers (2004). Indeed, small daughter cells spend more time growing during G1 Johnston (1977); Hartwell and Unger (1977) while duration of S/G2/M was observed to depend weakly on size in most studies. In addition to controlling size, passage through start is also nutrient-sensitive Turner et al. (2012); Jorgensen and Tyers (2004). Although the classical view of budding yeast cell cycle is that it is a combination of size control in G1 and a timer afterward, several studies currently challenge this view. The role of another size control mechanism that integrates nutrient cues and takes place during G2/M was brought up to discussion by two studies Leitao et al. (2016); Mayhew et al. (2016).

3.2.2.2 Lack of consensus about the growth behaviour of *S. cerevisiae*.

Important work from Di Talia et al. (2007) stated that the budding yeast *S. cerevisiae* grew exponentially at the single-cell level. This was confirmed later by Soifer et al. (2016); Godin et al. (2010). However, others claimed that growth in G1 is closer to linear Ferrezuelo et al. (2012). Two studies also reported phase-dependent growth rates. It was first shown that arrested cells grow faster in anaphase and G1 than in S and early mitosis Goranov et al. (2009). The second study matched the result that growth rate was higher during anaphase but contradicted the rest of the results by observing higher growth rate in metaphase and lower growth rate during other periods including G1 Leitao et al. (2016). The variability of these results is probably explained by the variability of the approaches to measure size: some performed measurement at the single-cell level using bulk mRNA amount reporter Di Talia et al. (2007), suspended micro-channel resonator for mass Godin et al. (2010) and density Bryan et al. (2010) or phase contrast imaging Leitao et al. (2016); Ferrezuelo et al. (2012); Soifer et al. (2016), while others favoured cell-population approaches and Coulter counter based measurement Goranov et al. (2009).

3.2.2.3 Daughter cell of *S. cerevisiae* behave in an adder-like manner.

It is clear from several studies that the size-sensing mechanism of *S. cerevisiae* does not impose a perfect size-threshold since variability of size between mother and daughter cells is not fully resolved at entry into S phase Di Talia et al. (2007, 2009). In Di Talia et al. (2007), the famous size-growth plot: αT *vs.* $ln(V_{birth})$ Sveiczer et al. (1996) was used for the first time as a systematic way to decipher between adder, sizer or timer (see figure 2.1). The slope of this plot is 0, 0.5 or 1 in case of a timer, adder and sizer respectively. In this work, it was reported that the size-growth plot yielded a slope coefficient of 0.06 for the mother cells and 0.43 for the daughter cells over the total cell cycle, indicating that mother cells did not show any size control whereas daughter cells clearly did. Interestingly, extremely small daughter cells showed an even stronger size control with a slope coefficient of 0.66. Later on, this result was reproduced Ferrezuelo et al. (2012) and defined as an adder-behaviour Soifer et al. (2016).

It is worth noting that before the size homeostatic process of *S. cerevisiae* was characterized as an adder Soifer et al. (2016), following the results in bacteria Campos et al. (2014); Taheri-Araghi et al. (2015), other approaches had been proposed to explain why size control was 'weak' (compared to the famous sizer of *S. pombe* for example). In a first study where growth was defined as exponential with a growth rate α, it was hypothesized that volume gained during G1 is the result of a size-dependent

growth process ($f(V_i)$) and gene expression noise-related fluctuations of timing (η) : $\alpha T = f(V_i) + \eta$ Di Talia et al. (2007). Alternatively, others suggested that added volume depended on cell-to-cell variability in growth rate Ferrezuelo et al. (2012). The model from this last study is perhaps less convincing as it is based on the description of G1 as the sum of a timer (k) and a size-dependent time ($T - k$) whose relevance from the data is unclear.

3.2.2.4 Whi5 and the inhibitor-dilution size sensor model for G1/S transition

It is commonly thought that the size sensing mechanism for *S. cerevisiae* is based on protein synthesis rate measurement (reviewed in Turner et al. (2012); Jorgensen and Tyers (2004)). In a synthesis-rate based model, the initiator protein that reflects total protein biosynthesis is titrated against a fixed compartment (*i.e.* DNA) or protein and ultimately triggers cell cycle transition in a dose-dependent manner (see also figure 2.4 and section 2.3). The G1 cyclin Cln3, has long been identified as the initiator protein of Start transition in budding yeast (reviewed in Turner et al. (2012)). The titration mechanism however is still debated.

It was first hypothesized that Cln3 localized in the nucleus where its concentration increased as the nucleus volume grew slower than that of the cytoplasm Futcher (1996) but this hypothesis was rejected by measurement showing that nucleus size scaled with cell size Jorgensen et al. (2007). Later, the idea that Cln3 was titrated against specific DNA binding sites was raised Wang et al. (2009), but the fact that increasing DNA copy of these binding site led to an increase of cell size indicated a lack of understanding in the chore mechanism. A third hypothesis suggested that Cln3 was actually sequestrated in the ER and released in a growth rate-dependent manner Vergés et al. (2007). More recently, work showing that Whi5, the inhibitor of Cln3, was present in constant amount throughout G1 led the authors to propose that Cln3 was in fact titrated against Whi5 Schmoller et al. (2015) (see figure 2.4, also reviewed in Schmoller and Skotheim (2015); Amodeo and Skotheim (2016)).

Although appealing, this last mechanism still needs clarification. Indeed, in its initial description, precise characterization of the rates of synthesis and degradation of both the inhibitor and the initiator were missing. Several refinements to the model are in fact currently debated. In a first study, authors emphasized the need of segregating the inhibitor protein proportionately to cell size at cytokinesis Soifer et al. (2016) and noted that the asymmetric segregation described in the initial model Schmoller et al. (2015) would otherwise lead to a weaker size control than observed experimentally. A second implementation to the model was proposed by Delarue et al. (2016). In this case, instead of accumulating proportionately to cell volume and thus being of constant concentration, ($dN_I/dV = C$), the initiator Cln3 is produced at a rate proportional to cell volume (κ_p, rate per unit volume) and degraded at a constant rate (k_d). The authors show that assuming exponential growth at a rate γ, the number of Cln3 molecules increases as:

$$\frac{dN_I}{dV} = \frac{\kappa_p - k_d N_I/V}{\gamma} \tag{3.1}$$

In this case, the authors show that two regimes are observed. For very small cells, the accumulation of Cln3 is very slow at the beginning of G1 and occurs mostly at the end of the phase, which enforces a minimum final volume that is independent of volume at birth (sizer regime). On the contrary, for very large cells, the rate of a of Cln3 varies little throughout G1, therefore resembling the initial model described in Schmoller et al. (2015); Soifer et al. (2016) that leads to an adder-like behaviour.

3.3 Lessons from yeast and bacteria

For the question of size control in proliferating cells, studies in yeast and bacteria bring a wealth of findings and concepts that pave the way for research in metazoan cells. A first lesson from these studies is the importance of dynamic measurement performed at the single-cell level. In both yeast and bacteria, these measurement almost systematically focused on cell volume. The relevance of this size parameter in the molecular mechanisms explaining size control has been demonstrated in both *E. coli* and *S. cerevisiae*. Second, in both organisms, size control is most often thought to be the result of one or several processes that adapt cell-cycle progression to cell growth through size checkpoints. These checkpoints are highly debated in both communities but they emphasize the need of accurate characterization of growth during each sub-period.

In the next section, we discuss the current knowledge about size control in metazoan cells. We show that due to technical difficulties, no measurement of single-cell volume over complete cell cycle trajectories was ever reported. Dynamic characterization of metazoan cells growth and progression through cell cycle progression are in fact very rare Son et al. (2012); Mir et al. (2014) and models for size control are mostly at the state of hypotheses Kafri et al. (2013). In fact the very idea of the existence of size control is debated in metazoan cells Lloyd (2013); Conlon and Raff (2003); Sveiczer et al. (2004); Ginzberg et al. (2015).

Chapter 4

Cell size homeostasis in metazoan cells

4.1 Growth and cell cycle pathways in mammalian cells 49
4.1.1 Pathways regulating the growth rate 49
4.1.2 Cell cycle regulation 53
4.2 Population-level studies and evidence of size control in early work . . 54
4.2.1 Evidence of size-sensing in G1 54
4.2.2 Results challenging the idea of size control in metazoan cells. 56
4.3 The challenging problem of characterizing cell growth in metazoan cells 56
4.4 Current views on the homeostatic process in metazoan cells 57
4.4.1 Cells grow exponentially or super-linearly 57
4.4.2 No clear role for time modulation, possible existence of a growth-rate modulation 58
4.5 Conclusion 58

4.1 Growth and cell cycle pathways in mammalian cells

In this section, we do not intend to present an exhaustive description of the growth and cell cycle pathways in mammalian cells. These networks have been widely studied and their details are beyond the scope of this study. However, the understanding of the cross-talks between cell cycle progression and cell growth pathways seems to be one of the missing element of the picture Mchedlishvili et al. (2015), although its existence is argued Lloyd (2013). Studying how size control is exerted and characterizing the relationship between growth and cell cycle progression might be key towards a unified vision of these two aspects of cell physiology. Here we describe the main characteristics of growth and cell cycle progression pathways and choose a few examples that illustrate their importance in size control.

4.1.1 Pathways regulating the growth rate

In metazoan cells, growth pathways typically translate extra-cellular (amino acids, growth factors) and intra-cellular (energy status, oxygen, amnio acids) cues into regulatory signals for growth processes. To increase cell growth, these pathways can either activate protein and lipid synthesis or reduce protein

degradation and cell autophagy. These pathways are also important for the regulation of energy level and metabolism (reviewed in Locasale and Cantley (2011)).

In metazoan cells where growth regulation is also set at the tissue level, growth factors are central: their presence is required to stimulate cell growth Conlon et al. (2001); Rathmell et al. (2000) and their absence, even when nutrients are in sufficient amounts, leads to cell skrinking Lum et al. (2005); Saucedo and Edgar (2002); Rathmell et al. (2000). Nevertheless, growth factors are not sufficient to induce cell growth, as amino-acids are also required Rathmell et al. (2000); Saucedo and Edgar (2002); Sonenberg and Hinnebusch (2009). This co-regulation of growth by nutrients and growth factors is thought to ensure that growth occurs only when enough amount of nutrients is available Edgar (2006).

Most of the growth factors act through the activation of transmembrane receptor tyrosine kinase (RTK) whose intracellular portion auto-phosphorylates upon binding of an extracellular ligand. This leads to the recruitment of an intracellular adapter protein that will trigger a downstream signaling cascade regulating growth processes Lemmon and Schlessinger (2010).

4.1.1.1 The mTOR pathway

The mechanistic target of rapamycine (mTOR) is central in the regulation of biogenesis and broadly conserved across eukaryotes Roustan et al. (2016), from yeast to mamals. This complex is formed by TOR atypical serine/threonine kinases that associate in complexes containing 6 (mTORC1) or 7 (mTORC2) proteins. These complexes integrate a plethora of environmental and intracellular cues and are involved in the regulation of all the important processes for cell growth (reviewed in Laplante and Sabatini (2012); Caron et al. (2015); Eltschinger and Loewith (2016).

Upstream of mTORC1: growth factor dependent pathways. One of the most famous signaling cascade upstream of mTOR is the IGF/PI3K/AKT/mTORC1 which transfers extra-cellular signaling through growth factors to the mTORC1 complex. In this cascade, the insulin growth factor (IGF) binds to its receptor (IGFR), a member of the RTK family. The auto-phosphorylation of IGFR induces the recruitment of the phosphoinositide 3-kinase (PI3K) via the adapter insuline receptor substrate adapter proteins (IRS 1-4). Once PI3K is recruited to the plasma membrane, it phosphorylates phosphatidylinositol (4,5)-biphosphate (PIP2) to generate PI(3,4,5)P3 (PIP3) which results in the activation of AKT. Active AKT then phosphorylates and inhibits the negative regulators of mTORC1, TSC2 and TSC2. Active TSC inhibits mTORC1 by converting the Ras-homolog enriched in brain (Rheb)GTPase protein into its inactive GDP form. The active form of Rheb, Rheb-GTP is the key activator of mTORC1 (reviewed in Laplante and Sabatini (2012); Caron et al. (2015)). Alternatively, IGF can also lead to the inhibition of the TSC1/TSC2 complex via the IGF/IGFR/Ras/Raf/MEK/ERK cascade (Laplante and Sabatini (2012); Caron et al. (2015)).

Upstream of mTORC1: amino acids. Amino acids, especially leucine, are crucial for the activity of mTORC1, since their withdrawal completely abolishes mTORC1 activity. This is due to a signaling cascade that ultimately leads to the localization of mTORC1 at the lysosomal surface where it is activated by Rheb Caron et al. (2015). Amino acids present in the inner compartment of the lysosome activate Ragulator, a protein complex at the lysosome membrane through a mechanism that involves the lysosomal H^+-adenosine triphosphate ATPase Zoncu (2011). This enables the anchoring of the heterodimer RagA/B-GTP which recruits mTORC1 at the lysosome via the tuberus sclerosis complex (TSC1/2). Therefore, amino-acids mediated recruitment of mTORC1 at its site of activation is a pre-requisite for all its other functions Nobukuni et al. (2005). The biological meaning of this is that biogenesis activation via mTORC1 is only possible when sufficient nutrients are available.

Finally in addition to amino acids and growth factors, hypoxia and energy levels, via the activation of the adenosine monophosphate-activated protein kinase (AMPK) phosphorylate and inhibit TSC2 to activate mTORC1 Laplante and Sabatini (2012).

Downstream of mTORC1: increased biogenesis, decreased autophagy. Activation of mTORC1 leads to the downstream up-regulation of protein synthesis (reviewed in Ma and Blenis (2004)), mainly through the phosphorylation of the eukaryotic translation initiation factor 4E (eIF4E)-binding proteins 1 and 2 (E4-BP1/2) and the ribosomal protein S6 kinase 1 (S6K1). Moreover, mTORC1 also promotes lipogenesis which is crucial for membrane addition (thus volume growth) and metabolism (reviewed in Caron et al. (2015); Teixeira and Costa (2016)). This is mainly achieved through the up-regulation of a family of transcription factors of genes involved in lipid synthesis, the sterol regulatory element-binding proteins (SREBPs) Horton et al. (2002). Finally, mTORC1 also regulates mitochondria synthesis and ATP production Zhang and Xu (2016); Dennis et al. (2001); Laplante and Sabatini (2012). In addition to these positive effects, activation of mTORC1 also down-regulates autophagy Russell et al. (2014); Feng et al. (2015); Eltschinger and Loewith (2016).

Feedback loops in the mTORC1 network. Importantly, the mTORC1 pathway comprises several feedback loops where downstream effectors regulate upstream effectors . For example, both mTORC1 and S6K1 phosphorylate the RTK IRS-1 which induces its degradation and therefore reduces the cell's sensitivity to extra-cellular growth factors Harrington et al. (2004); Um et al. (2004); Tzatsos and Kandror (2006). The recent progress in the characterization of such feedback loops suggests a new view on the mTOR pathway where it is not only a simple transducer of environmental cues but plays an active role in cellular homeostasis Eltschinger and Loewith (2016). This characteristic might be important in the light of recent works suggesting that active growth regulation is key in cell size control in mamalian cells Kafri et al. (2013); Ginzberg (2015).

Regulation via mTORC2. The signaling through mTORC2 is less characterized but it is known to be activated by growth factors and to be involved in cell survival, lipid synthesis as well as cytokseletal organization Teixeira and Costa (2016); Caron et al. (2015); Eltschinger and Loewith (2016). In *S. cerevisiae*, mTORC2 has been shown to be involved in plasma membrane tension regulation. Although some aspects of the underlying mechanism are still unclear, the current view is that membrane tension increase causes the proteins Slm1 and Slm2 to translocate from invaginated plasma membrane nanodomains (eisosomes) to membrane domains containing mTORC2 (MCTs) where they activate mTORC2 Niles and Powers (2012); Berchtold et al. (2012). Activation of mTORC2 ultimately leads to the up-regulation of lipidogenesis, specifically limiting lipids for membrane synthesis such as sphingolipids Berchtold et al. (2012); Eltschinger and Loewith (2016). How these findings in yeast translate to mammalian cells is an interesting future line of research that might help understanding how two key growth processes, namely mass acumulation (via mTORC1) and volume growth (via mTORC2) are co-regulated.

4.1.1.2 Other pathways

Myc is another central regulator of cell growth. This family of highly conserved transcription factors forms a heterodimer with the protein Max to regulate the transcription of thousands of genes (up to 15% of the genome) involved in several key functions such as cell proliferation, cell growth, or development (reviewed in Adhikary and Eilers (2005); Dang (2012)). Additionally, Myc expression increases ribosome biogenesis through enhancing transcription of ribosomal RNA, proteins and cofactors and translation of mRNA van Riggelen et al. (2010); Grewal et al. (2005). Finally, the

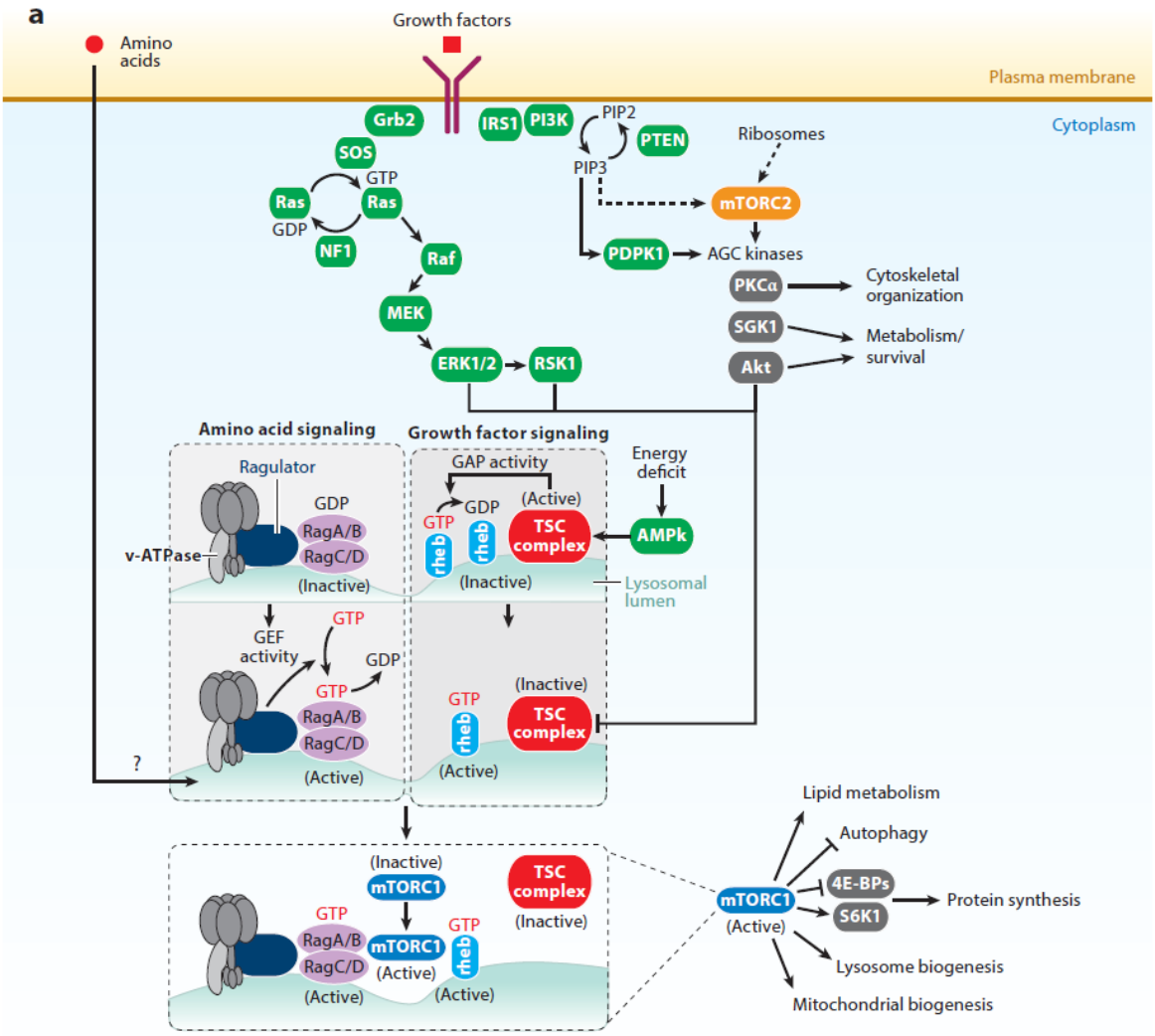

Figure 4.1: The mTOR pathway in mammalian cells. Extra-cellular amino acid and growth factors activate the mTOR pathway. Amino acid are imported to the lysosomal compartment through an unknown mechanism where they ultimately lead to the activation of Rheb which in turn recuits to the lysosome and activate mTORC1. Growth factors pathways, the IGF/IGFR/Ras/Raf/MEK/ERK and IGF/PI3K/AKT further activate mTORC1 via the inhibition of the TSC complex. Activated mTORC1 then enhances protein synthesis via inhibition of 4E-BPs and activation of S6K1. It also enhances lysosome, lipid and mitochondria biogenesis and decreases autophagy. mTORC2 is less well understood, it is activated by growth factors and regulates cytoskeletal organization, metabolism and survival. Its role in membrane tension is not shown here since this is best understood in *S. cerevisiae* for the moment. *(See main text for more details, figure from Caron et al. (2015)).*

Hippo pathway is a key transducer of mechanical cues at the tissue level into regulatory signals for cell proliferation and apoptosis (reviewed in Piccolo et al. (2014); Yu et al. (2015)). A more complete overview of the different pathways regulating cell growth in mammalian cells can be found in Lloyd (2013); Roberts (2013).

4.1.1.3 Conclusion.

In metazaon cells, growth factors are central for cell growth, and nutrient only are not sufficient to trigger growth Rathmell et al. (2000). We described here the main pathways involved in growth regulation. Importantly, these pathways do not have the same impact on cell growth. In *Drosophila* for example, both Myc and PI3K over-expression induce cell hypertrophy but this seems to be mostly due to an accumulation of protein and ribosomes for the cells over-expressing Myc or lipids and sugars for the cells over-expressing PI3K Saucedo and Edgar (2002). The Hippo pathway instead regulates cell number rather than cell growth. As our understanding of these pathways improves, cross-talks between these pathways are unraveled, suggesting a complex coordinated regulation of cell growth and cell proliferation from the organ level to each individual cell Lloyd (2013).

The important question for the purpose of our work is to understand how such growth regulatory pathways are linked with the cell cycle network in order to maintain size control. We will briefly describe the principles of mammalian cell cycle regulation before discussing the experimental evidence of such links.

4.1.2 Cell cycle regulation

4.1.2.1 Brief overview of the mammalian cell cycle

The regulatory network driving cell cycle progression in mammalian cells relies on the same principles than in yeasts although the expansion of the family of cyclins and cyclin-dependent kinases (Cdk) through genetic evolution adds another layer of complexity Malumbres (2014). The precise description of the regulatory mechanisms that set the cell cycle clock in mammalian cells is beyond the scope of this work. Here we only briefly mention the main characteristics of this regulation with an emphasis on the checkpoints that potentially play a role in cell size control.

Briefly, the classical view of cell cycle progression involves four different couples of cyclin-Cdk that regulate the progression through the cell cycle (figure 4.2). Upon mitogen stimulation (*i.e.* EGF), cyclin expression starts and marks the beginning of G1. Cyclin D-Cdk4/6 complex induces the expression of cyclin E in mid-G1. cyclin E-cdk2 drives the G1/S transition after which cyclin E is rapidly degraded. Finally, cyclin A-cdk1 and cyclin B-cdk1 complexes drive the transition from G2 to M when they are degraded (reviewed in Malumbres and Barbacid (2009)). However, all these Cdk except Cdk1 are dispensable for cell cycle progression Santamaría et al. (2007), thus suggesting that the core mechanism driving cell cycle progression is driven by a unique cyclin-Cdk complex, similarly to yeast.

The cyclic and timely regulated activity of these cyclin-Cdk complexes is at the heart of the successive cell cycle checkpoints that drive cell cycle progression Kastan and Bartek (2004). Although much is known about the molecular networks underlying each of these cell cycle transitions, often, the initial trigger is unknown. Mitotic entry for instance is well known to depend on a bistable switch in Cdk1 activity regulated by Cdc25/Wee1 but the initial trigger to this switch is still mysterious Mchedlishvili et al. (2015). Similarly, G1/S transition occurs in a switch-like manner via a network that involves cyclin E-Cdk2 Barr et al. (2016); Bertoli et al. (2013); Cappell et al. (2016) and several experimental

results suggest that this transition depends on cell growth or cell size (discussed in the next section 4.2.1). Yet, the molecular links between these two observations are still mostly unknown. We will first describe the known links between growth regulatory pathways such as mTOR and cell cycle checkpoints during G0 and G1. In the next section, we will then discuss the results suggesting that progression through G1 is also size-dependent.

4.1.2.2 Commitment to a new the cell cycle: checkpoint(s) for growth during G0 and G1

After division, cells can either enter a quiescent state (G0) or commit to a new round of division and progress through G1 phase (figure 4.2). A restriction point (R) occuring in G1 and checking nutrient availability, similarly to Start checkpoint in *S. cerevisiae* (section 3.2) was first proposed in Pardee (1974). The existence of such commitment point was further supported by the description of a point in early G1 after which cells complete their cell cycle independently of serum removal Zetterberg and Larsson (1985). The molecular basis of the restriction point is thought to be the hyperphosphorylation of Rb that leads to the activation of E2F, a major transcription factor for cell cycle Bertoli et al. (2013)

Since these first influential studies, much work to identify the mechanism(s) underlying this restriction point has been done. A unified vision of how these mechanisms define the restriction point is however still missing (reviewed in Fisher (2016)). A first interesting idea emerging from these works is that signaling during the previous cell cycle plays a role in the decision to commit into a new round of division. Newborn MCF10A cells were shown to be separated into two sub-populations displaying either low or intermediate Cdk2 activity Spencer et al. (2013). The low levels of Cdk2 caused the cells to enter a transient G0-like quiescent state in contrast with the high level Cdk2 cells that immediately entered G1. The proportion of low Cdk2 cells increased as serum was removed during a period of time lasting 8 hours prior to division. Therefore, in addition to the classical view of cyclin D-Cdk4/6 dependent R passage, Cdk2 activity inherited at birth also plays a role in cell-cycle commitment.

A second interesting emergent concept is that decision to commit to the next cell cycle depends on several signaling processes. It has been proposed that two independent checkpoints exist during G1. The first depends on growth factors via the Ras/Raf/MAPK/Cyclin D pathway and the second one occurs later, checks nutrient availability via the mTORC1 pathway which ultimately enhances cyclin E-Cdk2 activity Foster et al. (2010). Even more recently, another checkpoint for extracellular lipids was also proposed Patel et al. (2016).

Overall, it seems that several processes occurring in G0 and G1 and that both depends on signaling during the previous cell cycle and cues from the external environment have a role in the cell committing to a new round of division and growth. Better understanding of the links between the growth regulatory pathways such as mTORC1 and the cell cycle network will help refining our understanding of the potentially several restriction points occurring during G1. Furthermore, similarly to *S. cerevisiae*, G1/S transition is thought to be size-dependent.

4.2 Population-level studies and evidence of size control in early work

4.2.1 Evidence of size-sensing in G1

Famous work by Zetterberg and Killander using interferometric microscopy on fibroblasts in the 1960s produced the first result suggestive of a size-dependent G1 phase. They showed that variability in

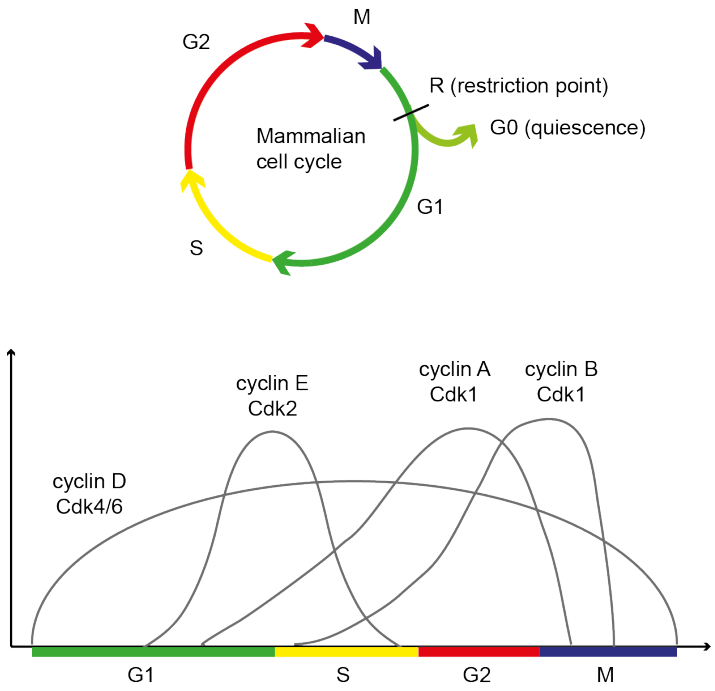

Figure 4.2: Cell cycle progression in mammalian cells. Top: Early in the cell cycle, the cell can either enter a quiescent state (G0) or commit to a new round of division and enter G1. This commitment point is thought to be gated by a restriction point (R) that checks that sufficient nutrients and growth factors are available. There are however possibly multiple restriction points occuring during G1 (see main text) and G1/S transition is possibly at least partly dependent on cell size. S phase is the phase when replication occurs while G2 is a less well-defined additional growth phase before mitosis. **Bottom: Cyclin-Cdk regulate progression through cell cycle phases.** CyclinD expression starts at the begining of G1 and assocites with cdk4/6 to induce the expression od cyclin E in mid G1. CyclinE-Cdk2 levels and activity reach a peak at G1/S transition after which cyclin E is rapidly degraded, cyclin A-Cdk1 and cyclin B-Cdk1 drive the transition from G2 to M.

size when entering S phase was less important than after birth and that entry into S phase depended more on cell size than on cell age (time spent from birth to S phase) Killander and Zetterberg (1965). Since then, other works have concluded a same size-dependence progression in G1 phase in different cell types (Shields et al. (1978); Gao and Raff (1997), reviewed in Jorgensen and Tyers (2004)). An elegant work from Dolznig et al. (2004) brought strong arguments in favor of a size-sensing mechanism in G1. By inducing avian erythroblasts to proliferate under the control of either normal c-Kit/EpoR physiological cytokines or constitutively active oncogene v-ErB, the authors could tune the rate of proliferation and the final size of cells. v-ERB cells cycled faster and were larger: they had a faster growth rate and division rate and entered the cell cycle with a volume that was 1.3 fold higher than the control cells. When switched back c-Kit/EpoR, v-ERB cells growth rate was immediately reduced but G1 phase was shorter than control cells so that v-ErB cells would grow less and correct for their larger size. The second cell cycle showed similar G1 phase length in both conditions. This result led the authors Dolznig et al. (2004) and others Ginzberg et al. (2015) to the conclusion that a critical size threshold exists in G1 phase. However, it should be noted from their results that v-ErB cells size takes more than one cell cycle to regress towards the mean size in the c-Kit/EpoR condition, therefore suggesting a mechanism more complex than a simple critical sizer in G1: an adder or a mechanism where a timer limits the reduction of cell cycle length and thus leads to an uncomplete correction could for example be considered.

4.2.2 Results challenging the idea of size control in metazoan cells.

It is important to recall that not all studies agree on the existence of a size-sensing mechanism in metazoan cells, as exposed in the first part of this introduction. In a study based on Coulter counter volume measurement performed at the population level, it was proposed that primary Schwann cells grow linearly and therefore do not need to regulate their size Conlon and Raff (2003). In this study, cells were blocked in S phase by aphidicolin and increased linearly their volume over a five-fold increase during 5 days. Theses conclusion were however challenged by theoretical considerations emphasizing the need of direct and dynamic measurement on single-cells Sveiczer et al. (2004). Moreover, since recent result suggested that a coupling between growth rate and size occurs in G1 Son et al. (2012), it will be interesting to see whether this result came from the fact that cells were blocked later in the cell cycle, in S phase. Later in the same lab, it was shown that growth factors and mitogens independently regulate growth and proliferation and that their amount in the culture media sets cell size, therefore suggesting the absence of size checkpoint in Schwann cells Echave et al. (2007).

As the recent progress in the characterization of size control in yeast and bacteria (chapter 3) illustrate, direct measurement of cell growth at the single-cell level is key to make the next steps in the understanding of size control in metazoan cells.

4.3 The challenging problem of characterizing cell growth in metazoan cells

Aiming at characterizing mammalian cells growth is challenging for at least two reasons. First, these cells are irregularly shaped objects whose volume is constantly evolving. Unlike with yeast or bacteria, the precise measurement of a geometric-size parameter such as volume is therefore difficult to obtain. For this reason, all the recent work but one Tzur et al. (2009) chose to measure other parameters than volume such as mass Park et al. (2010); Sung et al. (2013); Mir et al. (2011), buoyant mass Son et al. (2012); Godin et al. (2010), or density Grover et al. (2011). Findings in *S. cerevisiae* and *E. coli* however strongly support the idea that volume is an important size parameter and molecular

mechanisms for size sensing currently debated in both these organisms most often rely on cell volume measurement Zheng et al. (2016); Si et al. (2016); Ho and Amir (2015); Soifer et al. (2016); Schmoller et al. (2015).

Second, cell cycle duration in these cell types is usually around 20 to 25 hours. Obtaining single-cell growth trajectories over full cell cycles thus requires very stable and non-invasive techniques. Among the recent methods developed for single-cell measurement, three only enable tracking over complete cell cycle trajectories Park et al. (2010); Mir et al. (2011); Son et al. (2012) with a throughput of maximum ≈ 100 cells Son et al. (2012). In the other methods which do not allow repetitive measurements of cell size, indirect approaches to mathematically infer growth curves from measurement on asynchronous populations at steady state were reported using either the Collins-Richmond method Tzur et al. (2009); Sung et al. (2013) or the ergodic rate analysis Kafri et al. (2013). However, as illustrated by the recent findings in yeast and bacteria, population-level studies have some flaws and dynamic measurement of cell growth throughout the cell cycle at the single-cell level is crucial to gain understanding in cell size control. This is probably the most important challenge currently facing research in size control in metazoan cells. In the methods chapter, we will discuss the technical aspects of this challenge (table 6.1). Here, we discuss the results obtained with the techniques currently available (table 4.1).

4.4 Current views on the homeostatic process in metazoan cells

4.4.1 Cells grow exponentially or super-linearly

Results provided with these different methods measuring different size parameters and on different cell types argue in favor of different growth models, making it currently difficult to propose a clear answer.

Several studies agree on an exponential growth model, strongly suggesting, according to the authors the need of a size-sensing mechanism Tzur et al. (2009); Sung et al. (2013); Godin et al. (2010). Further reinforcing the requirement of a size control in these exponentially growing cells, is the finding that the symmetry of division accepts an error of 7-10% depending on the cell type when measuring dry mass Sung et al. (2013) or volume Tzur et al. (2009). To prevent the exponential spreading of these asymmetries, a size-sensing mechanism must exist to correct them within the following cell. It is however important to note that in all these reported studies, there is no direct size measurement on the same cell over long periods of time and growth profiles are mathematically extracted using the Collins-Richmond method Sung et al. (2013); Tzur et al. (2009).

Further suggesting that these growth trajectories extracted mathematically might omit some of the complexity of the problem, are the more precise results provided by mass measurement on single adherent cells over 50 hours Park et al. (2010). In this study, although the authors focus on exponential growth profiles, it is clear from the results that both linear and exponential growth behavior can be found on single cells over periods of time as long as 25 hours. In the study conducted by Mir et al. (2011), spatial light interference microscopy (SLIM) enabling dry mass measurement was combined with fluorescent imaging of probe indicating the cell cycle phase. This allowed the characterization of growth during the different phases of the cell cycles. Results showed that in G2 phase, growth was exponential whereas the growth profile was less clear in G1 phase. Surprisingly, the authors also report that growth continues during mitosis.

4.4.2 No clear role for time modulation, possible existence of a growth-rate modulation

Two of these recent studies provide a hypothetical model to explain the size homeostatic process. By combining buoyant mass measurement and FUCCI system Sakaue-Sawano et al. (2008) imaging to track progression through the cell cycle, Son *et al.* proposed an interesting and new solution to the problem where growth rate rather than size or time is the key regulator Son et al. (2012). They show that: (i) there is no correlation between mass at birth and total cell cycle or G1 phase duration; (ii) there is no correlation between mass and growth rate (iii) there is however a clear correlation between G1 phase duration and early growth rate in G1; (iv) the variability of growth rates decrease as cells approach to the G1/S transition, and diverges again after passing that point; (v) size variability is also decreased, but to a much lesser extent at the G1/S transition compared to birth; and (vi) when cells are grown in limiting isoleucine conditions, growth rate is reduced and the duration of G1 phase increases so that the size range at both G1/S transition or end of cell cycle is conserved compared to control conditions. Altogether, these data led to a model where G1 duration is tuned to early growth rate so that slow growing cells spend more time growing in G1 than fast growing cells.

The other model suggested that there is a negative correlation between growth rate and size: small cells grow faster than big cells so that the variability of sizes is reduced at the G1/S transition Kafri et al. (2013). However, this surprising result might be taken with caution regarding the fact that growth curves are extracted from fixed asynchronous populations at steady state using Ergordic Rate Analysis (ERA), a mathematical model based on the assumption that there is no variation of cell cycle duration depending on size. Following on this, the same lab implemented the ERA by directly obtaining individual cell age through long-term live-imaging before cell fixation and protein amount measurement Ginzberg (2015). This enabled the authors to refine their model by proposing that cell size feedbacks on growth rate: cells larger than the target size will down-regulate their growth rate while cells smaller than the targe size will up-regulate their growth rate.

All the studies on mammalian cells mentioned in this paragraph are listed in table 4.1.

4.5 Conclusion

There is to date a convergence of evidence in the field towards the existence of growth control occurring during G1 phase in different metazoan cells.

Recent technical improvement enabled measuring single-cell dry mass Park et al. (2010); Sung et al. (2013); Mir et al. (2011) or buoyant mass Godin et al. (2010); Son et al. (2012). However, although direct single-cell growth trajectories is crucial for size homesotasis characterization (see section 2.4.2.2), only two of these studies successfully tackled the many challenges of performing such measurement in metazoan cells Son et al. (2012); Mir et al. (2011). Moreover, volume, which appears to be a potentially crucial parameter for size sensing in both yeast and bacteria (section 2.3) has never been measured throughout the cell cycle in metazoan cells.

The most recent works in metazoan cells have not yet reached a clear consensus on the size homeostasis mechanism. A common feature however, is that these studies are suggesting that classical sizer and adder models should be replaced by growth rate-dependent size homeostasis models Son et al. (2012); Kafri et al. (2013). These new models however still lack direct experimental proof. As description of the homeostatic process is getting more complex, taking into account the differential regulations of growth occurring during distinct phases of the cell cycle will be important. Experiments where growth rates and sizes are perturbed while single-cell tracking of cell size and cell cycle phase is performed

Reference	Size parameter	Cell type	Measurement method	Analysis of growth curves
Exponential growth, no model for size homeostasis				
Tzur et al. (2009)	volume	Lymphoblastoid cells	Optical measurement of cells in suspension	Collins-Richmond method
Godin et al. (2010)	buoyant mass	Lymphoblastoid cells	Suspended microchannel resonator	No measurement over full cell cycles
Park et al. (2010)	mass	HT29	Resonant mass sensor	Single-cell tracking over 50hrs
Sung et al. (2013)	dry mass	Lymphoblastoid cells, RKO, HT29	Synthetic phase microscopy	Adapted Colins-Richmond method
Exponential growth, or linear growth no model for size homeostasis				
Mir et al. (2011)	dry mass	U2OS	spatial light interference microscopy	Single-cell tracking over full cell cycles + pcNA probes
Exponential growth, growth rate transition at G1/S				
Son et al. (2012)	Buoyant mass	Lymphoblastoid cells (L1210, FL5.12)	Suspended microchannel resonator	Single-cell tracking over full cell cycle + FUCCI system
Constant time, active growth rate regulation				
Kafri et al. (2013)	dry mass	HeLa	Protein amount staining	Egodic rate analysis

Table 4.1: Summary of recent studies in animal cells

are needed to gain understanding in what could be the possible homeostatic process. It will also be very helpful to combine these experiments with predictions from mathematical modeling to test the generality of these observed features of cell size regulation.

Chapter 5

General conclusion and aims of this study

5.1 General conclusion 61
5.2 Aims of this study 62

5.1 General conclusion

Studies in yeast and bacteria demonstrate that size control is central in the coordination of two key processes in cells, namely cell cycle progression and cell growth. In these organisms, the development of techniques enabling live single-cell volume measurement over successive generations marked a significant step in the understanding of size control. Phenomenologically, the size homeostasis mechanism could be characterized as a sizer for *S. pombe* Fantes (1977), and an adder for daughter cells of *S. cerevisiae* Soifer et al. (2016) and several bacteria cell types Campos et al. (2014); Taheri-Araghi et al. (2015); Soifer et al. (2016). Research in these two types of organisms is now aiming at identifying the underlying molecular mechanism. This is currently hotly debated but volume appears as a potentially crucial parameter Schmoller et al. (2015); Delarue et al. (2016); Soifer et al. (2016); Ho and Amir (2015); Si et al. (2016); Zheng et al. (2016) for both *E coli* and *S. cerevisiae*. Moreover, it is possible that several mechanisms independently regulate cell cycle and growth regulation. In eukaryotes, the cell cycle is indeed described as the sequential progression through growth phases when most of the size control occurs and phases where DNA is replicated or divided.

Cell cycle and cell growth regulatory pathways have been intensively studied in metazoan cells and they show an additional layer of complexity compared to single-cell organisms. Evolutionary genetic expansion indeed led to the complication of the networks in higher eukaryotes. Moreover, metazoan cells do not behave like uni-cellular organisms in that they also integrate several growth and mitogen signals enabling homeostasis at the organ and body level. Finally, cell growth studies in metazoan cells are very challenging experimentally because these cells have long cell cycles and constantly fluctuating shapes, making it impossible to easily access cell volume through a measurement of the cell outline as in bacteria or yeasts. For all these reasons, very little is known about how size homeostasis occurs in mammalian cells. Only two studies reported mass measurement at the single cell level over full cell cycle trajectories Son et al. (2012); Mir et al. (2011) and volume has been poorly investigated. No phenomenological characterization of the homeostatic behaviour exists in these cells and the very existence of a size control is debated Lloyd (2013). Although early work suggested that G1 phase

duration was adapted to cell growth or size Zetterberg and Larsson (1985); Dolznig et al. (2004), reminiscent of what has been described in *S. cerevisiae* Hartwell and Unger (1977); Johnston (1977), this was contradicted by more recent work that instead suggested a central role for growth rate regulation Kafri et al. (2013); Son et al. (2012); Tzur et al. (2009). It is in this emerging, challenging and exciting context that I started my PhD.

5.2 Aims of this study

During my PhD, I aimed at characterizing the size homeostasis process of mammalian cells. To provide the first direct and dynamic measurement of mammalian cell volume over full cell cycles, I optimized a method previously established in the lab that enables fluorescence exclusion-based measurement (FXm) of volume Zlotek-Zlotkiewicz et al. (2015). These optimizations involved improving the robustness of the technique and guaranteeing good growth conditions throughout experiments that spanned from 1 to 2 days. The analysis protocol was also improved Cadart et al. (2017). Addressing these challenges took in fact the most important part of my PhD.

Size, growth and cell cycle duration are entangled processes. Identifying and testing the homeostasis mechanism requires the development of experimental tools that would enable decoupling these three parameters. Traditionally, chemical perturbations such as RNAi or drugs are used. However, since several cross-talks exists between growth pathway and cell cycle machinery, results from such experiments are not always easy to interpret. Mechanical decoupling of these parameters could therefore be an interesting complementary strategy. At the beginning of my PhD, I hypothesized that artificial induction of asymmetries of either total cytoplasm or specific organelles could be an interesting approach to study cell size homeostasis and homeostasis within the cell Cadart et al. (2014). I tried different micro-fabrication techniques to optimize tools to induce asymmetrical divisions of cell volume and mitochondria. The latter remains at a preliminary state but I could artificially induce asymmetrical divisions of cytoplasm through confinement in micro-channels. I observed that such asymmetries were reduced during the following cell cycle , thus showing the existence of a size homeostasis mechanism.

Combining volume measurement with cell-cycle tracking, I aimed at (i) providing a phenomenological description of the size homeostasis behaviour in several mammalian cells and (ii) characterizing how growth and cell cycle progression were coordinated in each sub-periods to make hypotheses about the mechanisms underlying size control in these cells. I found that most mammalian cell types behaved in an adder-like manner. I also showed that for HT29 and HeLa cells, cell cycle duration and more specifically G1 length was inversely correlated with initial size. This correlation seemed to be limited by a minimum duration of G1, as emphasized by the study of artificially induced large HeLa cells that all spent a constant minimum time in G1. However, even in these large cells that do not show time modulation anymore, the adder behaviour is conserved, suggesting complementary growth regulatory mechanisms that are still unclear. In collaboration with theoreticians, we propose a general frame to compare the homeostasis process of mammalian cells and bacteria.

In the following chapter, I describe the methods I developed for volume measurement and artificial induction of asymmetries.

METHODS

Chapter 6

Methods

6.1 Long time-lapse acquisition in animal cells to characterize growth: state of the art and challenges . . . 65
6.2 Fluorescence-exclusion based volume measurement . . . 67
6.2.1 Volume measurement method: principle and validation . . . 67
6.2.2 Image analysis optimization . . . 68
6.2.3 Protocol optimization for long time-lapse acquisition . . . 70
6.3 Cell growth analysis: clonal & single-cell curves, cell cycle transitions 77
6.3.1 Single-cell curves . . . 77
6.3.2 Clonal growth curves . . . 80
6.3.3 Cell cycle transitions keypoint analysis . . . 81
6.4 Developing tools to induce asymmetrical divisions . . . 84
6.4.1 Inducing asymmetrical divisions using micro-channels . . . 84
6.4.2 Asymmetrical patterns . . . 85
6.4.3 Drug-induced asymmetrical distribution of organelles . . . 85
6.5 Choice of cell types . . . 87
6.5.1 Description of the cell types used in this study . . . 87
6.5.2 Establishing new stable lineages . . . 88
6.6 Statistical analysis . . . 88

6.1 Long time-lapse acquisition in animal cells to characterize growth: state of the art and challenges

The study of cell growth regulation in animal cells has recently been renewed by sophisticated techniques aiming at dynamically measuring a size parameter on single cells over the entire cell cycle Park et al. (2010); Mir et al. (2014); Son et al. (2012). A reliable method for cell growth study must tackle several challenges: (i) the size measurement method chosen must allow accurate and repetitive measurements without perturbing cell′s physiology; (ii) the experimental set-up must be stable over several days because the typical cell cycle length of an animal cell ranges from 15 to 20 hours; (iii) the low frequency at which complete cell cycles occur in these cells makes it more difficult to obtain a satisfying number of observations and a method enabling measurement on several single cells in parallel might be preferable; (iv) a steady state of growth all throughout the experiment must be guaranteed, which requires for example that sufficient amounts of nutrients are provided or that cells in excess

	FXm	SLIM	SMR	RMS	SPM	Optical measurement	Protein staining	Coulter counter
Size parameter	volume	mass	density	mass	mass	volume	protein amount	volume
Single cell	xx	xx	xxx	xxx	xx	xx	x	no
Suspended cell	xx	no	xxx	no	xx	xxx	no	xxx
Adherent cells	xx	xx	no	xx	xx	no	xx	no
Accuracy	xx	xx	xxx	xx	xxx	x	x/xx	?
Throughput	xx	xx	x	x	x	xx	xxx	xxx
Easy to use	xx	xx	xx	x	x	xx	xx	xxx
Instrumentation	xx	xxx	xxx	xxx	xxx	xx	x	xxx
Dynamic measurement	xxx	xxx	xxx	xxx	xx	no	no	no
Long-time measurement	xx	xx	xxx	x	x	no	no	no
Reference	1	2	3	4	5	6	7	8

Table 6.1: Comparison of the available methods to measure animal cell size. References for the methods are: 1) Zlotek-Zlotkiewicz et al. (2015), 2) Mir et al. (2014), 3) Godin et al. (2010),Son et al. (2012),4) Park et al. (2010), 5) Sung et al. (2013) , 6) Tzur et al. (2009), 7) Kafri et al. (2013), 8) Conlon and Raff (2003).

are removed to prevent density-related effects on cell growth and proliferation. In addition to these requirements, compatibility of the method with traditional cell biology tools to assess biochemical processes within the cell such as fluorescent microscopy or transient drug treatments would very much improve the output of the experimental set-up.

The characteristics of the different methods that were used to study animal cell growth and size regulation are compared in table 6.1, a review on the first three methods can also be found in Popescu et al. (2014)). Overall, four main techniques enable dynamic mass measurement on single cells over long periods of time: Spatial Light Interference Microscopy (SLIM) Mir et al. (2014), Suspended microchannel resonator, (SMR) Son et al. (2012), Mass Resonant Sensor (MRS) Park et al. (2010) and Synthetic Phase Microscopy (SPM) Sung et al. (2013).

In the lab, a volume measurement technique based on fluorescence exclusion Zlotek-Zlotkiewicz et al. (2015) had been developped. This method has many advantages: it enables dynamic measurement of cell volume over long periods of time, it requires little instrumentation, it is also compatible with traditional cell biology tools such as drug treatment or fluorescence imaging.

During this PhD, we tried to adress three main technical challenges encountered when applying this technique to the study metazoan cell growth: (i) we improved the experimental and theoretical validation of the method and published a protocol paper Cadart et al. (2017), (ii) we optimized the protocol for long time-lapse acquisition and established a list of controls to rigorously assess the quality of growth in the device and finally (iii) we improved the image analysis protocol together with the company QuantaCell that writes Matlab softwares for image analysis in order to make it more robust and user-friendly. The protocol paper that fully explains the method is available in annexe B. Here we report additional controls and optimizations that are not described in this protocol paper.

6.2 Fluorescence-exclusion based volume measurement

6.2.1 Volume measurement method: principle and validation

6.2.1.1 Method principle

Fluorescence exclusion method (FXm) is a volume measurement method based on fluorescence intensity calculation. A description of the method can be found in Zlotek-Zlotkiewicz et al. (2015) and Cadart et al. (2017). Briefly, cells are placed in PDMS chambers of defined height (around 15-25μm) in the presence of fluorescent dextran (in our case 10kDa-Alexa488 or Alexa647). Dextran cannot penetrate the cellular membrane nor the PDMS. Thus, cells appear of lower fluorescence intensity than the surrounding media as any other object excluding the dye. The intensity of the fluorescence at a given pixel is proportionate to the height of the chamber. We can thus obtain the following relation:

$$I_{(x,y)} = I_{max} - \alpha \times h_{(x,y)} \tag{6.1}$$

The intensity of the fluorescence is maximal in the background, where no objects exclude the dye (I_{max}) and is minimal under the pillars that bind the roof of the chamber to the bottom of the dish and thus completely exclude fluorescence (I_{min}). We can deduce from these two measurements the value of α:

$$\alpha = \frac{I_{max} - I_{min}}{h_{chamber}} \tag{6.2}$$

Since the height of the pillars is known and constant, it is possible to deduce from the decrease of intensity the height of the fluorescence-excluding object, here the cell. We then integrate the heights found over the area covered by the cell to obtain its volume:

$$V_{cell} = \iint_{x,y} \frac{I_{max} - I_{x,y}}{\alpha} dxdy \tag{6.3}$$

6.2.1.2 Theoretical validation

It is important to note that the accuracy of volume measurement through this technique directly depends on a reliable measurement of the intensity signal over the entire height $h_{chamber}$ of the device. We therefore run a serie of tests both theoretical and experimental to validate the FXm method with our device. To validate the method theoretically, we initiated a collaboration with an optician, Olivier Thouvenin.

The image of single small fluorescent emitter recovered on the camera is described by a point spread function (PSF) which properties depend on the numerical aperture of the objective and the wavelength of the excitation light. If the excited point is on the focal plane, its image on the camera will look close to a point. On the contrary, the further this point from the focal plane, the more spread its image will be (figure 6.1 A). The range of acceptable focus, also called the depth of field, scales with the inverse square of the numerical aperture (NA):

$$\text{depth of field} = \frac{\lambda.n}{NA^2} + \frac{n}{M.NA}e \tag{6.4}$$

Where λ is the wavelength of detection, n is the refractive index of the medium between the coverslip and the objetive, e is the smallest lateral resolution at the focal plane and M is the magnification of the objective. Typically, a high numerical aperture objective gives a better lateral resolution of the point at the focal plane but looses focus very fast when the point is imaged out of focus. For our method, we need objectives with a large depth of field to make sure that the total fluorescence intensity signal

is recovered. Ideally, the depth of field should be as large as the height of our measurement device ($\approx 20\mu m$). Olivier Thouvenin's model showed that our method gives accurate volume measurement even when the depth of field calculated with the usual formula gives lower values than the height of our measurement device. Indeed, with an epifluorescence microscope, all fluorescence light is collected on the camera. The out-of-focus signal is simply diffracted on pixels around the real position of the object, as described by the PSF. With a depth of field smaller than the height of the measurement device, the height of an object calculated at a single pixel will be wrong, however its volume, calculated by integrating fluorescence intensity signal over a large area will be correct. As long as the area over which fluorescence intensity is collected is larger than the object's further diffracted points, volume calculation remains correct. The radius of this area for volume integration R_{int} was estimated by Olivier Thouvenin as:

$$R_{int} > R_{cell} + h_{chamber} \frac{1}{\sqrt{\left(\frac{n}{NA}\right)^2 - 1}} \tag{6.5}$$

where R_{cell} is the radius of the cell.

6.2.1.3 Experimental validation

We checked experimentally that the predictions of the model were right. We verified that volume calculated was constant over a wide range of z-planes, with different magnifications and numerical apertures as long as the area over which the calculation had been made was large enough. Results of these experiments, made together with Larisa Venkova, can be found in figure 5 of the protocol paper (appendix B). Additional controls showing that volume measurement is on average independent to cell shape can be found in Zlotek-Zlotkiewicz et al. (2015).

6.2.2 Image analysis optimization

Proper image analysis is a critical step of the FXm method. The main difficulty is to extract in the most robust and accurate manner the values of I_{min} and I_{max} used for the calculation of volume. Image analysis was initially performed using a custom-made Matlab programm, written by Sylvain Monnier and described in Zlotek-Zlotkiewicz et al. (2015). In order to develop a more robust and user-friendly code, a new Matlab code, written by Victor Racine from the company QuantaCell was established. Optimizing this code was in fact a lot of work, where we performed series of experimental and analytical tests to try establishing the most robust image treatment protocol. The final image analysis protocol is described in Cadart et al. (2017). Here we described the main tests that were made to best evaluate I_{min} and I_{max} .

I_{min}, the value under the pillar is supposed the be the value when no fluorescence is present and thus should be equal to the value of the camera offset. To check whether fluorescence intensity under the pillars was a reliable measurement of I_{min}, we tested its dependency upon variable source of fluorescence signal in the device and increasing power of fluorescence illumination (figure 6.2). This test showed that when we used phenol-red free medium to prevent additional fluorescent signal coming from the cell culture media and not the fluorescent probe, fluorescence intensity under the pillar was present but small with respect to the range over which fluorescence intensity was calibrated. A perfect approach would be to define I_{min} as the value of the camera offset which corresponds to the value measured by the camera in the absence of light and is always slightly above zero. However, for the sake of simplicity of the Matlab program, we decided to neglect the small over-estimation of I_{min} when measured as the intensity under the pillar.

I_{max}, the value of the background, where no object excludes the fluorescence is present. The main sources of fluctuations of I_{max} are: (i) fluctuations of fluorescence lamp in space or time, (ii)

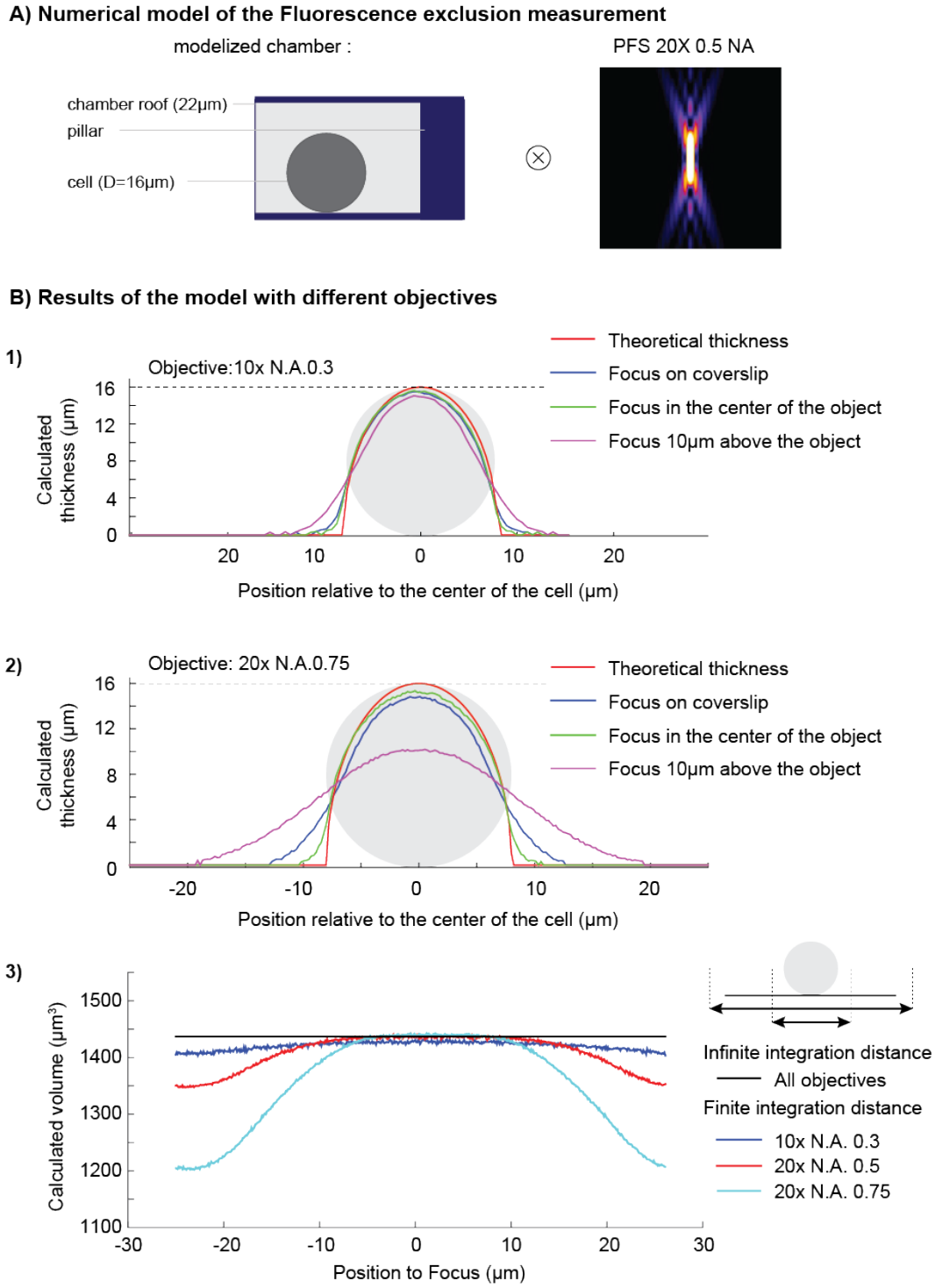

Figure 6.1: Theoretical validation of the method. A) 2D simulation of the FXM: The modelized chamber as a $22\mu m$ high chamber and a cell represented as a sphere of $16\mu m$ diameter. Perfect homogeneous fluorescence signal is assumed. The PSF was calculated for different objectives (here 20X NA0.5) and the program performs the convolution of this PSF with each (x, z) point of the chamber to calculate the fluorescence intensity signal recovered on the camera. The output is then used to calculate volume as shown in B).**B) Expected calculated volume with different objectives.** 1) and 2) show the calculated thickness of the simulated cell (grey disk) at different z-planes: this thickness is rapidly underestimated as fluorescence intensity is measured out of the focal plane and this effect is even more rapid as the numerical aperture increases. However, in 3), we see that the calculated volume, is correct as long as fluorescence intensity signal is integrated over a large enough area.*(figure adapted from Cadart et al. (2017))*

fluctuations of the height of the chamber, (iii) presence of dusts and small particles resulting in an inhomogeneous background. To adress these problems, the following steps were defined:

1. In the design of the chamber, the pillars that sustain the roof of the chamber were closely spaced to maintain a flat roof.
2. The presence of dusts and small particles was limited because of the several washing steps during the pre-incubation of the chamber with media and the injection of the cells (see protocol in the paper).
3. For all our experiments the fluorescence excitation source was a LED (Lumencor or Zeiss Colibi) to obtain the best possible homogeneity of field illumination. Prior to the experiment, the fluorescence lamp was re-aligned with the optical path using a chroma fluorescent slide if needed.
4. Finally, after the images were acquired, the first step of the Matlab program was a background normalization procedure which principle is described in the protocol paper. The optimization and the verification of the accuracy of this procedure took several months. It implied validating the procedure written by Victor Racine through the careful analysis of single-cell growth curves. These controls led to a significant change in the strategy we used for the background normalization. Initially, our normalization method was a classical image smoothing where borders are estimated by mirroring the local background. We realized that this method fails to estimate the background when there are gradients of illumination (in a corner of the field for example). Victor Racine then developed a very innovative approach to normalize the background using a surface fitting protocol that better extrapolates the intensity in the corners of the image John D'Errico (2005). This greatly improved the robustness of our volume measurement, even in cells that were in the corners of the field of illumination (figure 6.3).

6.2.3 Protocol optimization for long time-lapse acquisition

6.2.3.1 Improve nutrient access

As explained in 6.1, methods that guarantee and check the quality and steadiness of growth throughout long experiments performed on animal cells are still lacking currently. In the field of bacteria growth study, the development of microfluidic chips with continuous flow delivering fresh media to the cells such as the mother machine Wang et al. (2010) (also described in figure 3.1 B) led to an impressive increase of discoveries in the field of size control. Translating this strategy to experiments on animal cells is however difficult because the microfluidic system must now be robust for over 50hrs without any bubble appearing. It also makes it more difficult to image more than one condition (i.e. increased number of tubes are more difficult to keep away from the microscope motorized plane). In addition to this, our method requires the use of a fluorescent probe that must be homogeneous in the chamber and also has cost. After trying different approaches, for the sake of simplicity and reproducibility of our experiments, we therefore chose a static system to provide the culture medium. We added side reservoirs on each side of the volume measurement chamber 6.4 that passively diffused nutrients through to the cells. The chamber was designed and fabricated by Sylvain Monnier with a micro-milling machine. A comparison of the cell cycle duration of HT29 inside and outside the device is shown in figure 6.5

6.2.3.2 Standardized cell culture protocol to try reduce variability

When repeating experiments, we sometimes observed that cells doubled on average slower than expected. In addition to the improvements of the design of the chamber described just above, we

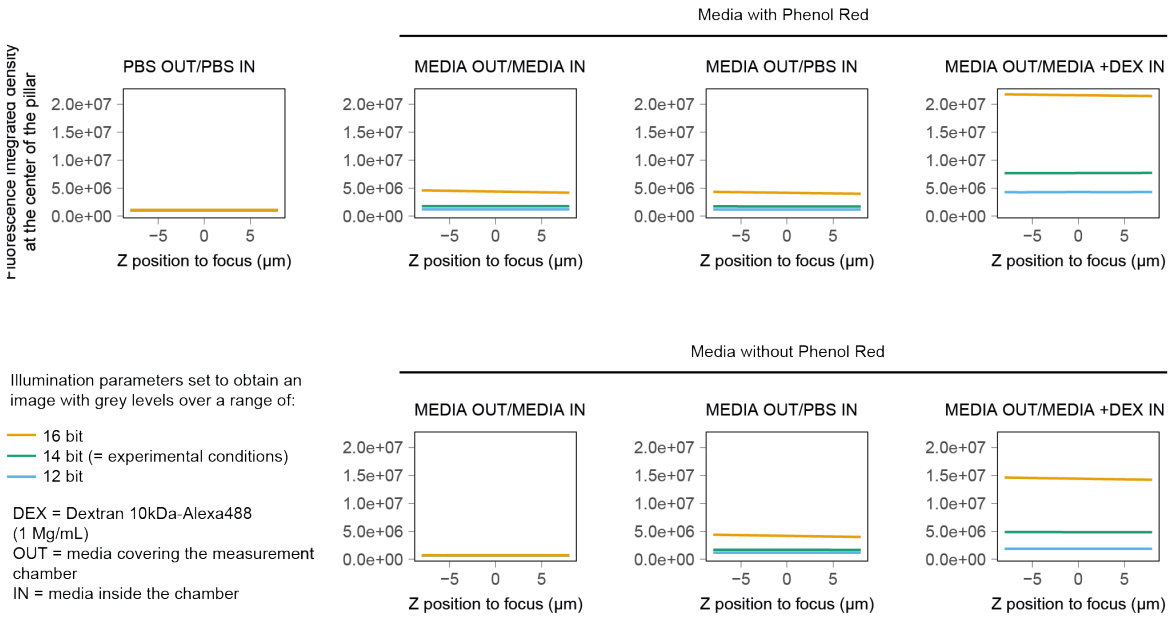

Figure 6.2: Accuracy of I_{min} estimation. We tested four different conditions: (i) PBS inside and outside (covering) the chamber; (ii) media covering the chamber and PBS inside the chamber; (iii) media covering the chamber and filling the chamber and (iv) the experimental condition where media covers the chamber and a mix of media + fluorescent dextran is injected inside the chamber. These four conditions enable distinguishing whether fluorescent signal under the pillar comes from the media covering the chamber and is therefore homogeneously added to all points (ii), whether it comes from media close to the pillar in the chamber generating artefactual signal due to light diffusion (iii) or whether it comes from fluorescent dextran in the chamber for the same reason. When media without phenol red is used, it seems that fluorescence coming from the media can be avoided, however fluorescence coming from the dextran and shadowing to the pillar is still observed. Under experimental illumination conditions (green slopes), the increase in fluorescence intensity remains small compared to the levels of intensity measured in the background.

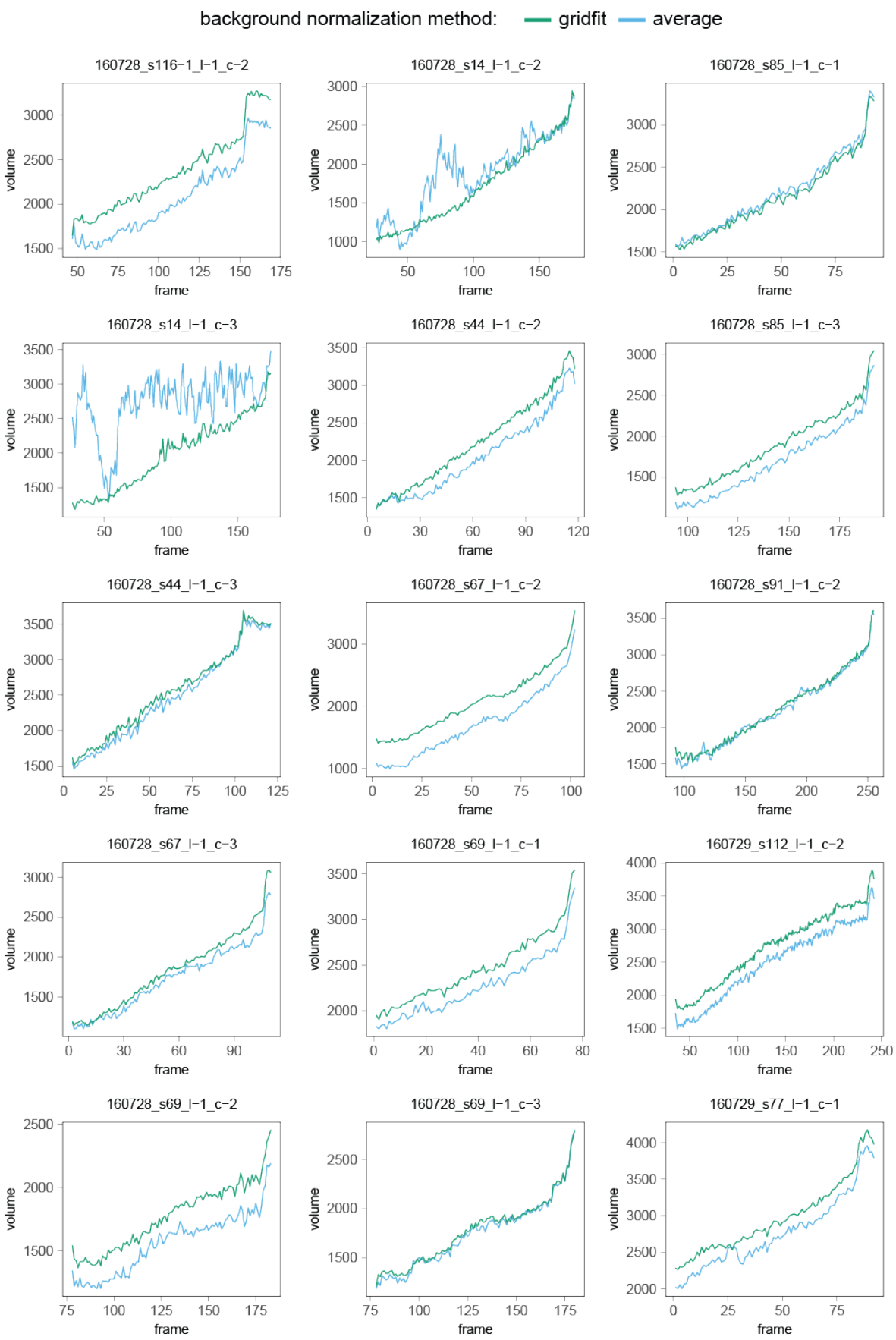

Figure 6.3: Robustness of the background normalization procedure to inhomogeneous fluorescent fields. Comparison of the volume curves obtained after two different background normalization procedures: the 'average' method is a classical method of image smoothing (blue curves) while the 'gridfit' method is based on a surface fitting protocol (green curve).

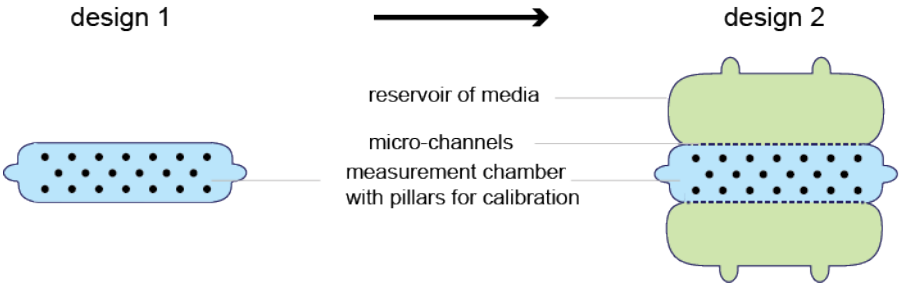

Figure 6.4: Evolution of the design of the volume measurement chamber to improve nutriment access Several designs were tested, we here show the initial design and the final design used for experiments. Cells are put in a chamber (blue) at low height ($\approx 20\mu m$) with pillars regularly spaced (dark circles). The pillars are important to ensure that the chamber roof is of constant height and to give a reference of I_{min} the minimum intensity. To improve the quality of growth throughout long experiments, we added two side reservoirs (green) of height $400\mu m$ that passively diffuse fresh media through narrow micro-channels (width $= 100\mu m$, height $= 5\mu m$ and length $= 300\mu m$) to the cells in the measurement chamber.

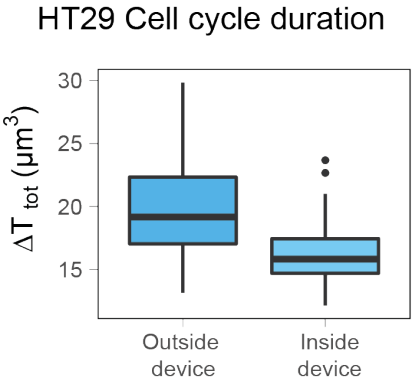

Figure 6.5: Cell cycle duration inside and outside the device. Duration of cell cycle length inside and outside the volume measurement device for HT29. Cells were plated at approximately the same density. Cell cycle duration is slightly higher outside the device, probably due to a faster equilibration of the media in the small volume of the measurement device. This control shows that cells cycle on expected durations in the measurement device.

tried to prevent potential sources of variability in the growth rate or doubling rate caused by different proliferative states in the population. We therefore always seeded cells in a six-well plate at a constant concentration two days before the experiment (table 6.2).

Cell type	Seeding density for routine cell culture in t25 flask (n/mL)	Seeding density in 6-well plate at Day - 2 (n)	Concentration injected in the chamber (n/mL)
HT29	50×10^4		2×10^5
HeLa	7×10^5	1.5×10^5	1.8×10^5
HeLa + roscovitine $20\mu M$		8×10^5	2×10^5

Table 6.2: Cell density seeded 2 days before the experiment and cell concentration injected in the volume measurement chambers. The volume injected in the chamber is $\approx 5\mu L$

6.2.3.3 Analytical validation of the quality of growth in the experiments

Careful validation of the quality and steadiness of growth in the chambers is a crucial step when measuring cell growth. Indeed, studying a population that for example progressively looses volume over time because of some growth problem can lead to misleading correlations.

In the field of bacteria or yeast recent devices improved significantly the control of nutrient access and cell number in the chambers, thus allowing the tracking of hundreds of successive generations in one single experiment while guaranteeing good growth conditions (reviewed in Duncombe et al. (2015); Okumus et al. (2014)). In these works, validation of the quality of growth in the experiment is usually made through a systematic quantification of several growth-related parameters such as the average growth rate, cell cycle duration or doubling ratio ($S_{final}/S_{initial}$). This ratio is expected to be close to 2 when the cells are at steady state and maintain a constant size through generations. This enable identifying a window of time in the experiment during which all these parameters are steady (see figure 6.6).

Aiming at such rigorous validation of the quality of growth in experiments performed on mammalian cells is more complicated because mammalian cells typically cycle over $\approx$ 20 hours. It is therefore difficult to observe more than 2 or 3 successive cell cycles and impossible to define a steady state in the population. In fact, in the case where cells are adherent, cell number increases through time in the experiment and one might observe changes in the proliferation speed due to cell-to-cell signaling effects. It is well known for example that when cells reach confluence, proliferation is inhibited: this is the so called contact inhibition effect. Another problem is that an increasing number of cell might exhaust nutrients available and lead to a reduction of the growth rate. This could be an interpretation to the progressive slow down of the slope of average cell mass over time observed in the experiments from Mir et al. (2011) (figure 6.6).

Until now, there has been little emphasis made on the importance of assessing the quality of growth in experiments performed in mammalian cells (figure 6.6). In this PhD, making sure that the data-sets we acquired were of enough quality to then build a robust characterization of the growth behaviour of different cell types was one of our major concern. We therefore developed a protocol to validate analytically the quality of growth of each data-set acquired. Because we only measure two to three generations in one experiment, we could not use the same strategy as in yeast or bacteria studies to validate our experiment but we verified that all growth-related parameters such as cell volume, cell cycle duration or average growth speed were constant throughout the 50 hours of the experiment. An example of how this was performed can be found in figure 6.7.

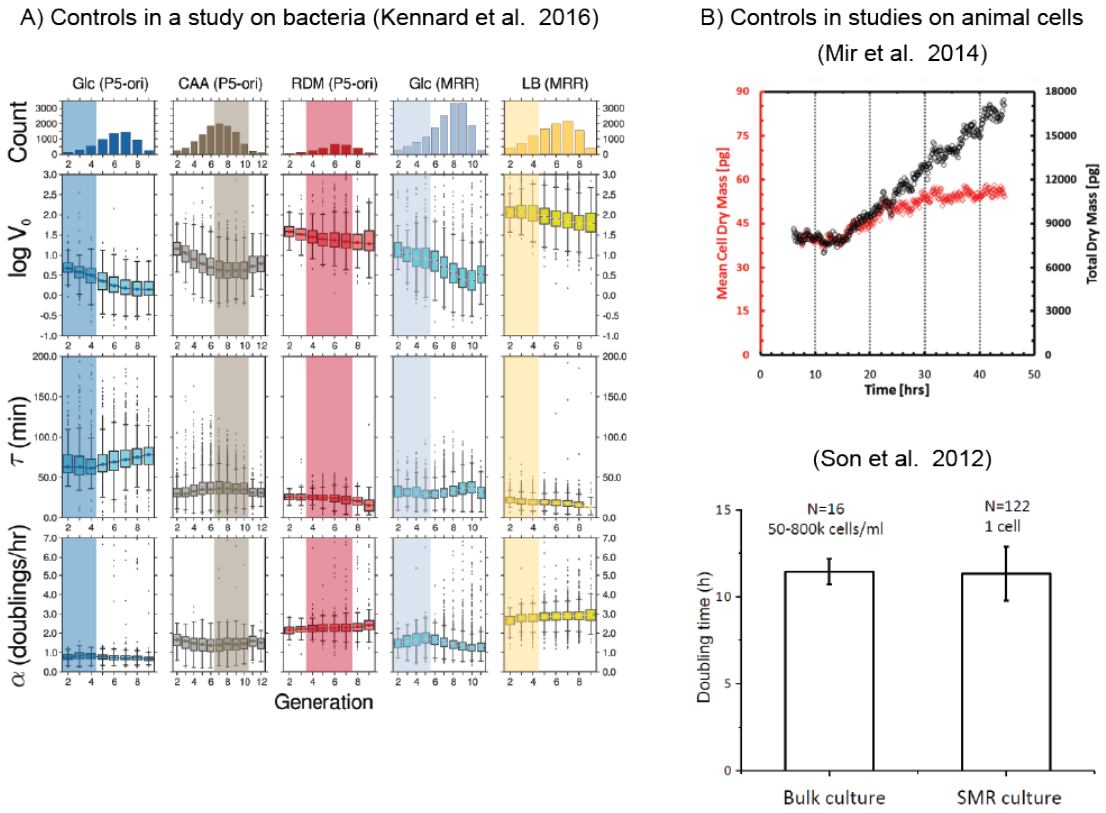

Figure 6.6: Examples of controls made to assess the quality and steadiness of growth in bacteria and animal cells. A) Controls in a study performed on bacteria: in bacteria, it is possible to measure high number of cells in several generations and then filter for the generations where the typical growth parameters are steady.(here: initial size V_0, cell cycle duration τ and the doubling rate α). *(Image adapted from Supplementary fig. 4 in Kennard et al. (2016)).* **B) Controls made in the two study reporting live measurement of animal cell size over complete cell cycles:** Top: In Mir et al. (2014), the average dry mass per cell (black) and the total dry mass (black) were measured over time from a synchronized population of U2OS cells. *(Image adapted from Supplementary fig. 2 in Mir et al. (2014)).* Bottom: In Son et al. (2012), L1210 suspended cells were measured one at a time with the Suspended Mass Resonator (SMR) device. To check that the device was not perturbing cell growth, cell cycle duration was compared to that of 16 cells in bulk culture.*(Image adapted from Supplementary fig. 1 in Son et al. (2012))*

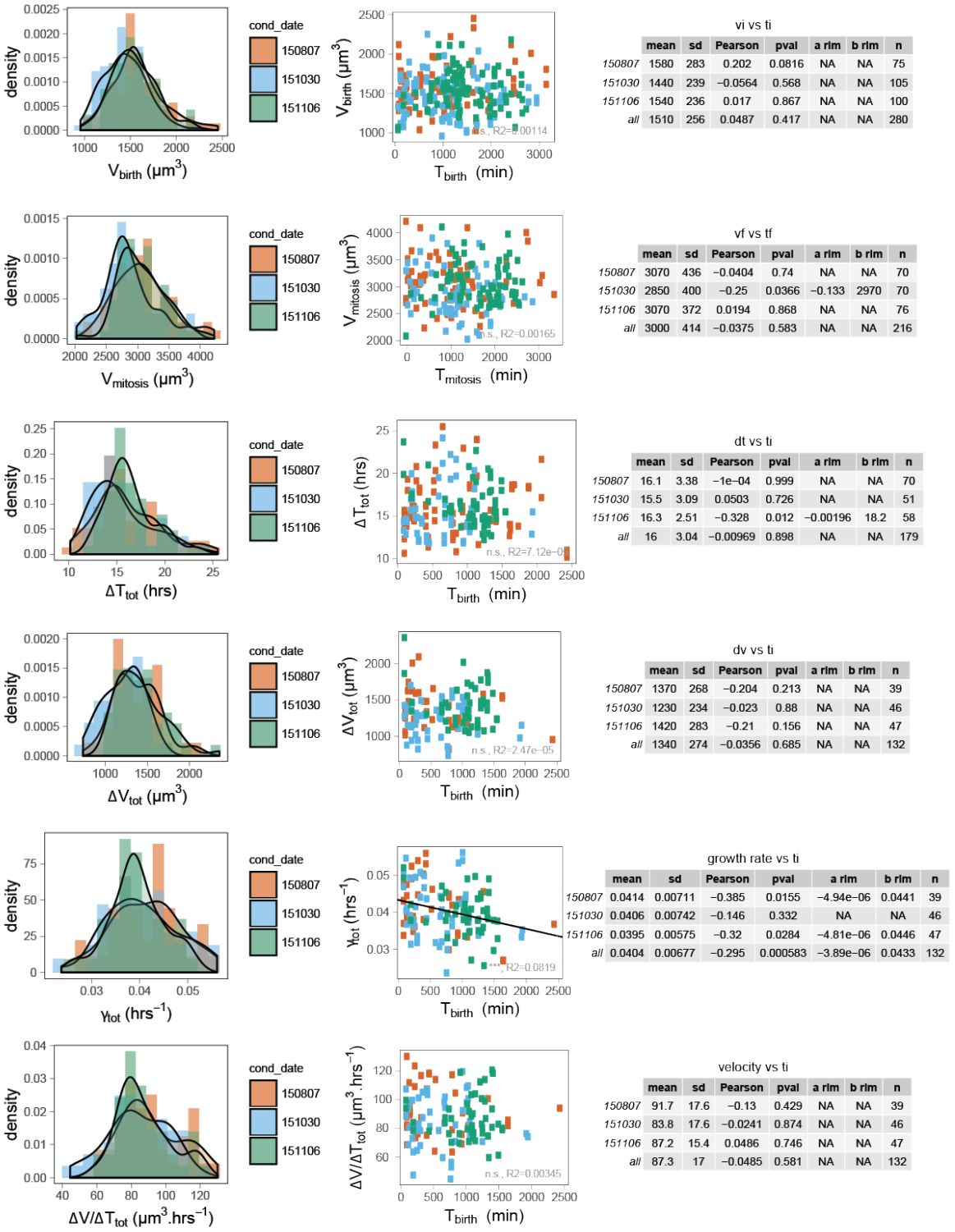

Figure 6.7: List of controls systematically made to assess the quality of growth in each experiment. An R program was written to automatically assess the quality and steadiness of growht in the chambers. Systematically, we checked that final and initial volumes($V_{mitosis}$,V_{birth}),cell cycle duration (ΔT_{tot}), volume gained per cell cycle (ΔV_{tot}), growth rate (γ_{tot}) and velocity ($\Delta V/\Delta T_{tot}$) were constant through time in the experiment and homogeneous across repeated experiments

6.2.3.4 Improving the fluorescent probes

An important line of improvement of the FXm method that we did not manage to address is the development of better fluorescent probes less prone to be uptaken by the cells through time. Indeed, although some cell types like HT29 cells have a poor endocytic activity and therefore uptake very little dextran through time in the experiment, others such as RPE1 cells rapidly uptake the probe which leads to an under-estimation of the volume. Improving the fluorescent probe would therefore enable extending the volume measurement to other cell types such as RPE1 cells which are often used in cell cycle studies.

We hypothesized that a probe is less likely to be uptaken if it interacts poorly with the negatively charged cell membrane and if it is bigger than the endocytosed molecules (the threshold is around $\approx 100nm$ of diameter). We tried three different types of probes (table 6.3) and systematically compared the uptake in RPE1 cells that uptake very fast our usual dextran with the uptake in HT29 cells which uptake close to zero dextran over long experiments:

1. Commercially available dextrans of different molecular weights. There was a slight decrease in the uptake of two dextran: the 70kDa-Alexa514 and 10kDa-Texas red. Trying even larger dextran molecules might be an interesting idea.
2. Home-made polythylne glycol chains (PEG) of different lengths bound to Alexa fluorescent probes using click-chemistry. The reasoning here was that PEG are neutral and should therefore poorly interact with the negatively charged cell membrane. However, these probes were uptaken even by the HT29 cells, probably suggesting that we failed to obtain a good purification of the unbound alexa molecules.
3. Quantum dots bound to zwiterrionic chains kindly offered by Thomas Pons, from the ESPCI Bouccara et al. (2014). These quantum dots however were toxic for our cells.

An important remark here is that when we optimized the injection method, we managed to reduce the uptake of dextran in some cells. As explained in the protocol (B), the fluorescent probe should be injected in the chamber after the cells were given enough time to adhere, not at the same time as the cells.

Overall, the optimization of better fluorescent probes is an important line of development that still needs to be solved.

6.3 Cell growth analysis: clonal & single-cell curves, cell cycle transitions

6.3.1 Single-cell curves

6.3.1.1 Careful control of the sources of volume curves fluctuations

Volume curves obtained with our method showed some rapid fluctuations at small timescales. In order to understand whether these fluctuations came from 'real' events or noise in our measurement that we could improve, we carefully checked 20 growth curves (figure 6.8). We performed the following controls:

1. We checked by eye, frame by frame, images from transmitted light and fluorescence-exclusion

$\lambda_{exc.}$	fluorophore	kDa	molecule	uptake in HT29	uptake in RPE1
680	Alexa	3	Dextran	no	yes
589	Texas-red	10	Dextran	no	20% of cells
647	Alexa	10	Dextran	no	yes
488	Alexa	10	Dextran	no	yes
514	Alexa	70	Dextran	no	20% of cells
488	Alexa	5	PEG	yes	yes
647	Alexa	5	PEG	yes	yes
650	Alexa	5	PEG	yes	yes
488	Alexa	20	PEG	yes	yes
647	Alexa	20	PEG	yes	yes
650	Alexa	20	PEG	yes	yes
450	Qdots		zwiterionic chains	toxic	toxic

Table 6.3: List of fluorescent probes tested for FXm. All the dextran probes were commercially available. PEG probes were made with click-chemistry. Zwiterrionic Quantum dots (Qdots) were a kind gift from Thomas Pons, ESPCI, Paris. Uptake is visually assessed 24 hours after the injection of the dextran in either RPE1 or HT29 as a control.

channel together with measurement of volume, to see whether obvious fluctuations in cell volume came from fluctuations in shape, or appearance of dusts in the field. The analysis was performed on HT29 cells which are fairly round throughout the cell cycle. Thus, no clear shape fluctuations could be associated to volume fluctuations. Repeating a systematic analysis of correlation between morphometric changes and volume fluctuations on more adherent cell types such as HeLa could provide different results.

2. We then checked whether fluctuations of background intensity *(I_{max})* and pillar intensity *(I_{min})* estimation that are used to calibrate volume measurement (see equation 6.2) caused artificial volume fluctuations. This led to several successive improvements of the background normalization procedure in Matlab to reach a stage where fluctuations of fluorescence background and minimum intensity (due for example to inhomogeneous fluorescence illumination through time or space) did not impact at all volume measurement. A comparison of the results from the final version of the procedure with the previous one is shown in figure 6.3.

3. We also quantified the error due to to wrong segmentation of cells close to each other and, more importantly, shadow effect of a neighboring cell in the collection of fluorescence intensity around the cell. Indeed, as explained in section 6.2.1.2, our method of measurement is based on the collection of all fluorescence intensity from top to bottom of the chamber under the cell area but out-of-focus light is retrieved by collecting light on a larger area than that of the cell. Close objects present in this larger area thus generate a 'shadow' on the measured cell. The quantification described in figure 6.8 shows that the error introduced by neighboring cells is in fact very small: volume is under-estimated of $\approx 200\mu m^3$ which is maximum 10% of the volume of a small cell at birth.

6.3.1.2 Semi-automated analysis of hundreds of single-growth curves

Once the automated background normalization and automated tracking steps were validated on a few trajectories, we established a protocol for semi-automated analysis of hundreds single-cell curves. We favoured a semi-automated approach rather than a fully automated one because much can be learned and optimized from apparently abnormal tracks and because outlier removal from experimental or

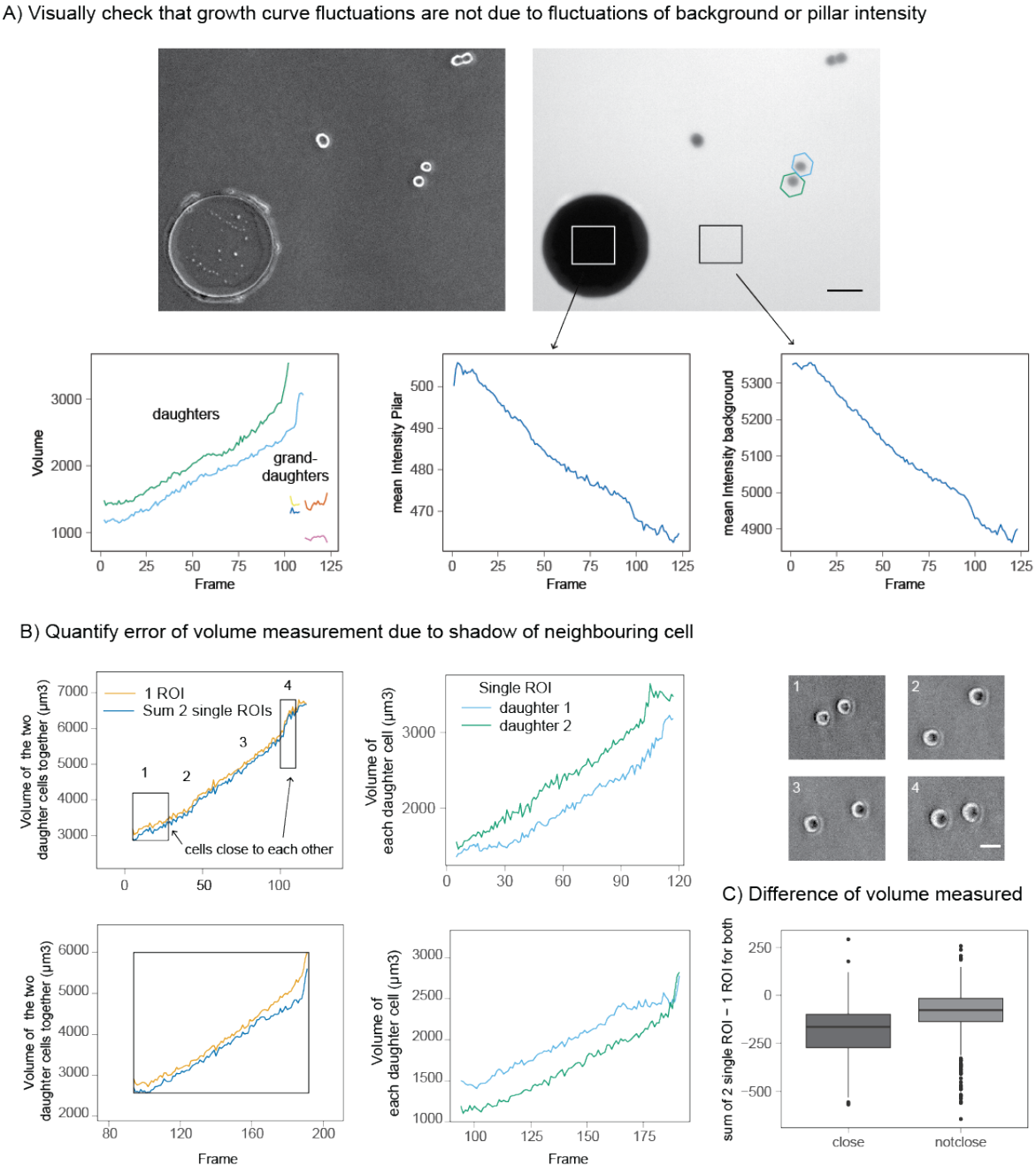

Figure 6.8: Control accuracy of the accuracy of single growth curve measurement. A) We checked that our measurement was robust to o fluctuations of the estimation of the values of background (I_{max}) or pillar (I_{min}) intensity used for volume calculation. We visually checked for several single growth curved that fluctuations of volume curves were not correlated with fluctuations of pillar or background intensity. *(Scale bar* $= 50\mu m$*).***B)** We quantified the error of volume measurement due to the presence of a close neighboring cell generating a shadow on the cell measured. Two examples of pairs of daughter cells are shown. Left: Comparison the volume calculated when measuring volume over one Region Of Interest (ROI) covering the two daughter cells or when measuring volume for each individual cell. Right: Single curves obtained for each daughter cells. The pictures represent the first pair of cells at different timepoints, the rectangles on the graphs represent periods where cells are very close to each other.*(Scale bar* $= 20\mu m$*)* **C)** Difference between volume calculated using one single ROI for the two cells or the sum of two individual ROI. The difference is slightly negative when the cells were close two each other, indicating that volume is slightly underestimated in these situations due to the shadow of the neighboring cell.*(Difference measured at every frame and for 20 growth curves).*

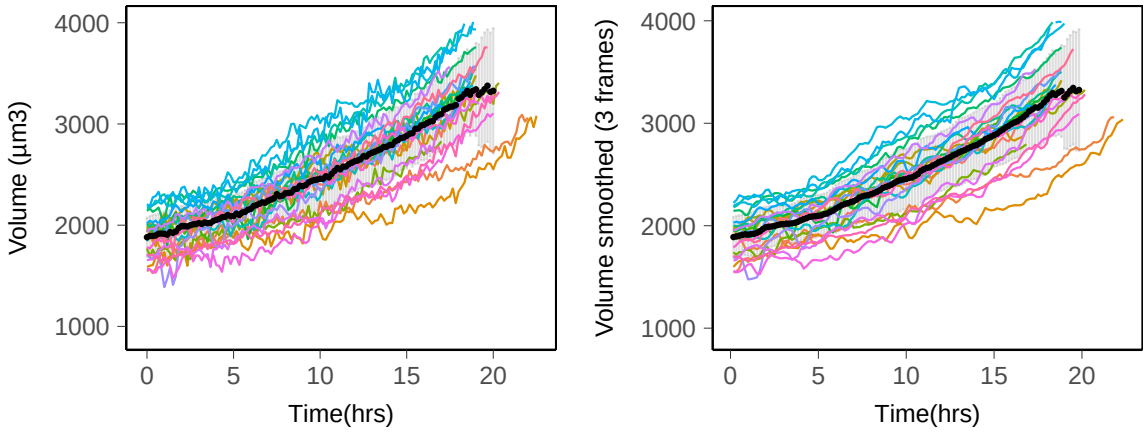

Figure 6.9: HeLa cells single-growth curves obtained with the automated tracking Matlab program. Left, raw trajectories obtained after step 3 of the semi-automated protocol for analysis of single-cell curves detailed in 6.3.1. Right: same trajectories after smoothing described in step 5.

visual criteria seems more biologically relevant than that based on purely analytical criteria. Our analysis protocol, written in R, was the following:

1. automated tracking with the MatLab program after manual determination of the segmentation parameters
2. each curve that was longer than 40 frames ($= 400min$) was visualized, curves that were clearly abnormal (due to one cell partly escaping the field or merging with another cell for example) were removed;
3. during the same step, the user indicates whether the trajectory is complete (between 2 identified mitotic overshoots) or, if it's a portion of trajectory, whether it can be aligned with respect to birth or mitosis.
4. the geminin-mcherry fluorescence intensity curve was then plotted so that the user indicates manually the transition point where fluorescence signal changes from zero to an increasing slope, this point corresponds to the G1/S transition.
5. finally, a small smoothing using sliding average over a window of 3 frames was performed.

An example of the outcome of this analysis is shown in figure 6.9. The raw trajectories still show some important fluctuations at short time scales. Considering the controls and optimization of our program described in section 6.3 and figures 6.8 and 6.3, we are confident that these fluctuations are not related to errors in the estimation I_{min} and I_{max}. However, we cannot rule out that some of these fluctuations come from shape and adhesion changes. An important consideration is that volume growth curves might fluctuate much more than mass growth curves on the same cells: volume indeed rapidly fluctuates upon shape changes. On the contrary, the typical phase delay techniques used to measure mass to date only measure large proteins and lipid contents that are unlikely to fluctuate rapidly at short timescales. More work to identify other potential sources of noise in our measurement is still possible but our trajectories are already satisfying enough to perform growth rate analysis.

6.3.2 Clonal growth curves

For cell types that badly separate from each other (HT29), it was very difficult to obtain high statistics on single-cell trajectories. To establish whether growth was exponential or linear, we sought to analyze

growth rate at the population level rather than at the single-cell level. To do so, we combined together any growth-curve trajectory of either single-cell or cell aggregates. After the automated tracking, two sources of artefactual fluctuations were identified: (i) error of segmentation with 2 cells merging for example; (ii) error in the mask segmenting cells during the background normalization. A third type of volume fluctuation irrelevant in the context our study was caused by mitotic volume overshoot which is a transient increase of cell volume at mitotic onset (see Zlotek-Zlotkiewicz et al. (2015) and discussion in the next section, figure 6.10).

After several tests, we established the following semi-automated protocol to filter these three types of fluctuations:

1. Visually check each trajectory that were longer than $> 50 frames = 500 min$, remove the few trajectories that are clearly wrong (unusual big and rapid fluctuations of volumes that were due to problems in the mask for the segmentation). Split trajectories when a step-wise increase or volume appeared due to cells merging or separating .
2. Smoothing by averaging over 3 frames.
3. Manually cut the trajectories before and after every overshoot (The cut was made a bit after the overshoot to avoid the plateau in growth observed at the very beginning of the cell cycle).
4. Outlier removal (to remove very rare cases where 1 or 2 points are clearly out of the curve): on sliding windows of 11 frames, points that were $>$ or $<$ to 25% or 75% $\pm$ IQR (Inter Quantile Range) were removed.

6.3.3 Cell cycle transitions keypoint analysis

A complementary efficient measure to that of single-cell trajectories was to collect volume measurement at key-points of the cell cycle (birth, G1/S transition and mitosis). This was important because the software enabling automated tracking of single-cell took long to optimize. Meanwhile, we implemented the home-made Matlab software previously developed by Sylvain Monnier Zlotek-Zlotkiewicz et al. (2015) in order to record volume, cell cycle time and lineage information at key-points in the cell cycle. We performed the following controls to validate this approach:

1. It was previously shown in the lab that volume shows an abrupt change of $\approx 20\%$ at mitotic onset Zlotek-Zlotkiewicz et al. (2015). To ensure that our measurement of volume at mitosis and birth were taken outside of this specific overshoot, we defined mitosis as the time-point occurring 60 minutes before cytokinesis and birth as the time-point occuring 40 mintues after cytokinesis. In figure 6.10, we show that these points are well out of the range of the mitotic volume overshoot (that starts around 40 minutes before cytokinesis and ends 20 minutes after).
2. G1/S transition was assessed by eye as the firt time-point where fluorescent h-geminin is expressed. h-geminin is a protein whose amount rises progressively from S to mitosis; it is then rapidly degraded at the end of mitosis and has therefore been proposed as a marker for S-G2 phase in the famous FUCCI system Sakaue-Sawano et al. (2008) (cell types are discussed in section 6.5). We verified that our visual assessment was in good agreement with fluorescence intensity curve-based analysis of the G1/S transition (figure 6.10).

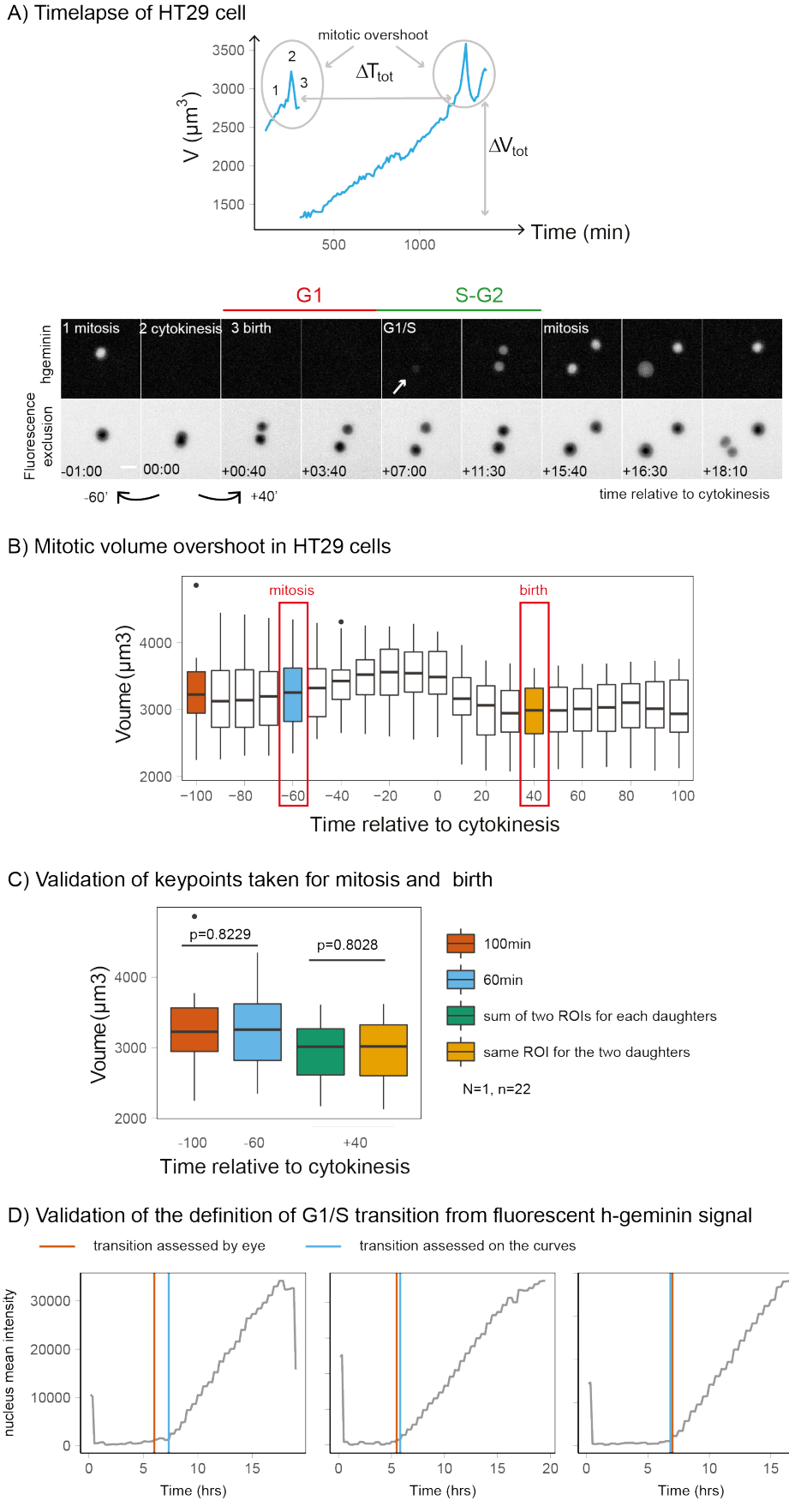

Figure 6.10: Definition and validation of volume measurement at keypoints in the cell cycle. (continued next page)

Figure 6.10: (continued) Definition and validation of volume measurement at keypoints in the cell cycle. A) Timelapse and volume curve of a HT29 cell over a complete cell cycle. The events in the circles correspond to the mitotic volume overshoots. Mitosis and birth are defined as the time-points occurring 60 min before or 40 min after cytokinesis respectively. G1/S transition is identified visually as the first point where fluorescent h-geminin is expressed (white arrow). **B) and C) Definition of mitosis and birth time-points outside of the mitotic volume overshoot.** To measure volume outside the mitotic volume overshoot, volume at mitosis is measured 60 minutes before cytokinesis and volume at birth 40 minutes after cytokinesis. The boxplot in C) shows that 60 minutes before cytokinesis, the average volume is not significantly higher than 100 minutes before cytokinesis, thus indicating that we the measurement is made before the mitotic volume overshoot. We also checked that the manual segmentation of daughter cells just after division was correct despite the cells being still close to each others. To do so, we compared the sum of the volumes of the two daughter cells measured separately (green) with the value obtained when measuring the two cells at once (orange). On average, these two calculation are not significantly different. **D) Validation of the G1/S transition time-point.** The G1/S transition was assessed visually as the first time-point when fluorescent h-geminin appeared in the nucleus. To verify that this method was correct, we compared our visual definition of the transition (red) with a definition based on the analysis of the nuclear fluorescence intensity profile through time (blue). We compared ≈ 10 curves and show here the most imprecise evaluation (left), the average type of error observed (middle) and the best evaluation (right). A quantification of the error made on more cells still needs to be done but this first empirical check shows that on average the error was small.

6.4 Developing tools to induce asymmetrical divisions

At the beginning of this PhD, we hypothesized that artificially inducing asymmetrical divisions of either total cytoplasmic content or specific organelles could be an interesting tool to study size homeostasis and intracellular homeostasis Cadart et al. (2014). We therefore worked on developing tools to induce asymmetries of cytoplasm or mitochondria distribution at mitosis. Since we later focused our work on cell size homeostasis study, our results on artificial segregation of mitochondria remained at a preliminary stage. On the contrary, the micro-channel induced segregation of cytoplasm at mitosis were useful to test the robustness of the size homeostasis mechanism in mammalian cells (figure 2 of the paper in the Results section).

6.4.1 Inducing asymmetrical divisions using micro-channels

6.4.1.1 Micro-channels induce asymmetrical cell divisions and allow volume measurement

In order to test the existence of a size-correcting mechanism in animal cells, we developed a tool to artificially induce asymmetrical divisions. This method consists in confining cells in micro-channels: the confinement prevents complete rounding of the cell at entry to mitosis. This induces defects in mitotic spindle positioning Le Berre et al. (2014) and leads to asymmetrical divisions. The other advantage of the confinement is that it enables volume calculation. Because they try to round-up during mitosis, cells take the shape of an approximate cylinder; by measuring the length l of the cell and integrating it over the channel cross section CS, we obtain:

$$V_{cell} \approx l \times CS$$

We tried several cross-section areas ranging from rom 60 to 150 μm^2 and chose the $98\mu m^2$ cross-section area channels ($12.9\mu m$ width by $7.6\mu m$ height) to perform all further experiments because this dimension enabled inducing asymmetrical divisions without inducing too often other defects such as death in mitosis or multipolar divisions. However, if such an event happened, it was systematically removed from the analysis.

This method unfortunately shows a major issue as it revealed to be difficult to guarantee good conditions in micro-channels. Optimization of the micro-channel design was therefore needed to improve nutrient access in the micro-channels.

6.4.1.2 Optimization of the micro-channels device to improve nutrient access

Preserving good growth conditions in a confined environment such as micro-channels over 50hrs long periods of time required some improvements. Indeed, experiments made using the initial chamber design (figure 6.12) showed an important decrease of ΔV, the volume gained per cell, over time during the acquisition. A second design that allowed both a reduction of the number of cells deposited at the entry of the micro-channels and the possibility of easily renewing the medium in the channels was fabricated (figure 6.12). Even without media renewal, this design improved growth conditions in the channels since volume gained became constant and independent of the time in the acquisition. With this design, it is also possible to plug inlet and outlet tubes and deliver a constant flux of fresh medium throughout the experiment, using a pressure controller, a syringe pump or a simple set-up with two tubes at different heights, generating a difference of pressure. All three were tested but it proved difficult to obtain a robust set-up for 50hrs and there were many limitations to such experiments:

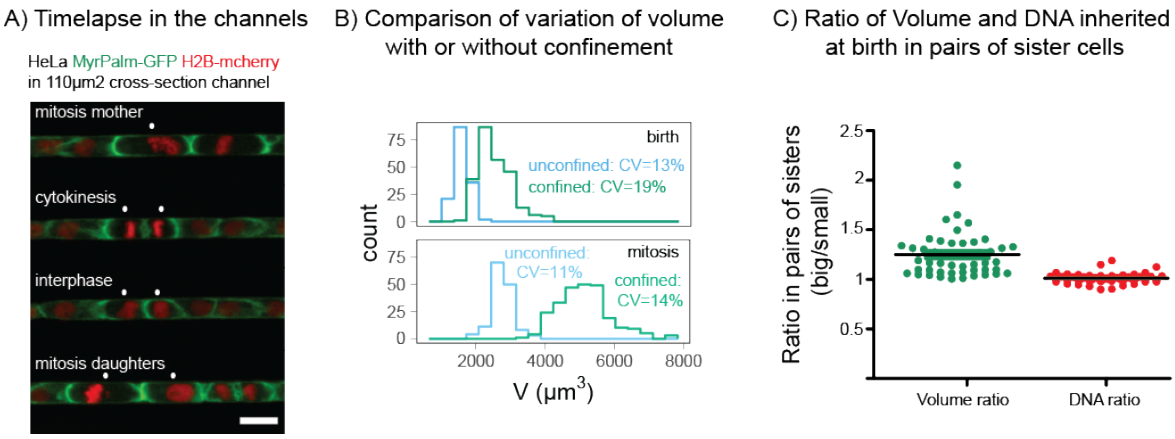

Figure 6.11: Confinement in micro-channels induces asymmetrical divisions. A) Timelapse of a HeLa cells in the microchannels over an entire cell cycle. HeLa cells are MyrPalm-GFP (membrane) H2B-mcherry (DNA). The white point indicate, from top to bottom, the mother cell at mitosis when it rounds up, the daughter cells asymmetrically dividing at cytokinesis, te daughter cells in interphase and the daughter cells roudnign upon entry into mitosis. **B) Comparison of the distribution of volume at birth and mitosis with or without confinement.** The unconfined condition corresponds to cells in the Fxm volume measurement chambers while the confined condition corresponds to cells in $110\mu m^2 CS$ channels. The coefficient of variation of the distributions (CV) are indicated for each conditions. **C) Confinement induces asymmetrical division of volume but not DNA.** DNA ratio was measured by measuring the fluorescence intensity of H2B-mcherry in each daughter cells right after cytokinesis. This ratio is close to 1, thus showing that confinement in the micro-channels did not induce error of segregation of DNA.

appearance of air-bubbles in the system were often stopping fluxes coming in the chambers, it was also complicated to acquire images on more than one or two devices because of the number of tubings on the plate, thus reducing the possibilities of having different conditions.

6.4.2 Asymmetrical patterns

We designed new motifs of asymmetrical adhesive micro-patterns hoping to favor the occurrence of asymmetrical divisions. This trial was based on the observation that RPE1 cells naturally tend to leave long retraction fibers upon rounding at mitosis that eventually lead to asymmetrical volume division when the retraction fiber rejoins the rest of the cytoplasm of one of the two daughter cells at mitosis exit (figure 6.13). Reinforcing that idea, came the observation that asymmetric adhesive micro-patterns initially designed to induce asymmetrical DNA segregation also seemed to induce asymmetrical volume division Freida et al. (2013). The designs were made using AutoCad software. The trials with these micro-patterns were unsuccessful since results showed that: (i) asymmetrical divisions were more likely to happen in the total absence of patterns or on thin $9\mu m$ wide lines where cells can produce retraction fibers of undefined length, (ii) confinement in height using micro-pillars Le Berre et al. (2014) was a more efficient way to induce asymmetrical divisions 6.13.

6.4.3 Drug-induced asymmetrical distribution of organelles

We then moved to chemical and genetic tools to perturb the segregation of mitochondria. Mitochondria structure is the result of the balance between fusion and fission events reviewed in Elgass et al. (2013). Upon mitosis, the activation of cyclinB-Cdk promotes the activation of the main fission actor, DRP1, via the protein RALBP1 Kashatus et al. (2011). Targeting DRP1 using the inhibiting drug Mdivi

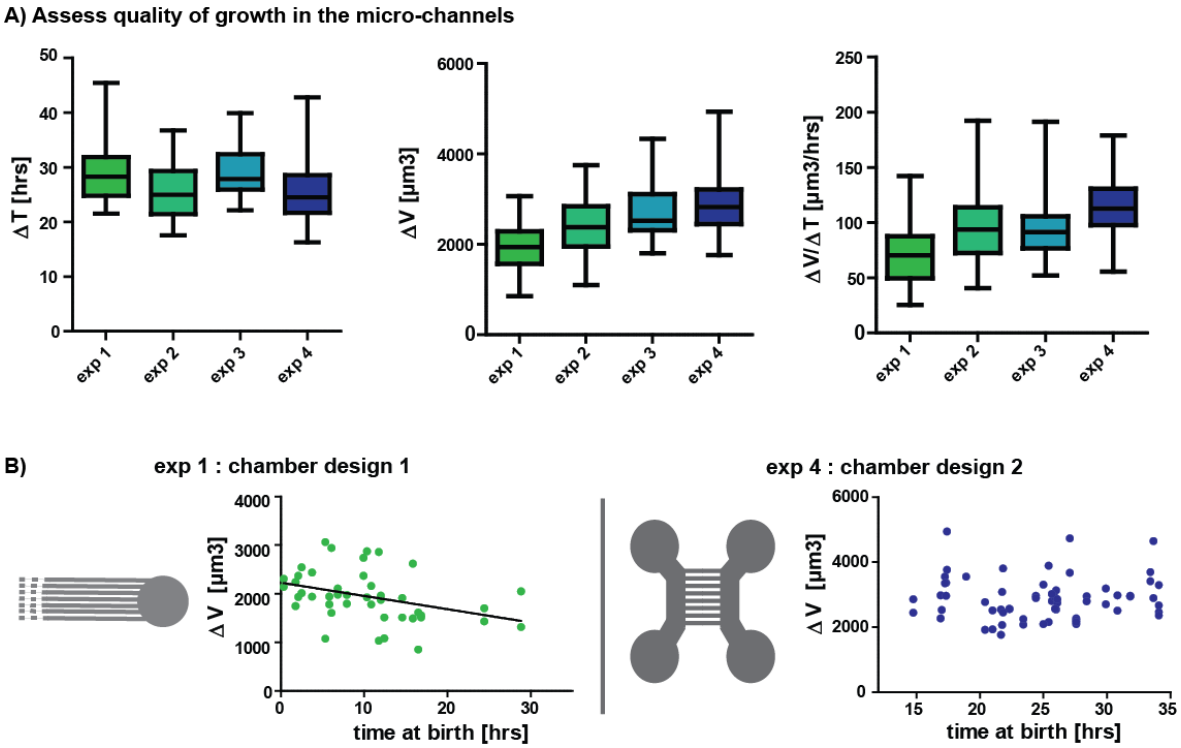

Figure 6.12: Optimization of the microchannels design. ΔV, ΔT, $\Delta V/\Delta T$ were measured in 4 different experiments made on HeLa cells in micro-channels for 50hrs. Variability can to some extend be explained by the quality of nutrient access in the chamber used and the time the experiment was made. Experiment 1 and 2 are made with chamber design 1(cross section of the channels = $102\mu m^2$) where the volume of medium directly accessible to the cells in the channels is small. Experiments 3 and 4 were made with chamber design 2 (channel cross-section=$98\mu m^2$) but experiment 3 was started 24 hours later than experiment 4 (compared to time of cell loading in the chambers): ΔV is the same for these two experiments *(t test, $p = 0.1667$)* and higher than in the previous experiments made with chamber design 1 *(t test: exp1 vs. exp3 and exp4 $p < 0.0001$; exp2 vs. exp3 and exp4 $p = 0.0003$)* ; however, in experiment 3 that started 24 hours later then experiment 4, the growth rate $\Delta V/\Delta T$ is lower than in experiment 4 *(t test, $p < 0.0001$)*, since ΔT is higher *(t test, $p = 0.0006$).(exp1: $n = 44$, exp2: $n = 48$, exp3: $n = 39$, exp4: $n = 62$).*

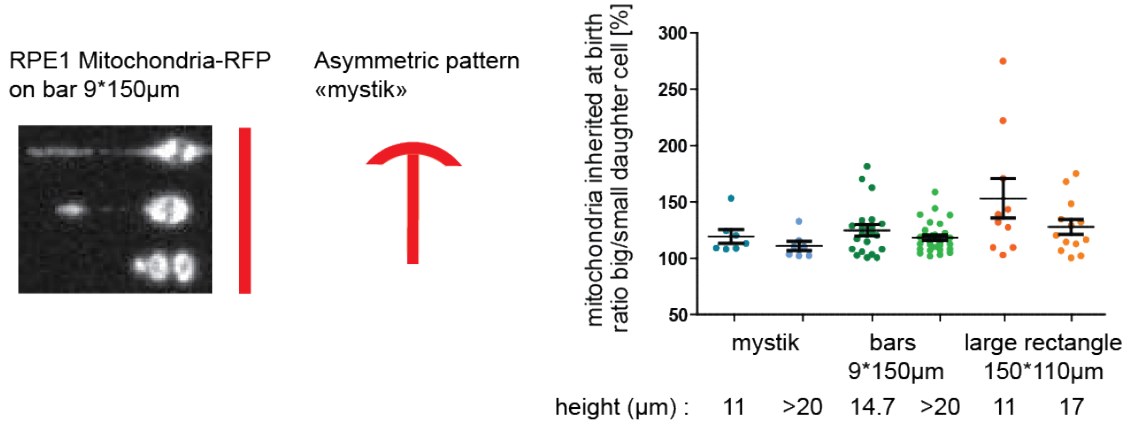

Figure 6.13: Artificially inducing asymmetrical divisions using asymmetric micro-patterns and confinement. Left: RPE1 cells constitutively expressing RFP fused with a Mitochondria Localizing Signal (MLS) on $9 * 150\mu m$ bar pattern, RFP image. **Middle:** Asymmetric pattern 'mystic'. **Right:** Quantification of mitochondria distribution asymmetries in pairs of daughter cells induced by different patterns and confinement in heights. Higher confinement in height leads to more spread distribution of asymmetries on bars and big squares *(t test to compare variances: bars* $9 * 150\mu m$*,* $h = 14.7$ *vs.* $h > 20\mu m$*,* $p = 0.0144$*; large rectangles* $150 * 110\mu m$ $h = 11$ *vs.* $h = 17\mu m$*,* $p = 0.0084$*).* Large rectangles that do not restrict the formation of retraction fibers in any directions induce a wider distribution of asymmetries than $9 * 150\mu m$ bars in the absence of confinement *(t test to compare variances: large rectangle* $h = 17\mu m$ *vs. bars* $9 * 150\mu m$*,* $p = 0.0146$*).*

or RNAi silencing revealed to be not ideal since it induced very long delays of mitosis and overall cell cycle length. RNAi silencing of Myo19, a non-conventional myosin that was recently reported to induce asymmetrical divisions in HeLa cells Rohn et al. (2014) seems on the contrary very promising since it induces asymmetrical mitochondria divisions without delaying the cell cycle in RPE1 cells (figure 6.14).

6.5 Choice of cell types

6.5.1 Description of the cell types used in this study

The cell types we chose for our study are HeLa cells, HT29, MDCK and Raji cells.
HeLa cells are human epithelial cells from adenocarcinoma. These cells have huge aneuploidy with a mean number of chromosomes of 82 (range 70 to 164, source: ATCC). These cells thus show important variability and are not an optimal system for cell growth and cell cycle progression studies. However they are useful to compare our results with previously established results on adherent cells Kafri et al. (2013). In addition to that, stably expressing HeLa-FUCCI cells were already available which made them attractive to track the distinct phases of the cell cycle Sakaue-Sawano et al. (2008). We used HeLa Kyoto either stably expressing MyrPalm-GFP (membrane marker for the experiments in the micro-channels) or the FUCCI system.
HT29 are human cancerous cells coming from colorectal adenocarcinoma. They have a model number of 71 chromosomes ranging from 68 to 72 (source: ATCC). These cells have four main interests: they have already been used in size homeostasis studies Park et al. (2010),Sung et al. (2013), they do not migrate much which makes them easy to track, they have a simple spherical shape which first helped making sure that volume fluctuation measured were not due to shape fluctuations but actual volume changes, they seem to show robust and reproducible behaviors in our hand. However, these cells are

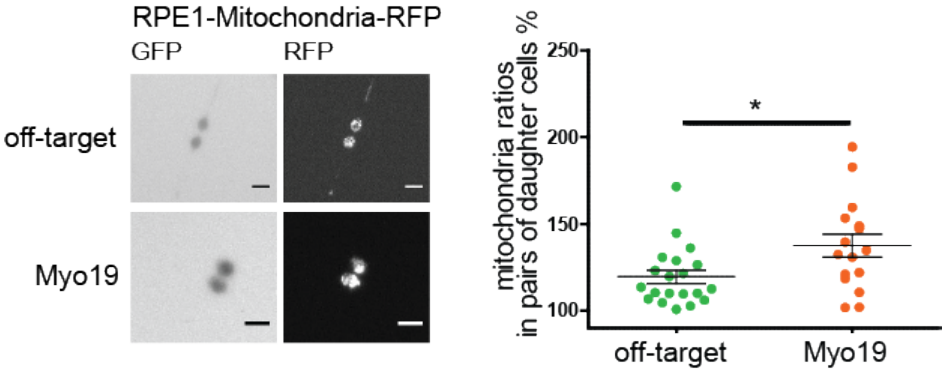

Figure 6.14: Asymmetrical division of mitochondria induced by Myo19 RNAi. Left: RPE1-mitochondria-RFP in volume measurement chambers filled with dextran (signal in GFP), scale bars = $20\mu m$. **Right:** Myo19 RNAi induces asymmetrical distribution of mitochondria at birth (ratios calculated in pairs of daughter cells, t test comparing means: $p = 0.0187$; t test comparing variances shows non-significant different: $p = 0.0746$).

very adherent to each other which makes it difficult to obtain single-cell trajectories over full cell cycles.

MDCK were derived from the kidney of an apparently normal female dog in 1958 (source: ATCC). They however are hyperdiploid with a modal chromosome number ranging from 77 to 80 or 87 to 90 (instead of 78 normally in that specie). As they seem to have reproducible behaviors in our hand and an MDCK-FUCCI cell line already exists, they would be an interesting tool. Unfortunately, they are very attached to each other which make them poorly suitable for single-cell tracking. We therefore used the cells for the micro-channels experiments and not in the Fxm chambers.

Finally, Raji cells are human B lymphoblast of stable diploid karyotype that were derived from a lumphoma in 1963 (source: ATCC). These cells enabled us comparing our results to results obtained in lymphoblastoid cells: in Son et al. (2012), the authors use mouse lymphoblastoid cells FL5.12 and L1210. Unfortunately, we could not reproduce the author's measurements on L1210 in our set-up because they eat the fluorescent probe used for volume measurement.

Overall, our study would benefit from reproducing the observations made on HT29 with an other adherent cell type. RPE1 which are human immortalized cells from the retinal epithelium could be a good candidate: they are near-diploid and they were already used in cell cycle studies. We built a stable cell line expressing RPE1-hgem-mcherry and we are currently trying to reproduce the previous results with these cells.

6.5.2 Establishing new stable lineages

To generate MDCK-MyrPalm-GFP, HT29-hgem-mcherry and RPE1-hgem-mcherry stable cell lines, we optimized an electroporation protocol because transfection with lipofectamine gave poor results on these cell types. Cells were electroporated and then selected for antibiotic resistance. Each lineages were then FACS-sorted to obtain a polyclonal population homogeneous in fluorescence.

6.6 Statistical analysis

All the analysis was made using R software.

Optimization of the linear fit method In order to analyze simple linear correlations between measurements, a common approach is to perform linear fits. We tried several ways to perform this fit (figure 6.15) before finding the method that most robustly described our data, considering their noise and relatively low statistical power ($n \approx 100 - 300$ events). In the end we chose a classic linear fit performed on median bins and weighted by the number of event in each bin. The number of bins for the analysis on our small data-sets was usually arbitrarily set to 8 and bins containing less than 8 observations were automatically excluded from the fit measurement. For the analysis of the bacteria data sets coming from Osella et al. (2014); Iyer-Biswas et al. (2014); Wallden et al. (2016), the number of bins and limit was adapted to the number of observations since some data-sets contained more than 4000 events.

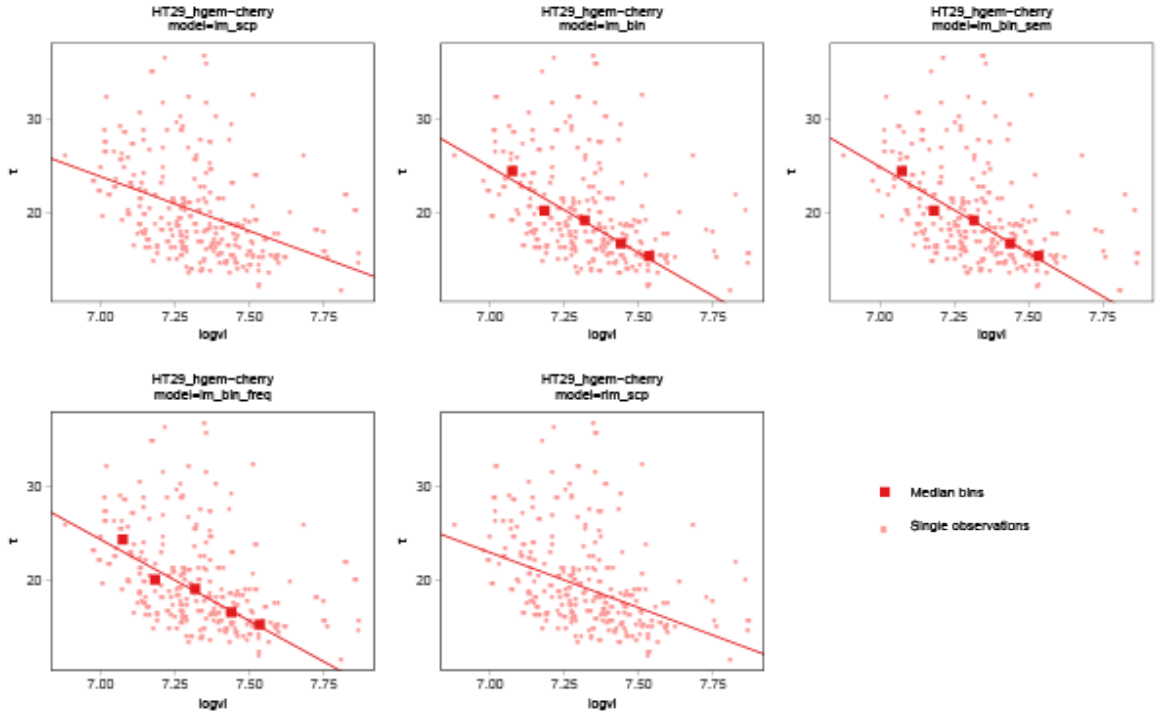

coefficients estimation

	model	beta (y intercept)	alpha slope
1	lm_scp = linear fit on scatter plot	105.0940	−11.61159
2	lm_bin = linear fit on median bins	153.4609	−18.37602
3	lm_bin_sem = linear fit on median bins, weights =SEM	154.2829	−18.48593
4	lm_bin_freq = linear fit on median bins, weights = n	146.2600	−17.40718
5	rlm_scp = robust linear fit on scatter plot	105.6136	−11.79918

pvalue

	model	beta pval	alpha pval
1	lm_scp	5.3878e−15	9.6516e−11
2	lm_bin	0.0038591	0.0056620
3	lm_bin_sem	0.0526740	0.0640242
4	lm_bin_freq	< 2.22e−16	< 2.22e−16
5	rlm_scp	1.97327431253162e−18	1.32540297282981e−13

standard−error

	model	beta stderror	alpha std error
1	lm_scp	12.553382	1.7117056
2	lm_bin	18.822645	2.5745919
3	lm_bin_sem	26.819776	3.6743597
4	lm_bin_freq	2.434169	0.3327512
5	rlm_scp	11.062398	1.4987766

Figure 6.15: Optimization of the linear fit method. Using a typical set of data analyzed in our study, 5 different approaches are compared: (1) linear fit on the single observations (lm_scp), (2) linear fit on the median bins, (3) linear fit on the median bins weighted by the standard error on the mean (SEM) of each bin (lm_bin_sem), (4) linear fit weighted by the number of observations in each bin (lm_bin_freq) and (5) a robust fit on the single observations calculated with the 'MASS' package from R (rlm_scp). The accuracy of the fit is assessed visually by checking which represents best the data and is less sensitive to outliers.

RESULTS

Chapter 7

Results

7.1 Summary **93**
7.2 Manuscript in preparation for submission **95**
7.3 Concluding remarks **139**
7.3.1 Analysis planed before the submission 139
7.3.2 Important experiments needed to complete the work 139

The results obtained during this PhD are briefly summarized and then presented in the format of the manuscript in preparation for submission.

7.1 Summary

The way unicellular organisms such as yeast or bacteria maintain homeostasis is thought to occur through an adaptation of cell cycle progression to growth Turner et al. (2012); Osella et al. (2017). This ensures that for these cells, which most often grow exponentially, large cells at birth will grow for less time than small cells so that they grow less, relatively to their initial size, than small cells. At the phenomenological level, the relationship between initial and final size defines the strength of size control and ranges from perfect size control, where all cells reach the same final size before dividing ('sizer'), intermediate size control, where all cells add the same amount of size per cell cycle ('adder') and no control, where cells grow by the same amount of time and diverge in sizes if they grow exponentially ('timer') (section 2.1). Recent technological developments enabled high-throughput measurement of single cell growth in bacteria Wang et al. (2010); Iyer-Biswas et al. (2014) and yeast Nobs and Maerkl (2014) and led to the observation that the adder behaviour was very common across bacteria and daughter cells of *S. cerevisiae* Campos et al. (2014); Taheri-Araghi et al. (2015); Deforet et al. (2015); Santi et al. (2013); Soifer et al. (2016). Such a characterization, at the phenomenological level, of size homeostasis behaviour in mammalian cells is still lacking.

How size homeostasis is achieved in mammalian cell is in fact highly debated. First, studies showing that some mammalian cells grew linearly Conlon and Raff (2003) or that growth and cell cycle progression were independently regulated at the organ level in *Drosophila in vivo* Edgar (2006); Lloyd (2013), raised a doubt about the existence of active size control through the coordination of these two pathways. Second, although early work had suggested that progression through G1 was size-dependent Killander and Zetterberg (1965); Dolznig et al. (2004), similarly to what has been shown in *S. cerevisiae* Johnston (1977); Hartwell and Unger (1977), more recent work rather provided evidence that growth rate displayed modulations that could participate in size control Son et al.

(2012); Tzur et al. (2009); Kafri et al. (2013). Third, very few characterization of growth at the single cell level have been reported and their conclusions vary depending on the cell type, size parameter and methodology used. Given the difficulty of measuring cell volume in adherent mammalian cells, which shape constantly fluctuates, most approaches favored the measurement of cell mass Sung et al. (2013); Mir et al. (2011); Park et al. (2010), buoyant mass Godin et al. (2010); Son et al. (2012) or protein amount Kafri et al. (2013). Volume was measured on suspended cells that have spherical shapes Tzur et al. (2009). Moreover, most of the studies did not capture dynamic measurement and rather mathematically inferred single cell behaviours from population measurements Tzur et al. (2009); Kafri et al. (2013); Sung et al. (2013). Together, these studies concluded that growth was exponential, at least in some parts of the cell cycle Son et al. (2012); Tzur et al. (2009); Mir et al. (2011); Sung et al. (2013); Godin et al. (2010).

To characterize cell size homeostasis behaviour in mammalian cells, direct and dynamic measurement of cell size through complete cell cycles is crucial. We used two techniques enabling single cell volume measurement. The first method relies on confinement in micro-channels Cadart et al. (2014). The second method is based on fluorescence exclusion (FXm) Zlotek-Zlotkiewicz et al. (2015); Cadart et al. (2017) and enables single cell volume measurement. Improving this technique and adapting it to the study of complete cell cycles, where growth conditions are maintained constant throughout long experiments (24 to 50 hours), required several developments and took the longest part of this PhD (methods, 6.2). When these developments were made, we could provide the first set of data reporting single cell volume measurement in mammalian cells throughout complete cell cycles. These measurements, together with the ones acquired with the micro-channels and the analysis of previously published data on L1210 cells Son et al. (2012) enabled providing the first evidence that the adder was the most common behaviour in mammalian cells.

We also observed that cell growth was overall exponential during the cell cycle for both HT29 and HeLa cells, consistent with previous direct or indirect findings Son et al. (2012); Tzur et al. (2009); Mir et al. (2011); Sung et al. (2013); Godin et al. (2010). In this case, cell cycle progression must be coordinated to cell growth in order to enable small cells, that grow slowly, to gain the same absolute amount of volume than large cells. To test this hypothesis, we therefore combined FXm volume measurement with cell-cycle tracking Sakaue-Sawano et al. (2008). We found that G1 duration was inversely correlated with initial volume, thus confirming results from indirect approaches that had suggested that size control occured during this phase Dolznig et al. (2004); Killander and Zetterberg (1965). However, large cells seemed to saturate this time adaptation and proceed through G1 in a constant, minimal time that was near 4-5 hours. These large cells however still displayed a homeostatic behaviour, which would be impossible if they grew linearly.

To further investigate whether growth was different in these large cells, we artificially generated large HeLa cells through a 48 hours roscovitine-induced cell cycle block. Under this treatment, cells are blocked in the cell cycle Meijer and Raymond (2003) but keep growing and therefore reach volumes that are 1.7 fold higher than the average control cells. In these large HeLa cells, G1 duration was around 4-5 hours and was not negatively correlated with initial volume. Moreover, preliminary results suggested that these cells grew linearly. The combination of linear growth with a near constant cell cycle time yielded an effective adder behaviour. Our results therefore point to three distinct processes that modulate cell growth or cell cycle progression and appear depending on the conditions: (i) a size-dependent progression through G1; (ii) a minimal timer in G1 and (iii) a non-linear dependence of growth rate on size.

To study how modulations of growth and cell cycle progression contribute to the effective size homeostasis behaviour, we established a mathematical framework that applies to all kinds of proliferating cells, from bacteria to mammalian cells. This analysis points to the robustness of the adder behavior in single cells across kingdoms, although this behavior can emerge from a variety of

coupling between cell growth and cell division cycle.

Our work provides the first direct and dynamic measurement of cell volume through complete cell cycles on several cell types and enables concluding that the adder is the most common homeostatic behaviour. Moreover, our results points to several processes limiting or modulating cell cycle progression and cell growth and participating in cell size control. The first one is a volume-dependent progression through G1, reminiscent of the size control mechanism found in *S. cerevisiae*. Given the similarities with *S. cerevisiae* Fisher (2016), the molecular mechanisms currently debated in this yeast to explain size control in G1 Schmoller et al. (2015); Soifer et al. (2016); Delarue et al. (2016) are a starting point for the study of the equivalent mechanism in mammalian cells. The second process we identify is the existence of a minimum G1 duration, reminiscent of the minimal G1 duration defined by APC_{Cdh1} levels recently identified in mammalian cells Cappell et al. (2016). Finally, the third process is a non-linear modulation of growth rate as a function of size where growth rate saturates for very large cells. This result echoes previous observations in L1210 Tzur et al. (2009); Son et al. (2012) and HeLa cells Kafri et al. (2013), although our interpretation of this result does not go as far as speculating on an active growth rate regulation as suggested by some authors Kafri et al. (2013); Ginzberg et al. (2015); Ginzberg (2015). It is possible indeed that more general constraints on cell metabolism or surface-to-volume ratio explain this non linear dependence of growth rate on cell size Miettinen and Bjo (2015); Glazier (2014). Possible interpretations and developments for each of these three observations are further discussed in the discussion (chapter 8).

Overall, our work brings a significant contribution to the study of cell size homeostasis in mammalian cells by providing the first characterization of the homeostatic behaviour at the phenomenological level and identifying some of the important growth and time modulation contributing to size control.

7.2 Manuscript in preparation for submission

Size homeostasis in mammalian cells involves several growth or time-dependent limiting processes

Authors:

Clotilde Cadart, Sylvain Monnier, Jacopo Grilli, Jacopo Marchi, Rafaele Attia, Emmanuel Terriac, Buzz Baum, Marco Cosentino-Lagomarsino, Matthieu Piel

Abstract

Whether size control exists in mammalian cells and whether it relies on a modulation of growth or cell cycle progression is currently debated. Answers to this question have been limited by the difficulty of directly measuring growth at the single cell level. We report the first direct measurement of single cell volume over complete cell cycle trajectories in mammalian cells. This enables showing that the most common homeostatic behavior for these cells is that of an adder. This behavior is the result of an adaptation of G1 duration to volume at birth and a saturation of growth rate for large cells. We establish a mathematical framework to compare the size homeostasis mechanism from bacteria to mammalian cells and show that although the adder at the phenomenological level is very common, it arises from a variety of coupling between growth and time modulations.

Introduction

Cells exist in a large variety of shapes and sizes, but most single celled organisms and cell types display a stereotypical shape and steady-state size distribution for a given set of environmental parameters. Understanding how proliferating cells maintain this distribution of sizes through cycles of growth and division has recently made spectacular progresses (Sauls, Li, and Jun 2016). This was made possible thanks to live cell imaging and quantitative image analysis combined with the development of microfluidics platforms which maintained a constant number of cell and amount of nutrients throughout the experiments(Wang et al. 2010; Iyer-Biswas et al. 2014). In model single celled organisms, such as bacteria and yeasts, which have a simple shape due to a rigid cell wall, the natural measure of size has been cell volume, and other morphometric parameters such as surface area, length, diameter or width which can be measured directly by detection of cell boundaries on transmitted light images. Implementation of automated algorithms gave access to a large number of single cell measures, combined with detection of cell division cycle stage. These rich datasets helped define a small number of simple rules for cell size homeostasis in these organisms (Sauls, Li, and Jun 2016) .

Cell size homeostasis in proliferating cells is achieved through adapting the amount of growth produced during one cell division cycle to the initial size of the cell: large cells should grow less while small cells should grow more, relatively to their initial size. The strength of this correction varies. Size homeostatic behaviors are usually sorted into three main categories: the sizer, the adder and the timer. Historically, the most famous model for size homeostasis is that of the sizer where a size threshold restricts the transition to the next event of the cell cycle. This ensures that the entry into the next phase of the cell cycle is not triggered until the size threshold is reached. The classical example of a sizer behavior is that of the yeast *S. Pombe* (Fantes 1977).

Alternatively, the adder mechanism relies on the addition of a constant amount of growth at each cell cycle, independently of initial size (Amir 2014; Voorn and Koppes 1998), leading to a convergence of cells with too big or too small size at birth, toward the mean added volume. This was observed in several datasets for bacteria and daughter cells of budding yeast (Campos et al. 2014; Taheri-Araghi et al. 2015; Soifer et al. 2016). Growing by a constant amount could simply be achieved combining linear growth and a constant cell cycle time (a process called ‘timer’). But in most cells and conditions studied, growth was reported to be exponential, and the timer mechanism would thus not ensure homeostasis, because bigger cells would grow more than small cells. Importantly, the phenomenological description of the size homeostatic process using the terminology of sizer, adder or timer only defines the rate of size convergence in a population of proliferating cells, and several distinct molecular mechanisms can achieve the same global behavior. Moreover, the simple categories of sizers, adders, etc. are only extreme cases of complex correlation patterns that may occur between size, duration of the cycle, and growth during different cell-cycle stages. The entry time into the next stage may depend on both size and time (‘concerted control’ (Osella, Nugent, and Cosentino Lagomarsino 2014)), or an “Imperfect” adder or sizer (Jun and Taheri-Araghi 2015). Additionally, different cell-cycle sub-periods may be subject to different controls (Adiciptaningrum et al. 2015; Wallden et al. 2016; Delarue, Weissman, and Hallatschek 2016), so that the overall emergent pattern could become complex. These factors make it all the more remarkable that in some cases simple patterns, like a near adder, were observed.

Standard hypotheses for size regulatory mechanisms postulate a coupling of the cell division cycle control network with a pathway which provides a measure of a cell size related parameter. The two best studied pathways rely, in budding yeast, on dilution of a negative regulator of cell division cycle

entry (activation of G1 cyclins,(Schmoller et al. 2015)), and in fission yeast, on the accumulation of a positive regulator of mitotic entry in a specific region of the cortex proportionally to surface area (Pan et al. 2014). In bacteria, which do not have cyclins, titration was proposed to depend on added surface area (Harris and Theriot 2016) or the accumulation of a constant amount of volume per replication origin (Zheng et al. 2016; Ho and Amir 2015), possibly via the titration of the protein DnaA on replication origins (reviewed in (Robert 2015) . In all these cases, regulation relies on a titration phenomenon with a threshold value triggering entry in the next phase of the cycle.

In multicellular organisms, the question of size regulation is more complex because, as studies suggest in *Drosophila,* growth and proliferation are also determined at the organ or body level both during developmental programs and at the adult stage to maintain tissue homeostasis (Edgar 2006). Examples of such extrinsic control of cell size are rife and led some authors to doubt the importance of an intrinsic regulatory mechanism coordinating growth and cell cycle progression at the single cell level (Lloyd 2013; Edgar 2006). This however remains debated because no model currently explains how metazoan cells, both in tissue and cell culture maintain size uniformity (Ginzberg, Kafri, and Kirschner 2015). Importantly, loss of cell size uniformity is a marker of tumorigenic transformation (Ginzberg, Kafri, and Kirschner 2015). Evidence of a size or growth dependent progression through G1, which could indicate cell size control, was reported in cultured mammalian cells (Killander and Zetterberg 1965; Dolznig et al. 2004), and *in vivo* in *Drosophila* cells (Edgar 2006), reminiscent of what has been observed in budding yeast (Johnston 1977; Hartwell and Unger 1977).

Cultured animal cells, just like single celled organisms, maintain a distribution of sizes through cycles of growth and division. Contrary to bacteria and yeasts, cultured mammalian cells display complex and fast changing shapes. As a consequence, the natural choice for measures of cell size is less clear and a variety of parameters related to cell size have been investigated, such as cell mass (Park et al. 2010; Sung et al. 2013; Mir et al. 2011), buoyant mass (Son et al. 2012) or density (Grover et al. 2011). These measurements almost always involved indirect methods (Popescu et al. 2014). Morever, animal cells often display long cell division cycles (typically around 20 hours long), thus requiring non-invasive and stable measurement methods and limiting the throughput of the measurement. For this reason, most of the studies on animal cell growth were performed at the population level (Ian Conlon and Raff 2003; Dolznig et al. 2004; Echave, Conlon, and Lloyd 2007; Killander and Zetterberg 1965), with a few attempts to mathematically extrapolate growth dynamics from size measurement at fixed time-points (R. Kafri et al. 2013; Sung et al. 2013; Tzur et al. 2009). Recently, several studies reported single live cell measurement of mass (Mir et al. 2014; Park et al. 2010) or buoyant mass (Son et al. 2012) on animal cells over complete cell cycles.

Altogether, these works raised the hypothesis that growth rate, although exponential on average, is modulated at some specific points of the cell cycle and participates in cell size control. Direct evidence supporting this was provided for lymphoblastoid cells, which display no significant cell cycle time modulation but for which the growth rate was found to be slower in large cells than in small cells at G1/S transition (Son et al. 2012). The role of time modulation in G1 which had been hypothesized in earlier work (Dolznig et al. 2004; Killander and Zetterberg 1965) was not always confirmed by these more recent studies, although the question remains open, as there has been no extensive studies of single cell growth trajectories over entire cell division cycles.

While this recent body of literature on cultured mammalian cells homeostasis clarified several important questions, it remains difficult to compare what is known on bacteria and yeasts and on mammalian cells. For example, the simple question of the relation between final volume (at mitosis onset) and initial volume (at birth) for individual cultured mammalian cycling cells, has not been

documented yet. As a consequence, it is not known if mammalian cells behave more like adders, sizers or timers or do not follow any simple rule. This lack of answer to such basic questions is primarily due to a methodological issue: there has been no direct measurements of single live animal cells sizes (for example volume) through cycles of growth and division, performed on a large enough number of cells to obtain reliable statistics. The available datasets are indirect (measure of phase shift to infer dry mass (Sung et al. 2013; Mir et al. 2011), or buoyant mass to infer mass and volume (Son, et al. 2012; Godin et al. 2010; Grover et al. 2011), and/or performed on a too small number of cells through entire cycles (for example (Son et al. 2012) provides the most precise measure of buoyant mass on complete cycles for single cells, but only on 49 cells, and only on 18 cells combined with cell cycle markers). It appears important to bridge that gap in knowledge for cultured mammalian cells. The generality of the models proposed for size regulation in yeasts and bacteria make it likely that some will apply also to mammalian cells. Most of these mechanisms rely on titration effects and thus point to the importance of cell volume as a central parameter to couple growth and cell division cycle progression.

We recently developed a method to precisely measure the volume of single live cells over several days, on a large number of cells, independently of their shape (Cadart et al. 2017; Zlotek-Zlotkiewicz et al. 2015). This method, which we also coupled to live cell measure of dry mass by quantitative phase microscopy, can overcome the current technical limitations for the study of cultured mammalian cells size homeostasis and provide the datasets required to answer the main elementary questions related to size homeostasis in mammalian cells. In this article, we measured the size of hundreds of cells, for several immortalized cultured mammalian cell lines, over up to 50 hours, covering two complete cell cycles. This revealed, that the so called ‘adder’ is, like in bacteria and yeasts, the most common behavior followed by mammalian cells in culture. Combining this study with live cell markers of cell division cycle stage, we found that this apparent adder was achieved, despite a global exponential growth, thanks to a modulation of G1 duration according to initial cell size. We identified three distinct constraints on cell growth and cell cycle progression: (i) G1 duration is size-dependent with small cells spending more time than large cells; (ii) G1 duration is also gated by a minimal time; (iii) growth rate saturates and becomes linear for very large cells. In order to compare the behavior of proliferating single cells, from bacteria to mammalian cells, we propose a general unbiased mathematical framework. This analysis points to the robustness of the adder behavior in single cells across kingdoms, although this behavior can emerge from a variety of coupling between cell growth and cell division cycle. We further speculate on the physical and evolutionary origin of this apparently universal behavior in cultured cells and on the limits of its physiological relevance. Our study constitutes the first direct observation of cell size homeostasis through cycles of growth and division for cultured mammalian cells and reveals the elementary rules underlying this phenomenon.

Results

Single cell measurement of volume over complete cell cycles with a good throughput

Cultured mammalian cells display a broad range of sizes (Ginzberg, Kafri, and Kirschner 2015) (Figure S1A), which is due in part to the various cell cycle stages present in a population of cycling cells, and in part to the distribution of their size at birth. It is a general belief that proliferating cultured cells double their size between two divisions, yet the relation, for single cells, between their size at mitotic entry and their size at birth, has never been reported for cultured mammalian cells.

To establish this relation, it is necessary to track single proliferating cells and measure the volume of the same cell at birth and at mitotic entry. We implemented two distinct methods to obtain these measures. First, we grew cells inside microchannels of a well-defined cross-sectional area (Figure S1B, and (Cadart et al. 2014)). In such a geometry, dividing cells occupied the whole section of the channels and we could infer their volume from their length, like for yeasts and bacteria. The second method we used was based on fluorescence exclusion (FXm, (Zlotek-Zlotkiewicz et al. 2015; Cadart et al. 2017), Figure 1A) and has been optimized for long term recording and automated analysis of populations of growing cells ((Cadart et al. 2017), Figure S1C). It is more precise than the channels method and also produces complete growth trajectories for single cells (Figure 1B, Figure S1D). Visual inspection of the movies was used to determine key points in the cell division cycle for each single cell tracked. The most precise reference point is cytokinesis onset. Volume at birth was defined as the volume of a daughter cell 40 minutes after cytokinesis onset, while volume at mitotic entry was defined as volume of the same cell 60 minutes prior to the next cytokinesis onset (Figure 1B). These intervals were chosen to avoid the period of volume overshoot corresponding to mitosis (Zlotek-Zlotkiewicz et al. 2015; Son et al. 2015) (Figure S1E). We verified that the sum of the volumes of the two daughter cells at birth corresponded to the volume of the mother cell prior to mitotic entry, when birth and mitotic entry volumes were determined this way (Figure S1E-F). For each experiment performed, the dataset was checked for quality: we verified that the distribution of volumes at birth and the average growth rate did not change throughout the experiment (Figure 1C and Figure S1H), and that these values did not change from one experiment to another (Figure 1D). Experiments which did not match these quality criteria were eliminated from the dataset. Single growth trajectories were also examined and showed a steady growth (Figure S1D), and analysis of growth rates as a function of size, for a large number of single cells and cell aggregates showed global exponential growth, as expected (Figure S1G) (Tzur et al. 2009; Mir et al. 2011; Sung et al. 2013; Son et al. 2012). We were thus able, with these methods, to produce fully validated high quality datasets of single cell volume along cycles of growth and division, which can be further used to ask elementary questions on volume homeostasis for proliferating cultured mammalian cells.

The adder is the most common homeostatic behavior to mammalian cells

The first elementary question is the relation between the added volume and the volume at birth. We thus made that plot, together with the equivalent plot of volume at mitotic onset versus volume at birth, for each cell line and condition in our dataset (Figure 2A and Figure S2A). If cells were doubling their volume, the added volume would be equal to the volume at birth, thus the two values would linearly correlate with a slope of 1, and the final versus initial volume plot would show a slope of 2. On the other hand, if cells were perfectly correcting for differences in size, added volume would be smaller for bigger cells, so the slope would be negative, while the final volume would be identical for all cells independently of their initial volume. We found neither of these two extremes. With the exception of Raji cells (human B lymphoblast), which showed a large dispersion of added volumes,

and for which added volume slightly correlated with initial volume, we instead found that added volume showed no correlation with initial volume. Consistently, the volume at mitotic entry showed a clear linear correlation with volume at birth, with a slope close to 1 (Figure 2B), suggesting that cells grow by the same amount, in average, independently of their volume at birth. This growth behavior is known as an adder, and was already described for several bacteria species and for the buds of budding yeast cells (Campos et al. 2014; Taheri-Araghi et al. 2015; Soifer et al. 2016). This weak form of volume homeostasis was shown, theoretically and experimentally for bacteria and yeasts, to be enough to maintain a constant size distribution in a population of growing cells (Amir 2014) and should compensate for asymmetries in sizes during division. A direct prediction is that, after an asymmetric division, the difference in size of the two daughter cells would be reduced by half in one division cycle, but not completely compensated. We artificially induced asymmetric divisions by growing cells in microchannels. Confinement prevents mitotic rounding which leads to errors in the mitotic spindle positioning and ultimately generates uneven division of the mother cell (Figures 2C and S2B, (Lancaster et al. 2013; C. Cadart et al. 2014)). We then compared the asymmetry in volume, at birth and at the next mitosis, between pairs of daughter cells that had divided inside these channels. We found that their level of volume asymmetry at birth was much higher than in control cells that divided outside of the channels, and that it was significantly reduced at entry into the next mitosis, but not completely compensated (Figure 2D), as predicted with an adder behavior. In conclusion, this first analysis of our dataset revealed that most cultured mammalian cell lines display a typical adder behavior.

G1 duration is negatively correlated with volume at birth

When cells are growing exponentially (Figure S1G) smaller cells grow less, in the same amount of time, than large cells. A simple way for small cells to add as much volume as big cells, is to grow for a longer time. This modulation of cell cycle duration, which is well established for the budding yeast (Hartwell and Unger 1977; Johnston 1977) was also proposed in the past for mammalian cells (Killander and Zetterberg 1965; Dolznig et al. 2004) but was not verified in more recent contributions (R. Kafri et al. 2013; Son et al. 2012) opening a controversy on this question, with few direct observation available to clarify this point. In our dataset, cells grown in the volume measurement chamber, but not inside micro-channels, showed a longer cell division cycle for smaller cells, (Figure S2A). To investigate this point in more details, we combined cell volume measurements with a classical marker of cell cycle phases, hgeminin-mcherry, which accumulates in the cell nucleus at S-phase entry (Sakaue-Sawano et al. 2008) (Figures 3A and S3A). This new dataset confirmed that, at the scale of the entire cell division cycle, cells added the same amount of volume independently of their volume at birth. During G1 phase, small cells at birth added slightly more volume than large ones, while during S-G2, large cells at G1/S added slightly more volume than small ones (Figure 3B). Consistently, the volume at G1/S transition plotted against volume at birth showed a slope below 1 ($\alpha = 0.7 \pm 0.01$), suggesting a homeostasis mechanism more efficient than an adder, while the slope of the volume at mitosis entry versus volume at the G1/S transition was 1.4 ± 0.02, suggesting a poor homeostasis mechanism (Figure S3A). Consistent with a regulation occurring mostly in G1, the distribution of G1 durations was right-squewed, resembling the distribution of entire cell division cycle durations (Figure S3C), while S-G2 showed a very narrow and symmetrical distribution of durations (test comparing the standard deviation, $p<0.0001$) and the duration of G1 was highly correlated with the total duration of the cell cycle, while it was less for S-G2 (Figure S3D). Plotting the time spent for single cells in a given phase versus its volume at the beginning of that phase, confirmed that smaller cells at birth had a longer G1 phase, while smaller cells at the G1/S transition spent as much time as bigger cells in S/G2 (Figures 3D and S3B). This graph also suggested that there

was a minimal time cells spent in G1, and that dispersion of G1 duration was larger for smaller than for larger cells, which tend to spend only the minimal time in G1. This is well illustrated by the cumulative distribution function of the time spent in G1 for various ranges of volumes at birth (Figure 3E). These data together suggest that, despite an overall exponential growth, smaller cells can add, in average, as much volume as bigger cells, thus achieving an adder behavior, by extending the duration of the G1 phase, while S-G2 phase rather resembles a timer, with a duration independent of size at the G1/S transition.

Abnormal large cells reveal two limit phenomena: a saturation of growth rate for larger cells and a minimal G1 duration

Figure 3D shows a lower limit on the duration of G1 phase, which implies that, if growth was exponential, it would not be possible to have homeostasis for larger cells. To produce larger cells at birth, we arrested cells using Roscovitine, an inhibitor of major interphase cyclin dependent kinases, like Cdk2 (Meijer and Raymond 2003). For this experiment, we used HeLa cells, because HT29 cells, despite long arrest with Roscovitine treatment, only slightly increased their volume. After a 48hours block with Roscovitine, the drug was rinsed, and cells were injected in the volume measurement chamber. Recording started after the first mitosis following the release from Roscovitine. As expected, cells which had been treated with Roscovitine were on average 1.7 fold higher than the controls ($p<0.0001$) (Figure 4A, right axis of the graph). Single cell growth curves showed that Roscovitine treated cells behaved similarly to large control cells (Figure 4A). As expected, they G1 duration was shifted towards a minimal time (Figure 4B right axis) and was on average close to a minimal G1 duration (≈ 4 hours) independently of volume at birth (Figure 4B). Interestingly, this duration was the same as the duration displayed by large control cells. But, surprisingly, large Roscovitine treated cells still grew, during G1, by the same amount of volume than smaller control cells, independently of volume at birth (Figure 4C). If G1 duration is not modulated and larger cells grow by the same amount, an alternative mechanism is a modulation of the growth rate. We thus analyzed single cells growth curves in G1 and plotted their growth rate against their volume. It showed that, while, for control cells, smaller cells displayed a smaller growth rate than larger ones, compatible with an exponential growth, for Roscovitine treated cells, growth rate was independent of size and was similar to the growth rate of the larger control cells (Figures 4D and S4C-F). This suggests that larger cells reached a saturation of their growth rate and instead displayed a linear growth. Consistent with a minimal G1 duration, Roscovitine treated cells, which were as big at birth as larger controlled cells, displayed a G1 duration independent of their volume at birth and equal to the minimal G1 duration found for control cells. They still added the same amount of volume as smaller cells, due to a saturation of their growth rate. By producing larger cells at birth, we were able to observe two limit phenomena: a saturation of growth rate for larger cells, and a minimal G1 duration.

General mathematical framework to compare the homeostatic process from bacteria to eukaryotes

This result prompted us to perform a comparative analysis on our whole dataset, and on other published datasets, to ask how general is the adder behavior and how general are G1 duration or growth rate modulation. In order to be able to perform this comparison, it was necessary to define a simplified mathematical framework (described in SI) applicable to the whole cell cycle or to single cell-cycle stages (to remain simple, we will discuss it hereon for an entire cycle). Motivated by the compatibility with the most commonly observed exponential growth behavior, our model assumes that each cell grows exponentially and chooses its rate from a probability distribution, which may

depend on its volume at birth (and hence perform size correction). Equally, the interdivision time may be chosen based on volume at birth and has a stochastic component. All such correlations are accounted to linear order, motivated by the fact that such linear correlations are able to explain most patterns in existing data (at least for bacteria, (Grilli et al. 2016)). The resulting model is able to characterize the joint correction of size by timing and growth with a small number of parameters.

A first parameter, λ, describes how total relative growth depends on volume at birth. If $\lambda = 1$, the system behaves like a sizer, if it is 0.5, it is an adder and if it is 0, growth is uncoupled from volume at birth. This parameter can be described, for each dataset, by performing a linear regression on the plot of $\log(V_{mitosis}/V_{birth})$ versus of $\log(V_{birth})$ (Figure S5A). The second parameter, γ describes how interdivision time depends on volume at birth. This parameter can again be described, for each dataset, by performing a linear regression on the plot of cell cycle duration ($\tau = \Delta T$) versus $\log(V_{birth})$ (Figure S5B). If this correlation is negative, it means that larger cells will tend to divide in shorter times, hence these cells operate size correction due to a modulation of timing. Finally, the third parameter θ, describes the link between initial size and a variation in growth rate with respect to its mean value. Again, this can be in principle obtained by linear regression, if this measurement is available (e.g. in data from bacteria).

These three parameters are linked by a balance relation, which expresses the concept that the overall size correction results from a combination of timing and growth rate corrections.

$$\lambda = \theta \langle\alpha\rangle \langle\tau\rangle + \gamma \langle\alpha\rangle \langle\tau\rangle \quad \text{(Eq.1)}$$

Additional (less relevant) parameters concern the intrinsic stochasticity of interdivision timing, growth rates and net growth (see SI). For eukaryotes where $\langle\alpha\rangle$ is not accessible, the product $\langle\alpha\rangle \langle\tau\rangle$ was approximated to $\langle G\rangle = \langle \log(V_{mitosis})/\log(V_{birth})\rangle$

Using these dimensionless parameters, it was then possible to compare datasets obtained from different cell types in different conditions and estimate whether they displayed volume homeostasis ($\lambda > 0$) with an adder behavior ($\lambda = 0.5$) or better ($\lambda = 1$). It was also possible to know if homeostasis relied more on time modulation ($\theta > 0$) or growth rate modulation ($\gamma > 0$). For bacteria, which have clearly identifiable exponential growth for single cells, all three parameters can be evaluated directly. We used previously published datasets (Wallden et al. 2016; Osella, Nugent, and Cosentino Lagomarsino 2014) in order to evaluate the validity of the balance relationship expressed by Eq. (1) (Figure S5D). These data were also analyzed using the same framework (Figure 5A). All the datasets mostly fell around the line of $\lambda = 0.5$ indicative of a near-adder behavior. In these datasets, all cells showed a consistent degree of time modulation when performing correction. A small subset also showed positive growth rate modulation, but many also had instead a strong negative growth rate modulation (i.e. growth rate modulations contribute to noise in size instead of correcting it).

The adder behavior emerges from a variety of coupling of growth and time modulations

For datasets in mammalian cells, and particularly our own, the growth rate fluctuations (θ) were not directly measurable. Hence, we assumed the validity of Eq. (1) and evaluate them indirectly as the difference between the other two corrections (λ and γ) (see SI). Each cell line and condition was characterized by one value for each parameter and thus one point on the graph shows γ versus θ. Most cells displayed volume homeostasis close to an adder behavior (all points fell between the lines representing $\lambda = 0.5$ and $\lambda = 0$) (Figure 5B), consistent with the findings from Figure 2B. As

expected, control Hela cells showed a modulation of cell cycle duration, like control HT29 cells, while in large Roscovitine treated HeLa the adder was the result of the combination of a near-constant cell cycle time and linear growth.

For cells that deviate from exponential growth, the model, and equation, are still valid. However, the interpretation of the correlation coefficients as active corrections becomes more delicate. For example, for cells that grow linearly and divide according to a timer, $\lambda = 0.5$, and $\gamma = 0$, so that the control appears to operate fully through growth-rate modulation (which is correct, as there is no timing modulation for a timer). However, the size correction is not active, since there are also strong correlations between α and τ, (α is defined as $1/\tau \,.\log(V_{mitosis}/V_{birth})$) and in the case of linear growth ($V_{mitosis} = V_{birt} \;\; + \nu\tau$) makes it a function of τ. In other words, in this case one has to be careful not to mistake the intrinsic properties of a timer for a linearly growing cells with an active mechanism of growth modulation.

Data obtained from Son et al (Son et al. 2012) on L1210 showed that these cells were also adders, with mostly growth rate modulation (in accordance with the results of that study), but also some level of time modulation, possibly explained by the negative correlation between G1 duration and early growth rate observed in these cells (Son et al. 2012) (Figure 5B, red star). For both mammalian cells and bacteria, no dataset showed a negative time modulation (bigger cells at birth having a longer cell division cycle), while negative growth rate modulation (larger cells with a faster exponential growth rate than smaller cells at birth) was rarer in mammalian cells than in bacteria, but nevertheless observed in some cases (for Raji cells, Figure 5B, black diamond). Our analysis method, by providing a summarized overview of a large dataset comprising various cell types and culture conditions, demonstrated the robustness of the adder behavior, and also revealed the diversity of underlying homeostatic mechanisms, relying either on growth rate modulation or cell cycle duration modulation, even for a given cell line.

Discussion

Size homeostasis in cultured mammalian cells can be described phenomenologically as an adder behavior

Cell size homeostasis, or how cells regulate their size through cycles of growth and division, is one of the central questions of cell biology. Due to technical limitations to measure size related parameters, the progress in answering this question have been slow for animal cells and the current general understanding of this process mostly derives from a large body of indirect evidence (Conlon et al. 2001; Ian Conlon and Raff 2003; Echave, Conlon, and Lloyd 2007; Tzur et al. 2009; Sung et al. 2013; R. Kafri et al. 2013; Dolznig et al. 2004), nurturing controversies which have proven hard to resolve without direct observations at the single cell level. In this study, we used two different methods to follow the volume of single cultured mammalian cells. This provides the first large dataset providing direct size measurement of proliferating cultured animal cells. It allowed us to answer a simple fundamental question: how volume at mitotic entry relates to volume at birth, for single cells. We found, for four different cell lines out of five tested, measured in three different devices, that these two volumes were linearly related with a slope of 1, meaning that the added volume was independent of the volume at birth. This corresponds to what was called an adder behavior in bacteria and yeast. Below, we discuss in more details the significance of this finding and the complexity hidden behind this apparently simple phenomenological description.

Generality of the adder mechanism

Over the past 3 years the adder mechanism was observed in a variety of organisms, from bacteria (Soifer et al. 2016; Campos et al. 2014; Taheri-Araghi et al. 2015; Deforet, Van Ditmarsch, and Xavier 2015) to yeast (Soifer et al. 2016). However, the simplicity and apparent universality of this result could be deceiving.

One limitation comes from the quality of the dataset and analysis method. Indeed, even in studies on bacteria where the number of cells measured can reach several thousands, theoretical work showed that the threshold for detectability of a given homeostatic behavior has not been reached yet (Grilli et al. 2016). To prove the adder, additional experimental perturbations that test its robustness are therefore important. By inducing asymmetric divisions, we are able to provide another evidence of the adder. Our observation validated a strong prediction of the adder behavior: size asymmetry was reduced only by half in one division cycle (Figure 2D) (Sauls, Li, and Jun 2016).

Additionally, the use of the term adder has evolved from a simple phenomenological description of a behavior common to several organisms (Sauls, Li, and Jun 2016), to a more complex picture. The same organism can display a range of effective homeostatic behaviors depending on its growth rate both at the population level (Wallden et al. 2016) and the individual cell level (Kennard et al. 2016); and, within the same population, small cells will show a sizer-like behavior while large cells will show an adder behavior (Delarue, Weissman, and Hallatschek 2016). The adder therefore appears as a behavior resulting from a specific set of external conditions. Understanding whether and how one or several molecular processes result in an effective homeostatic behavior that varies upon environmental condition is the current challenge for research on size homeostasis in bacteria and yeasts.

Modulation of cell cycle timing, with a minimal G1 duration

To understand how cell size homeostasis can be achieved in exponentially growing cells, the simplest hypothesis is a modulation of cell cycle timing, to allow smaller cells to grow longer. Indeed, a role of

the timing of G1/S transition in cell size control, similarly to budding yeast (Hartwell and Unger 1977; Di Talia et al. 2007; Schmoller et al. 2015), has long been hypothesized in mammalian cells (Zetterberg and Killander 1965; Dolznig et al. 2004). Direct measurement of the correlation between G1 duration and initial size had however never been reported in mammalian cells so far. Among the studies that combined dynamic cell mass measurement with cell cycle tracking, only one discussed specific events occurring in G1 and reported a decrease in the variability of growth rate at the G1/S transition and an inverse correlation between early growth rate in G1 and G1 duration (Son et al. 2012). Here we observed, for the two cell lines that we tested, HT29 and HeLa cells, a clear negative correlation between G1 duration and volume at birth (Figures 3D and 4B), thus reinforcing the notion that G1 progression and size are coupled in mammalian cells.

In HT29 cells, progression through G1 depended both on volume and time (Figure 3D), thus suggesting that volume is not the sole variable limiting cell cycle progression for these cells. Given the similarities both at the phenomenological and molecular level between *S. cerevisiae* and mammalian cells (Fisher 2016), it is possible to speculate that time modulation in G1 would depend on dilution of an inhibitor as was proposed for *S. cerevisiae* (Schmoller et al. 2015). Moreover, our results on control HeLa (Figure 4B) and HT29 (Figure 3D) and on Roscovitine induced large HeLa cells (Figure 4B) reveal the existence of a minimum G1 duration of about 4 hours, independent of cell volume. A potential candidate for this minimal period could be the inactivation of the APC-Cdh1 complex which has recently been proposed to set a minimal window of time of 4 hours before the commitment point to S phase in mammalian cells (Cappell et al. 2016). Together with this study, our results raise the hypothesis that G1 comprises two distinct periods: a first period, which length depends on cell size, possibly involving pRb-E2F activation, and a second period of constant duration of 4 hours ending with the inactivation of APC-Cdh1.

Our conclusions about S and G2 phases are less clear. We found that S/G2 duration was less variable than G1 and that it is poorly correlated with total cycle length (Figure S3D). Moreover, there was no correlation between S-G2 duration and volume at G1/S transition in HT29 cells (Figure S3B). A small negative trend was however observed in HeLa cells (Figure S4A), suggesting that this phase has little impact on cell size homeostasis. This could be because, similarly to yeast and bacteria, S duration would be simply dependent on the completion of DNA replication (Zhang et al. 2017). A possible explanation for the slight negative trend observed in HeLa cells is that these cells have very variable amounts of chromosomes and that larger cells, which are more likely to have more chromosomes, could take longer to replicate their genome. What drives the transition from G2 to M remains mysterious in eukaryotes and the possibility that cell size could be the trigger for entry in mitosis remains debated (Mchedlishvili, Jonak, and Saurin 2015).

Exponential versus linear growth rates: saturation for larger cells and limitation for confined cells

Because the exponential character of growth is central to the question of cell size homeostasis (Mitchison 2003; Ginzberg, Kafri, and Kirschner 2015), we measured growth rates for individual cells and for cell aggregates. We found that, in control cycling cells, growth was globally exponential (Figures S1G and S3C). However the picture was more complicated when investigating growth rates from single cell growth curves, in different phases of the cell cycle, and for different sizes. For HeLa cells in the FXm chamber, growth was clearly exponential in G1 but seemed to saturate and become more linear in S/G2 (it did not depend very much on cell size anymore, (Figure S3C-D). Consistently, growth rate was also found to saturate, for the same volume, for Roscovitine induced large G1 cells of the same size as control S/G2 cells (around 2000μm3, Figure S4C and S4E). Remarkably, several published results already suggested, based on indirect measurements, that growth rate is linear or

starts decreasing when reaching very large sizes both for mammalian cells (Ian Conlon and Raff 2003; Tzur et al. 2009; R. Kafri et al. 2013) and unicellular organisms (Marañón 2014; Prescott 1956). This raises the question of how cells grow, and of the factor that can limit growth.

Three types of constraints on growth are discussed: limitations of protein synthesis, nonlinear metabolic scaling with cell size and physical constraints on volume growth via the addition of surface area. A first hypothesis to explain growth saturation for large cells invokes the possibility that protein synthesis rate slows down when mRNA supplies, which depend on the transcription from a finite number of DNA copies become limiting (Hu and Zhu 2014; M. Kafri et al. 2016). A second hypothesis could be that metabolism does not scale linearly with cell volume. This is supported by the recent observation that mitochondria function and cell fitness was maximum at a specific optimal size, after which it starts decreasing (Miettinen and Bjorklund 2016). Finally, it is also possible that limitations to nutrient uptake via the surface area appear as the surface to volume ratio decreases. Our experiments with HeLa and MDCK cells growing inside micro-channels are another potential illustration of such restriction of growth by surface exchange area. Due to the confinement, the surface exchange with the medium was limited and these cells showed indirect evidence of linear growth (they added the same amount of volume in the same amount of time independently of their initial size (Figure S2A)).

Evidence that growth rate can vary as a function of the cell cycle phase also exist although there is no consensus about the precise description of these phenomenon in the literature (Son et al. 2012; Mir et al. 2011) and in our results (Figure S4C-F), perhaps partly due to cell-type specific behaviors. It was proposed that cells could `sense' their size and actively tune their growth rate accordingly (R. Kafri et al. 2013; Ginzberg, Kafri, and Kirschner 2015). Our results and those from the literature do not provide, to our opinion, sufficient evidence for this to date. First, phase-dependent growth rate is well documented in *S. pombe* (Sveiczer, Novak, and Mitchison 1996; Nobs and Maerkl 2014) and *S. cerevisiae* (Bryan et al. 2010; Leitao, Pham, and Kellogg 2016; Ferrezuelo et al. 2012; Goranov et al. 2009) and an interesting hypothesis, consistent with our observation, is that phases of the cell cycle are distinctly devoted to either growth (i.e. G1) or replication (i.e. S) (Goranov and Amon 2010). Second, in eukaryotes, the variability of the pathways involved in the regulation of growth (Lloyd 2013; Turner, Ewald, and Skotheim 2012) make it complicated to imagine a unique and robust molecular mechanism `sensing' size and translating this into the regulation of overall growth rate. Finally, testing the hypothesis of active growth rate regulation as a function of cell volume would require: (i) direct measurement of single cell growth curves with a much higher throughput than currently possible with any method given the great variability observed in these cells; (ii) clarifying what are the determinants of mass and volume fluctuations and which of these two parameters is relevant for such a model. On the contrary, a potentially simpler hypothesis is that more general rules such as the ones that dictate metabolic scaling with cell size exert constraints on the growth.

A simple general framework to summarize these complex behaviors and compare homeostatic phenomenology in different datasets

Our study provides the first large dataset for direct measurement of cells size through cycles of growth and division, with two different cell culture devices, four different cell lines and a perturbation of cell size at birth using Roscovitine treatment, combined with a marker for G1/S transition. The most robust feature we observed is an apparent adder behavior, although it can rely on different types of cell growth and coupling with cell cycle progression. We thus proposed a general framework to compare the relative contribution of growth and time modulation (Figure 5). We can summarize our findings by defining three main types of growth and cell cycle coupling.

First, when cultured in FXm chambers, epithelial HT29 and HeLa cells grow exponentially, at least during G1 phase (Figures S1G and S4C-F). In this case, consistent with previous indirect findings on mammalian cells (Zetterberg and Killander 1965; Dolznig et al. 2004), and reminiscent of the size control mechanism occurring in *S.cerevisiae* (Johnston 1977; Hartwell and Unger 1977; Di Talia et al. 2007), G1/S transition is negatively correlated with cell volume at birth.

Second, large HeLa cells seem to reach a limiting growth rate (supplementary Figure 4E-F) and a minimum duration of G1 (Figure 3D and Figure 4B). The combination of linear growth with a timer-like G1 phase results in an adder, although growth rate here is maximal and cell cycle time minimal. A saturation of the growth rate was also proposed to explain size control in L1210 cells (Son et al. 2012). We analyzed the dataset from this article (kindly sent by the authors). It shows that, while these cells do not adapt cell cycle duration (Son et al. (2012)), they still display an adder behavior (Figure 5).

Third, when grown under confinement inside 1D channels, MDCK and HeLa cells show indirect evidence of linear growth. These cells grow slower than in the FXm chambers and display a longer cell cycle, resulting in an overall constant added volume and a similar homeostatic size (Figure S2). Although one could argue that the constant added amount of volume is just the result of the combination of linear growth with a constant time, the similarity of the added volume to other conditions of growth, despite a lower growth rate, again argues in favor of a size or added volume sensing mechanism.

Overall, our work reveals that there are at least three main aspects limiting cell growth and cell cycle progression: first, the points detailed above suggests that volume or the addition of a constant volume limits progression through G1, consistent with the hypothesis of a titration mechanism coupling growth and cell cycle timing (Schmoller et al. 2015; Soifer et al. 2016; Delarue, Weissman, and Hallatschek 2016). Second, G1 duration appears to have a lower boundary close to 4 hours, consistent with recent findings on G1 regulation (Cappell et al. 2016). Third, growth speed is limited for large cells. These limitations on either growth speed or cell cycle timing were revealed by studying specific environmental growth conditions and abnormal sizes. A striking observation is that in all these conditions, the overall effective size homeostasis is that of an adder. An intriguing question is therefore whether a unique mechanism leading to an adder can recapitulate all these phenomena.

Physiological relevance of the adder behavior

In E. coli, Wallden and colleague recently showed that as cells were grown in slow conditions, they tended to show stronger size homeostasis mechanism, closer to a sizer than to an adder (Wallden et al. 2016). Similarly, in *S. cerevisiae*, cells grown in glycerol/ethanol instead of glucose grew slower and showed stronger size control in G1 (Di Talia et al. 2007). Direct experimental proof of such variability of the strength of size control upon the change in growth conditions is currently lacking in mammalian cells.

Any homeostasis behavior observed is potentially valid only for the experimental growth conditions that were used. In most cases in the literature, this corresponds to the maximum growth speed of the cells, since cell culture protocols tend to maximize the doubling time and growth speed. For this reason, one of the hypotheses raised to explain the generality of the adder is that it is a simple evolutionary convergence of selection for a mode of growth and cycling that is the fastest possible while preventing size divergence.

Alternatively, or in addition, the adder mechanism could emerge from the physics of cell growth and cell size control, which is not yet well understood. The mechanisms that couple metabolism, cell

mass and cell volume are still debated. Similarly to the role played by the cell wall for yeasts and bacteria, a central player of cell size physics is the cell membrane. Indeed, cell volume results from a balance of forces (Stewart et al. 2011) mostly regulated by ion fluxes at the plasma membrane. These fluxes are in turn modulated by surface tension (Tao and Sun 2015; Jiang and Sun 2013), and thus growth could be limited by the addition of membrane surface area through the synthesis of new lipids and the appropriate balance of endocytosis and exocytosis (McCusker and Kellogg 2012; Morris and Homann 2001), but also by the mechanical state of the cytoskeleton (Dang and Gautreau 2012) and the degree of adhesion of the cell to its environment, which all contribute to cell surface mechanical properties. How membrane addition is regulated remains poorly understood but links between membrane growth and the cell cycle have been found in *S. cerevisiae* (McCusker and Kellogg 2012; Goranov and Amon 2010). Moreover, lipid synthesis appears to involve membrane tension via the mTORC2 pathway in budding yeast (Niles and Powers 2012; Berchtold et al. 2012; Eltschinger and Loewith 2016). The role of membrane tension sensing in regulating cell volume growth via the synthesis of lipids and addition of new membrane is interesting because it could suggest a mechanism where volume increase and not mass (or protein synthesis) is the primary driver of cell growth. In this scenario, an intriguing question is how mass production follows volume and how cell density is maintained constant or on the contrary, fluctuates through the cell cycle (Grover et al. 2011; Bryan et al. 2010; Son et al. 2015; Zlotek-Zlotkiewicz et al. 2015). Additionally if this membrane tension mediated regulation of volume growth is confirmed in mammalian cells, it could suggest a mechanism linking tension sensing in the tissue and translation into enhanced volume growth at the single cell level.

Perspective: size homeostasis mechanism adapts to various condition by involving diverse time and growth modulation processes

Our work points to the existence of several distinct limiting processes that contribute to size homeostasis: a size-dependent progression through G1, a minimum G1 duration and a maximum growth rate. It is likely that further studies, exploring other types of perturbation (i.e. slow growth conditions (Son et al. 2012) or artificially induced small cells) will unravel other limiting processes. Importantly, our observations are compatible with previous findings that had raised a doubt about the existence of size control in mammalian cells such as the fact that large cells grow linearly (Ian Conlon and Raff 2003) or that at very fast growth, the duration of the cell cycle reaches an intrinsic minimal duration (Edgar 2006). As our description of size homeostasis evolves towards that of a flexible process that involves several types of regulation of growth and cell cycle progression depending on the growth conditions, we therefore envision that a unified understanding of the role of size homeostasis from the single-cell to the tissue-level will become possible.

FIGURE 1

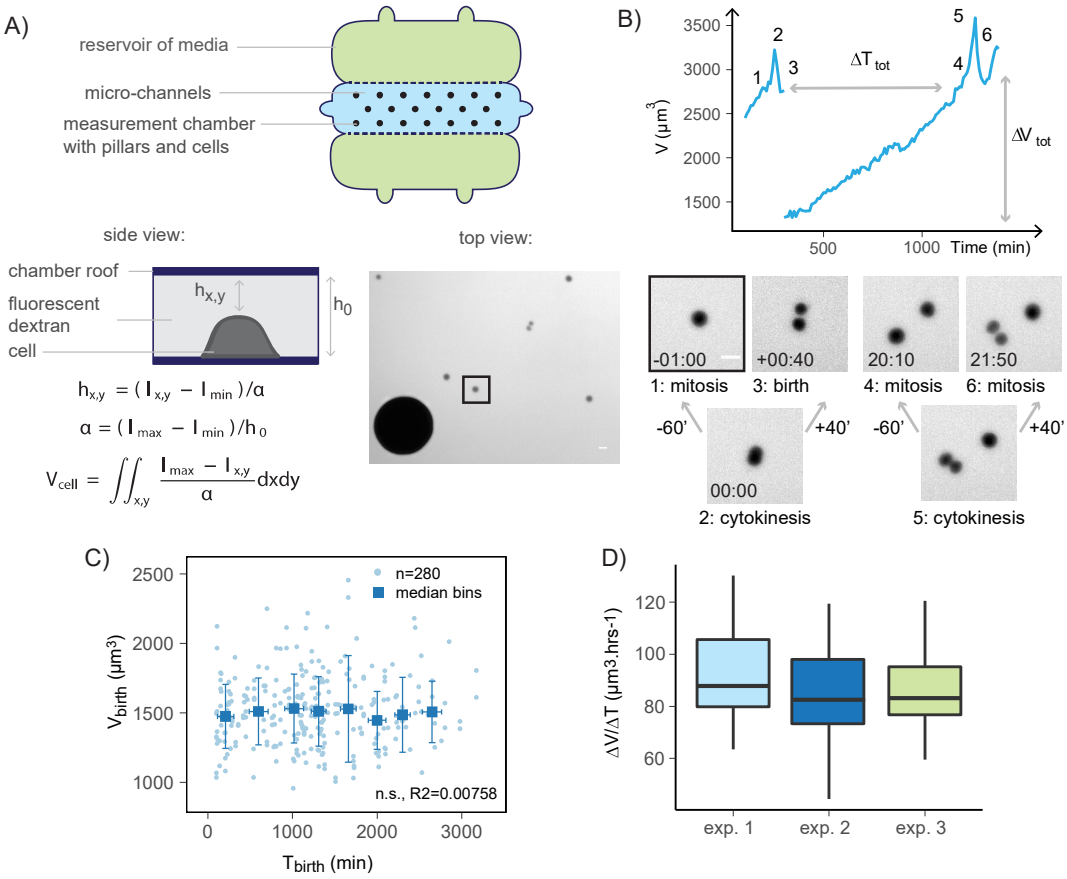
A)
reservoir of media
micro-channels
measurement chamber
with pillars and cells
side view:
top view:
chamber roof
fluorescent
dextran
cell
$h_{x,y}$
h_0
$h_{x,y} = (I_{x,y} - I_{min})/\alpha$
$\alpha = (I_{max} - I_{min})/h_0$
$V_{cell} = \iint_{x,y} \frac{I_{max} - I_{x,y}}{\alpha} dxdy$
B)
V (µm³)
3500
3000
2500
2000
1500
500
1000
Time (min)
1
2
3
4
5
6
ΔT_{tot}
ΔV_{tot}
-01:00
+00:40
20:10
21:50
1: mitosis
3: birth
4: mitosis
6: mitosis
-60'
+40'
00:00
2: cytokinesis
5: cytokinesis
C)
n=280
median bins
V_{birth} (µm³)
2500
2000
1500
1000
0
1000
2000
3000
T_{birth} (min)
n.s., R2=0.00758
D)
ΔV/ΔT (µm³.hrs⁻¹)
120
100
80
60
exp. 1
exp. 2
exp. 3

Figure 1: Single-cell volume tracking over full cell cycles.

A) Principle of the fluorescence exclusion-based volume measurement method (Fxm): Cells are put in chambers of a known height and in presence of a fluorescent dye (10kDa-Dextran-Alexa488) that cannot enter the cells. The fluorescence intensity (I) is linearly related to the height of any object that excludes the fluorescence by a coefficient α. Volume is obtained by integrating the fluorescence intensity over the surface area of the cell. More description of this method can be found in (Zlotek-Zlotkiewicz et al. 2015; Cadart et al. 2017) Top: design of the measurement chambers used for 50hrs long time-lapse acquisitions: side reservoirs contain media that passively diffuse through micro-channels to provide nutrients to the cells in the middle of the chamber. Bottom left: scheme of a side view in the chamber showing how cell height is calculated at each pixel and how volume is inferred. Bottom right: typical image of 10X field imaged with HT29 cells for the Fxm measurement, the dark square shows the cell tracked in B). *(The scale bar indicates 20µm).*

B) Single-cell growth curve and identified key-points: cytokinesis is identified visually as the first time-point where daughter cells start separating; mitosis and birth are defined as the time-points 60 min before and 40 min after cytokinesis respectively. This time frame ensures that volume is measured out of the volume over-shoot period that occurs during mitosis (Zlotek-Zlotkiewicz et al. 2015). ΔT_{tot} is the total duration of the cell cycle from birth to mitosis. Scale bar indicates 20µm.

C) and D) Example of controls were systematically made for all the experiments to check that cells grew at a constant rate and reached a constant size on average both through time in the experiment and across repeated experiments *(experiments on HT29 wild-type; for graph D), n= 39 (exp1), n=46 (exp2), n=47 (exp3)).* More examples of controls are shown in (Figure S1H)

FIGURE 2

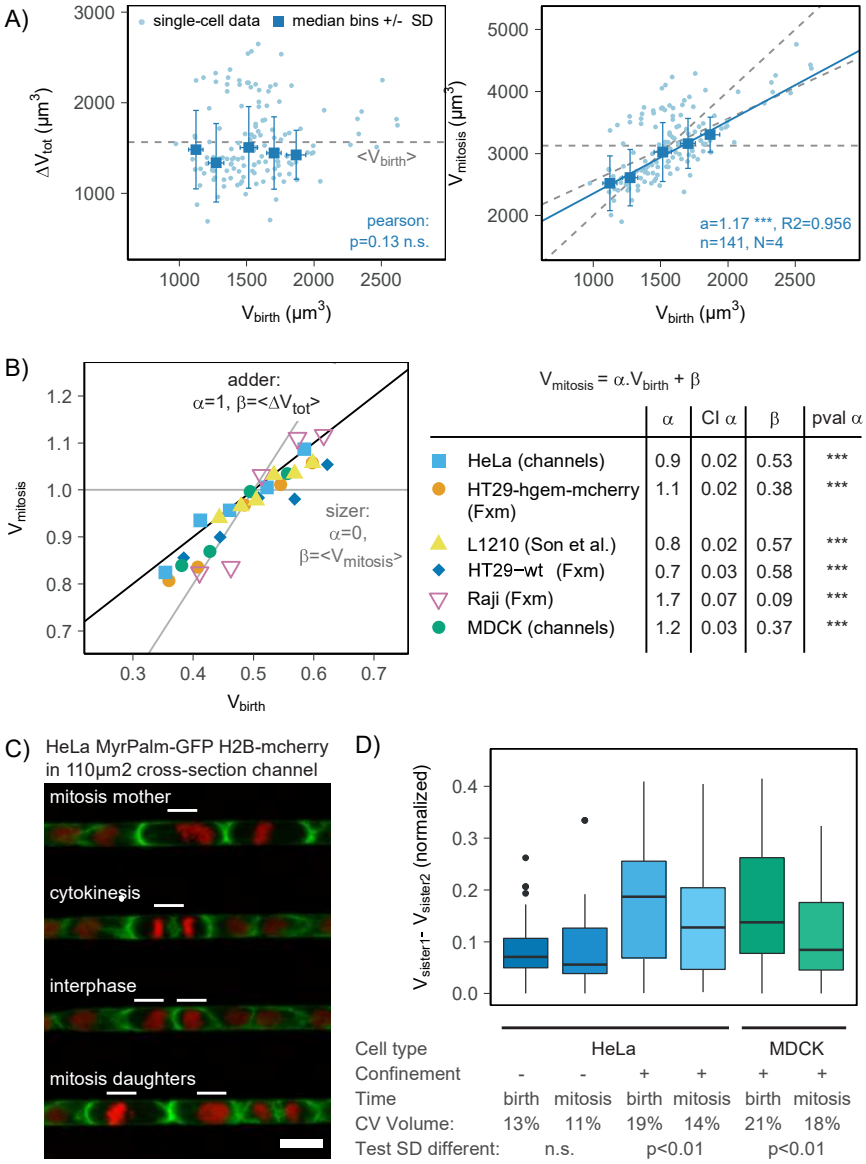

	α	CI α	β	pval α
HeLa (channels)	0.9	0.02	0.53	***
HT29-hgem-mcherry (Fxm)	1.1	0.02	0.38	***
L1210 (Son et al.)	0.8	0.02	0.57	***
HT29−wt (Fxm)	0.7	0.03	0.58	***
Raji (Fxm)	1.7	0.07	0.09	***
MDCK (channels)	1.2	0.03	0.37	***

Figure 2: Adder-like behavior in most animal cell types

A) Adder-like behavior in HT29 cells (n=141, N=4). Total volume gained during the cell cycle ΔV_{tot} is not correlated to volume at birth V_{birth} and the slope coefficient of $V_{mitosis}$ vs. V_{birth} is very close to 1, the value expected in the case of an adder mechanism. Fit is made on the binned data, the slope coefficient α is indicated together with its p value and R^2 *(n.s: p>0.05, * p<0.05, ** p<0.01, *** p<0.001).*

B) Left: comparison of the strength of size control across several animal cell types. The plot $V_{mitosis} = \alpha . V_{birth} + \beta$ shows the range of possible size control mechanisms: (i) timer: in the absence of size control and if cells grow exponentially for a constant time, $V_{mitosis} = 2 . V_{birth}$, and sizes in the population diverge through generations; (ii) in the sizer model, cells all divide at the same size so $V_{mitosis} = Constant$; (iii) in the adder model, a constant ΔV_{tot} is added at each cell cycle, independently of initial size so $V_{mitosis} = 1 . V_{birth} + \Delta V_{tot}$ where ΔV_{tot} is constant. To compare cell types, $V_{mitosis}$ and V_{birt} were rescaled to the mean $\langle V_{mitosis} \rangle$. Cell types analyzed are: Raji *(n=108, N=2)*, HT29 *(n=273, N=7)*, HeLa *(n=137, N=3)*, MDCK *(n=87, N=3)* and L1210 re-analyzed from (Son et al. 2012). Apart from the L1210, the data were acquired either with the Fxm method or with the micro-channels method described in C). For all cell types, the slope coefficient is estimated by performing a fit on the binned data. Right: table showing the values of the slope coefficient α, the intercept β, the 95% Confidence Interval and p value of α estimation *(***: p<0.001)*.

C) Artificially-induced asymmetrical divisions using confinement in micro-channels. Timelapse of a HeLa MyrPalm-GFP (membrane) – H2B-mcherry (nucleus) cell in 110µm2 cross section area channel. Time-points shown are, from top to bottom: mother cell's mitosis (first time-point after rounding upon entry in mitosis), mother cell's cytokinesis, daughter cells in interphase and daughter cells' mitosis. White dots indicate the mother than the two daughter cells*. (Scale bar=20µm).*

D) Rescaled difference of volume in pairs of daughter cells at birth (just after the mother's asymmetrical division) and at mitosis (at the end of the daughter's cell cycles). The dataset correspond to MDCK (channels), HeLa (channels) and, for a control in unconfined condition HeLa cells measured with Fxm**.** A test comparing the standard deviations (SD) at birth and at mitosis in each condition is performed *(CV=coefficient of variation)*.

FIGURE 3

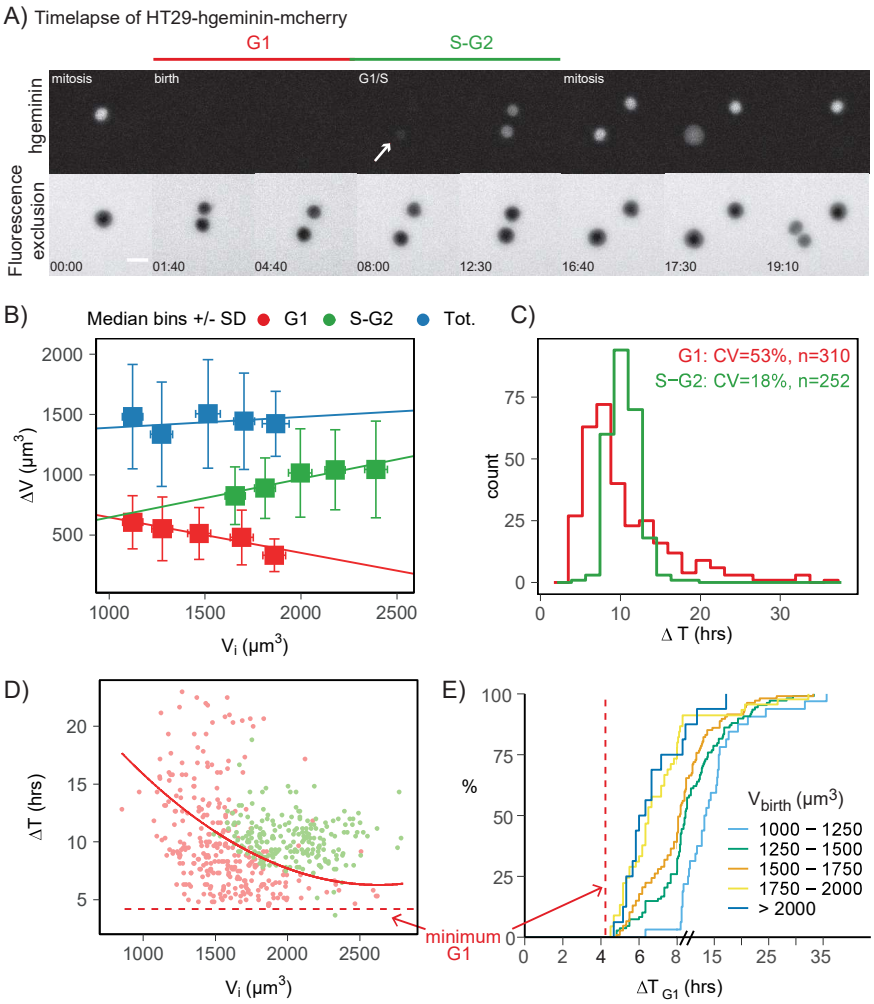
A) Timelapse of HT29-hgeminin-mcherry
G1
S-G2
mitosis
birth
G1/S
mitosis
hgeminin
Fluorescence exclusion
00:00
01:40
04:40
08:00
12:30
16:40
17:30
19:10
B)
Median bins +/- SD
G1
S-G2
Tot.
ΔV (μm3)
Vi (μm3)
C)
G1: CV=53%, n=310
S−G2: CV=18%, n=252
count
Δ T (hrs)
D)
ΔT (hrs)
Vi (μm3)
minimum G1
E)
%
Vbirth (μm3)
1000 – 1250
1250 – 1500
1500 – 1750
1750 – 2000
> 2000
ΔT G1 (hrs)

Figure 3: G1 duration is inversely correlated to V_{birth}

A) Sub-periods were identified using h-geminin coupled to a fluorophore. Example with HT29-hgeminin-mcherry: G1/S transition is defined visually as the first timepoint where h-geminin-mcherry appears (white arrow), G1 phase spans from birth to G1/S and S-G2 phase from G1/S to mitosis. *(Scale bar=20µm.)*

B) Although the total added volume ΔV has the properties of an adder and is not correlated to initial volume, size control seems slightly more efficient than an adder in G1 and oppositely in S-G2 *(the slope coefficient, p value, R square and number of observation of are: a=-0.3 *** R2=0.83, n=244 (G1 phase); a=0.3 *** R2=0.83, n=144 (S-G2 phases) and a=0.1 *** R2=0.1, n=141 (total cell cycle). Results obtained in HT29-hgem-mcherry (N=4).*

C) S-G2 duration shows little variation whereas G1 duration varies a lot. Histogram of ΔT_{G1} and ΔT_{S-G2} showing that the coefficient of variation of ΔT in S-G2 is very narrow compared to that of *G1 (CV: coefficient of variation, the standard deviations are significantly different p<0.0001; results obtained in HT29-hgem-mcherry, N=4).*

D) G1 duration correlates with V_{bir} but this correlation is limited by a minimum G1 duration. ΔT_{G1} and ΔT_{S-G2} vs. V_{birth}. G1 duration correlates negatively with V_{birth} while S-G2 does not *(ΔT_{G1}: polynomial fit, f(x)=-33.9x+8.5x^2+0.4, R2=0.1, n=310; ΔT_{S-G2}: f(x)=-3.3x+10.3, R2=0.1, n=225).* The negative correlation observed in G1 reaches a plateau for large V_{birth}, suggesting a minimum G1 duration around 4-5 hours (red dashed line).

E) Cumulative frequency of ΔT_{G1} with data binned by V_{birth} shows that: (i) the probability of passing G1/S increases with both initial size V_{birth} and time spent in G1, (ii) this probability is null before $\Delta T_{G1} \simeq 4 - 5hrs$. *Results obtained in HT29-hgem-mcherry (N=4).*

FIGURE 4

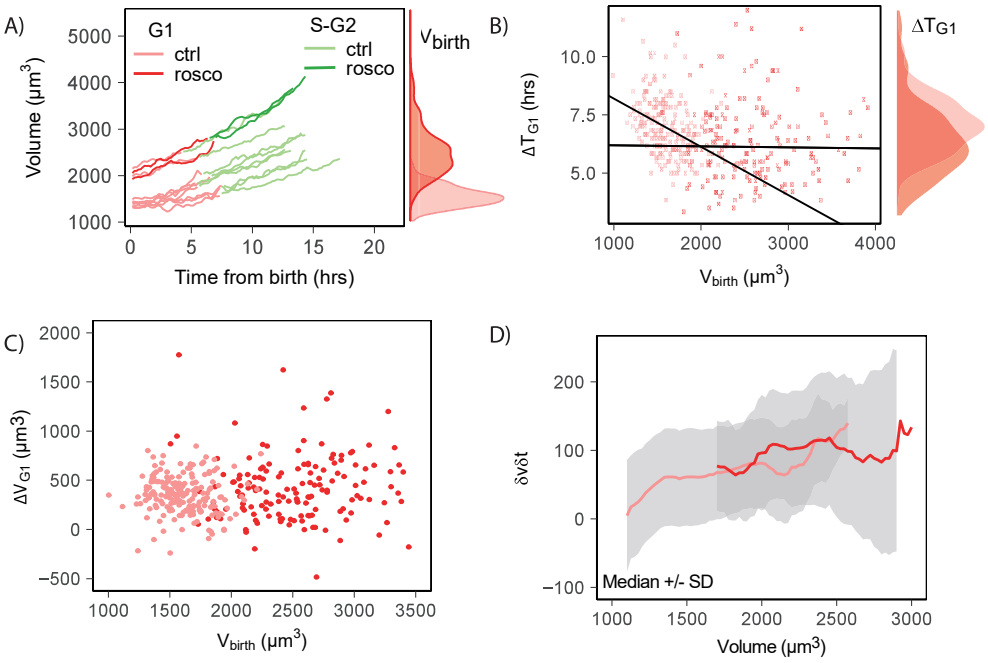
A)
G1
ctrl
rosco
S-G2
ctrl
rosco
Volume (µm3)
Time from birth (hrs)
Vbirth
B)
ΔTG1 (hrs)
Vbirth (µm3)
ΔTG1
C)
ΔVG1 (µm3)
Vbirth (µm3)
D)
δvδt
Median +/- SD
Volume (µm3)

Figure 4: Time adaptation in G1 saturates for large cells but adder is still observed.

To obtain abnormal large cell sizes, HeLa cells were treated with roscovitine 20µM for 48 hours.

A) Example of single-cell growth trajectories of HeLa cells treated with roscovitine or control cells. The histogram shows the distribution of V_{birth} . Roscovitine-treated cells are on average 1.7 larger than control *cells (roscovitine: mean=2500, n=309; control: mean=1500, n=261; Welch t test comparing the means: p<0.0001)*.

B) G1 duration (ΔT_{G1}) as a function of volume at birth in both roscovitine-treated and control HeLa cells. The trend seen in HT29 in Figure 3D) with a negative correlation for small cells and a plateau for larger cells is reproduced. Note that control HeLa cells are already very close to the minimum G1 time compared to the HT29 cells *(robust fit, roscovitine: n.s. n=184; control: a=-0.002±0.0004, R2=0.1, p<0.0001, n=214; N=2).*

C) Added volume in G1 (ΔV_{G1}) is not correlated with volume at birth in both control and roscovitine treated cells *(robust linear fit not significant, roscovitine: n=201; control: n=181; N=2).*

D) Instantaneous growth velocity $\partial v \partial t$ as a function of volume during G1. The velocity for the control cells seems to increase with volume for control cells while it is constant for large roscovitine-treated cells.

FIGURE 5

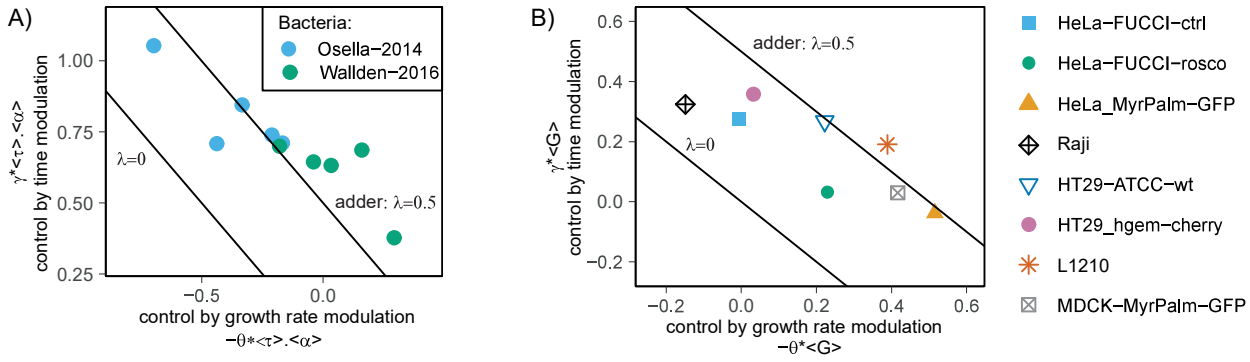
A)
Bacteria:
Osella−2014
Wallden−2016
λ=0
adder: λ=0.5
1.00
0.75
0.50
0.25
−0.5
0.0
control by time modulation
γ*<τ>.<α>
control by growth rate modulation
−θ*<τ>.<α>
B)
adder: λ=0.5
λ=0
0.6
0.4
0.2
0.0
−0.2
−0.2
0.0
0.2
0.4
0.6
control by time modulation
γ*<G>
control by growth rate modulation
−θ*<G>
HeLa−FUCCI−ctrl
HeLa−FUCCI−rosco
HeLa_MyrPalm−GFP
Raji
HT29−ATCC−wt
HT29_hgem−cherry
L1210
MDCK−MyrPalm−GFP

Figure 5: Roles of growth and time modulation in overall size control.

A) and B) Model to estimate the respective contribution of growth and time adaptation to size in the overall size-control. The model is described in the SI. γ and θ describe the strength of time and growth modulation respectively, when they are positive values, they contribute to size control while when they are negative they contribute to loss of size control. λ describes the strength of the overall size control, in case of an adder $\lambda = 0.5$, in case of no control, $\lambda = 0$, in case of a sizer, $\lambda = 1$. Left: results with bacteria data from (Osella, Nugent, and Cosentino Lagomarsino 2014; Wallden et al. 2016), right results in animal cells.

SUPPLEMENTARY FIGURE 1 (part1)

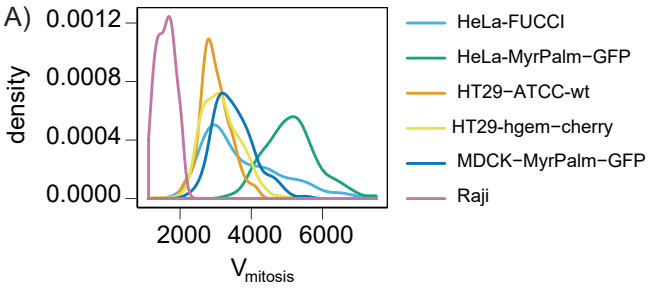

B) Design of the micro-channels

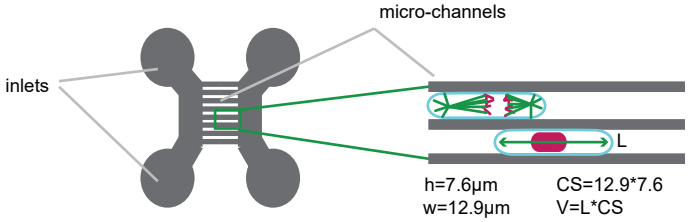

C) HT29 Cell cycle duration

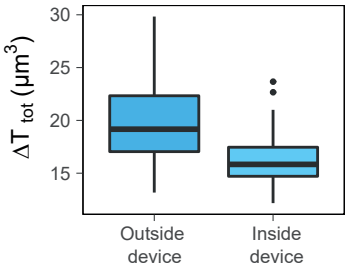

D) HT29 Growth curves

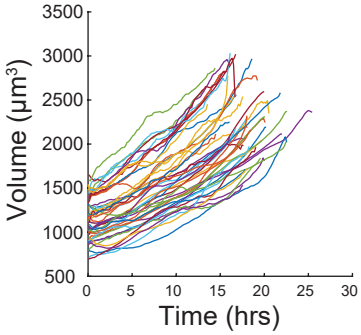

E) Mitotic volume overshoot in HT29 hgem-mcherry cells

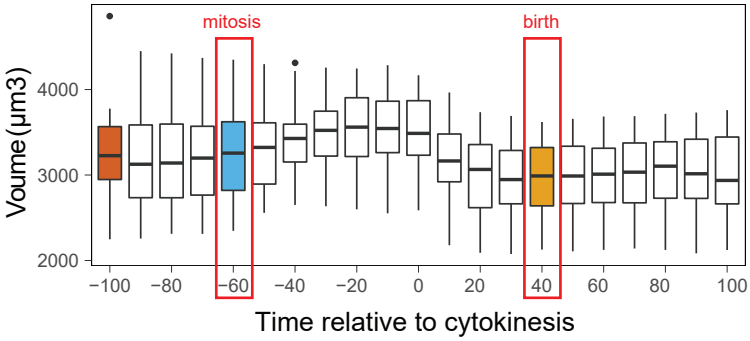

F) Timepoints at birth and mitosis

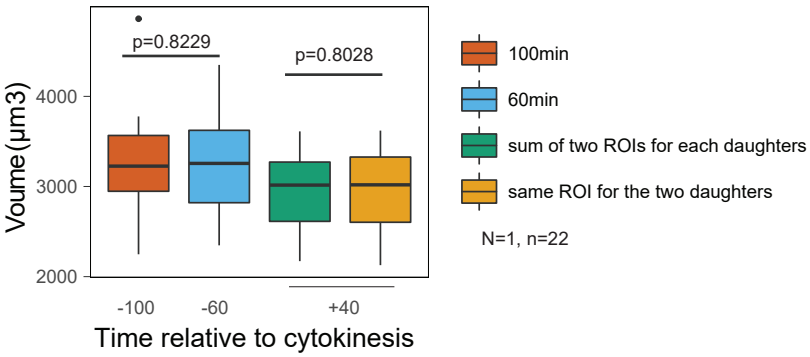

G) Bulk growth in HT29-hgem-mcherry

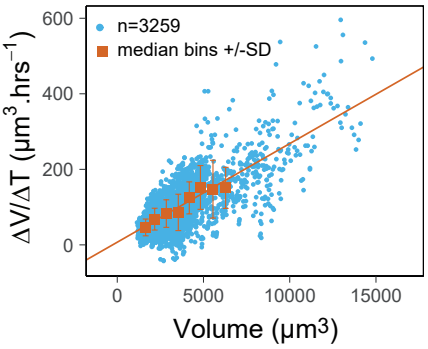

SUPPLEMENTARY FIGURE 1 (part2)

H) Control of growth quality for each experiment

Raji (Fxm)

number of cells per experiment:

- n = 50
- n = 58

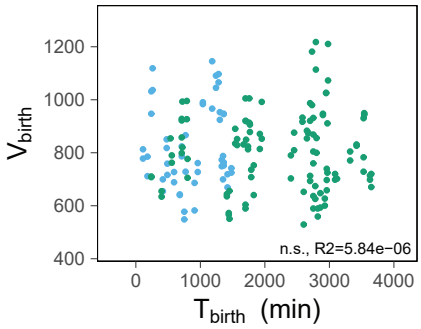

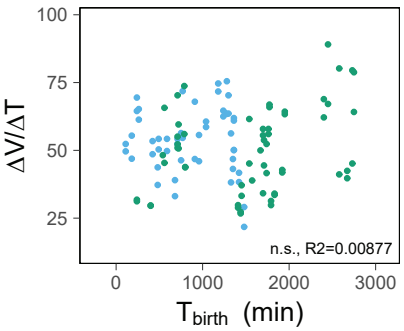

HT29 hgem-mcherry (Fxm)

number of cells per experiment:

- n = 31
- n = 20
- n = 41
- n = 49

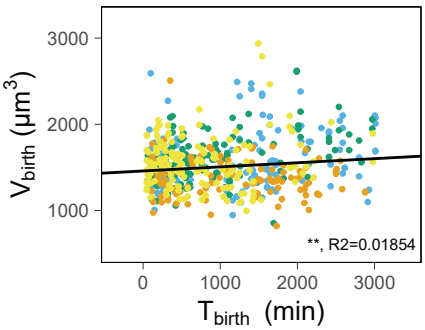

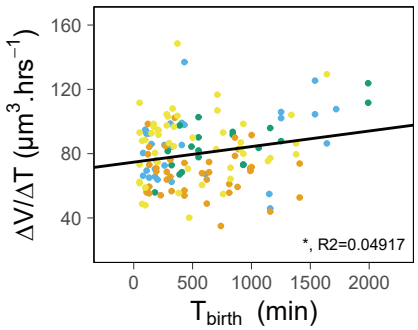

HeLa MyrPalm-GFP (channels)

number of cells per experiment:

- n = 38
- n = 59
- n = 40

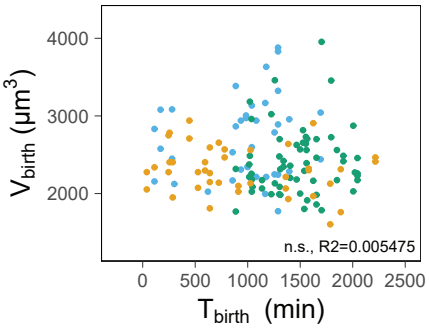

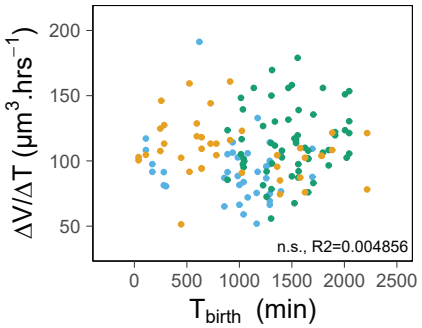

MDCK MyrPalm-GFP (channels)

number of cells per experiment:

- n = 44
- n = 12
- n = 31

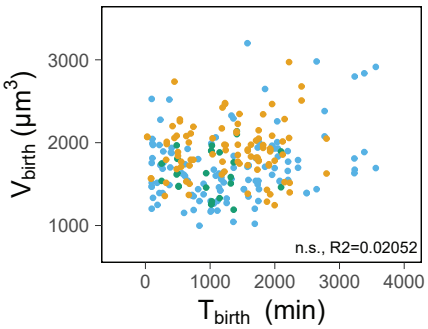

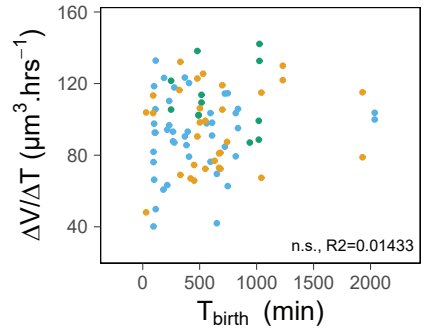

Figure S1

A) Volume distribution for all the cell types analyzed in this study.

B) Design of the micro-channels: the micro-channels have a cross section (CS=98µm2, h=7.6µm; w=12.9µm); they confine cells at mitosis which induces asymmetric divisions. Two large perpendicular channels enable injecting the cells via the inlets. Volume is estimated by measuring the length of a rounded cell and multiplying it by the cross section area of the channel.

C) Duration of cell cycle length inside and outside the measurement device for HT29. Cells were plated at approximately the same density. Cell cycle duration is slightly higher outside the device, probably due to a faster equilibration of the media in the small volume of the measurement device. This control shows that cells cycle on expected durations in the measurement device.

D) Examples of complete single growth curves of HT29-WT obtained with the Fxm method.

E) Boxplot of the average volumes centered on cytokinesis shows the mitotic volume overshoot in HT29 cells (Zlotek-Zlotkiewicz et al. 2015). The time-points highlighted are compared in figure F).

F) Volume at mitosis was defined as the volume 60 minutes before cytokinesis to be outside of the mitotic volume over shoot (at this time-point, volume is not significantly higher than 100 minutes before the cytokinesis). We also checked that the manual segmentation of daughter cells just after division was correct despite the cells being still close to each others. To do so, we compared the sum of the volumes of the two daughter cells measured separately (green) with the value obtained when measuring the two cells at once (orange). On average, these two calculation are not significantly different.

G) Growth velocity as a function of size of individual or groups of HT29 h-geminin-mcherry cells show that growth is superlinear.

H) Controls for the quality of growth made for all the experiments described in Figure 2.

SUPPLEMENTARY FIGURE 2 PART1

A) Trends for each cell type

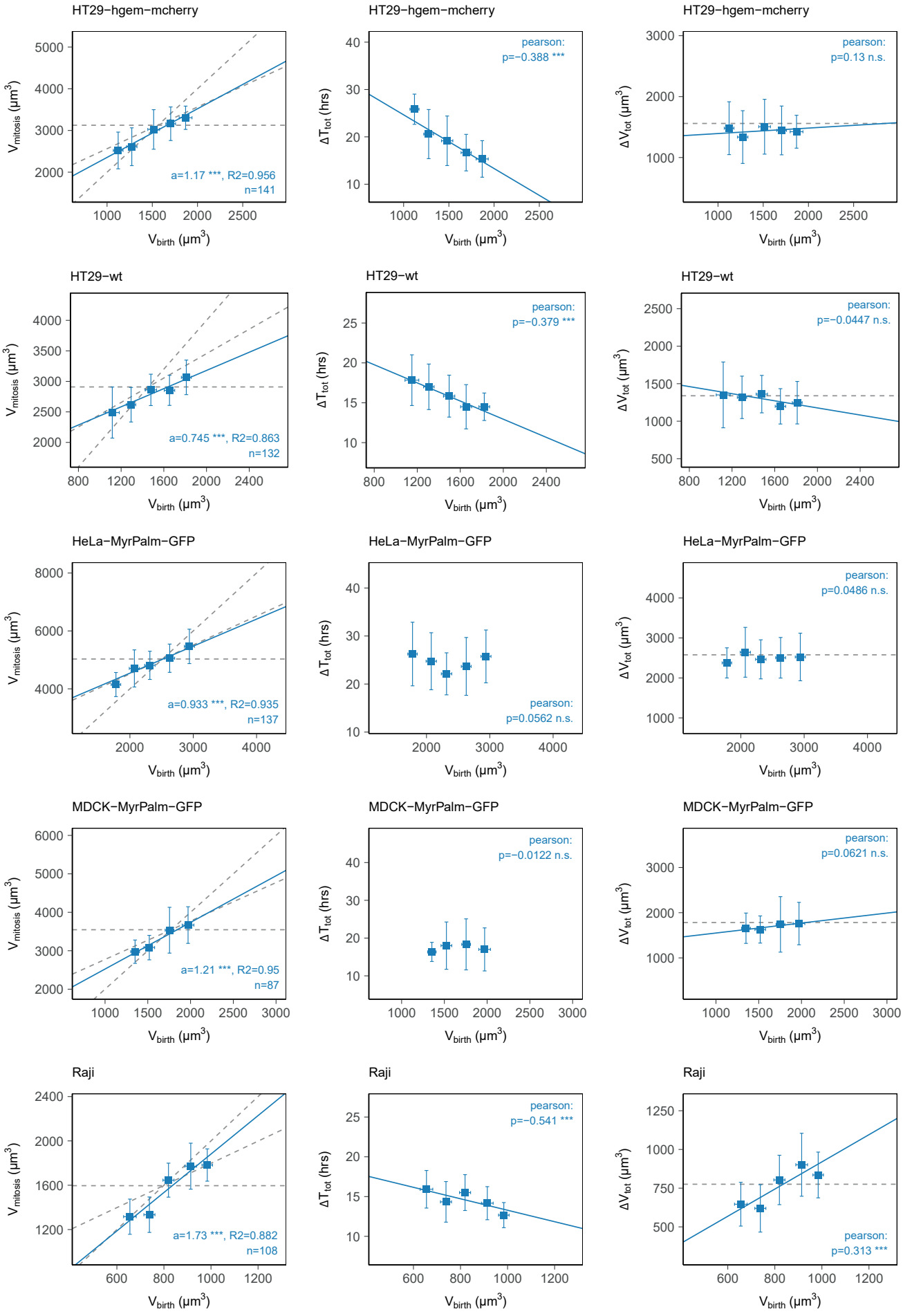

SUPPLEMENTARY FIGURE 2 PART2

B) Volume distribution inside our outside the channels, HeLa cells

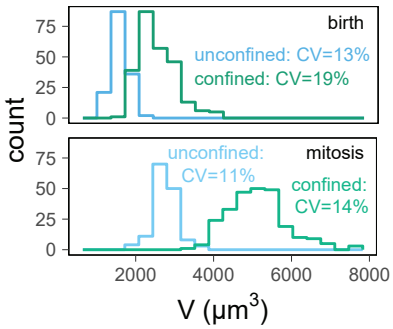

Figure S2

A) Plots for each individual cell type showing the homeostatic process efficiency and if any, presence of correlation between duration and initial volume. For ΔV_{tot} vs. V_{birth}, the dashed line indicates $\langle \Delta V_{tot} \rangle$. For the $V_{mitosis}$ vs V_{birth} plot, the dashed line indicates the slopes of timer, adder and sizer as in Figure 2B).

B) Volume distribution of HeLa cells inside (confined) and outside (unconfined) the micro-channel device: asymmetrical divisions in the micro-channels induces a spread of the distribution of sizes at birth which is then reduced at mitosis.

SUPPLEMENTARY FIGURE 3

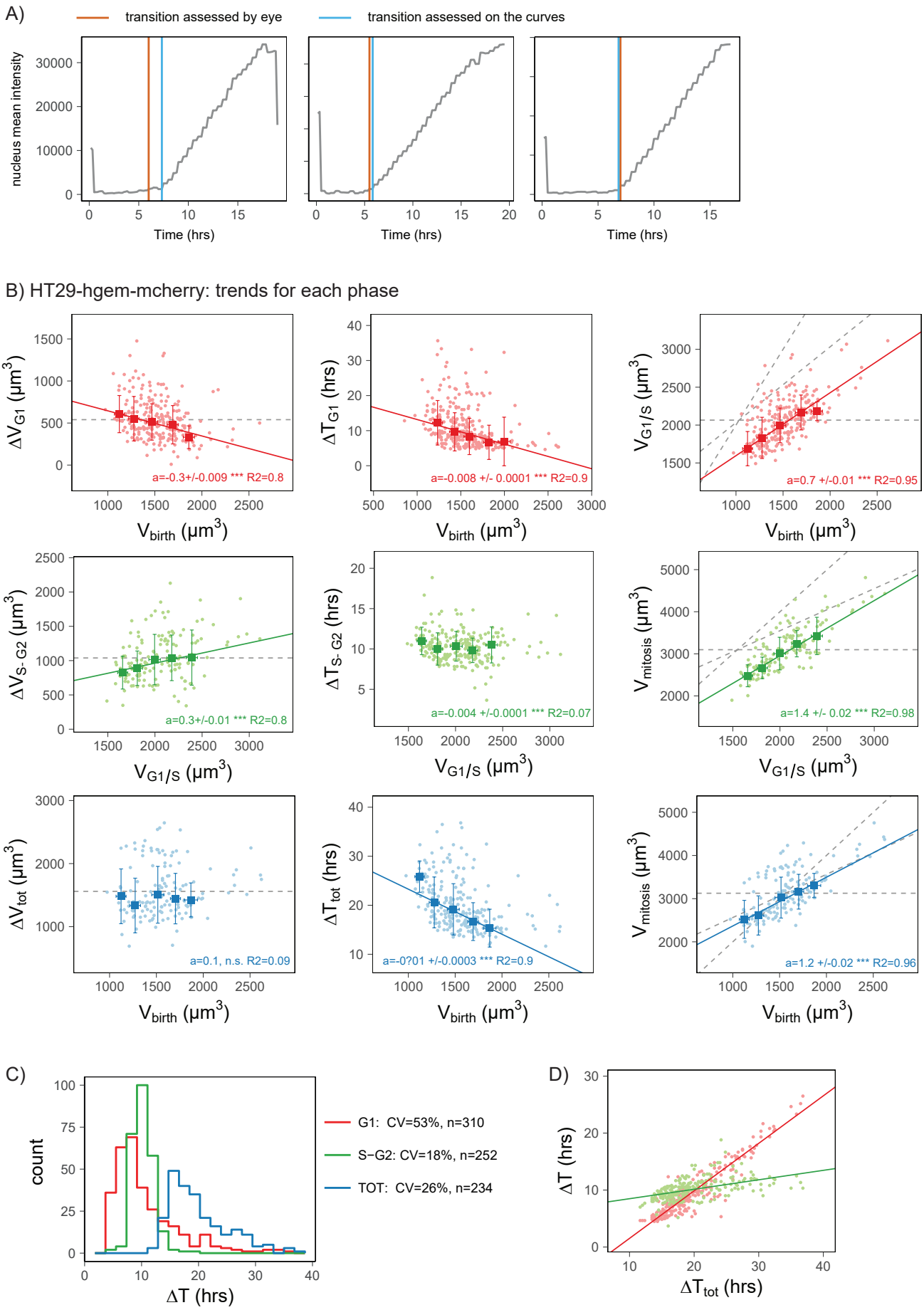

Figure S3:

A) Validation of the G1/S transition time-point. The G1/S transition was assessed visually as the first time-point when fluorescent h-geminin appeared in the nucleus. To verify that this method was correct, we compared our visual definition of the transition (red) with a definition based on the analysis of the nuclear fluorescence intensity profile through time (blue). We compared 10 curves and show here the most imprecise evaluation (left), the average type of error observed (middle) and the best evaluation (right). This empirical check shows that on average the error was small.

B) Trends in each sub-periods for HT29 experiments. The legend indicates the slope coefficient a +/- the 95% confidence interval, the p value of the slope coefficient and the R square.

C) Same histogram as in Figure 3C but also showing the total cell cycle duration. *Results obtained in HT29-hgem-mcherry (N=3).*

D) Duration of G1 or S-G2 phase with respect to total cell cycle duration (n=228). ΔT_{G1} correlates strongly with ΔT_{tot} *(Pearson's correlation coefficient P=0.9 ***)* while ΔT_{S-G2} does less *(P=0.5 ***). Results obtained in HT29-hgem-mcherry (N=3).*

SUPPLEMENTARY FIGURE 4

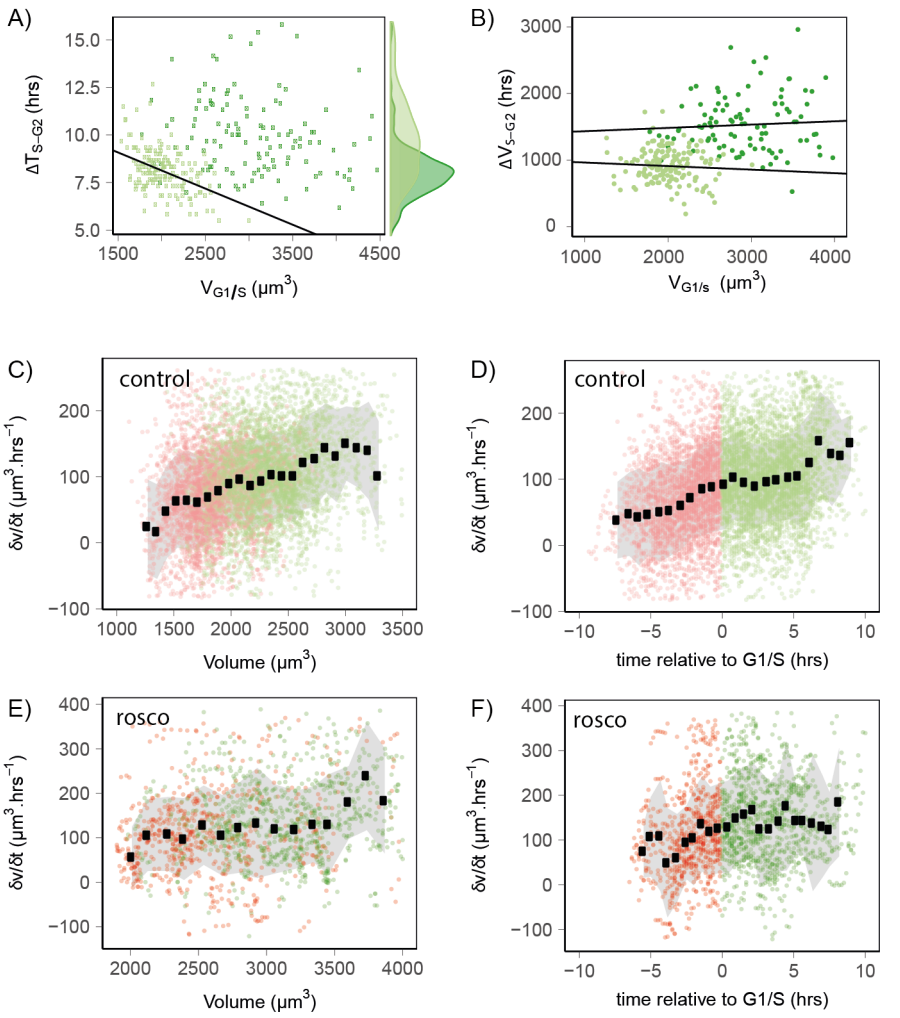

G) Control of the quality of growth in HeLa control

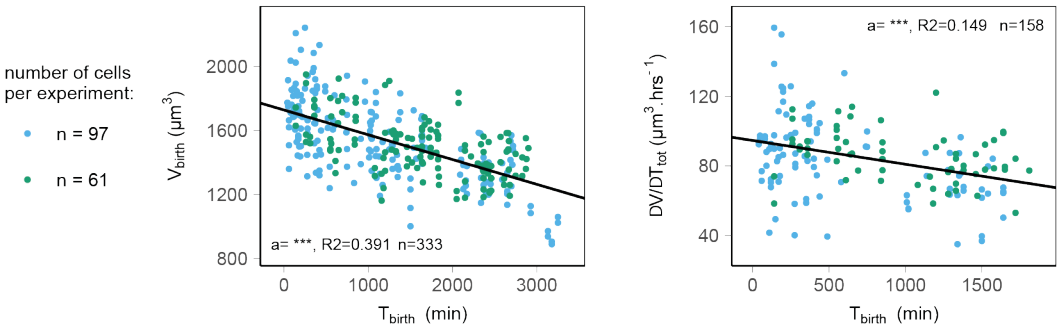

H) Control of the quality of growth in HeLa treated with Roscovitine 20µM for 48 hours

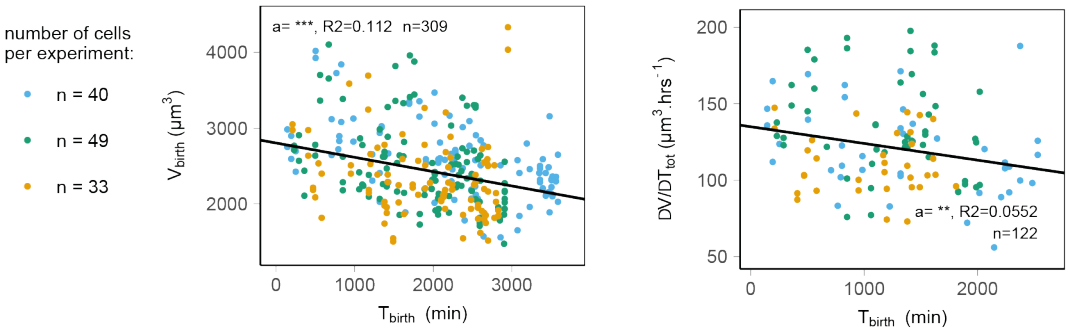

Figure S4:

A) S-G2 duration (ΔT_{S-G2}) is slightly correlated with volume at G1/S transition in control HeLa cells but not in roscovitine treated cells *(robust fit, roscovitine: a=-0.0007±0.0003, p<0.05, R2=0.04, n=124, N=3; control: a=-0.002±0.0004, R2=0.2,p<0.0001, n=157; N=2)*. Moreover, S-G2 duration is longer for roscovitine treated cells, perhaps because of problems occurring in S phase. *(roscovitine: mean=10 hrs; control: mean=8 hrs, Welch t test comparing the mean: p<0.0001).*

B) Added volume in G2 (ΔV_{G2}) is not correlated with volume at birth in both control and roscovitine treated HeLacells (robust fit not significant, roscovitine: n=101, N=3; control: n=146; N=2). However, volume added in roscovitine treated cells is on average significantly higher than in control cells (roscovitine: mean=1600; control: mean=900, Welch t test comparing the means:p<0.0001).

C, D, E and F): Instantaneous growth velocity $\partial v \partial t$ as a function of volume or time during the whole cell cycle (red=G1, green = S-G2, median bins with standard deviation). The velocity for the control cells seems to increase with volume for control cells, thus indicating superlinear growth while it is constant for large roscovitine-treated cells which therefore seem to grow linearly. Potentially, a transition in velocity might be observed at G1/S for control cells. This however still requires more quantification.

G) and H) Control of the quality of growth for experiments with HeLa and Roscovitine-treated HeLa cells as in Figure S1H. HeLa cells tend to internalize the dextran which leads to a progressive apparent decrease of volume at birth through time in the experiment. For this reason, the growth curves shown in Figures S4C-F and Figure 4D were only measured on the first 25 hours of the experiment to reduce underestimation of volume. This decrease needs to be solved by further experiments. However the error made on the correlations analyzed here should be minimal as the trend $\Delta V/\Delta T$ vs. T remains small.

SUPPLEMENTARY FIGURE 5

A)

size-growth plot:

$\alpha\tau_{V_0} = \langle\alpha\tau\rangle - \lambda\,(\log(V_i) - \langle\log(V_i)\rangle)$

Example eukaryote: HT29-WT

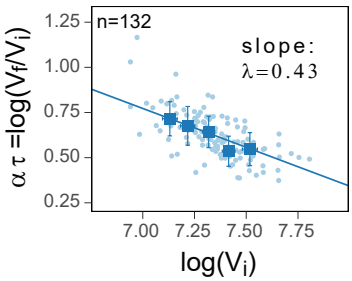

Example Bacteria: Osella E.Coli_MRR_LB

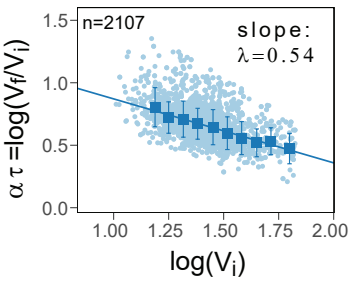

B)

time vs. size

$\tau_{V_0} = \langle\tau\rangle - \gamma\,(\log(V_i) - \langle\log(V_i)\rangle)$

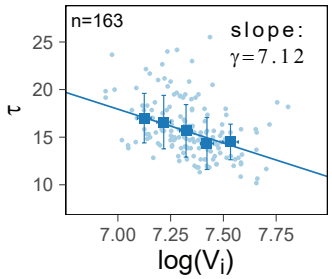

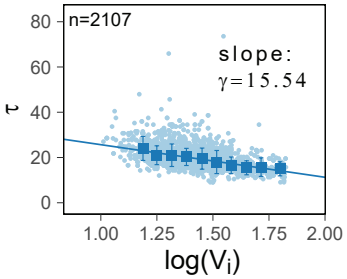

C) Validation of the method of trends estimation using the covariance

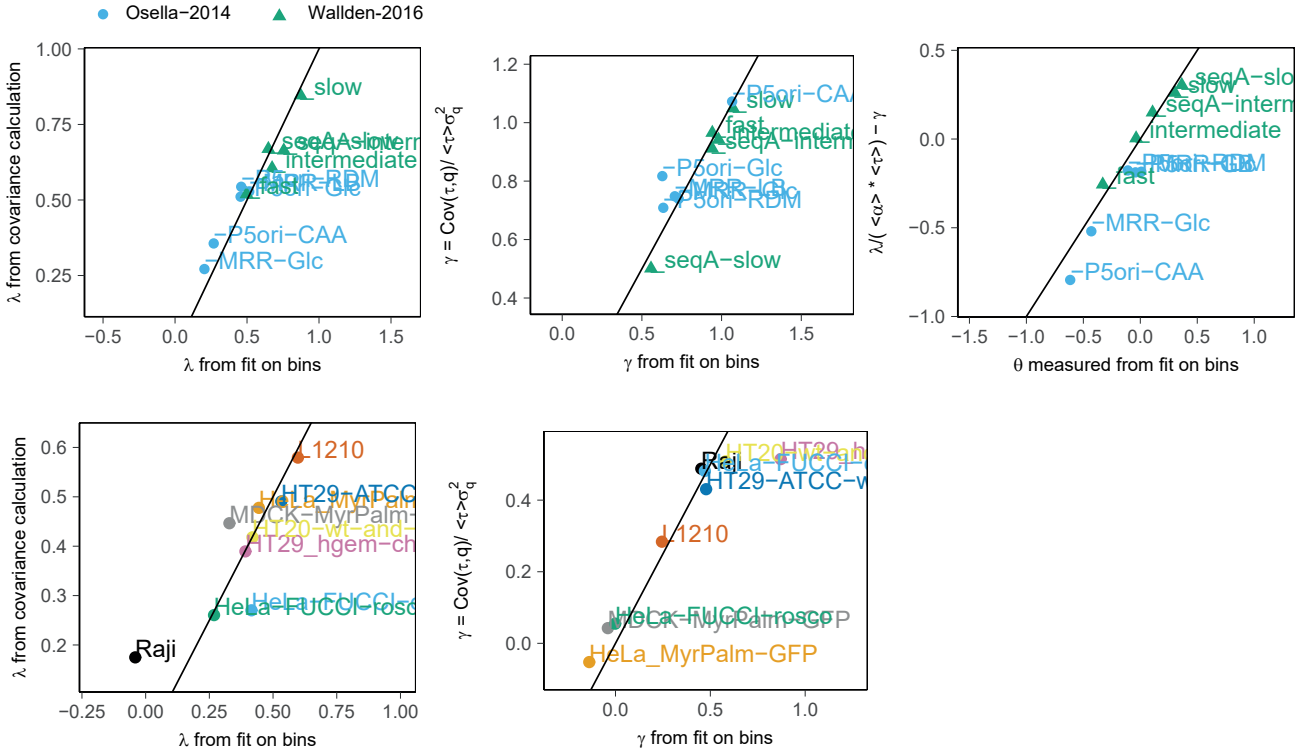

D) Validation of the model using bacteria

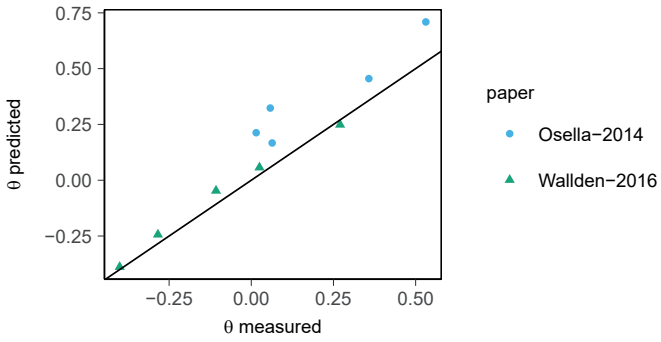

Figure S5

A) Example of the size-growth plot for one mammalian cell type and one dataset from a study in bacteria. The slope of the plot λ describes how total relative growth depends on initial size.

B) Example of the plot testing the control by time modulation in one of our dataset and one dataset from a study in bacteria.

C) Comparison of the estimation of trends using a calculation of the covariance or a fit on the binned data as in A) or B). The two methods show excellent agreement except for the Raji cells which showed a very noisy behavior and low sampling (see Figure S2 A)

D) Validation of the model using bacteria: the value of θ as predicted by the model matches very well with that measured from a fit on the data.

Supplementary Informations 1: experiments and analysis

Cell culture & reagents

Cells were cultured in media supplemented with 10% FBS and 1% penicillin-streptomycin. Media, EDTA, trypsin, penicillin-streptomycin and glutamax were purchased from ThermoFisher. For HeLa, MDCK, HT29, cell culture medium was DMEM-GlutaMAX (HeLa, MDCK, HT29) and medium for microscopy imaging was DMEM with no phenol red (#31053044) supplemented with Glutamax (#35050061). For Raji cells, medium used was RPMI supplemented with either GutaMAX. Zeocin (#10072492) was purchased from Life Technologies and Puromycin (#BML-GR312-0050) from Enzo life sciences. Dextran (#D-22910, #D-22914) and roscovitine (#R7772-1G) were purchased from Sigma Alrich.

Cell lines and plasmids

HeLa S-FUCCI were obtained from the Riken Brain Center and were initially characterized in (Sakaue-Sawano et al. 2011). HeLa Kyoto MyrPalm-mEGFP-H2B-mRFP are a kind gift from Daniel Gerlich's lab (ETH, Zurich, Switzerland). HT29 HTB-38 were bought from ATCC. A stable HT29 hgem-mcherry cell line was established using the lentiviral vector mCherry-hGeminin(1/60) / pCSII-EF (Sakaue-Sawano et al. 2013): electroporation was used to transfect the cells, the cells were then selected with zeomycin 200µg/mL and FACS-sorted for mCherry fluorescence. The resulting polyclonal population showed good homogeneity in fluorescence intensity. MDCK cells were obtained from Buzz Baum lab (UCL, London, United Kingdom). Similarly to the protocol used for HT29 hgem-mcherry, a stable MDCK-MyPalm-GFP cell line was established by electroporating cells with the plasmid pMyrPalm-mEGFP-IRES_puro2b offered by Daniel Gerlich's lab. Selection was made with Puromycin 2µg/mL prior to FACS sorting. For all the transfected cell lines, antibiotic were removed from the culture media after FACS sorting. Raji cells were obtained from Claire Hivroz's lab (Institut Curie, Paris, France).

Roscovitine experiment

For the roscovitine experiments, HeLa cells were seeded in six-well plates at 1.9*10^4 (control) and 8.3*10^4 (treated) cells per cm2 52 hours before the experiment. 4 hours later (48 hours before the experiment), when cells were spread, media was changed to 2 mL +/- 20µM roscovitine. Roscovitine stock solution was 50mM in DMSO.

Live-cell imaging

Phenol red-free media was used for FXm experiments. Acquisitions were performed on a Ti inverted (Nikon) or Axio Ob-server microscope (Carl Zeiss) at 37°C with 5% C02 atmosphere, a 10× dry objective (NA 0.30 phase) for FXm experiments or a 20× dry objective (NA 0.45 phase) for micro-channels experiments. Images were acquired using MetaMorph (Molecular Devices) or Axio Vision (Carl Zeiss) software. The excitation source was systematically a LED for FXm experiments to obtain the best possible homogeneity of field illumination (Lumencor or Zeiss Colibri); or a mercury arc lamp for some of the micro-channel experiments. Images were acquired with a CoolSnap HQ2 camera (Photometrics) or an ORCA-Flash4.0 camera (Hammamatsu).

For timelapse experiment, images were acquired every 5min (micro-channel experiments), 10min (FXm measurements: fluorescence-exclusion channel and phase channel) and 30min (fluorescent geminin channel) for up to 50hours in order to obtain 1 to 2 full cell cycles per lineage.

Volume measurement with Fxm

The FXm method was initially described in (Zlotek-Zlotkiewicz et al. 2015) and a detailed protocol is available in (ref (Cadart et al. 2017)**.** We only describe here specifications from this protocol.

Except for Raji experiments, the design of the volume measurement chamber (fig 1.A) included two side reservoirs that diffused nutrients to cells in the middle of the chamber. Side reservoirs were 400µm high and diffusion to the observation part was achieved through a grid of channels (w=100µm, l=300µm and h=5µm). The height of the chambers was around 20-24µm (depending on the chambers) for HT29 and HeLa cells and 15.5 or 18.2µm for the Raji cells.

The chambers were coated with fibronectin 50µg/mL, and then incubated over night with the appropriate phenol-red-free media. During the acquisition, the chambers were covered with media to prevent desiccation of the PDMS and subsequent changes of the osmolarity of the media in the chamber. To prevent dextran leakage outside the chambers, the height of the inlets was risen by sticking 3-4 mm high PDMS cubes on top of each inlet, then 2mm diameter punches were made for every inlets.

To prevent potential sources of variability in the growth rate or doubling rate caused by different proliferative states in the population, cells were seeded at constant concentration two days before the experiment (1*10^5/cm² for HT29 cells and 1.9*10^4/cm² for HeLa). Cells were detached using trypLE (thermofisher #12605036) (HT29) or EDTA (HeLa), to avoid cell aggregates and optimize adhesion time f to the glass-bottom, fibronectin-coated chamber. Cells were injected in the middle part of the chamber (see scheme in fig. 1A) at a concentration ranging from 1.5 to 2*10^5 cells /mL in order to obtain the appropriate density in the chambers. For adherent cells (HT29 and HeLa), 4 hours after seeding, media was changed with equilibrated media containing 1mg/mL of 10kDA-Dextran. Raji cells were injected together with the Dextran at the same concentration. 10kDa Dextran could be coupled either toAlexa-645 (HeLa-FUCCI experiments) or Alexa-488 (all other experiments). Imaging started 2 to 4 hours after changing the media to give time to for media to equilibrate in the chamber and avoid possible inhomogeneity of dextran just after injection.

Micro-channel experiments

Microchannels molds were made with classical lithography technics and then replicated in epoxy molds. Microchannels had a 98µm2 cross-section area (12.9µm width by 7.6µm height) (supplementary figure 1B). They were crossed perpendicularly by two large distributing channels (5mm width by 50µm height). The micro-channels chips were replicated in PDMS, plasma-treated, bound to glass-bottom fluorodishes, coated with fibronectin 50µg/mL and incubated over night with the culture media. The large distributing channels were used both to inject the cells and as reservoirs of media. Cells were injected at a concentration of 3.8*10^6/mL, in the upper distributing channel; the dishes were then tilted with the large distributing channels axis parallel to the bench plane. This helped deposing a thin layer of cells at the entry of the micro-channels while minimizing the number of cells injected for nutrient amount economy and appropriate density's sake. The

opposing distributing branch contained only media and thus diffused nutrients to the channels. This was indeed important to guarantee enough nutrient stock and good growth conditions throughout the 50hrs of the acquisition in this confined design. Cells were then let to migrate in the microchannels over-night and experiments were started the morning after. For the analysis, mitosis was defined as the first time-point where the cell rounds-up and displays a cylinder shape and birth was the last time-point after cytokinesis where the cell is still in the shape of a cylinder.

Image analysis

For FXm experiments, image analysis was performed using a home-made Matlab program described in (Zlotek-Zlotkiewicz et al. 2015) . Rapidly, fluorescent signal was calibrated for every time points using the fluorescence intensity of the pillars and around the cell of interest to obtain the linear relationship between height and fluorescence. After background cleaning, the fluorescence intensity was integrated for the whole cell and its surroundings to obtain the cell volume.

For the micro-channels experiments, image analysis was performed on ImageJ. Cells entering mitosis roughly adopt the shape of a cylinder. Volume was calculated by measuring the length (ℓ) of the cell and integrate it on the channel cross section ($\mathcal{CS}$): $V \approx \ell.\mathcal{CS}$ (supplementary figure 1B).

Data filtering and analysis

For the data on the animal cells obtained by us (or analyzed from (Son et al. 2012)), only clear outliers that were higher or lower than the mean+/-3*SD were removed. This corresponded on average to 0 to 5 points maximum per dataset (each dataset being n>100). These outliers were removed for visual purposes (scale of the plot adapted to the range of the data) and analytical robustness.

For the bacteria data, a filter based on the IQR (interquantile range) was performed: cells which log(Vi) and log (Vf) where higher or lower than 1.5*IQR+/-median of log(Vi) and log(Vf) respectively were removed.

For the growth curves, a filter removed the points further from the 1*IQR +/- median on sliding windows of 11 frames. Then the points were averaged on sliding windows of 3 frames for smoothing.

Statistical analysis

All the figures and statistical analysis were performed in R. Packages used were: “robust”, “robustbase”,“ggplot2”,”grid”,”gridExtra”,”xtable”,”stringr”.

For the boxplots, the upper and lower hinges correspond to the first and third quartiles, the upper and lower whiskers extend from the hinge to the highest (lowest) value within 1.5*IQR (Inter Quantile Range) of the hinge. Data beyond the whiskers are shown as outliers.

For the comparison of the variances in fig. 2D, the test was a Fligner-Killeen test because distribution of the variables were non normal and the median were not always equal.

Robust linear fits on single points were performed using the “robust” package in R. When error is indicated on the slope coefficient and intercept, the error corresponds to the 95% confidence

interval. When the fit is performed on the binned data, the formula used is a linear fit weighted by the number of observations in each bins. The bins are median bins along the x axis of the plot, and bins that contain less than a minimum number of events are removed. The bin number and the minimum size of the bin was adapted to the size of the datasets as follows:

Cell type	n number of events observed	Bin number	Minimum number of events per bin
Animal cells	80-300	8	8
Bacteria cells	<100	8	8
	<1000	10	15
	<5000	13	60
	>5000	15	150

Supplementary Information 2: Mathematical framework to compare size homeostasis mechanism in various organisms

Linear response theory of size control

We assume that the final volume (in a cell cycle or subperiod) is a result of a size-dependent growth and timing:

$$V_f = V_0 \exp\left[\alpha(V_0)\tau(V_0,\alpha)\right] \ ,$$

where V_x is volume and α and τ quantify the growth rate and duration in the period (or cell cycle) and they are both random variables. Note that there is no hypothesis of exponential growth rate, just that growth during a period is represented as en effective exponential growth.

We also define:

$$q_f - q_0 = G(V_0) + \nu$$

where ν is the noise, $q_x = \log(V_x)$ and $G(V_0) = \alpha(V_0)\tau(V_0,\alpha)$ and $q_f - q_0 = \log\frac{V_f}{V_0}$ so the previous equation is just the size-growth plot.

A. Notation and general form of control

Introducing the notation:

$$\delta q = q_0 - \langle q_0 \rangle$$

and:

$$\delta\alpha = \alpha - \langle\alpha\rangle \ ,$$

we can write:

$$\tau = \langle\tau\rangle\left(1 - \varphi_\tau\delta_q + T_\tau\delta\alpha\right) + \nu_\tau$$

and:

$$G = \langle G\rangle - \varphi_G\delta_q + T_G\delta\alpha + \nu_G$$

Using $G = \alpha\tau$ and $\alpha = \langle\alpha\rangle + \delta\alpha$, we can write:

$$G = \langle\alpha\rangle\tau + \tau\delta\alpha = \langle\alpha\rangle\langle\tau\rangle - \langle\alpha\rangle\langle\tau\rangle\varphi_\tau\delta_q + \langle\tau\rangle(1 + \langle\alpha\rangle T_\tau)\delta_\alpha + \text{nonlinear terms} + \text{noise}$$

And therefore we obtain the equivalence between the two parameterizations:

$$\varphi_G = \langle\alpha\rangle\langle\tau\rangle\varphi_\tau$$

and:

$$T_G = \langle\tau\rangle(1 + \langle\alpha\rangle T_\tau)$$

In principle α can depend on size as well:

$$\alpha = \langle\alpha\rangle\left(1 + \theta\delta q\right) + \nu_\alpha$$

The slope λ of the size-growth plot is defined considering the conditional average of G over q:

$$\langle G\rangle_q = \langle G\rangle - \lambda\delta_q \tag{1}$$

Computing this average on the expression above, we obtain:

$$\langle G\rangle_q = \langle G\rangle - \varphi_G\delta_q + T_G\langle\delta\alpha\rangle_q = \langle G\rangle - \left(\varphi_G - \theta\langle\alpha\rangle T_G\right)\delta_q$$

And therefore we have:

$$\lambda = \varphi_G - \theta\langle\alpha\rangle T_G$$

In a similar way, if we defined γ as:

$$\langle\tau\rangle_q = \langle\tau\rangle - \langle\tau\rangle\gamma\delta_q \tag{2}$$

we have that:

$$\langle\tau\rangle_q = \langle\tau\rangle - \langle\tau\rangle\varphi_\tau\delta_q + \langle\tau\rangle T_\tau\langle\delta\alpha\rangle_q = \langle\tau\rangle - \langle\tau\rangle\left(\varphi_\tau - \theta\langle\alpha\rangle T_\tau\right)\delta_q$$

and therefore we obtain:

$$\gamma = \varphi_\tau - \theta\langle\alpha\rangle T_\tau$$

Using $\varphi_G = \langle\alpha\rangle\langle\tau\rangle\varphi_\tau$ and $T_G = \langle\tau\rangle(1 + \langle\alpha\rangle T_\tau)$, we obtain:

$$\lambda = \langle\alpha\rangle\langle\tau\rangle\varphi_\tau - \theta\langle\alpha\rangle\langle\tau\rangle(1 + \langle\alpha\rangle T_\tau)$$

And therefore we obtain:

$$\frac{\lambda}{\langle\alpha\rangle\langle\tau\rangle} = \varphi_\tau - \theta(1 + \langle\alpha\rangle T_\tau)$$

Using the measurements of γ and λ we obtain:

$$\frac{\lambda}{\langle\alpha\rangle\langle\tau\rangle} - \gamma = \theta$$

We can therefore test the relationship (equation 1 in the main text):

$$\theta\langle\alpha\rangle\langle\tau\rangle = \lambda - \gamma\langle\alpha\rangle\langle\tau\rangle \tag{3}$$

For the bacteria datasets, both $\langle\alpha\rangle$ and $\langle\tau\rangle$ are accessible, therefore this correlation can be directly tested (figure 5B). For mammalian cells, since α cannot be measured, we do the following approximation: $\langle\alpha\rangle\langle\tau\rangle \approx \langle\, G\rangle$ (figure 5A).

B. How to measure λ and γ and infer θ in Eukaryotes

Both λ and γ can be determined using correlation between variables. Since by definition:

$$\langle G\rangle_q = \langle G\rangle - \lambda\delta_q$$

and:

$$\mathrm{cov}(G, q) := \langle\langle G\rangle_q \delta q\rangle \ ,$$

we have that:

$$\mathrm{cov}(G, q) := -\lambda\sigma_q^2 \ ,$$

where σ_q^2 is the variance of q. Analogously, we have that:

$$\mathrm{cov}(\tau, q) := -\langle\tau\rangle\gamma\sigma_q^2 \ ,$$

We can therefore obtain λ and γ using

$$\lambda = -\frac{\mathrm{cov}(G, q)}{\sigma_q^2} \ ,$$

and:

$$\gamma = -\frac{\mathrm{cov}(\tau, q)}{\langle\tau\rangle\sigma_q^2} \ .$$

Figure S5 C) shows a comparison of the values obtained for λ and γ from either the covariances or a linear fit testing the relationships (equations 1 and 2 respectively). The final prediction is that:

$$\theta_{pred} = \frac{1}{\sigma_q^2}\left(\frac{\mathrm{cov}(G, q)}{\langle\tau\rangle\langle\alpha\rangle} - \frac{\mathrm{cov}(\tau, q)}{\langle\tau\rangle}\right)$$

If individual growth rates are available, as with the bacteria datasets, θ can be estimated as:

$$\theta_{meas} = \frac{\mathrm{cov}(\alpha, q)}{\sigma_q^2\langle\alpha\rangle} \ .$$

Figure S5 D) shows that θ_{meas} and θ_{pred} are in very good agreement.

7.3 Concluding remarks

Some of the results presented in this manuscript are still preliminary. Here we summarize the weak points of this manuscript that require more analysis or experiments.

7.3.1 Analysis planed before the submission

The analysis of single growth curves of control and roscovitine-treated HeLa cells (figure 4 and S4) is the most important missing point of this manuscript. For the moment, only one experiment was analyzed and low sampling limits our conclusion regarding the linearity of growth. When more curves will be analyzed it will be possible to validate or invalidate the following preliminary observations: (i) that there is a growth rate transition at G1/S in control cells, (ii) that growth rate increases with cell volume and then reaches a plateau. This is important to compare our results with the results from previous studies in mammalian cells Son et al. (2012); Kafri et al. (2013); Tzur et al. (2009).

Moreover, the statistical analysis of figure S4 A-B and figure 4 B-C still needs to be performed with the same method than the rest of the manuscript (linear fits on the bins), although this will not change the final result.

Finally, an important missing control is the accuracy of the definition of G1/S transition via the imaging of h-geminin-mcherry signal in HT29 cells. We need to (i) validate our home-made lineage through immunofluorescence labeling a marker of G1, S and G2 phases and (ii) rigorously quantify the error made when assessing the transition visually rather than from the curve of fluorescence intensity over time (figure S3 D).

7.3.2 Important experiments needed to complete the work

In addition to this, one of the weakness of our work is that we point to several types of modulation of growth and cell cycle timing but lack direct testing of each of these modulation. In the perspective of the revisions, the following experiments will be important:

- The adaptation of G1 to initial volume should be further tested by studying artificially induced small cells (techniques discussed in the discussion 8.2.1.3).
- The experiment in the micro-channels suggests that these cells grow slowly and linearly but nevertheless adapt their cell cycle time to add a constant amount of volume. This should be tested by reducing the growth rate of cells without confinement (for example by growing cells in limited isoleucine conditions Son et al. (2012)).
- It might be interesting to extend the characterization of the homeostatic process to primary cells or at least non-primary cells. We already tried several cell types for this but the main limitation remains the fact that the fluorescent probe used for FXm measurement is rapidly internalized by many cell types (see discussion 8.1.2).
- Parallel measurement of mass and volume will be important to: (i) compare our results with the rest of the literature previously published in mammalian cells that report mass-related measurement Sung et al. (2013); Mir et al. (2011); Son et al. (2012); Godin et al. (2010), (ii) establish whether mass and volume growth constantly evolve the same (*i.e.* density is constant) or whether more complex behaviour are observed for example at the begining of the cell cycle (as our preliminary results, not shown here suggest).

DISCUSSION

Chapter 8

Discussion

8.1 Single cell growth measurement in mammalian cells 143
8.1.1 Single cell measurement of volume with the FXm 143
8.1.2 Current limitations of the FXm 145
8.2 Growth and time modulation 146
8.2.1 Time modulation 146
8.2.2 Growth modulation 151
8.2.3 Conclusion on the respective contribution of time and growth modulation in size control 156
8.3 Is there a unique mechanism or several processes resulting in the adder? 157
8.3.1 Generality of the adder, from bacteria to mammalian cells 157
8.3.2 Is there enough evidence to conclude that size homeostasis is an adder in mammalian cells? 158
8.3.3 Size homeostasis is a flexible process 158
8.3.4 Several scenarios can explain the apparent adder in mammalian cells 160
8.4 Perspectives: a combination of processes, both single and tissue-level determined? 162

8.1 Single cell growth measurement in mammalian cells

8.1.1 Single cell measurement of volume with the FXm

Growth measurements at the single cell level are key in understanding cell size homeostasis. Such data, with rigorous control of the steadiness and of growth, only recently became available in yeast Nobs and Maerkl (2014) or bacteria Wang et al. (2010); Iyer-Biswas et al. (2014) and led to several important discoveries in these fields (section 2.4.2.2). In mammalian cells however, this technical challenge remains the main limiting factor. In this context, our method, which enables dynamic measurement of mammalian cell growth at the single cell level over full trajectories for the first time, brings a number of interesting improvements.

8.1.1.1 FXm allows measurement of both suspended and adherent cells

While some techniques only apply to suspended Son et al. (2012); Tzur et al. (2009) or adherent Park et al. (2010), our method is compatible with both types as we report measurement on HT29,

HeLa cells but also Raji which are lymphoblastoid. Such a versatility will be helpful when trying to understand whether the constraints on size homeostasis vary upon the cell type chosen Lloyd (2013).

8.1.1.2 FXm allows measurement of cell volume

In contrast with yeast or bacteria, methods for mammalian cells most often aimed at measuring cell mass or density Sung et al. (2013); Park et al. (2010); Godin et al. (2010); Mir et al. (2011); Son et al. (2012); Grover et al. (2011) to overcome the difficulty of measuring cell volume in these cells whose shape constantly fluctuate. Therefore very little is known about volume homeostasis in mammalian cells, with a few studies focusing on a specific period of the cell cycle such as mitosis Zlotek-Zlotkiewicz et al. (2015); Son et al. (2015a). Nevertheless, volume is potentially a central parameter in size control and most of the models of size sensing are based on titration effects, both in *S. cerevisiae* and bacteria Sompayrac and Maaloe (1973); Soifer et al. (2016); Ho and Amir (2015); Robert (2015); Schmoller et al. (2015); Si et al. (2016); Zheng et al. (2016).

8.1.1.3 Results from direct measurement of single cell growth might precise some of the previous findings

Most of the results on mammalian cell size homeostasis rely on inferences from indirect measurement at the population-level Tzur et al. (2009); Kafri et al. (2013); Conlon and Raff (2003); Echave et al. (2007); Dolznig et al. (2004). Nonetheless, one of the lessons from yeast or bacteria studies is that single deviate from the population average Kennard et al. (2016); Taheri-Araghi et al. (2015); Lin and Amir (2016); Hashimoto et al. (2016); Amir (2017); Delarue et al. (2016). Coulter counter measurement of average size in the population led to the observation that population growth was linear and therefore no size control was needed Conlon and Raff (2003); Echave et al. (2007). It was however argued that no clear conclusion could be drawn until single cells growth curves were analyzed Sveiczer et al. (2004). Another study proposed mathematical extraction of growth curves from fixed population. The main assumption of this method was that HeLa cells do not modulate their cell cycle timing in order to maintain size homeostasis. The conclusion from this work was that these cells therefore relied on the adaptation of cell growth rate to achieve homeostasis Kafri et al. (2013). The central assumption of the model contrasts with our direct measurements on HeLa cells where we observe that G1 duration is negatively correlated with initial volume, at least for the range of volumes in unperturbed conditions. It is therefore possible that some of the conclusions drawn from indirect techniques will be revisited by our work and future studies enabling live single cell growth measurement.

8.1.1.4 FXm measurements provide a robust set of data for the study of size homeostasis

Our FXm method, compared with other available techniques is probably one of the most versatile and easy to use method for single cell growth measurement in mammalian cells. It enables measuring volume, a parameter rarely quantified in such cells. It also has the advantage tof being compatible with classical biological tools such as fluorescence imaging of cell cycle markers. One of the challenges for growth studies in mammalian cells is guaranteeing good and steady growth conditions. For our work, this was one of our main concerns. Having in mind the standards set from studies in bacteria and yeast, we improved both our device to enhance nutrient access and our method to validate analytically each experiment (section 6.2.3.3). With all this, we are able to provide a robust set of results on HT29 and Raji cells with the FXm method. However, experiments on HeLa cells highlight some of limitations of our technique (figure S4G-H).

8.1.2 Current limitations of the FXm

8.1.2.1 Limitation to cells which do not internalize the probe

As explained in the method chapter (section 6.2.3.4), the main limitation of our technique is that it requires the use of a fluorescent probe that is not internalized by the cell. Our current data on HeLa cells for example show a decrease of volume through time in the experiment caused by the progressive uptake of fluorescent dextran (figure S4G-H). It would also have been interesting to confirm our findings with measurement on primary cells or RPE1 cells because these cells are immortalized cells often used for cell cycle studies. These cells rapidly showed a rapid internalization of the fluorescent dextran that we used even after the injection of the probe was optimized. To address this issue, we tried to develop and test other fluorescent probes. This needs further work because no clearly satisfying probe was found. We will continue our tests with dextran of even higher molecular weight than those already used. It is however possible that FXm method will remain unadapted to cell types that have very high endocytic activity such as macrophages for example. An interesting idea for such cells would be to design a system enabling rapid change of the media to switch to media containing a different fluorescent probe, this would also enable quantifying the volume endocytosed.

8.1.2.2 FXm currently requires a device confining the cells

The other main drawback of our technique is that the calibration of the fluorescence intensity signal requires performing the measurements in a chamber of known height (section 6.2.1.1). Since the technique relies on the accurate measurement of the fluorescence intensity over the full height of the chamber (section 6.2.1.2), this height is kept relatively low ($\approx 20-25\mu m$), within the range of depth of field given by the objective used. This has several disadvantages: (i) the volume of media contained by the device is very small, thus nutrients might become limiting over long experiments; (ii) controlling the density of cells seeded in the chamber via their injection us not easy; (iii) when trying to rinse the chamber (with dextran or with a drug for example), one might generate some shear stress perturbing the cells; (iv) the device is made of PDMS which tends to absorb many hydrophobic drugs, thus making it difficult to control the concentration of drug active on the cells.

Our collaborator Olivier Thouvenin suggested an alternative to this method where the chamber is replaced by controlling the optical section. On a microscope such as the confocal laser scanning microscopy platform TCS SP8 from Leia, it is indeed possible to tune the pinhole size and thus the height of the optical section. In this set-up, the optical section acts like a virtual chamber that controls the height over which fluorescence intensity is retrieved. For the fluorescence signal calibration (Eq. 6.2), I_{min} is the camera offset and I_{max} is the height of the optical section.

Together with Olivier Thouvenin, Larisa Venkova and Mathieu Maurin we therefore initiated a project to test and optimize this idea. Our results are still very preliminary but comparing the same cells measured with either an optical section set to $10\mu m$ with the confocal or our classical method gave encouraging results (figure 8.1). The main difficulty of this technique is however to precisely find the zero plane (the bottom of the dish) from which the optical section (or virtual chamber) will be added. We are currently trying different approaches such as adding beads of known height in the dish (the zero plane is therefore the focal plane of the beads minus the radius of the bead) or performing a short z-stack around the expected value of the zero plane to then infer its actual value in image post-treatment.

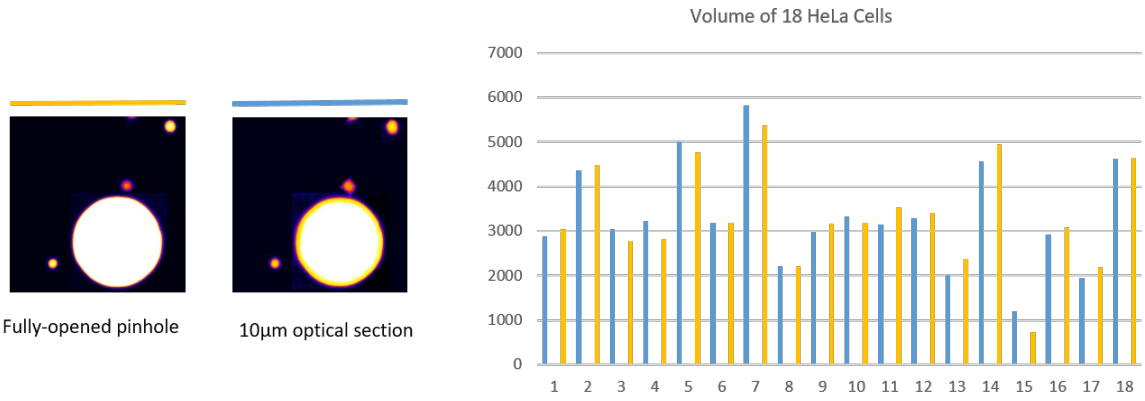

Figure 8.1: FXm through optical sectioning using a confocal. HeLa cells were seeded in the classical FXm chambers. We compared volume measured with (i) a fully opened pinhole giving an optical section higher than that of the chamber and thus mimicking our classical measurement using an with epifluorescence microscope (yellow) and (ii) a 10 μm high optical section obtained by setting the appropriate pinhole diameter (blue). This preliminary result on 18 HeLa cells shows a good match between values obtained from the two techniques.

8.2 Growth and time modulation

8.2.1 Time modulation

8.2.1.1 G1 duration is correlated with volume in HT29 and HeLa cells and gated by a minimum duration

The role of G1/S transition in cell size control similarly to that in budding yeast Hartwell and Unger (1977); Di Talia et al. (2007); Schmoller et al. (2015), has long been hypothesized in mammalian cells Killander and Zetterberg (1965); Dolznig et al. (2004) (section 4.2.1). Direct measurement of the correlation between G1 duration and initial size has however never been reported in mammalian cells. Among the studies that combined dynamic cell mass measurement with cell cycle tracking only one discussed specific events ocuring in G1 with a decrease in the variability of growth rate at G1/S transition and an inverse correlation between early growth rate in G1 and G1 duration Son et al. (2012). Here we observe that both HT29 and HeLa cells show a negative correlation between G1 duration and initial volume (chapter 7, figure 3D and 4B), thus reinforcing the idea that coordination between G1 progression and growth exists in mammalian cells.

Several clarifications to this observation are however needed. First, it is important to note here that our assessment of G1/S transition as the starting point of the accumulation of the fluorescent h-geminin, which comes from the FUCCI system Sakaue-Sawano et al. (2008) (methods, 6.10) is less precise than other techniques for example based on the detection of PCNA speckles in the nucleus Sporbert et al. (2005). PCNA imaging would also have enabled distinguishing between S and G2 phases. The drawback of using PCNA is that it requires higher magnification (40X) than the one suitable for FXm (10X with low numerical aperture, providing a large field for long term cell tracking) which is the reason why we used the FUCCI system.

Second, the results in HT29 cells show that progression through G1 depends both on volume and time (chapter 7, figure 3D), thus suggesting that volume is not the sole variable limiting cell cycle progression for these cells. Cyclines, Cdks and CKI dynamics during G1 phase were recently characterized in mammalian cells Barr et al. (2016); Cappell et al. (2016), although some details are still debated. The reporters from these studies could be combined with our FXm volume measurement

to analyze the concentrations of Cyclin D, Cdk4/6 and their inhibitors, the Rb family which are the mammalian cells functional equivalents of Cln3-Cdk1 and Whi5 respectively in budding yeast Fisher (2016). This would enable testing whether a dilution inhibitor such as the one proposed in *S. cerevisiae* Schmoller et al. (2015) explains the volume dependence of G1 duration.

Moreover, our results in large control HT29 and HeLa cells and roscovitine induced large HeLa cells (chapter 7, figure 4D and 3C) unravel the existence of a minimum G1 duration which is near 4 hours and is independent of cell volume. This suggest a minimal refractory period before transiting through S phase. A potential candidate for this could be the inactivation of APC^{Cdh1} complex which has been proposed as the ultimate and irreversible commitment point to S phase in mammalian cells Cappell et al. (2016). Knockdown of Cdh1 had already been shown to cause shortened G1 phase and accumulation of DNA damage Sigl et al. (2009). The current model now posits that APC^{Cdh1}, which activation occurs during the previous anaphase Peters (2006), is inactivated in a switch-like manner by cyclinE/Cdk2 within less then one hour prior to DNA replication. In proliferating cells that directly enter G1, a minimum time window of 4 hours before the inactivation of APC^{Cdh1} is defined Cappell et al. (2016), reminiscent of the minimum G1 duration observed in our large HeLa cells. In this work, authors propose that G1 can be decomposed into two distinct steps: a first restriction point gating G0 to G1 transition driven by pRb-E2F activation, followed by a window of reversibility lasting 4 hours and ended by the inactivation of APC^{Cdh1} during which it is always possible to exit to quiescence Cappell et al. (2016). An interesting question will be to understand whether the dependency of G1 duration on volume we observed is the result of a clear size-dependent phase prior to pRb-E2F activation and the subsequent 'timer' phase in G1 or whether it is rate-limiting later during the window of reversibility prior to APC^{Cdh1} inactivation (figure 8.2 A-B).

8.2.1.2 S and G2 phases

Our work brings less clear conclusions about S and G2 phases. In HT29 cells, we observe that the coefficient of variation of S-G2 is lower than that of G1 ($CV = 53\%$ in G1 and 18% in S-G2, chapter 7, figure 3). Figure 8.3 here also shows that the majority of the variation of the total cell cycle is due to variations of G1 phase. This difference in the variability of G1 and S-G2 is however less marked in HeLa cells (chapter 7, figure 4 $CV = 29\%$ for G1 and 22% for S-G2). Further reinforcing the idea that S-G2 duration adaptation plays little role in size control, is the absence of correlation between S-G2 duration and volume at G1/S transition in HT29 cells. A small negative trend was however observed in HeLa cells (chapter 7, supplementary figure 4A).

An easy speculation would be that, similarly to yeast and bacteria, S duration is fairly constant because its timing is dependent on the completion of a discrete task: DNA replication Zhang et al. (2017). However, arguments in favour of the existence of variability in S phase were also reported. In mammalian cells, it was recently argued that all the phases of the cell cycle except mitosis displayed important variability Araujo et al. (2016). It has also been shown that when G1 is artificially shortened through the knockdown of APC^{Cdh1} the subsequent S phase is lengthened Sigl et al. (2009); Yuan et al. (2014).

What drives the transition from G2 to M remains mysterious in eukaryotes and the possibility that cell size is the ultimate trigger for entry in mitosis is debated Mchedlishvili et al. (2015). In *S. cerevisiae*, the dogma that size control occurred at Start in late G1 was recently contradicted with findings that G2 phase duration was also negatively correlated with volume Leitao et al. (2016).

To better answer the question of the role of S and G2 phases, our work would need to be continued with distinct measurement of each phase duration. Our experiments suggest that G1 time adaption to size seems preponderant to that of S-G2 but it does not rule out the existence of additional control

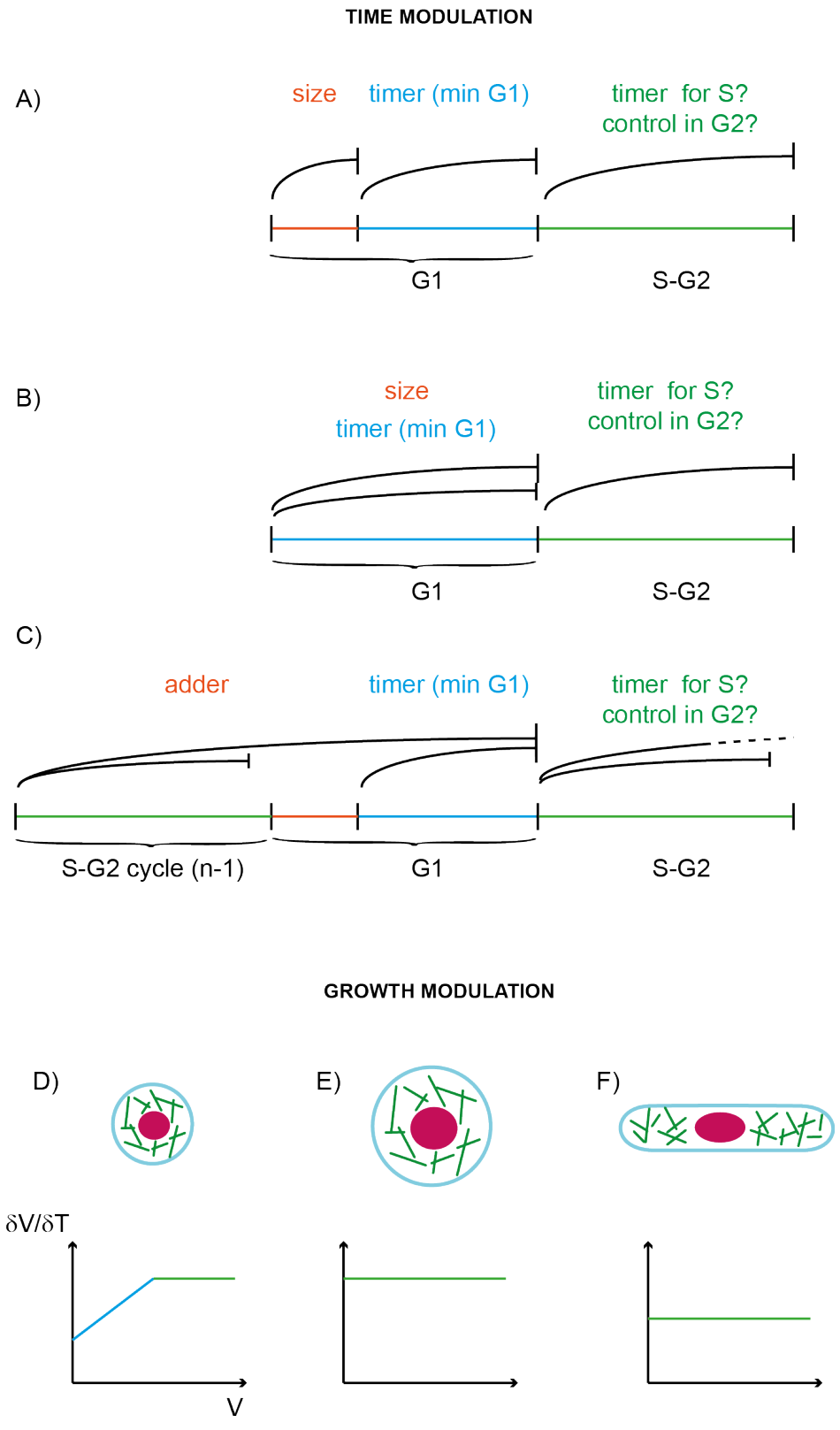

Figure 8.2: Time and growth modulations (Legend continued on the next page.)

Figure 8.2: Time and growth modulations (continued) Our results identify two main constraints on **time:** a volume dependent duration of G1 phase and a minimal duration of G1. Hypothetically, these constraints could be effective A) sequentially (as in proposed for *S. cerevisiae* by Schmoller et al. (2015); Di Talia et al. (2007) and for *E. coli* by Adiciptaningrum et al. (2015), B) concomitantly, C) sequentially but with the constraint on added volume overlapping two cell cycles and acting parallel to other controls in sub-periods (*i.e.* timer in S-G2 or late G1). This last possibility is hypothesized both in *S. cerevisiae* Soifer et al. (2016) and *E. coli* Amir (2014); Ho and Amir (2015). Our results also suggest that S-G2 display timer properties but we cannot rule out that additional rate-limiting processes existing during these phases could be unraveled by studies in different growth conditions. We also observe three types of **growth:** D) HeLa cells with sizes observed in classical cell culture conditions inceased their growth speed through G1, suggesting an exponential growth mode while S-G2 was closer to linear; E) large HeLa cells showed a saturation of growth speed regardless of cell cycle phase; F) cells confined in micro-channels showed indirect evidence of slow linear growth, possibly due to limitations of their surface exchange with the medium mostly occuring through their tips.

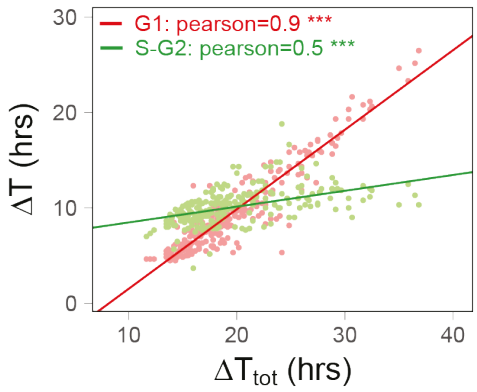

Figure 8.3: Most of the variability in total cell cycle duration is due to variability in G1 in HT29. Duration of G1 phase shows a strong positive correlation with total cell cycle duration ΔT_{tot} IN HT29 cells.

of size in these later phases. Similarly to what has been observed in both fission yeast and budding yeast (section 3.2), performing experiments in various growth conditions or with artificially induced abnormally small sizes might unravel additional 'cryptic' size controls in G1 or other phases than G1.

8.2.1.3 Conclusion on the role of time adaptation

Our work identifies a dependency of G1 duration on initial volume in both HT29 and HeLa cells which adds up to the previously more indirect results suggesting that G1/S transition is size-dependent Killander and Zetterberg (1965); Dolznig et al. (2004). There is however a lower boundary to this adaptation of time since G1 has a minimum duration of approximately 4 hours for the largest HT29 and HeLa cells. This limitation was confirmed with artificially induced large roscovitine treated cells and might be explained by the minimum window of time required for the inactivation of APC^{Cdh1} complex Cappell et al. (2016).

The straightforward question from this result is to understand how the cell cycle network is regulated in a way that adapts to cell size. For this, the model currently identified in *S. cerevisiae* and based on the dilution of the G1 cyclin inhibitor is appealing Schmoller et al. (2015). Investigating this model is now possible in mammalian cells with the recent development of reporters of the main actors of the G1/S transition Barr et al. (2016); Cappell et al. (2016). Moreover, perturbations of initial sizes, for example to identify a potential upper boundary to G1 time adaption for very small cells and studies in variable growth environments will be helpful to refine the understanding of the role of G1 adaptation in size control and the possible existence of other controls later in the cell cycle (7.3.2). Small sizes could for example be obtained by transient treatment with rapamycine, an inhibitor of mTORC1 or culture in nutrient poor medium. Alternatively, mechanical ablation of part of the cytoplasm could be used. For this, classical enuclation protocols enabling the recovery of karyoplasts containing the nucleus and a very small amount of cytoplasm with the centrosome could be interesting Karsenti et al. (1984); Piel et al. (2000). An alternative and original approach consists in transiently inducing blebbing using latrunculin treatment and then detaching the blebs from the cells by a step of centrifugation in a gradient of ficoll Biro et al. (2013).

All our results however are not explained only by time adaptation and we will now discuss the potential role of variations of growth rate in cell size control.

8.2.2 Growth modulation

8.2.2.1 Experimental evidence

Several observation from our work show that growth is a fluctuating process during the cell cycle and that constraints on growth might play a role in cell size control.

Phase-dependent growth rate in L1210 and HeLa cells First, for HeLa cells, our preliminary results suggest a transition from exponential growth in G1 to linear growth in S-G2 phase (chapter 7, supplementary figure 4 C-D). This needs further confirmation with more analysis but it is interesting to compare this transition with already published work since the hypothesis of active regulation of growth speed in mammalian cells has recently gained interest. From the two studies reporting dynamic measurement of growth, one indeed reported that in lymphoblastoid L1210 cells, G1/S transition was concomitant with a decrease in the variability of growth speed Son et al. (2012), while the second one observed that adherent U2OS cells showed exponential growth in S-G2 and linear growth in G1. Direct evidence that growth fluctuates over the cell cycle is thus starting to appear although there is no consensus about the precise description of these fluctuations, possibly partly because of cell-type specific behaviours. Another study reported growth trajectories on HeLa cells before us Kafri et al. (2013). It is however important to note that these trajectories were established from fixed population samples and based on the assumption that cell cycle timing did not vary upon size. This probably explains why we do not reproduce the results from the study: the authors indeed claim that they observe a constant growth speed over time in G1, followed by a decrease in growth rate in late G1 and an increase in S-G2. Phase-dependent growth speed are well documented in both *S. pombe* (section 3.2.1.3, Sveiczer et al. (1996); Nobs and Maerkl (2014)) and *S. cerevisiae* (section 3.2.2.2 and Goranov et al. (2009); Leitao et al. (2016); Ferrezuelo et al. (2012)). An interesting hypothesis, consistent with our observation is that, alike *S. cerevisiae* mammalian cell cycle phases are separated between phases where growth occurs (*i.e.* G1) and phases where the energy is allocated to other processes such as replication (S phase) Goranov and Amon (2010). Alternative hypotheses such as active growth rate regulation will be discussed in the next sub-section 8.2.2.2.

Large HeLa cells grow linearly A second important observation from our work is that growth speed seems to saturate in very large cells. Roscovitine treated HeLa cells indeed show a growth speed that is constant with respect to volume (chapter 7, supplementary figure 4E-F), although we need to fully confirm this result with more statistics. Remarkably, several published results already suggest that growth rate is linear or saturates for very large cells Conlon and Raff (2003); Tzur et al. (2009); Son et al. (2012).

These observations lead us to wonder whether and how growth speed is regulated in the cell.

8.2.2.2 Growth regulation and cellular homeostasis

Because unicellular organisms grow exponentially at the population level, and because single cell growth is often thought to be well described by a mono-exponential curve in *E. coli* Wang et al. (2010); Osella et al. (2014); Godin et al. (2010); Iyer-Biswas et al. (2014), *S. cerevisiae* Di Talia et al. (2007); Godin et al. (2010); Soifer et al. (2016) or mammalian cells Tzur et al. (2009); Godin et al. (2010); Park et al. (2010); Sung et al. (2013), the idea that growth rate can be constrained and that this potentially plays a role in cell size control was long neglected. This question however appears more and more important as observations in this line are emerging in diverse organisms Goranov and Amon (2010); Kafri et al. (2013) (also see section 2.4.1). Three types of constraints on growth are

discussed: metabolic scaling with cell size, physical constraints on volume growth via the addition of surface area and limitations of protein synthesis.

Metabolic scaling with cell size Allometry studies how metabolic rate scales with body mass (reviewed in Glazier (2014)). The characterization of such relationship at the unicellular level is less understood to date. We observed that growth rate is slower for large roscovitine-induced HeLa cells. This result echoes the observation that growth rate of L1210 cells starts decreasing after reaching very large sizes Tzur et al. (2009) later confirmed by direct measurement showing that large cells grow slower than small cells at G1/S transition Son et al. (2012). In the same line, indirect approaches reported that Schwan cells blocked in S phase grew linearly Conlon and Raff (2003) and that growth rate was negatively correlated with cell size at some specific time-points in the cell cycle Kafri et al. (2013). Evidence in various unicellular organisms were also found. In *Amoeba proteus*, early work took advantage of the fact that light exposure inuced asymmetrical divisions to study the growth rate of abnormally small or large cells Prescott (1956). Results showed that the growth rate of these cells decreased through time and that this decrease was faster for large cells than for small cells. The observation that growth rate does not scale linearly with size but is rather maximum at intermediate size has also been documented in phytoplankton (reviewed in Marañón (2014)). A potential explanation for this non linear allometry was proposed by Miettinen and colleague who showed that although mitochondria content scaled linearly with cell size (reviewed in Marshall (2015)), mitochondria function did not in several types of metazoan cells Miettinen and Bjorklund (2016) and rather displayed an optimum of fitness at intermediate size. Mitochondria homeostasis therefore appears to be central for cell metabolism and growth rate.

Intracellular homeostasis of organelles & growth homeostasis Early during this PhD, we hypothesized that perturbing the symmetry of segregation of specific cellular sub-compartments could be an interesting tool to study intracellular homeotasis and its impact on cell fate. These ideas are reviewed in Cadart et al. (2014) (annexe A). Considering the central role of mitochondria in cell metabolism, we focused on this organelle and proposed a project to an intern, Camille Blakely, which aimed at finding tools to decouple mitochondria from volume segregation at mitosis. Our hypothesis was that this would generate populations of cells of different growth rates, uncoupled from cell size.

Mitochondria structure is the result of the balance between fusion and fission events (reviewed in Elgass et al. (2013)). At mitotic onset, the activation of CyclinB-Cdk promotes the activation of the main fission actor, DRP1 Kashatus et al. (2011), the organelle becomes fragmented throughout the cytoplasm, thus allowing uniform partitioning during cell division. As explained in the method chapter (method sections 6.4.2 and 6.4.3), this mechanism made it very difficult to find a tool that successfully uncoupled mitochondria from volume sgregation. Proportional segregation of mitochondria was robust to all the mechanical perturbations we tried (asymmetric micro-patterns, confinement, combination of asymmetric micro-patterns and confinement) (figure 8.4 B). We then turned to chemical perturbations, although we were aware of the fact that with this approach it might be difficult to alter specifically mitochondria segregation and not mitochondria function. After trying different drugs and siRNA, we found that RNA silencing of the non-conventional Myosin 19 Rohn et al. (2014) led to asymmetrical segregation of mitochondria that were not accompanied by asymmetrical segregation of cytoplasmic volume (figure 8.4 A-D). Unfortunately, we did not have time to develope the project any further but this tool might be very interesting to study mitochondria homeostasis within the cell Marshall (2015) and its role in growth rate and cell size control Miettinen and Bjorklund (2016).

Surface area, a limiting factor for growth? Among the other models for cellular allometry the role of surface area which limits nutrient uptake an exchange with the environment is also discussed

Glazier (2014). In the experiments with HeLa and MDCK cells in the micro-channels, cells seem to grow linearly since they add the same amount of volume in the same amount of time independently of their initial size (see chapter 7, figure supplementary 2). In this case, it is likely that due to their confinement in the micro-channels (chapter 7, figure 2C), cells only uptake nutrient by their tips which have a constant area through the cell cycle, reminiscent of the linear growth mode of *S. pombe* which grow by their poles (section 3.2.1.3).

Another reason to think that surface area is an important parameter of size homeostasis is because volume growth is limited by the addition of membrane through the synthesis of new lipids, the appropriate balance of endocytosis and exocytosis and secretion of vesicles from the Golgi McCusker and Kellogg (2012); Morris and Homann (2001). How membrane addition is regulated remains poorly understood but links between membrane growth and the cell cycle have been found in *S. cerevisiae* (McCusker and Kellogg (2012); Goranov et al. (2009); Goranov and Amon (2010)). Moreover, lipid synthesis appears to be under the influence of both extracellular nutrients via mTORC1 pathway Caron et al. (2015); Teixeira and Costa (2016); Horton et al. (2002) in mammalian cells and membrane tension via the mTORC2 pathway in budding yeast Niles and Powers (2012); Berchtold et al. (2012); Eltschinger and Loewith (2016) (section 4.1.1.1). The role of membrane tension sensing in regulating cell volume growth via the synthesis of lipids and new membrane is interesting because it could suggest a mechanism where volume growth is the primary driver of cell growth. In this scenario, an intriguing question is how mass production follows volume and how cell density is maintained constant Grover et al. (2011) or on the contrary, fluctuates through the cell cycle Bryan et al. (2010). Additionally if this membrane tension mediated regulation of volume growth is confirmed in mammalian cells, it could suggest a mechanism linking tension sensing in the tissue and translation into enhanced volume growth at the single cell level.

The growth law: ribosomes and limitations of protein synthesis Traditionally, the minimal model to describe growth stated that protein synthesis was directly proportional to the amount of ribosomes (reviewed in Kafri et al. (2016a), section 2.4.1.2). In this model, total protein synthesis rate scales linearly with the fraction of ribosomes and the theoretical limit to protein synthesis rate is reached when all ribosomes are allocated to the synthesis of new ribosomes. Refinements to this model were however recently brought to discussion. They for example propose that mRNA supplies, which depends on the transcription from a finite number of DNA copies can become limiting for very large cells and lead to a deviation from exponential growth Hu and Zhu (2014); Kafri et al. (2016a). This model has been hypothesized to explain the reduced growth rate for large L1210 cells in Hu and Zhu (2014). Direct testing of such hypothesis in mammalian cells would require actively perturbing the transcription rate and assessing the impact on cell growth.

8.2.2.3 Conclusions on the role of growth modulation

Several growth modes Our work identifies several modes of growth. For HeLa cells cultured in the traditional way (*i.e.* seeded on a dish with no confinement), we observe that growth is exponential in G1 and closer to linear in S-G2 (chapter 7, supplementary figure 4C-D). However, when cells are grown under 2D confinement in the micro-channels, our results indirectly indicate that growth is linear (chapter 7, supplementary figure 2, MDCK and HeLa cells in micro-channels), possibly because of the limited active suface exchange for nutrient uptake. Moreover, growth speed seems to saturate for very abnormally roscovitine-induced large cells (chapter 7, supplementary figure 4E-F). This explains why these cells which cycle in a minimum G1 duration still maintain an adder in this phase.

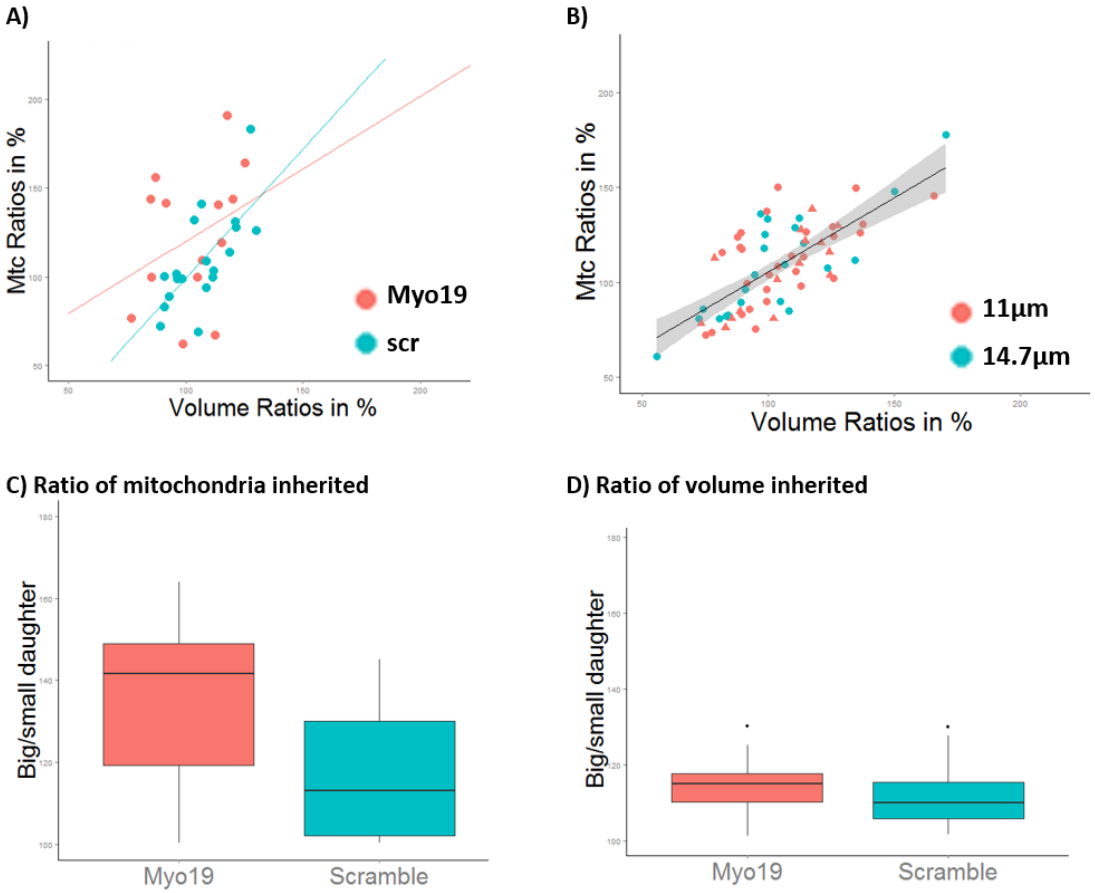

Figure 8.4: Decoupling mitochondria from volume segregation. We combined the FXm method with and fluorescence imaging of RPE1 cells tagged with a fluorescent mitochondria localizing signal (GFP-MLS RPE1). This enabled quantifying the symmetry of segregation of both volume and mitochondria amount. We looked at whether the ratio of mitochondria and the ratio of volume inherited at birth in pairs of sister cells were decoupled in several perturbations. **A) Myo19 RNAi:** mitochondria are distributed proportionately to volume in scramble condition *(*$R2 = 0.45$, $p = 0.0011$, $n = 19$, $N = 1$*), this proportional distribution is lost when asymmetrical mitochondria segregation is induced by Myo19 RNAi (*$R2 = 0.03$, $p = 0.24$, $n = 14$*).* **B) asymmetrical divisions by confining cells at different heights,** mitochondria remains segregated proportionately to volume *(*$R2 = 0.52$, $p < 0.0001$, *colors represent confinement height of* $11\mu m$ *(red) or* $14.7\mu m$ *(blue), symbols represent two different data-sets).*).**C)** Myo19 RNAi induces asymmetrical divisions of mitochondria *(t test* $p = 0.025$*)*, while **D)** it doesnt modify the symmetry of volume distribution *(t test,* $p = 0.17$*;* $N = 1$, $n = 19$ *for scramble and* $n = 14$ *for Myo19).*

The hypothesis of active regulation of growth rate as a function of size A recent hypothesis raised in mammalian cells is that active growth rate regulation is the basis of cell size control. Specifically, it is proposed that cells 'sense' their size and actively tune their growth rate accordingly Ginzberg (2015); Kafri et al. (2013). Our results and those from the literature do not provide, to our opinion, convincing evidence for this to date. Testing this would require (i) direct and dynamic measurement of single cell growth curves with a much higher throughput than currently possible with any method given the great variability observed in these cells; (ii) clarifying what are the determinant for mass and volume fluctuations and which of these two parameters is relevant for such a model. Moreover, in eukaryotes at least, the variability of the pathways involved in the regulation of growth (Lloyd (2013); Turner et al. (2012), section 4.1.1) depending on environmental signals and the resulting variability in intracellular content depending on the pathway stimulated (*i.e.* growth by increase of protein or lipid production or nutrient uptake) Saucedo and Edgar (2002); Son et al. (2015b) make it complicated to imagine a unique and robust molecular mechanism 'sensing' size and translating this into the regulation of overall growth rate.

On the contrary, a potentially simpler hypothesis is that more general rules such as the ones that dictate metabolic scaling with cell size exert constraints on the growth.

Non linear allometry in single cells We raised several hypotheses that could explain the non linear allometry of mammalian cells. A first hypothesis is the role of mitochondria and we proposed an experimental approach based on decoupling of mitochondria partitioning from volume segregation to further investigate this role (figure 8.4). A second hypothesis is the role of membrane synthesis as a limiting factor for either nutrient uptake or volume extension. The regulation of membrane synthesis and dynamics and their implications for cell growth is poorly understood McCusker and Kellogg (2012); Morris and Homann (2001); Gauthier et al. (2012). Several types of investigations are needed. Assessing cell growth in conditions where the production of limiting lipids for membrane synthesis such as sphingolipids is constrained or where membrane tension is induced through confinement Stewart et al. (2011) or hyper-osmotic shocks will probably be informative. It will also be interesting to understand where membrane addition occurs in mammalian cells (*i.e.* whether it occurs uniformly or at specific sites); this is however challenging technically as it would require controlling the synthesis of fluorescently-labelled lipids during a specific time-window and tracking their association with the membrane similarly to what has been done to study protein secretion Boncompain et al. (2012). Finally, revisions of the ribosome centered model of growth recently suggested that mRNA levels, in addition to ribosome amounts, limit protein synthesis rate are proposed. To investigate this, forcing cells to synthesize or transcribe useless proteins or transcripts similarly to what has been done in yeast and bacteria Basan et al. (2015); Kafri et al. (2016a) might reveal saturation of the growth process. The underlying hypothesis behind the idea that mRNA transcripts become limiting for large cells is that they depend on the transcription from a finite number of DNA copies. Endocycling and increased number of nuclei is a very common strategy to sustain cell size increase Edgar et al. (2014). It would therefore be interesting the compare the relationship between ploidy, cell volume and cell growth rate. Artificial induction of asymmetries in the micro-channels produce sister cells that have the same ploidy but different initial volumes. Transient starvation has been shown to induce cytokinesis failure in HeLa cells and could thus be used to generate small, binucleated cells Nishimura et al. (2016).

We tried to provide a description of the growth and time modulations evidenced by our work and the many open questions they raise. We now want to discuss whether and how these modulations might be combined to maintain size homeostasis.

8.2.3 Conclusion on the respective contribution of time and growth modulation in size control

8.2.3.1 Classification of the results into three types of combinations of growth and time modulation

We performed experiments in several conditions. We studied growth in both confined (micro-channels, chapter 7, figure 2C and supplementary figure 2) and unconfined (FXm device chapter 7, figure 1) environments. We also perturbed the initial distribution of cell volume with either wider distribution induced by asymmetrical divisions (chapter 7, supplementary figure 2) or higher average value through 48hrs roscovitine block (chapter 7, figure 4). The most common feature to all these conditions is that cells behave in an adder-like manner (chapter 7, figure 2B). The central question is to understand how growth and cell cycle progression are coordinated in order to generate this adder (chapter 7, figures 3-4). We propose a general mathematical frame to compare the relative contribution of growth and time modulation (chapter 7, figure 5) and we show that these fluctuate upon the cell type and the growth condition. We can attempt to rationalize these behaviours into 3 different categories (figure 8.2):

- When cultured in 1D, epithelial HT29 and HeLa cells seem to grow exponentially, at least during G1 phase (chapter 7, supplementary figure 1B and supplementary figure 4C-D). In this case, cell cycle delay with respect to size is required to maintain size homeostasis. Consistent with previous indirect findings Killander and Zetterberg (1965); Dolznig et al. (2004), G1/S transition is negatively correlated with initial size. Given the similarity of the cell cycle network between *S. cerevisiae* and mammalian cells Fisher (2016), it is tempting to wonder whether a mechanism where added volume Schmoller et al. (2015); Soifer et al. (2016); Delarue et al. (2016) rather than absolute volume is sensed in these cells.

- When grown under confinement, MDCK and HeLa cells show indirect evidence of linear growth. Results with these cells further suggest the idea that the addition of a constant volume might be one of the rate-limiting factor of cell cycle progression. Indeed, these cells, which grow slower than when cultured without confinement, take longer than a normal cell cycle and overall add a constant amount of volume (chapter 7, supplementary figure 2). In appearance, one could argue that the constant added amount of volume is just the result of the combination of linear growth with a timer. However, a hypothesis for why cell cycle duration is lengthened compared to the normal timing observed under exponential growth is needed. Lengthening caused by a restriction point sensing nutrients or growth factors is unlikely since HeLa the restriction point is not intact, as in most cancerous cells Moody and Laimins (2010). A potential explanation is therefore that at least part of this cell cycle lengthening is due to a size or added volume sensing mechanism. The key experiment to test the robustness of the molecular adder would be to perform experiments with the same cells at slow growth rate induced by another perturbation than confinement (*i.e.* nutrient deprivation) and at fast growth and then compare the value of ΔV gained in each of these conditions.

- Finally, large HeLa and HT29 cells seem to reach both a limiting growth rate (chapter 7, supplementary figure 4E-F) and a minimum duration of G1 (chapter 7, figure 3D and figure 4B). The combination of linear growth with a timer-like G1 phase results in an adder. The saturation of growth rate is also hypothesized to explain size control in L1210 cells Son et al. (2012); Tzur et al. (2009) which do not adapt cell cycle time Son et al. (2012) but still generate an adder (chapter 7, figure 5).

The fact that Raji cells behaviour does not fall in any of these three categories however suggests that

we are missing some of the elements. Overall, our work hints at three distinct rate-limiting processes for the cell cycle but others will still be unravelled by future research.

8.2.3.2 Identification of three distinct rate-limiting processes for cell cycle and cell growth

Our results identify with different levels of certainty discussed above three main rate-limting processes to cell cycle and cell growth:

- ΔV **or** V**:** as explained just above, the lengthening of G1 in a volume dependent manner in HT29 and HeLa cells as well as the conservation of an adder behaviour in cells that grow very slowly (MDCK and HeLa in micro-channels) strongly suggests that the addition of a constant ΔV limits cell cycle progression.
- ΔT_{min} **in G1:** G1 duration appears to have a lower boundary close to 4-5 hours. This is shown in the largest cells of unperturbed populations of HT29 and HeLa cells and in abnormal large cells induced by roscovitine block.
- $\Delta V/\Delta T_{max}$ **for large cells:** growth speed is limited for large cells.

These limitation on either growth speed or cell cycle timing are not all observed at once, they are rather revealed by specific environmental growth conditions or limit sizes. A striking observation is that in all these conditions, the overall effective size homeostasis is that of an adder. A intriguing question is therefore whether a unique mechanism leading to an adder can recapitulate all these phenomenon.

8.3 Is there a unique mechanism or several processes resulting in the adder?

8.3.1 Generality of the adder, from bacteria to mammalian cells

8.3.1.1 Generality of the adder in our results

The most striking result from our work is that mammalian cells most often behave in an adder-like manner (chapter 7, figure 2). We observe this behaviour in both HT29 and HeLa cells measured with the FXm method but also in cells grown under confinement in micro-channels (MDCK and HeLa) or HeLa cells induced to be abnormally large (chapter 7, figure 4). We also find this adder behaviour in L1210 cells from a previous study on dynamic measurement of cell mass Son et al. (2012). One notable exception to this behaviour is that of Raji cells which showed a very weak homeostasis mechanism with a slope coefficient of the plot V_f vs. V_i equals to 1.7.

8.3.1.2 Generality of the adder in the litterature

Over the past 3 years the adder mechanism was observed in a variety of organisms, from bacteria Campos et al. (2014); Taheri-Araghi et al. (2015); Soifer et al. (2016); Deforet et al. (2015) to yeast Soifer et al. (2016). At the phenomenological level, this mechanism is characterized by an absence of correlation between volume gained and initial volume and a correlation between final and initial volume that gives a slope close to one (figure 2.1). An adder behaviour predicts that, for cells that divide

symmetrically, the difference of volume between a given cell and the mean volume is divided by two at each division (equation 2.5, Sauls et al. (2016); Amir (2014)), which our experiment in micro-channels reproduces (chapter 7, figure 3C-D). However, the emphasis made on the adder behaviour should not prevent from a more precise and complex description of the homeostasis behaviour in any cell type. At this stage of our discussion, it is thus important to recall several results that balance the apparent universality and simplicity of the adder.

8.3.2 Is there enough evidence to conclude that size homeostasis is an adder in mammalian cells?

8.3.2.1 Statistical resolution is currently lacking to confirm the adder in any organism.

Even in bacteria studies where the number of cells measured can reach $1.2 * 10^4$, theoretical work showed that no study currently has the statistical power to validate a given homeostasis mechanism Grilli et al. (2016) (section 3.1.4.2). In this work, it is shown that the more variability in the data, the more a distinction between different trends and mechanisms becomes possible. The drawback is that low sampling in the tails of the distribution reduces the confidence in the trends observed. An example of the sensitivity of the conclusions depending on the method used for correlation analysis can be found with the analysis of the same data-set obtained in *C. crescentus*: the initial study had concluded in a weak size homeostasis behaviour with a slope coefficient of the plot V_f vs. V_i equals to 1.8 Iyer-Biswas et al. (2014) while it was later re-evaluated to be closer to an adder Jun and Taheri-Araghi (2015).

Aware of this problem, we looked for the statistical method that was best adapted to our data (see methods chapter 6.15). However, the statistical resolution of our data is far from that of bacteria. In addition to gaining statistical power, validation or invalidation of the adder mechanism will require further experimental testing.

8.3.2.2 Testing the adder

A good starting point to test the adder behaviour is the measurement of the rate of convergence of sizes in cells after an initial perturbation of cells Sauls et al. (2016) (section 2.1). In this regard the reduction by half of artificially induced asymmetrical divisions through confinement in the micro-channels is a convincing argument in favor of an adder mechanism in mammalian cells (chapter 7, figure 2C). It is worth noting however that in this experiment, the growth mode of cells is different than that observed in the absence of confinement (see above discussion 8.2.3.1).

Other experimental strategies testing the robustness of the adder observation to various growth conditions for example as has been done in *E. coli* Wallden et al. (2016); Kennard et al. (2016) will be important. It is also possible that such testing will in fact reveal that size homeostasis is a flexible process.

8.3.3 Size homeostasis is a flexible process

In the introduction of this thesis, we emphasized on the fact that size control is a process that must be both robust (prevent size divergence) and flexible (adapt to environmental changes) (figure 1.1) and that taking into account this flexibility is an important guide in the characterization of the homeostatic process (section 2.6.2).

8.3.3.1 Bacteria and *S. cerevisiae*: not always an adder

In *E. coli*, Wallden and colleague recently showed that as cells were grown in slow conditions, they tended to show stronger size homeostasis mechanism, closer to a sizer than to an adder Wallden et al. (2016). Similarly, in *S. cerevisiae*, cells grown in glycerol/ethanol instead of glucose grew slower and showed stronger size control in G1 Di Talia et al. (2007). Direct experimental proof of such variability of the strength of size control upon the change in growth conditions is currently lacking in mammalian cells. Performing such experiments is in fact difficult because the observation of full cell cycle trajectories would require performing even longer experiments than the ones made on normal growth conditions. Son *et al.* performed experiments in limited isoleucine conditions but did not comment on the effective strength of size homeostasis Son et al. (2012). In figure 8.5, we show a preliminary result on HeLa cells suggesting that the strength of size control might be negatively correlated with the average growth speed but more experiments are needed to confirm this. Our work already shows that the homeostatic behaviours are all (except for Raji cells) near-adder (chapter 7, figure 4B) albeit with some variability of the slopes of the plot V_f vs. V_i that range from 0.7 to 1.2 (chapter 7, figure 2B).

Another interesting idea raised in *S. cerevisiae* is that in the case where the molecular mechanism for size sensing depends not only on the absolute accumulation of an activator molecule but also on its rate of accumulation (see section 3.2.2.4), within the same population, small cells will show a sizer-like behaviour while large cells will show an adder behaviour Delarue et al. (2016). In *E. coli* as well, large and small cells in a population were shown to deviate from the mean behaviour Kennard et al. (2016).

8.3.3.2 Why flexibility is important when trying to build a model for size homeostasis

The observation that size homeostasis behaviour changes upon environmental conditions or initial size is important for at least two reasons. First, one must keep in mind that any homeostasis behaviour observed is potentially valid only for the experimental growth conditions that were tested. In most cases in the literature, this corresponds to the maximum growth speed of the cells, since cell culture protocols and reagents tend to maximize the doubling time and growth speed. For this reason, one of the hypotheses raised to explain the generality of the adder is that it is a simple evolutionary convergence of selection for a mode of growth and cycling that is the fastest possible while preventing size divergence. Our experiment showing that large roscovitine treated HeLa cells reach a maximum speed of growth and start growing linearly could be interpreted in this line of thought: a possible interpretation indeed is that these cells do not actively control size but show an effective adder because their mode of growth, at these maximal sizes, becomes linear and is combined with a minimal cell cycle duration.

Second, as explained in section 2.6.2, the apparent flexibility of size control is a helpful indicator of the potentially several rate-limiting processes to either growth or cell cycle progression that participate to the effective size control. For example, the C+D periods which were supposed to be a timer in *E. coli* were shown to be delayed at slow growth Wallden et al. (2016), unraveling an additional rate-limiting process occurring during these phases.

8.3.3.3 Conclusion: phenomenological adder and molecular adder

It is now clear from studies in bacteria that what people put behind the term 'adder' is not what it used to refer to initially. In the first studies, the 'adder' was proposed as a phenomenological behaviour very common to several organisms Sauls et al. (2016). However since then, evidence that

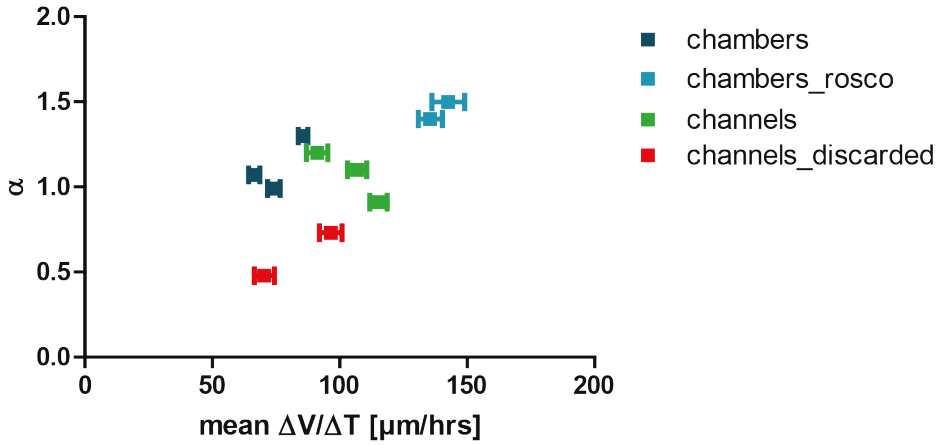

Figure 8.5: Efficiency of the homeostatic process is a function of growth speed? The coefficient α of the V_f vs. V_i plot is plotted against the mean growth spead $\langle \Delta V/\Delta T \rangle$ in each individual experiments performed with HeLa cells. Experiments in chambers correspond to HeLa-FUCCI measured with the FXm method with our without roscovitine treatment; among the experiments performed in the micro-channels, some were made prior to the optimization of the device and showed a low growth speed with a decreasing volume through time (see figure 6.12). These were discarded for the paper but provide data-sets with lower growth speed.

the same organism can display a range of effective homeostatic behaviours depending on growth rate both at the population level Wallden et al. (2016) and the individual cell level Kennard et al. (2016); Delarue et al. (2016) was reported. Phenomenologically, the adder therefore appears as the behaviour resulting from a specific set of external conditions. Importantly, the apparent flexibility of size control at the phenomenological level is not incompatible with a molecular adder. In *E. coli* indeed, one of the most popular model to describe size control is that of a molecular adder based on the addition of a constant amount of volume per origin of replication Zheng et al. (2016); Si et al. (2016); Ho and Amir (2015) while the effective homeostatic behaviour varies upon the growth conditions because of additional rate-limiting processes occurring in other periods of the cell cycle Wallden et al. (2016) or because this constant of volume addition occurs on overlapping cell cycles Ho and Amir (2015); Amir (2017). This is not however the only model envisioned and understanding whether and how one or several molecular processes result in an effective homeostatic behaviour that varies upon environmental condition is the current challenge in the fields of bacteria and yeasts.

8.3.4 Several scenarios can explain the apparent adder in mammalian cells

As described in section 2.5, several scenarios to explain size control in each organisms are currently debated. A distinction can be made between models that favour a unique molecular mechanism Ho and Amir (2015); Amir (2017); Zheng et al. (2016); Si et al. (2016); Amir (2014); Soifer et al. (2016); Harris and Theriot (2016) and models that rather hypothesize the contribution of several processes Adiciptaningrum et al. (2015); Wallden et al. (2016); Delarue et al. (2016); Osella et al. (2014). The debate in yeast and bacteria highlights the difficulty of answering this question. Here we discuss both possibilities for mammalian cells.

Scenario 1: Molecular adder At first sight, the generality of the adder in our experiments despite the variability of conditions and cell types tested suggests a molecular mechanism precisely maintaining the adder. In both *E. coli* and *S. cerevisiae*, an adder overlapping two cell cycles Soifer et al. (2016); Ho and Amir (2015) has been proposed (section 2.5.2). In *S. cerevisiae*, such a model predicts a

positive correlation between ΔV_{S-G2} of the mother cell and V_{birth} of the daughter cell and a negative correlation between ΔV_{G1} and V_{birth} of the daughter cell. These contributions cancel and give an effective adder Soifer et al. (2016). In HT29, these trends are reproduced (figure 8.6, although we do not have enough observations to confirm the last prediction of the model which is that volume added between two G1/S transition is not correlated with volume at birth. HeLa cells however give a less convincing result with no negative correlation between ΔV_{G1} and V_{birth} (chapter 7, figure 4D).

Scenario 2: Sizer in G1, timer in S-G2 An alternative scenario to the overlapping adder is that each phase of the cell cycle behaves independently and that the sum of the controls in each period yields an effective homeostatic behaviour Adiciptaningrum et al. (2015); Delarue et al. (2016) (see section 2.5.1). Classically, a strong size control operates during a fist phase (G1 for *S. cerevisiae*, B period for *E. coli*) while a second phase, dedicated to replication, displays timer properties with no control on size (S phase, or $C + D$ period respectively). The sum of these two phases results in an apparent adder although no phase actually counts added size. Our results in HT29 are also compatible with this model (chapter 7, supplementary figure 3). Again, HeLa cells which give an apparent adder in both G1 and S-G2 are less conclusive (chapter 7, figure 4D, supplementary figure 4B). It is possible that the weaker size control observed in G1 in these cells is due to the fact that they already cycle in times very close to the minimum G1 duration (chapter 7, figure 4B)

In *S. cerevisiae*, where the molecular mechanism for size sensing in G1 is proposed to rely on the progressive dilution of the cyclin inhibitor Whi5 whose amount is constant during G1 Schmoller et al. (2015), it was recently suggested that the Start transition activator Cln3 accumulates proportionately to the growth rate, not volume Delarue et al. (2016) (discussed in details in figure 3.2.2.4). Notably, a correlation between early growth rate in G1 and G1 duration was found in L1210 Son et al. (2012) and it will be interesting to see if this observations fits with this last model. Another prediction of the model is that very small cells will behave more like a sizer. Testing this result could be done via artificially inducing small cells (see discussion above 8.2.1.3).

Deciphering between scenario 1 and scenario 2 How the study of correlations can be used to decipher between scenarios 1 and 2 is not clear from the literature. Comparing the variability of added volume between two G1/S transitions with the added volume between two birth event could provide a first test. However, we do not have sufficient measurements of successive cell cycles to test this in HT29 (figure 8.6)

Scenario 3: combination of processes A final possible description of the cell cycle is that several parallel and concurrent processes operate constrains on the timing or growth. Each of these process can become rate-limiting in certain conditions and overall the system composed of all these processes evolved to maintain size homeostasis in various growth environments (section 2.5.3). In addition to suggesting that an important part of size control occurs in G1 through an adaptation of cell cycle duration, our work identifies two rate-limiting processes: a minimum duration of G1 and a maximum growth speed for large cells and points to a constraint on added volume (above section 8.2.3.2). The combination of the different processes always yields an homeostatic behaviour resembling that of an adder (chapter 7, figure 5B and section 8.2.3.1). In yeast, the existence of cryptic size controls that are unraveled by culture conditions different from the traditional ones suggest that several processes coordinating growth and cell cycle progression exist and that a unique mechanism cannot account for the robustness of size homeostasis in various conditions.

Therefore, although this last scenario is perhaps less satisfying at first sight because it does not propose a unique and simple mechanism recapitulating all the behaviours observed it might enable an accurate description of the cell cycle and growth processes compatible with the many layers of

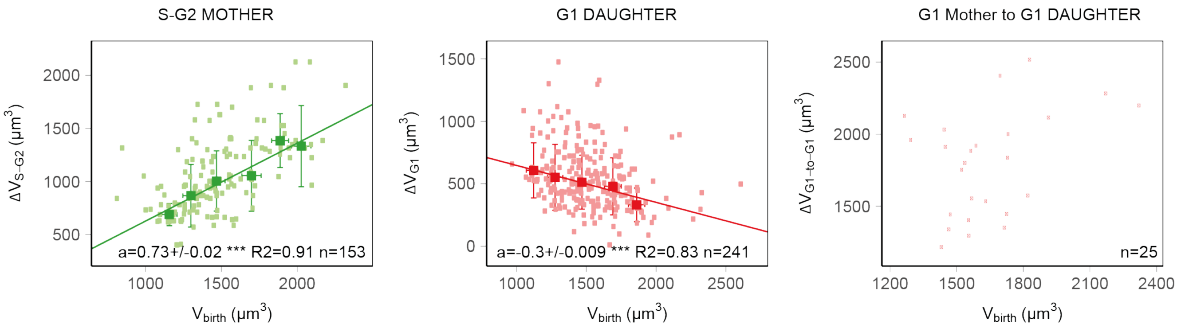

Figure 8.6: Testing the existence of an adder between two G1/S transitions. The model of an adder overlapping two cell cycles gives three predictions Soifer et al. (2016): (i) ΔV_{S-G2} in the cell cycle (n) is positively correlated with V_{birth} (left); (ii) ΔV_{G1} in the cell cycle $(n+1)$ is negatively correlated with V_{birth} (middle) and (iii) $\Delta V_{G1-to-G1}$ is not correlated with V_{birth} (right plot with not enough observations to test the significance of the plot). *Experiments on HT29-hgem-mcherry, N=4*

regulations observed in mammalian cells.

8.4 Perspectives: a combination of processes, both single and tissue-level determined?

The complexity of the regulation of growth and cell cycle progression in cells from multicellular organisms lies in the fact it can be decomposed into two layers: one exerted at the tissue or body level and one at the intrinsic cell level. Whether the second layer of regulation, which hypothesizes an active coordination of growth and cell cycle progression, exists at the single cell level is still argued (discussed in details in section 1.2, Lloyd (2013); Ginzberg et al. (2015); Saucedo and Edgar (2002)).

Among the arguments against the existence of a cell size homeostasis process is the claim that cell growth and cell cycle progression are two separate and independent processes Lloyd (2013). Our work however shows that cell cycle duration, more specifically G1 duration is correlated with initial cell volume in cells growing exponentially. We also observe that slow growing cells delay their cell cycle and ultimately add a constant amount of volume per cell cycle. These findings confirm previous indirect evidence of a size-dependent progression through G1 in mammalian cells Dolznig et al. (2004); Killander and Zetterberg (1965), alike what has long been characterized in *S. cerevisiae* Hartwell and Unger (1977). Importantly, it is commonly observed that overall in *Drosophila* mitotic tissues such as the wing, artificially induced increased growth rates through over expression of Ras Prober et al. (2000), dMyc Johnston et al. (1999), Rheb Saucedo et al. (2003) or proteins of the PI3K class Weinkove et al. (1999) accelerates passage through G1/S, through a mechanism that involves cyclin E Prober et al. (2000). However, in these studies S-G2 does not adapt to growth rate (or size) and cells reach larger sizes than in normal conditions which led some authors to conclude that the maximum rate of division is set by a developmental program at the tissue level and that growth rate and division rate are determined separately Edgar (2006); Edgar and Nijhout (2004). An alternative explanation however could be that S-G2 display timer properties and that G1 duration also reaches a minimum value, as our experiments and others Cappell et al. (2016) suggest the existence of a minimal cycling time. Our identification of rate-limiting processes constraining cell growth or cell cycle progression are thus helpful to revisit some of the published results that had led to the conclusion that size control does not exist in metazoan cells. A famous argument for example, was that *in vitro* cells blocked in S phase increased their sizes linearly with time Conlon and Raff (2003). Yet, this observation is potentially compatible with our finding that large cells change from exponential growth to linear growth.

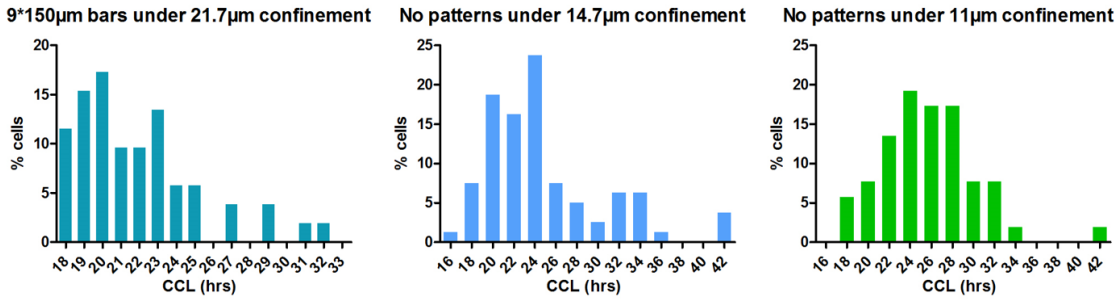

Figure 8.7: Confinement during mitosis impacts daughter's cell cycle duration in RPE1 cells. Cells were cultured in FXm chambers of decreasing heights. These heights were above $7\mu m$, the typical height of a cell in interphase and thus only mitotic cells 'sensed' the confinement. As the height decreases and the cell confinement at mitosis increases, cell cycle length (CCL) are shifted towards higher values. (In some cases micro-patterns were added to prevent cell migration out of the imaging field).

The interest of studying of growth and cell cycle progression at the single cell level on proliferating mammalian cells has sometimes been debated Lloyd (2013). Our work in fact highlights two aspects of size homeostasis that are, to our opinion, fully compatible with the more classical view of size homeostasis in multicellular organisms. First, it shows that G1 progression is size (or added size) dependent, a result that has been observed not only in single cultured cells Dolznig et al. (2004); Killander and Zetterberg (1965) but also in proliferating tissues of model organisms Edgar (2006). Second, and perhaps more convincingly to reconciliate with the view that growth and cell cycle progression are independently regulated Lloyd (2013), our results point at the existence of several rate-limiting processes constraining either growth or cell cycle timing. These processes are revealed by studying cells in different growth environments (*i.e.* confined or not) and suggest that multiple mechanisms are potentially involved in cell size homeostasis and overall maintain a coherent size homeostasis behaviour often close to that of an adder.

In addition to investigating the precise mechanistic details of the modulations of cell cycle and growth ensuring size homeostasis at the single cell level, it will be interesting to assess how these mechanisms are relevant in more complex environments mimicking cells in healthy or cancerous tissues for example. This could be done in organoids Delarue et al. (2014). Remarkably however, we observed that very reductionist approaches can already point at additional layers of regulations to that discussed in this work. Indeed, when we cultured RPE1 cells in chambers confining cell's height only at mitosis, we could observe that the cell cycle following a mitosis was lengthened (figure 8.7). This suggests that even at the single cell level, mechanical confinement sensed during mitosis can be translated into signaling to the cell cycle network, possibly via a mechanism involving the regulation of p21 and Rb levels Spencer et al. (2013). This result is reminiscent of our observation that cells in micro-channels also cycle slower. It is therefore tempting to speculate that complex layers of regulations, integrating not only cell growth at the single cell level as discussed in this study but also external mechanical signals mimicking for example confinement in a tissue can be approached by single cell studies in controlled environments.

Overall, as our understanding of size homeostasis evolves towards a flexible process that involves several types of constrains on growth and cell cycle, we envision that a unified vision of the role of size homeostasis from the single-cell level to the tissue-level will become possible.

Chapter 9

Conclusion

Whether size homeostasis in mammalian cells is the result of active regulation of growth and cell cycle progression is debated and poorly understood Lloyd (2013); Ginzberg et al. (2015). Our work brings a significant contribution to this question by proving the first direct and dynamic measurement of single cell volume through cell cycles.

Combining live volume measurement with cell cycle tracking, we show that G1 duration is adapted to cell volume, confirming more indirect previous observations in cultured cells Killander and Zetterberg (1965); Dolznig et al. (2004) and *Drosophila* Edgar (2006). Studying the underlying molecular mechanism to understand whether G1 adapts to volume or added volume will probably benefit from the findings in *S. cerevisiae* Di Talia et al. (2007); Schmoller et al. (2015); Delarue et al. (2016); Soifer et al. (2016), which shows remarkable similarities with mammalian cells both at the phenomenological and molecular levels Fisher (2016).

Additionally, the importance of growth modulations was hinted by live measurement of growth trajectories Son et al. (2012); Mir et al. (2011) and more indirect approaches Tzur et al. (2009); Kafri et al. (2013). Our results provide a possible interpretation for these observations since we show that growth rate saturates for very large cells and becomes linear. This enables maintaining size homeostasis even in large cells that no longer adapt G1 duration to volume because they cycle in a minimal time. The mechanism behind growth modulations is hypothetical at the moment. Notably, such modulation likely depend on very distinct regulatory types of signals than those acting on the cell cycle machinery. Indeed, the cell cycle network is a system optimized for irreversible and switch-like decisions such as commitment into a new round of division Tyson and Novak (2014). On the contrary, constrains on cell growth might be defined by more general metabolic and physical principles Glazier (2014).

In order to compare the behaviour of proliferating single cells, from bacteria to mammalian cells, we propose a general unbiased mathematical framework. This analysis points to the robustness of size control across kingdoms and growth conditions, often resembling an adder. However, the generality of this observation can be the result of a variety of coupling between cell growth and cell cycle. Size homeostasis therefore appears as a flexible process that involves modulations of growth and cell cycle to provide a robust response of cells to fluctuating environments both in unicellular and muticellular organisms.

Bibliography

S. Adhikary and M. Eilers. Transcriptional regulation and transformation by Myc proteins. *Nature reviews. Molecular cell biology*, 6(8):635–45, 2005. ISSN 1471-0072. doi: 10.1038/nrm1703. URL http://www.ncbi.nlm.nih.gov/pubmed/16064138.

A. Adiciptaningrum, M. Osella, M. C. Moolman, M. Cosentino Lagomarsino, and S. J. Tans. Stochasticity and homeostasis in the E. coli replication and division cycle. *Scientific reports*, 5 (November):18261, 2015. ISSN 2045-2322. doi: 10.1038/srep18261. URL http://www.ncbi.nlm.nih.gov/pubmed/26671779.

A. Amir. Cell Size Regulation in Bacteria. *Physical Review Letters*, 112(20):208102, may 2014. ISSN 0031-9007. doi: 10.1103/PhysRevLett.112.208102. URL http://link.aps.org/doi/10.1103/PhysRevLett.112.208102.

A. Amir. Is cell size a spandrel? *eLife*, 6:1–8, 2017. ISSN 2050-084X. doi: 10.7554/eLife.22186. URL http://elifesciences.org/lookup/doi/10.7554/eLife.22186.

A. Amodeo and J. Skotheim. Cell-Size Control. *Cold Spring Harbor Perspectives in Biology*, 8, 2016. ISSN 1943-0264. doi: 10.1101/cshperspect.a019083.

A. R. Araujo, L. Gelens, R. S. M. Sheriff, and S. D. M. Santos. Positive Feedback Keeps Duration of Mitosis Temporally Insulated from Upstream Cell-Cycle Events. *Molecular Cell*, 64(2):362–375, 2016. ISSN 10974164. doi: 10.1016/j.molcel.2016.09.018. URL http://dx.doi.org/10.1016/j.molcel.2016.09.018.

O. Atay and J. M. Skotheim. Modularity and predictability in cell signaling and decision making. *Mol Biol Cell*, 25(22):3445–3450, 2014. ISSN 1939-4586. doi: 10.1091/mbc.E14-02-0718. URL http://www.ncbi.nlm.nih.gov/pubmed/25368418.

W. Baldwin and H. E. Kubitschek. Buoyant density variation during the cell cycle in microorganisms. *Journal of Bacteriology*, 158(2):701–704, 1984. ISSN 1040-841X. doi: 10.3109/10408418709104436.

A. R. Barr, F. S. Heldt, T. Zhang, C. Bakal, and B. Novák. A Dynamical Framework for the All-or-None G1/S Transition. *Cell Systems*, 2(1):27–37, 2016. ISSN 24054712. doi: 10.1016/j.cels.2016.01.001.

M. Basan, M. Zhu, X. Dai, M. Warren, D. Sévin, Y. Wang, and T. Hwa. Inflating bacterial cells by increased protein synthesis. *Molecular Systems Biology*, 11(10):836–836, 2015. ISSN 1744-4292. doi: 10.15252/msb.20156178. URL http://msb.embopress.org/cgi/doi/10.15252/msb.20156178.

D. Berchtold, M. Piccolis, N. Chiaruttini, I. Riezman, H. Riezman, A. Roux, T. C. Walther, and R. Loewith. Plasma membrane stress induces relocalization of Slm proteins and activation of TORC2 to promote sphingolipid synthesis. TL - 14. *Nature cell biology*, 14 VN - r(5):542–547, 2012. ISSN 1465-7392. doi: 10.1038/ncb2480. URL /Users/yurikoharigaya/Documents/ReadCubeMedia/NatCellBiol2012BerchtoldD.pdf{%}5Cnhttp://dx.doi.org/10.1038/ncb2480.

C. Bertoli, J. M. Skotheim, and R. a. M. de Bruin. Control of cell cycle transcription during G1 and S phases. *Nature reviews. Molecular cell biology*, 14(8):518–28, aug 2013. ISSN 1471-0080. doi: 10.1038/nrm3629. URL http://www.ncbi.nlm.nih.gov/pubmed/23877564.

P. Bhatia, O. Hachet, M. Hersch, S. a. Rincon, M. Berthelot-Grosjean, S. Dalessi, L. Basterra, S. Bergmann, A. Paoletti, and S. G. Martin. Distinct levels in Pom1 gradients limit Cdr2 activity and localization to time and position division. *Cell cycle (Georgetown, Tex.)*, 13(4):538–52, feb 2014. ISSN 1551-4005. doi: 10.4161/cc.27411. URL http://www.ncbi.nlm.nih.gov/pubmed/24316795.

M. Biro, Y. Romeo, S. Kroschwald, M. Bovellan, A. Boden, J. Tcherkezian, P. P. Roux, G. Charras, and E. K. Paluch. Cell cortex composition and homeostasis resolved by integrating proteomics and quantitative imaging. *Cytoskeleton*, 70(11):741–754, 2013. ISSN 19493584. doi: 10.1002/cm.21142.

G. Boncompain, S. Divoux, N. Gareil, H. de Forges, A. Lescure, L. Latreche, V. Mercanti, F. Jollivet, G. Raposo, and F. Perez. Synchronization of secretory protein traffic in populations of cells. *Nature Methods*, 9(5):493–498, 2012. ISSN 1548-7091. doi: 10.1038/nmeth.1928.

S. Bouccara, A. Fragola, E. Giovanelli, G. Sitbon, N. Lequeux, T. Pons, and V. Loriette. Time-gated cell imaging using long lifetime near-infrared-emitting quantum dots for autofluorescence rejection. *Journal of biomedical optics*, 19(5):051208, 2014. ISSN 1560-2281. doi: 10.1117/1.JBO.19.5.051208. URL http://www.ncbi.nlm.nih.gov/pubmed/24395624.

A. K. Bryan, A. Goranov, A. Amon, and S. R. Manalis. Measurement of mass, density, and volume during the cell cycle of yeast. *Proceedings of the National Academy of Sciences of the United States of America*, 107(3):999–1004, 2010. ISSN 0027-8424. doi: 10.1073/pnas.0901851107.

A. K. Bryan, V. C. Hecht, W. Shen, K. Payer, W. H. Grover, and S. R. Manalis. Measuring single cell mass, volume, and density with dual suspended microchannel resonators. *Lab on a chip*, 14 (3):569–76, feb 2014. ISSN 1473-0189. doi: 10.1039/c3lc51022k. URL http://www.ncbi.nlm.nih.gov/pubmed/24296901.

C. Cadart, E. Zlotek-Zlotkiewicz, M. Le Berre, M. Piel, and H. Matthews. Exploring the function of cell shape and size during mitosis. *Developmental Cell*, 29(2), 2014. ISSN 18781551 15345807. doi: 10.1016/j.devcel.2014.04.009.

C. Cadart, E. Zlotek-Zlotkiewicz, L. Venkova, O. Thouvenin, V. Raacine, M. Le Berre, S. Monnier, and M. Piel. Fluorescence eXclusion Measurement of volume in live cells. *Methods in cell biology*, 139(Cell polarity and morphogenesis):103–120, 2017. doi: 10.1016/j.jwb.2007.10.005. URL http://www.elsevier.com/copyright.

M. Campos, I. Surovtsev, S. Kato, A. Paintdakhi, B. Beltran, S. Ebmeier, and C. Jacobs-Wagner. A Constant Size Extension Drives Bacterial Cell Size Homeostasis. *Cell*, 159(6):1433–1446, dec 2014. ISSN 00928674. doi: 10.1016/j.cell.2014.11.022. URL http://linkinghub.elsevier.com/retrieve/pii/S0092867414014998.

S. Cappell, M. Chung, A. Jaimovich, S. Spencer, and T. Meyer. Irreversible APCCdh1 Inactivation Underlies the Point of No Return for Cell-Cycle Entry. *Cell*, 166(1):167–180, 2016. ISSN 10974172. doi: 10.1016/j.cell.2016.05.077.

A. Caron, D. Richard, and M. Laplante. The Roles of mTOR Complexes in Lipid Metabolism. *Annual review of nutrition*, 35:321–348, 2015. ISSN 1545-4312. doi: 10.1146/annurev-nutr-071714-034355. URL http://www.ncbi.nlm.nih.gov/pubmed/26185979.

N. Cermak, S. Olcum, F. F. Delgado, S. C. Wasserman, K. R. Payer, M. A Murakami, S. M. Knudsen, R. J. Kimmerling, M. M. Stevens, Y. Kikuchi, A. Sandikci, M. Ogawa, V. Agache, F. Baleras, D. M. Weinstock, and S. R. Manalis. High-throughput measurement of single-cell growth rates using serial microfluidic mass sensor arrays. *Nat Biotech*, 34(10):1052–1059, 2016. ISSN

1087-0156. doi: 10.1038/nbt.3666. URL http://dx.doi.org/10.1038/nbt.3666{%}5Cnhttp://10.1038/nbt.3666{%}5Cnhttp://www.nature.com/nbt/journal/v34/n10/abs/nbt.3666.html{#}supplementary-information.

N. Chica, A. E. Rozalén, L. Pérez-Hidalgo, A. Rubio, B. Novak, and S. Moreno. Nutritional control of cell size by the greatwall-endosulfine-PP2A·B55 pathway. *Current Biology*, 26(3):319–330, 2016. ISSN 09609822. doi: 10.1016/j.cub.2015.12.035.

I. Conlon and M. Raff. Size control in animal development, 1999. ISSN 00928674.

I. Conlon and M. Raff. Differences in the way a mammalian cell and yeast cells coordinate cell growth and cell-cycle progression. *Journal of biology*, 2(1):7, jan 2003. ISSN 1475-4924. doi: 10.1186/1475-4924-2-7. URL /pmc/articles/PMC156598/?report=abstract.

I. Conlon, G. Dunn, A. Mudge, and M. Raff. Extracellular control of cell size. *Nature cell biology*, 3 (October 2001):3–7, 2001. URL http://discovery.ucl.ac.uk/186032/.

S. Cooper. Schizosaccharomyces pombe grows exponentially during the division cycle with no rate change points. *FEMS yeast research*, 13(7):650–8, nov 2013. ISSN 1567-1364. doi: 10.1111/1567-1364.12072. URL http://www.ncbi.nlm.nih.gov/pubmed/23981297.

S. Cooper and C. E. Helmstetter. Chromosome replication and the division cycle of Escherichia coli. *Journal of Molecular Biology*, 31(3):519–540, 1968. ISSN 00222836. doi: 10.1016/0022-2836(68)90425-7. URL http://www.sciencedirect.com/science/article/pii/0022283668904257.

D. Coudreuse and P. Nurse. Driving the cell cycle with a minimal CDK control network. *Nature*, 468 (7327):1074–1079, 2010. ISSN 0028-0836. doi: 10.1038/nature09543. URL http://dx.doi.org/10.1038/nature09543.

F. R. Cross, N. E. Buchler, and J. M. Skotheim. Evolution of networks and sequences in eukaryotic cell cycle control. *Philos Trans R Soc Lond B Biol Sci*, 366(1584):3532–3544, 2011. ISSN 0962-8436. doi: 10.1098/rstb.2011.0078. URL http://www.ncbi.nlm.nih.gov/pubmed/22084380.

J. K. L. da Silva, G. J. Garcia, and L. A. Barbosa. Allometric scaling laws of metabolism. *Physics of Life Reviews*, 3(4):229–261, 2006. ISSN 15710645. doi: 10.1016/j.plrev.2006.08.001.

C. V. Dang. MYC on the path to cancer. *Cell*, 149(1):22–35, 2012. ISSN 00928674. doi: 10.1016/j.cell.2012.03.003. URL http://dx.doi.org/10.1016/j.cell.2012.03.003.

E. Davie and J. Petersen. Environmental control of cell size at division. *Current opinion in cell biology*, 24(6):838–44, dec 2012. ISSN 1879-0410. doi: 10.1016/j.ceb.2012.08.003. URL http://www.ncbi.nlm.nih.gov/pubmed/22947494.

M. Deforet, D. Van Ditmarsch, and J. Xavier. Cell-Size Homeostasis and the Incremental Rule in a Bacterial Pathogen. *Biophysical Journal*, 109(3):521–528, 2015. ISSN 15420086. doi: 10.1016/j.bpj.2015.07.002.

M. Delarue, F. Montel, D. Vignjevic, J. Prost, J.-F. Joanny, and G. Cappello. Compressive Stress Inhibits Proliferation in Tumor Spheroids through a Volume Limitation. *Biophysical Journal*, 107(8):1821–1828, oct 2014. ISSN 00063495. doi: 10.1016/j.bpj.2014.08.031. URL http://linkinghub.elsevier.com/retrieve/pii/S0006349514009369.

M. Delarue, D. Weissman, and O. Hallatschek. A simple molecular mechanism explains multiple patterns of cell-size regulation. *bioRxiv*, 1(22):2013–2016, 2016.

P. B. Dennis, a. Jaeschke, M. Saitoh, B. Fowler, S. C. Kozma, and G. Thomas. Mammalian TOR: a homeostatic ATP sensor. *Science (New York, N.Y.)*, 294(5544):1102–1105, 2001. ISSN 00368075. doi: 10.1126/science.1063518.

S. Di Talia, J. M. Skotheim, J. M. Bean, E. D. Siggia, and F. R. Cross. The effects of molecular noise and size control on variability in the budding yeast cell cycle. *Nature*, 448(7156):947–51, aug 2007. ISSN 1476-4687. doi: 10.1038/nature06072. URL http://www.ncbi.nlm.nih.gov/pubmed/17713537.

S. Di Talia, H. Wang, J. M. Skotheim, A. P. Rosebrock, B. Futcher, and F. R. Cross. Daughter-specific transcription factors regulate cell size control in budding yeast. *PLoS biology*, 7(10):e1000221, oct 2009. ISSN 1545-7885. doi: 10.1371/journal.pbio.1000221. URL http://www.pubmedcentral.nih.gov/articlerender.fcgi?artid=2756959{&}tool=pmcentrez{&}rendertype=abstract.

H. Dolznig, F. Grebien, T. Sauer, H. Beug, and E. W. Müllner. Evidence for a size-sensing mechanism in animal cells. *Nature cell biology*, 6(9):899–905, sep 2004. ISSN 1465-7392. doi: 10.1038/ncb1166. URL http://www.ncbi.nlm.nih.gov/pubmed/15322555.

W. D. Donachie. Relationship between Cell Size and Time of Initiation of DNA Replication. *Nature*, 219(5158):1077–1079, sep 1968. ISSN 0028-0836. doi: 10.1038/2191077a0. URL http://www.nature.com/doifinder/10.1038/2191077a0.

W. D. Donachie and G. W. Blakely. Coupling the initiation of chromosome replication to cell size in Escherichia coli. *Current Opinion in Microbiology*, 6(2):146–150, 2003. ISSN 13695274. doi: 10.1016/S1369-5274(03)00026-2.

T. A. Duncombe, A. M. Tentori, and A. E. Herr. Microfluidics: reframing biological enquiry. *Nature reviews. Molecular cell biology*, 16(9):554–567, 2015. ISSN 1471-0080. doi: 10.1038/nrm4041. URL http://dx.doi.org/10.1038/nrm4041.

P. Echave, I. J. Conlon, and A. C. Lloyd. Cell Size Regulation in Mammalian Cells. *Cell Cycle*, 6 (2):218–224, oct 2007. ISSN 1538-4101. doi: 10.4161/cc.6.2.3744. URL http://www.tandfonline.com/doi/abs/10.4161/cc.6.2.3744.

E. Eden, N. Geva-zatorsky, I. Issaeva, A. Cohen, E. Dekel, T. Danon, L. Cohen, and A. Mayo. Proteome Half-Life Dynamics in Living Human Cells. *Science*, 331(January), 2011.

B. A. Edgar. How flies get their size: genetics meets physiology. *Nature Reviews Genetics*, 7(12): 907–916, 2006. ISSN 1471-0056. doi: 10.1038/nrg1989. URL http://www.nature.com/doifinder/10.1038/nrg1989.

B. a. Edgar and H. F. Nijhout. *Cell growth: control of cell size. Chapter 2 : Growth and Cell Cycle Control in Drosophila.* Cold Spring Harbor Laboratory Press, cold sprin edition, 2004. ISBN 0879696729.

B. a. Edgar, N. Zielke, and C. Gutierrez. Endocycles: a recurrent evolutionary innovation for post-mitotic cell growth. *Nature reviews. Molecular cell biology*, 15(3):197–210, 2014. ISSN 1471-0080. doi: 10.1038/nrm3756. URL http://www.ncbi.nlm.nih.gov/pubmed/24556841.

K. Elgass, J. Pakay, M. T. Ryan, and C. S. Palmer. Recent advances into the understanding of mitochondrial fission. *Biochimica et biophysica acta*, 1833(1):150–61, jan 2013. ISSN 0006-3002. doi: 10.1016/j.bbamcr.2012.05.002. URL http://www.ncbi.nlm.nih.gov/pubmed/22580041.

S. Eltschinger and R. Loewith. TOR Complexes and the Maintenance of Cellular Homeostasis. *Trends in Cell Biology*, 26(2):148–159, 2016. ISSN 18793088. doi: 10.1016/j.tcb.2015.10.003. URL http://dx.doi.org/10.1016/j.tcb.2015.10.003.

P. A. Fantes. Control of cell size and cycle time in Schizosaccharomyces pombe. *J Cell Sci*, 24:51–67, 1977. URL http://jcs.biologists.org/cgi/reprint/24/1/51.

Y. Feng, Z. Yao, and D. J. Klionsky. How to control self-digestion: Transcriptional, post-transcriptional, and post-translational regulation of autophagy. *Trends in Cell Biology*, 25 (6):354–363, 2015. ISSN 18793088. doi: 10.1016/j.tcb.2015.02.002. URL http://dx.doi.org/10.1016/j.tcb.2015.02.002.

F. Ferrezuelo, N. Colomina, A. Palmisano, E. Garí, C. Gallego, A. Csikász-Nagy, and M. Aldea. The critical size is set at a single-cell level by growth rate to attain homeostasis and adaptation. *Nature communications*, 3:1012, 2012. ISSN 2041-1723. doi: 10.1038/ncomms2015. URL http://eutils.ncbi.nlm.nih.gov/entrez/eutils/elink.fcgi?dbfrom=pubmed{&}id=22910358{&}retmode=ref{&}cmd=prlinks{%}5Cnpapers2://publication/doi/10.1038/ncomms2015.

D. Fisher, L. Krasinska, D. Coudreuse, and B. Novák. Phosphorylation network dynamics in the control of cell cycle transitions. *Journal of cell science*, 125(Pt 20):4703–11, oct 2012. ISSN 1477-9137. doi: 10.1242/jcs.106351. URL http://www.ncbi.nlm.nih.gov/pubmed/23223895.

R. P. Fisher. Getting to S: CDK functions and targets on the path to cell-cycle commitment. *F1000Research*, 5:2374, 2016. ISSN 2046-1402. doi: 10.12688/f1000research.9463.1. URL http://www.ncbi.nlm.nih.gov/pubmed/27746911.

D. a. Foster, P. Yellen, L. Xu, and M. Saqcena. Regulation of G1 Cell Cycle Progression: Distinguishing the Restriction Point from a Nutrient-Sensing Cell Growth Checkpoint(s). *Genes & cancer*, 1: 1124–1131, 2010. ISSN 1947-6019. doi: 10.1177/1947601910392989.

D. Freida, S. Lecourt, A. Cras, V. Vanneaux, G. Letort, X. Gidrol, L. Guyon, J. Larghero, and M. Thery. Human bone marrow mesenchymal stem cells regulate biased DNA segregation in response to cell adhesion asymmetry. *Cell reports*, 5(3):601–10, nov 2013. ISSN 2211-1247. doi: 10.1016/j.celrep.2013.09.019. URL http://www.ncbi.nlm.nih.gov/pubmed/24139805.

B. Futcher. Cyclins and the wiring of the yeast cell cycle. *Yeast*, 12(16):1635–1646, 1996. ISSN 0749503X. doi: 10.1002/(SICI)1097-0061(199612)12:16⟨1635::AID-YEA83⟩3.0.CO;2-O.

F. B. Gao and M. Raff. Cell size control and a cell-intrinsic maturation program in proliferating oligodendrocyte precursor cells. *Journal of Cell Biology*, 138(6):1367–1377, 1997. ISSN 00219525. doi: 10.1083/jcb.138.6.1367.

N. C. Gauthier, T. A. Masters, and M. P. Sheetz. Mechanical feedback between membrane tension and dynamics. *Trends in Cell Biology*, 22(10):527–535, 2012. ISSN 09628924. doi: 10.1016/j.tcb.2012.07.005. URL http://dx.doi.org/10.1016/j.tcb.2012.07.005.

M. B. Ginzberg. *Size Control and Uniformity in Animal Cells*. PhD thesis, Harvard, 2015.

M. B. Ginzberg, R. Kafri, and M. Kirschner. On being the right (cell) size. *Science*, 348 (6236):1245075–1245075, 2015. ISSN 0036-8075. doi: 10.1126/science.1245075. URL http://www.sciencemag.org/cgi/doi/10.1126/science.1245075.

A. Giometto, F. Altermatt, F. Carrara, A. Maritan, and A. Rinaldo. Scaling body size fl uctuations. *Proceedings of the National Academy of Sciences of the United States of America*, 110 (12):4646–4650, 2013. doi: 10.1073/pnas.1301552110/-/DCSupplemental.www.pnas.org/cgi/doi/10.1073/pnas.1301552110.

D. Glazier. Metabolic Scaling in Complex Living Systems. *Systems*, 2(4):451–540, oct 2014. ISSN 2079-8954. doi: 10.3390/systems2040451. URL http://www.mdpi.com/2079-8954/2/4/451/.

M. Godin, F. F. Delgado, S. Son, W. H. Grover, K. Andrea, A. Tzur, P. Jorgensen, K. Payer, A. D. Grossman, W. Marc, S. R. Manalis, A. K. Bryan, and M. W. Kirschner. Using buoyant mass to measure the growth of single cells. *Nature methods*, 7(5):387–90, may 2010. ISSN 1548-7105. doi: 10.1038/nmeth.1452. URL http://www.pubmedcentral.nih.gov/articlerender.fcgi?artid=2862099{&}tool=pmcentrez{&}rendertype=abstract.

A. I. Goranov and A. Amon. Growth and division-not a one-way road. *Current Opinion in Cell Biology*, 22(6):795–800, 2010. ISSN 09550674. doi: 10.1016/j.ceb.2010.06.004.

A. I. Goranov, M. Cook, M. Ricicova, G. Ben-Ari, C. Gonzalez, C. Hansen, M. Tyers, and A. Amon. The rate of cell growth is governed by cell cycle stage. *Genes and Development*, 23(12):1408–1422, jun 2009. ISSN 08909369. doi: 10.1101/gad.1777309. URL http://www.ncbi.nlm.nih.gov/pubmed/19528319http://www.pubmedcentral.nih.gov/articlerender.fcgi?artid=PMC2701574.

S. S. Grewal and B. a. Edgar. Controlling cell division in yeast and animals: does size matter? *Journal of biology*, 2(1):5, 2003. ISSN 1475-4924. doi: 10.1186/1475-4924-2-5.

S. S. Grewal, L. Li, A. Orian, R. N. Eisenman, and B. A. Edgar. Myc-dependent regulation of ribosomal RNA synthesis during Drosophila development. *Nature cell biology*, 7(3):295–302, 2005. ISSN 1465-7392. doi: 10.1038/ncb1223.

J. Grilli, M. Osella, A. S. Kennard, and M. C. Lagomarsino. Relevant parameters in models of cell division control. *bioRxiv*, jun 2016. URL http://arxiv.org/abs/1606.09284.

W. H. Grover, A. K. Bryan, M. Diez-Silva, S. Suresh, J. M. Higgins, and S. R. Manalis. Measuring single-cell density. *Proceedings of the National Academy of Sciences of the United States of America*, 108(27):10992–6, jul 2011. ISSN 1091-6490. doi: 10.1073/pnas.1104651108. URL http://www.pubmedcentral.nih.gov/articlerender.fcgi?artid=3131325{&}tool=pmcentrez{&}rendertype=abstract.

L. S. Harrington, G. M. Findlay, A. Gray, T. Tolkacheva, S. Wigfield, H. Rebholz, J. Barnett, N. R. Leslie, S. Cheng, P. R. Shepherd, I. Gout, C. P. Downes, and R. F. Lamb. The TSC1-2 tumor suppressor controls insulin-PI3K signaling via regulation of IRS proteins. *Journal of Cell Biology*, 166(2):213–223, 2004. ISSN 00219525. doi: 10.1083/jcb.200403069.

L. Harris and J. Theriot. Relative Rates of Surface and Volume Synthesis Set Bacterial Cell Size. *Cell*, 165(6):1479–1492, 2016. ISSN 00928674. doi: 10.1016/j.cell.2016.05.045. URL http://linkinghub.elsevier.com/retrieve/pii/S0092867416306481.

L. Hartwell and M. Unger. Unequal Division in the Control Division and Its Implications for the Control of Cell Division. *The Journal of cell biology*, 75:422–435, 1977.

L. H. Hartwell. Periodic Density Fluctuation During the Yeast Cell Cycle and the Selection of Synchronous Cultures. *JOURNAL OF BACTERIOLOGY*, 104(3):1280–1285, 1970.

M. Hashimoto, T. Nozoe, H. Nakaoka, R. Okura, S. Akiyoshi, K. Kaneko, E. Kussell, and Y. Wakamoto. Noise-driven growth rate gain in clonal cellular populations. *Proceedings of the National Academy of Sciences of the United States of America*, 113(12):3251–3256, 2016. ISSN 0027-8424. doi: 10.1073/pnas.1519412113. URL http://www.pnas.org/content/early/2016/03/04/1519412113.abstract.

P.-y. Ho and A. Amir. Simultaneous Regulation of Cell Size and Chromosome Replication in Bacteria. *Frontiers in Microbiology*, 6(July):1–10, 2015. ISSN 1664-302X. doi: 10.3389/fmicb.2015.00662.

C. Homem, V. Steinmann, T. Burkard, A. Jais, H. Esterbauer, and J. Knoblich. Ecdysone and Mediator Change Energy Metabolism to Terminate Proliferation in Drosophila Neural Stem Cells. *Cell*, 158(4):874–888, 2014. ISSN 00928674. doi: 10.1016/j.cell.2014.06.024. URL http://linkinghub.elsevier.com/retrieve/pii/S0092867414008149.

C. C. F. Homem, M. Repic, and J. A. Knoblich. Proliferation control in neural stem and progenitor cells. *Nature Reviews Neuroscience*, 16(November), 2015. ISSN 1471-003X. doi: 10.1038/nrn4021. URL http://www.nature.com/doifinder/10.1038/nrn4021.

J. D. Horton, J. L. Goldstein, and M. S. Brown. SREBPs: Transcriptional mediators of lipid homeostasis. *Cold Spring Harbor Symposia on Quantitative Biology*, 67:491–498, 2002. ISSN 00917451. doi: 10.1101/sqb.2002.67.491.

Y. Hu and T. Zhu. Cell growth and size homeostasis in silico. *Biophysical journal*, 106(5):991–7, mar 2014. ISSN 1542-0086. doi: 10.1016/j.bpj.2014.01.038. URL http://www.sciencedirect.com/science/article/pii/S0006349514001404.

M. Inoue, H. Zhai, H. Sakazaki, H. Furuyama, Y. Fukuyama, and M. Hirama. TMC-95A, a reversible proteasome inhibitor, induces neurite outgrowth in PC12 cells. *Bioorganic & medicinal chemistry letters*, 14(3):663–5, 2004. ISSN 0960-894X. doi: 10.1016/j.bmcl.2003.11.043. URL http://www.ncbi.nlm.nih.gov/pubmed/14741264.

S. Iyer-Biswas, C. S. Wright, J. T. Henry, K. Lo, S. Burov, Y. Lin, G. E. Crooks, S. Crosson, A. R. Dinner, and N. F. Scherer. Scaling laws governing stochastic growth and division of single bacterial cells. *Proceedings of the National Academy of Sciences*, pages 1403232111–, 2014. ISSN 0027-8424. doi: 10.1073/pnas.1403232111. URL http://www.pnas.org/content/early/2014/10/23/1403232111.abstract.html?etoc.

John D'Errico. Surface Fitting using gridfit - File Exchange - MATLAB Central, 2005. URL https://fr.mathworks.com/matlabcentral/fileexchange/8998-surface-fitting-using-gridfit?s{_}tid=srchtitle.

G. C. Johnston. Cell size and budding during starvation of the yeast Cell Size and Budding During Starvation of the Yeast. *Journal of Bacteriology*, 132(2):738–740, 1977.

L. A. Johnston, D. A. Prober, B. A. Edgar, R. N. Eisenman, P. Gallant, D. Doherty, D. Gratecos, M. Semeriva, T. Jones, A. Bejsovec, and et Al. Drosophila myc regulates cellular growth during development. *Cell*, 98(6):779–90, sep 1999. ISSN 0092-8674. doi: 10.1016/S0092-8674(00)81512-3. URL http://www.ncbi.nlm.nih.gov/pubmed/10499795.

P. Jorgensen. Systematic Identification of Pathways That Couple Cell Growth and Division in Yeast. *Science*, 297(5580):395–400, 2002. ISSN 00368075. doi: 10.1126/science.1070850. URL http://www.sciencemag.org/cgi/doi/10.1126/science.1070850.

P. Jorgensen and M. Tyers. How cells coordinate growth and division. *Current biology : CB*, 14(23): R1014–27, dec 2004. ISSN 0960-9822. doi: 10.1016/j.cub.2004.11.027. URL http://www.ncbi.nlm.nih.gov/pubmed/15589139.

P. Jorgensen, N. P. Edgington, B. L. Schneider, I. Rupes, M. Tyers, and B. Futcher. The size of the nucleus increases as yeast cells grow. *Molecular biology of the cell*, 18(9):3523–32, sep 2007. ISSN 1059-1524. doi: 10.1091/mbc.E06-10-0973. URL http://www.ncbi.nlm.nih.gov/pubmed/17596521http://www.pubmedcentral.nih.gov/articlerender.fcgi?artid=PMC1951755.

S. Jun and S. Taheri-Araghi. Cell-size maintenance: Universal strategy revealed. *Trends in Microbiology*, 23(1):4–6, 2015. ISSN 18784380. doi: 10.1016/j.tim.2014.12.001. URL http://dx.doi.org/10.1016/j.tim.2014.12.001.

M. Kafri, E. Metzl-Raz, G. Jona, N. Barkai, A. Mayo, E. Dekel, U. Alon, S. Itzkovitz, C. Hogue, H. Bussey, and et Al. The Cost of Protein Production. *Cell Reports*, 14(1):22–31, jan 2016a. ISSN 22111247. doi: 10.1016/j.celrep.2015.12.015. URL http://www.ncbi.nlm.nih.gov/pubmed/26725116http://www.pubmedcentral.nih.gov/articlerender.fcgi?artid=PMC4709330http://linkinghub.elsevier.com/retrieve/pii/S221112471501428X.

M. Kafri, E. Metzl-Raz, F. Jonas, and N. Barkai. Rethinking cell growth models. *FEMS Yeast Research*, 16(7):1–13, 2016b. ISSN 15671364. doi: 10.1093/femsyr/fow081.

R. Kafri, J. Levy, M. B. Ginzberg, S. Oh, G. Lahav, and M. W. Kirschner. Dynamics extracted from fixed cells reveal feedback linking cell growth to cell cycle. *Nature*, 494(7438):480–483, 2013. ISSN 0028-0836. doi: 10.1038/nature11897. URL http://dx.doi.org/10.1038/nature11897http://dx.doi.org/10.1038/nature11897{%}5Cnhttp://www.nature.com/nature/journal/v494/n7438/abs/nature11897.html{%}5Cnhttp://www.pubmedcentral.nih.gov/articlerender.fcgi?artid=3730528{&}tool=pmcentrez{&}rendertype=abstract.

J. Kaplon, L. van Dam, and D. Peeper. Two-way communication between the metabolic and cell cycle machineries: the molecular basis. *Cell Cycle*, 14(13):2022–2032, 2015. ISSN 1538-4101. doi: 10.1080/15384101.2015.1044172. URL http://www.tandfonline.com/doi/full/10.1080/15384101.2015.1044172.

E. Karsenti, J. Newport, and M. Kirschner. Respective roles of centrosomes and chromatin in the conversion of microtubule arrays from interphase to metaphase. *Journal of Cell Biology*, 99(1 II), 1984. ISSN 00219525. doi: 10.1083/jcb.99.1.47s.

D. F. Kashatus, K.-H. Lim, D. C. Brady, N. L. K. Pershing, A. D. Cox, and C. M. Counter. RALA and RALBP1 regulate mitochondrial fission at mitosis. *Nature cell biology*, 13(9):1108–15, sep 2011. ISSN 1476-4679. doi: 10.1038/ncb2310. URL http://www.pubmedcentral.nih.gov/articlerender.fcgi?artid=3167028{&}tool=pmcentrez{&}rendertype=abstract.

M. B. Kastan and J. Bartek. Cell-cycle checkpoints and cancer. *Nature*, 432(7015):316–323, 2004. ISSN 0028-0836. doi: 10.1038/nature03097.

P. Kavakebi, B. Hausott, A. Tomasino, S. Ingorokva, and L. Klimaschewski. The N-end rule ubiquitin-conjugating enzyme, HR6B, is up-regulated by nerve growth factor and required for neurite outgrowth. *Molecular and Cellular Neuroscience*, 29(4):559–568, 2005. ISSN 10447431. doi: 10.1016/j.mcn.2005.04.008.

H. Kempe, A. Schwabe, F. Crémazy, P. J. Verschure, and F. J. Bruggeman. The volumes and transcript counts of single cells reveal concentration homeostasis and capture biological noise. *Molecular biology of the cell*, 26(4):797–804, 2015. ISSN 1939-4586. doi: 10.1091/mbc.E14-08-1296. URL http://www.pubmedcentral.nih.gov/articlerender.fcgi?artid=4325848{&}tool=pmcentrez{&}rendertype=abstract.

A. S. Kennard, M. Osella, A. Javer, J. Grilli, P. Nghe, S. J. Tans, P. Cicuta, and M. Cosentino Lagomarsino. Individuality and universality in the growth-division laws of single E. Coli cells. *Physical Review E - Statistical, Nonlinear, and Soft Matter Physics*, 93(1):1–18, 2016. ISSN 15502376. doi: 10.1103/PhysRevE.93.012408.

D. Killander and A. Zetterberg. quantitative cytochemical studies on interphase growth II derivation of synthesis curves from the distribution of DNA, RNA and mass values of individual mouse fibroblasts in vitro. *Experimental Cell Research*, 39:22–32, 1965. ISSN 0014-4827.

D. J. Kiviet, P. Nghe, N. Walker, S. Boulineau, V. Sunderlikova, and S. J. Tans. Stochasticity of metabolism and growth at the single-cell level. *Nature*, 514(7522):376–9, 2014. ISSN 0028-0836. doi: 10.1038/nature13582. URL http://dx.doi.org/10.1038/nature13582.

M. Laplante and D. M. Sabatini. MTOR signaling in growth control and disease. *Cell*, 149(2):274–293, 2012. ISSN 00928674. doi: 10.1016/j.cell.2012.03.017. URL http://dx.doi.org/10.1016/j.cell.2012.03.017.

H. Laser, T. G. A. Mack, D. Wagner, and M. P. Coleman. Proteasome Inhibition Arrests Neurite Outgrowth and Causes "Dying-Back" Degeneration in Primary Culture. *Journal of Neuroscience Research*, 74(6):906–916, 2003. ISSN 03604012. doi: 10.1002/jnr.10806.

M. Le Berre, E. Zlotek-Zlotkiewicz, D. Bonazzi, F. Lautenschlaeger, and M. Piel. Methods for two-dimensional cell confinement. *Methods in cell biology*, 121:213–29, jan 2014. ISSN 0091-679X. doi: 10.1016/B978-0-12-800281-0.00014-2. URL http://www.ncbi.nlm.nih.gov/pubmed/24560512.

R. M. Leitao, A. Pham, and D. R. Kellogg. The duration of mitosis and daughter cell size are modulated by nutrients in budding yeast. *bioRxiv*, 2016.

M. A. Lemmon and J. Schlessinger. Cell Signaling by Receptor Tyrosine Kinases. *Cell*, 141(7): 1117–1134, 2010. ISSN 00928674. doi: 10.1016/j.cell.2010.06.011.

J. Lin and A. Amir. How does cell size regulation affect population growth? *bioRxiv*, pages 1–8, 2016. URL http://arxiv.org/abs/1611.07989.

A. C. Lloyd. The regulation of cell size. *Cell*, 154(6):1194–205, sep 2013. ISSN 1097-4172. doi: 10.1016/j.cell.2013.08.053. URL http://www.ncbi.nlm.nih.gov/pubmed/24034244.

J. Locasale and L. Cantley. Metabolic Flux and the Regulation of Mammalian Cell Growth. *Cell Metabolism*, 14(4):443–451, 2011. ISSN 15504131. doi: 10.1016/j.cmet.2011.07.014.

Z. Long, E. Nugent, A. Javer, P. Cicuta, B. Sclavi, M. Cosentino Lagomarsino, and K. D. Dorfman. Microfluidic chemostat for measuring single cell dynamics in bacteria. *Lab on a Chip*, 13(5):947, 2013. ISSN 1473-0197. doi: 10.1039/c2lc41196b. URL http://xlink.rsc.org/?DOI=c2lc41196b.

J. J. Lum, D. E. Bauer, M. Kong, M. H. Harris, C. Li, T. Lindsten, and C. B. Thompson. Growth factor regulation of autophagy and cell survival in the absence of apoptosis. *Cell*, 120(2):237–248, 2005. ISSN 00928674. doi: 10.1016/j.cell.2004.11.046.

X. M. Ma and J. Blenis. Molecular mechanisms of translational control. *Nat.Rev.Mol.Cell Biol.*, 5(1471-0072 (Print)):827–835, 2004. ISSN 1471-0072. doi: 10.1038/nrm2672. URL file://c/Users/clin1/Documents/PDF/Referent{_}manager{_}linked{_}PDFs/129.pdf{%}5Cnhttp://www.nature.com/nrm/journal/v5/n10/full/nrm1488.html.

M. Malumbres. Cyclin-dependent kinases. *Genome Biology*, 15(6):122, 2014. ISSN 1465-6906. doi: 10.1186/gb4184. URL http://genomebiology.com/2014/15/6/122.

M. Malumbres and M. Barbacid. Cell cycle, CDKs and cancer: a changing paradigm. *Nature reviews. Cancer*, 9(3):153–166, 2009. ISSN 1474-175X. doi: 10.1038/nrc2602.

E. Marañón. Cell Size as a Key Determinant of Phytoplankton Metabolism and Community Structure. *Annual Review of Marine Science*, 7(July 2014):241–64, 2014. ISSN 1941-1405. doi: 10.1146/annurev-marine-010814-015955. URL http://www.ncbi.nlm.nih.gov/pubmed/25062405.

W. F. Marshall. Cell Geometry: How Cells Count and Measure Size. *Annual Review of Biophysics*, (April):49–64, 2015. ISSN 1936-122X. doi: 10.1146/annurev-biophys-062215-010905.

S. G. Martin. Geometric control of the cell cycle, 2009. ISSN 15384101.

M. B. Mayhew, E. S. Iversen, and A. J. Hartemink. Characterization of Dependencies Between Growth and Division in Budding Yeast. *bioRxiv*, 2016.

D. McCusker and D. R. Kellogg. Plasma membrane growth during the cell cycle: unsolved mysteries and recent progress. *Current opinion in cell biology*, 24(6):845–51, dec 2012. ISSN 1879-0410. doi: 10.1016/j.ceb.2012.10.008. URL http://www.pubmedcentral.nih.gov/articlerender.fcgi?artid=3540179{&}tool=pmcentrez{&}rendertype=abstract.

N. Mchedlishvili, K. Jonak, and A. T. Saurin. Meeting report Getting Into and Out of Mitosis. *Journal of Cell Science*, 128(22), 2015.

L. Meijer and E. Raymond. Roscovitine and Other Purines as Kinase Inhibitors . From Starfish Oocytes to Clinical Trials Roscovitine and Other Purines as Kinase Inhibitors . From Starfish Oocytes to Clinical Trials. *Acc. Chem. Res*, 36(6):417–425, 2003. doi: 10.1021/ar0201198.

T. P. Miettinen and M. Bjo. Mevalonate Pathway Regulates Cell Size Homeostasis and Proteostasis through Autophagy. *Cell reports*, 13:1–11, 2015. ISSN 22111247. doi: 10.1016/j.celrep.2015.11.045.

T. P. Miettinen and M. Bjorklund. Cellular Allometry of Mitochondrial Functionality Establishes the Optimal Cell Size. *Developmental Cell*, 39(3):370–382, 2016. ISSN 18781551. doi: 10.1016/j.devcel.2016.09.004.

M. Mir, Z. Wang, Z. Shen, M. Bednarz, R. Bashir, I. Golding, S. G. Prasanth, and G. Popescu. Optical measurement of cycle-dependent cell growth. *Proceedings of the National Academy of Sciences of the United States of America*, 108(32):13124–9, aug 2011. ISSN 1091-6490. doi: 10.1073/pnas.1100506108. URL http://www.pubmedcentral.nih.gov/articlerender.fcgi?artid=3156192{&}tool=pmcentrez{&}rendertype=abstract.

M. Mir, A. Bergamaschi, B. S. Katzenellenbogen, and G. Popescu. Highly sensitive quantitative imaging for monitoring single cancer cell growth kinetics and drug response. *PloS one*, 9(2):e89000, jan 2014. ISSN 1932-6203. doi: 10.1371/journal.pone.0089000. URL /pmc/articles/PMC3928317/?report=abstract.

J. Mitchison. Growth During the Cell Cycle. *International Review of Cytology*, 226:165–258, 2003. ISSN 00747696. doi: 10.1016/S0074-7696(03)01004-0. URL http://www.sciencedirect.com/science/article/pii/S0074769603010040.

J. M. Mitchison. Single cell studies of the cell cycle and some models. *Theoretical biology & medical modelling*, 2:4, jan 2005. ISSN 1742-4682. doi: 10.1186/1742-4682-2-4. URL /pmc/articles/PMC550673/?report=abstract.

J. M. Mitchison and P. Nurse. GROWTH IN CELL LENGTH IN THE FISSION YEAST SCHIZOSACCHAROMYCES POM BE. *J. Cell Sri*, 75:357–376, 1985.

J. R. Moffitt, J. B. Lee, and P. Cluzel. The single-cell chemostat: an agarose-based, microfluidic device for high-throughput, single-cell studies of bacteria and bacterial communities. *Lab on a Chip*, 12 (8):1487, 2012. ISSN 1473-0197. doi: 10.1039/c2lc00009a.

C. A. Moody and L. A. Laimins. Human papillomavirus oncoproteins: pathways to transformation. *Nature Reviews Cancer*, 10(8):550–560, 2010. ISSN 1474-175X. doi: 10.1038/nrc2886. URL http://dx.doi.org/10.1038/nrc2886{%}5Cnhttp://www.nature.com/doifinder/10.1038/nrc2886.

C. E. Morris and U. Homann. Cell surface area regulation and membrane tension. *The Journal of membrane biology*, 179(2):79–102, 2001. ISSN 0022-2631. doi: 10.1007/s002320010040.

J. B. Moseley, A. Mayeux, A. Paoletti, and P. Nurse. A spatial gradient coordinates cell size and mitotic entry in fission yeast. *Nature*, 459(7248):857–60, jun 2009. ISSN 1476-4687. doi: 10.1038/nature08074. URL http://www.ncbi.nlm.nih.gov/pubmed/19474789.

J. R. S. Newman, S. Ghaemmaghami, J. Ihmels, D. K. Breslow, M. Noble, J. L. DeRisi, and J. S. Weissman. Single-cell proteomic analysis of S. cerevisiae reveals the architecture of biological noise TL - 441. *Nature*, 441 VN -(7095):840–846, 2006. ISSN 0028-0836. doi: 10.1038/nature04785. URL /Users/yurikoharigaya/Documents/ReadCubeMedia/nature04785.pdf{%}5Cnhttp://dx.doi.org/10.1038/nature04785.

B. J. Niles and T. Powers. Plasma membrane proteins Slm1 and Slm2 mediate activation of the AGC kinase Ypk1 by TORC2 and sphingolipids in S. cerevisiae, oct 2012. ISSN 15384101. URL http://www.tandfonline.com/doi/abs/10.4161/cc.21752.

K. Nishimura, S. Watanabe, R. Hayashida, S. Sugishima, T. Iwasaka, and T. Kaku. Binucleated HeLa cells are formed by cytokinesis failure in starvation and keep the potential of proliferation. *Cytotechnology*, 68(4):1123–1130, 2016. ISSN 0920-9069. doi: 10.1007/s10616-015-9869-6. URL http://link.springer.com/10.1007/s10616-015-9869-6.

J.-B. Nobs and S. J. Maerkl. Long-term single cell analysis of S. pombe on a microfluidic microchemostat array. *PloS one*, 9(4):e93466, apr 2014. ISSN 1932-6203. doi: 10.1371/journal.pone.0093466. URL http://dx.plos.org/10.1371/journal.pone.0093466http://www.pubmedcentral.nih.gov/articlerender.fcgi?artid=3977849{&}tool=pmcentrez{&}rendertype=abstract.

T. Nobukuni, M. Joaquin, M. Roccio, S. G. Dann, S. Y. Kim, P. Gulati, M. P. Byfield, J. M. Backer, F. Natt, J. L. Bos, F. J. T. Zwartkruis, and G. Thomas. Amino acids mediate mTOR/raptor signaling through activation of class 3 phosphatidylinositol 3OH-kinase. *Proceedings of the National Academy of Sciences of the United States of America*, 102:14238–14243, 2005. ISSN 0027-8424. doi: 10.1073/pnas.0506925102.

B. Novak, O. Kapuy, M. R. Domingo-Sananes, and J. J. Tyson. Regulated protein kinases and phosphatases in cell cycle decisions. *Current opinion in cell biology*, 22(6):801–8, dec 2010. ISSN 1879-0410. doi: 10.1016/j.ceb.2010.07.001. URL http://www.pubmedcentral.nih.gov/articlerender.fcgi?artid=3769698{&}tool=pmcentrez{&}rendertype=abstract.

P. Nurse. Genetic control of cell size at cell division in yeast. *Nature*, 256, 1975.

O'Farrell. How Metazoans Reach Their Full Size : The Natural History of Bigness. *Cell Growth: control of cell size*, 2004.

B. Okumus, S. Yildiz, and E. Toprak. Fluidic and microfluidic tools for quantitative systems biology. *Current Opinion in Biotechnology*, 25:30–38, 2014. ISSN 09581669. doi: 10.1016/j.copbio.2013.08.016. URL http://dx.doi.org/10.1016/j.copbio.2013.08.016.

M. Osella, E. Nugent, and M. Cosentino Lagomarsino. Concerted control of Escherichia coli cell division. *Proceedings of the National Academy of Sciences of the United States of America*, 111(9):3431–5, mar 2014. ISSN 1091-6490. doi: 10.1073/pnas.1313715111. URL http://www.pubmedcentral.nih.gov/articlerender.fcgi?artid=3948223{&}tool=pmcentrez{&}rendertype=abstract.

M. Osella, S. J. Tans, and M. Cosentino Lagomarsino. Step by Step, Cell by Cell: Quantification of the Bacterial Cell Cycle. *Trends in Microbiology*, xx:1–7, 2017. ISSN 0966842X. doi: 10.1016/j.tim.2016.12.005. URL http://linkinghub.elsevier.com/retrieve/pii/S0966842X16302001.

K. Z. Pan, T. E. Saunders, I. Flor-Parra, M. Howard, and F. Chang. Cortical regulation of cell size by a sizer cdr2p. *eLife*, 2014(3):e02040, mar 2014. ISSN 2050084X. doi: 10.7554/eLife.02040. URL http://www.ncbi.nlm.nih.gov/pubmed/24642412http://www.pubmedcentral.nih.gov/articlerender.fcgi?artid=PMC3956294http://elifesciences.org/lookup/doi/10.7554/eLife.02040.

A. B. Pardee. A restriction point for control of normal animal cell proliferation. *Proceedings of the National Academy of Sciences of the United States of America*, 71(4):1286–90, apr 1974. ISSN 0027-8424. doi: 10.1073/pnas.71.4.1286. URL http://www.ncbi.nlm.nih.gov/pubmed/4524638http://www.pubmedcentral.nih.gov/articlerender.fcgi?artid=PMC388211http://www.pubmedcentral.nih.gov/articlerender.fcgi?artid=388211{&}tool=pmcentrez{&}rendertype=abstract.

K. Park, L. J. Millet, N. Kim, H. Li, X. Jin, G. Popescu, N. R. Aluru, K. J. Hsia, and R. Bashir. Measurement of adherent cell mass and growth. *Proceedings of the National Academy*

of Sciences of the United States of America, 107(48):20691–6, nov 2010. ISSN 1091-6490. doi: 10.1073/pnas.1011365107. URL http://www.pubmedcentral.nih.gov/articlerender.fcgi?artid=2996435{&}tool=pmcentrez{&}rendertype=abstract.

D. Patel, D. Salloum, M. Saqcena, A. Chatterjee, V. Mroz, M. Ohh, and D. A. Foster. A Late G1 Lipid Checkpoint that is Dysregulated in Clear Cell Renal Carcinoma Cells. *The Journal of Biological Chemistry*, in press, 2016. ISSN 1083-351X. doi: 10.1074/jbc.M116.757864. URL http://www.ncbi.nlm.nih.gov/pubmed/27956548.

J. M. Peters. The anaphase promoting complex/cyclosome: a machine designed to destroy. *Nat Rev Mol Cell Biol*, 7(9):644–656, 2006. ISSN 1471-0072. doi: 10.1038/nrm1988. URL http://www.ncbi.nlm.nih.gov/pubmed/16896351.

S. Piccolo, S. Dupont, and M. Cordenonsi. The Biology of YAP/TAZ: Hippo Signaling and Beyond. *Physiological Reviews*, 94(4):1287–1312, 2014. ISSN 0031-9333. doi: 10.1152/physrev.00005.2014. URL http://physrev.physiology.org/cgi/doi/10.1152/physrev.00005.2014.

M. Piel, P. Meyer, A. Khodjakov, C. L. Rieder, and M. Bornens. The respective contributions of the mother and daughter centrioles to centrosome activity and behavior in vertebrate cells. *Journal of Cell Biology*, 149(2):317–329, 2000. ISSN 00219525. doi: 10.1083/jcb.149.2.317.

G. Popescu, K. Park, M. Mir, and R. Bashir. New technologies for measuring single cell mass. *Lab on a chip*, 14(4):646–52, 2014. ISSN 1473-0189. doi: 10.1039/c3lc51033f. URL http://www.ncbi.nlm.nih.gov/pubmed/24322181.

D. M. Prescott. Relation between cell growth and cell division. II. The effect of cell size on cell growth rate and generation time in Amoeba proteus. *Experimental Cell Research*, 11((1)):86–94, 1956.

D. A. Prober, B. A. Edgar, Y. Wang, W. Pledger, S. Leevers, P. Leder, J. DeCaprio, and M. Ewen. Ras1 promotes cellular growth in the Drosophila wing. *Cell*, 100(4):435–46, feb 2000. ISSN 0092-8674. doi: 10.1016/S0092-8674(00)80679-0. URL http://www.ncbi.nlm.nih.gov/pubmed/10693760.

A. Raj, C. S. Peskin, D. Tranchina, D. Y. Vargas, and S. Tyagi. Stochastic mRNA synthesis in mammalian cells. *PLoS Biology*, 4(10):1707–1719, 2006. ISSN 15457885. doi: 10.1371/journal.pbio.0040309.

J. C. Rathmell, M. G. Heiden, M. H. Harris, K. A. Frauwirth, and C. B. Thompson. In the Absence of Extrinsic Signals, Nutrient Utilization by Lymphocytes Is Insufficient to Maintain Either Cell Size or Viability. *Molecular Cell*, 6(3):683–692, 2000. ISSN 10972765. doi: 10.1016/S1097-2765(00)00066-6.

L. Robert. Size sensors in bacteria, cell cycle control, and size control. *Frontiers in microbiology*, 6(May):515, 2015. ISSN 1664-302X. doi: 10.3389/fmicb.2015.00515. URL http://journal.frontiersin.org/article/10.3389/fmicb.2015.00515/abstract.

L. Robert, M. Hoffmann, N. Krell, S. Aymerich, J. Robert, and M. Doumic. Division in Escherichia coli is triggered by a size-sensing rather than a timing mechanism. *BMC Biology*, 12(1):17, 2014. ISSN 1741-7007. doi: 10.1186/1741-7007-12-17. URL http://www.biomedcentral.com/1741-7007/12/17/abstract{%}5Cnhttp://www.biomedcentral.com/1741-7007/12/17{%}5Cnhttp://www.biomedcentral.com/content/pdf/1741-7007-12-17.pdf.

S. A. Roberts. *Mechanisms of Cell Growth*. PhD thesis, University College London, 2013.

S. a. Roberts and A. C. Lloyd. Aspects of cell growth control illustrated by the Schwann cell. *Current Opinion in Cell Biology*, 24(6):852–857, 2012. ISSN 09550674. doi: 10.1016/j.ceb.2012.10.003. URL http://dx.doi.org/10.1016/j.ceb.2012.10.003.

J. Rohn, J. Patel, B. Neumann, J. Bulkescher, N. Mchedlishvili, R. McMullan, O. Quintero, J. Ellenberg, and B. Baum. Myo19 Ensures Symmetric Partitioning of Mitochondria and Coupling of Mitochondrial Segregation to Cell Division. *Current Biology*, 24(21):2598–2605, oct 2014. ISSN 09609822. doi: 10.1016/j.cub.2014.09.045. URL http://linkinghub.elsevier.com/retrieve/pii/S0960982214012081.

V. Roustan, A. Jain, M. Teige, I. Ebersberger, and W. Weckwerth. An evolutionary perspective of AMPKTOR signaling in the three domains of life. *Journal of Experimental Botany*, 67(13): 3897–3907, jun 2016. ISSN 0022-0957. doi: 10.1093/jxb/erw211. URL https://academic.oup.com/jxb/article-lookup/doi/10.1093/jxb/erw211.

R. C. Russell, H.-X. Yuan, and K.-L. Guan. Autophagy regulation by nutrient signaling. *Cell research*, 24(1):42–57, 2014. ISSN 1748-7838. doi: 10.1038/cr.2013.166. URL http://www.ncbi.nlm.nih.gov/pubmed/24343578.

A. Sakaue-Sawano, H. Kurokawa, T. Morimura, A. Hanyu, H. Hama, H. Osawa, S. Kashiwagi, K. Fukami, T. Miyata, H. Miyoshi, T. Imamura, M. Ogawa, H. Masai, and A. Miyawaki. Visualizing Spatiotemporal Dynamics of Multicellular Cell-Cycle Progression. *Cell*, 132(3):487–498, 2008. ISSN 00928674. doi: 10.1016/j.cell.2007.12.033.

D. Santamaría, C. Barrière, A. Cerqueira, S. Hunt, C. Tardy, K. Newton, J. F. Cáceres, P. Dubus, M. Malumbres, and M. Barbacid. Cdk1 is sufficient to drive the mammalian cell cycle. *Nature*, 448 (7155):811–815, 2007. ISSN 0028-0836. doi: 10.1038/nature06046. URL http://www.ncbi.nlm.nih.gov/pubmed/17700700.

I. Santi, N. Dhar, D. Bousbaine, Y. Wakamoto, and J. D. McKinney. Single-cell dynamics of the chromosome replication and cell division cycles in mycobacteria. *Nature Communications*, 4:2470, sep 2013. ISSN 2041-1723. doi: 10.1038/ncomms3470. URL http://www.nature.com/doifinder/10.1038/ncomms3470.

S. D. M. Santos and J. E. Ferrell. On the cell cycle and its switches. *Nature*, 454(July):288–289, 2008. ISSN 1476-4679. doi: 10.1038/ncb1753. URL http://www.pubmedcentral.nih.gov/articlerender.fcgi?artid=2711503{&}tool=pmcentrez{&}rendertype=abstract.

L. J. Saucedo and B. a. Edgar. Why size matters: Altering cell size. *Current Opinion in Genetics and Development*, 12(5):565–571, 2002. ISSN 0959437X. doi: 10.1016/S0959-437X(02)00341-6.

L. J. Saucedo, X. Gao, D. a. Chiarelli, L. Li, D. Pan, and B. a. Edgar. Rheb promotes cell growth as a component of the insulin/TOR signalling network. *Nature cell biology*, 5(6):566–571, 2003. ISSN 14657392. doi: 10.1038/ncb996.

J. T. Sauls, D. Li, and S. Jun. Adder and a coarse-grained approach to cell size homeostasis in bacteria. *Current Opinion in Cell Biology*, 38:38–44, 2016. ISSN 18790410. doi: 10.1016/j.ceb.2016.02.004.

M. Schaechter, O. MaalOe, and N. O. Kjeldgaard. Dependency on Medium and Temperature of Cell Size and Chemical Composition during Balanced Growth of Salmonella typhimurium. *Journal of General Microbiology*, 19(3):592–606, 1958. ISSN 0022-1287. doi: 10.1099/00221287-19-3-592.

H. Schmidt-Glenewinkel and N. Barkai. Loss of growth homeostasis by genetic decoupling of cell division from biomass growth: implication for size control mechanisms. *Molecular systems biology*, 10:769, 2014. ISSN 1744-4292. doi: 10.15252/msb.20145513. URL http://www.pubmedcentral.nih.gov/articlerender.fcgi?artid=4300492{&}tool=pmcentrez{&}rendertype=abstract.

K. Schmoller, J. Turner, M. Kõivomägi, and J. Skotheim. Dilution of the cell cycle inhibitor Whi5 controls budding yeast cell size. *Nature*, (in press), 2015. ISSN 0028-0836. doi: 10.1038/nature14908.

K. M. Schmoller and J. M. Skotheim. The Biosynthetic Basis of Cell Size Control. *Trends in Cell Biology*, xx:1–10, 2015. ISSN 09628924. doi: 10.1016/j.tcb.2015.10.006. URL http://linkinghub.elsevier.com/retrieve/pii/S0962892415001932.

R. Shields, R. F. Brooks, P. N. Rmdle, D. F. Capellaros, and D. Delia. Cell Size , Cell Cycle and Transition in Mouse Fibroblasts. *Cell*, 15(October):469–474, 1978.

F. Si, D. Li, S. E. Cox, J. T. Sauls, O. Azizi, A. B. Schwartz, and M. J. Erickstad. Deconstructing cell size control into physiological modules in Escherichia coli. *bioRxiv*, (1):1–23, 2016.

R. Sigl, C. Wandke, V. Rauch, J. Kirk, T. Hunt, and S. Geley. Loss of the mammalian APC/C activator FZR1 shortens G1 and lengthens S phase but has little effect on exit from mitosis. *Journal of cell science*, 122(Pt 22):4208–17, 2009. ISSN 1477-9137. doi: 10.1242/jcs.054197. URL http://www.ncbi.nlm.nih.gov/pubmed/19861496.

I. Soifer and N. Barkai. Systematic identification of cell size regulators in budding yeast. *Molecular systems biology*, 10:761, 2014. ISSN 1744-4292. doi: 10.15252/msb.20145345. URL http://www.pubmedcentral.nih.gov/articlerender.fcgi?artid=4299602{&}tool=pmcentrez{&}rendertype=abstract.

I. Soifer, L. Robert, and A. Amir. Single-cell analysis of growth in budding yeast and bacteria reveals a common size regulation strategy. *Current Biology*, 26(3):356–361, 2016. ISSN 09609822. doi: 10.1016/j.cub.2015.11.067.

Sompayrac and O. Maaloe. Autorepressor Model for Control of DNA Replication. *Nature: new biology*, 241, 1973.

S. Son, A. Tzur, Y. Weng, P. Jorgensen, J. Kim, M. W. Kirschner, and S. R. Manalis. Direct observation of mammalian cell growth and size regulation. *Nature Methods*, 9(9):910–912, 2012. ISSN 1548-7091. doi: 10.1038/nmeth.2133.

S. Son, J. H. Kang, S. Oh, M. W. Kirschner, T. J. Mitchison, and S. Manalis. Resonant microchannel volume and mass measurements show that suspended cells swell during mitosis. *Journal of Cell Biology*, 211(4):757–763, 2015a. ISSN 15408140. doi: 10.1083/jcb.201505058.

S. Son, M. M. Stevens, H. X. Chao, C. Thoreen, A. M. Hosios, L. D. Schweitzer, Y. Weng, K. Wood, D. Sabatini, M. G. Vander Heiden, and S. Manalis. Cooperative nutrient accumulation sustains growth of mammalian cells. *Scientific Reports*, 5:17401, 2015b. ISSN 2045-2322. doi: 10.1038/srep17401. URL http://www.nature.com/articles/srep17401.

N. Sonenberg and A. G. Hinnebusch. Regulation of Translation Initiation in Eukaryotes: Mechanisms and Biological Targets. *Cell*, 136(4):731–745, 2009. ISSN 00928674. doi: 10.1016/j.cell.2009.01.042.

E. J. Song, H. M. Hong, and Y. S. Yoo. Proteasome inhibition induces neurite outgrowth through posttranslational modification of TrkA receptor. *International Journal of Biochemistry and Cell Biology*, 41(3):539–545, 2009. ISSN 13572725. doi: 10.1016/j.biocel.2008.04.022.

S. L. Spencer, S. D. Cappell, F. C. Tsai, K. W. Overton, C. L. Wang, and T. Meyer. The proliferation-quiescence decision is controlled by a bifurcation in CDK2 activity at mitotic exit. *Cell*, 155(2):369–383, 2013. ISSN 00928674. doi: 10.1016/j.cell.2013.08.062. URL http://dx.doi.org/10.1016/j.cell.2013.08.062.

A. Sporbert, P. Domaing, H. Leonhardt, and M. C. Cardoso. PCNA acts as a stationary loading platform for transiently interacting Okazaki fragment maturation proteins. *Nucleic Acids Research*, 33(11):3521–3528, 2005. ISSN 03051048. doi: 10.1093/nar/gki665.

M. P. Stewart, J. Helenius, Y. Toyoda, S. P. Ramanathan, D. J. Muller, and A. a. Hyman. Hydrostatic pressure and the actomyosin cortex drive mitotic cell rounding. *Nature*, 469(7329):226–30, jan 2011. ISSN 1476-4687. doi: 10.1038/nature09642. URL http://www.ncbi.nlm.nih.gov/pubmed/21196934.

T. T. Su and P. H. O'Farrell. Size control: cell proliferation does not equal growth. *Current biology : CB*, 8(19):R687–R689, 1998. ISSN 09609822. doi: 10.1016/S0960-9822(98)70436-1.

Y. Sung, A. Tzur, S. Oh, W. Choi, V. Li, R. R. Dasari, Z. Yaqoob, and M. W. Kirschner. Size homeostasis in adherent cells studied by synthetic phase microscopy. *Proceedings of the National Academy of Sciences of the United States of America*, 110(41):16687–92, oct 2013. ISSN 1091-6490. doi: 10.1073/pnas.1315290110. URL http://www.pubmedcentral.nih.gov/articlerender.fcgi?artid=3799364{&}tool=pmcentrez{&}rendertype=abstract.

Á. Sveiczer and A. Horváth. How do fission yeast cells grow and connect growth to the mitotic cycle? *Current Genetics*, pages 1–9, 2016. ISSN 14320983. doi: 10.1007/s00294-016-0632-0.

A. Sveiczer, B. Novak, and J. M. Mitchison. The size control of fission yeast revisited. *Journal of cell science*, 109:2947–2957, 1996.

A. Sveiczer, B. Novak, and J. M. Mitchison. Size control in growing yeast and mammalian cells. *Theoretical biology & medical modelling*, 1:12, 2004. ISSN 1742-4682. doi: 10.1186/1742-4682-1-12.

S. Taheri-Araghi, S. Bradde, J. Sauls, N. Hill, P. Levin, J. Paulsson, M. Vergassola, and S. Jun. Cell-Size Control and Homeostasis in Bacteria. *Current Biology*, 25(3):385–391, 2015. ISSN 09609822. doi: 10.1016/j.cub.2014.12.009. URL http://linkinghub.elsevier.com/retrieve/pii/S0960982214015735.

Y. Tanouchi, A. Pai, H. Park, S. Huang, R. Stamatov, N. E. Buchler, and L. You. A noisy linear map underlies oscillations in cell size and gene expression in bacteria. *Nature*, 523(7560):357–60, 2015. ISSN 1476-4687. doi: 10.1038/nature14562. URL http://www.ncbi.nlm.nih.gov/pubmed/26040722.

V. Teixeira and V. Costa. Unraveling the role of the Target of Rapamycin signaling in sphingolipid metabolism. *Progress in Lipid Research*, 61:109–133, 2016. ISSN 18732194. doi: 10.1016/j.plipres.2015.11.001.

J. J. Turner, J. C. Ewald, and J. M. Skotheim. Cell size control in yeast. *Current Biology*, 22(9), 2012. doi: 10.1016/j.cub.2012.02.041.Cell.

J. J. Tyson and B. Novak. Control of cell growth, division and death: information processing in living cells. *Interface focus*, 4(3):20130070, 2014. ISSN 2042-8898. doi: 10.1098/rsfs.2013.0070. URL http://rsfs.royalsocietypublishing.org/content/4/3/20130070.

J. J. Tyson and B. Novák. Models in biology: lessons from modeling regulation of the eukaryotic cell cycle. *BMC Biology*, 13(1):46, 2015. ISSN 1741-7007. doi: 10.1186/s12915-015-0158-9. URL http://www.biomedcentral.com/1741-7007/13/46.

A. Tzatsos and K. V. Kandror. Nutrients suppress phosphatidylinositol 3-kinase/Akt signaling via raptor-dependent mTOR-mediated insulin receptor substrate 1 phosphorylation. *Molecular and cellular biology*, 26(1):63–76, jan 2006. ISSN 0270-7306. doi: 10.1128/MCB.26.1.63-76.2006. URL http://www.ncbi.nlm.nih.gov/pubmed/16354680http://www.pubmedcentral.nih.gov/articlerender.fcgi?artid=PMC1317643.

A. Tzur, R. Kafri, V. S. Lebleu, G. Lahav, and M. W. Kirschner. Cell growth and size homeostasis in proliferating animal cells. *Science (New York, N.Y.)*, 325(5937):167–71, jul 2009. ISSN 1095-9203. doi: 10.1126/science.1174294. URL http://www.pubmedcentral.nih.gov/articlerender.fcgi?artid=2905160{&}tool=pmcentrez{&}rendertype=abstract.

G. Ullman, M. Wallden, E. G. Marklund, A. Mahmutovic, I. Razinkov, and J. Elf. High-throughput gene expression analysis at the level of single proteins using a microfluidic turbidostat and automated cell tracking. *Philosophical transactions of the Royal Society of London. Series B, Biological sciences*, 368(1611):20120025, 2013. ISSN 1471-2970. doi: 10.1098/rstb.2012.0025. URL http://rstb.royalsocietypublishing.org/content/368/1611/20120025.short.

S. H. Um, F. Frigerio, M. Watanabe, F. Picard, M. Joaquin, M. Sticker, S. Fumagalli, P. R. Allegrini, S. C. Kozma, J. Auwerx, and G. Thomas. Absence of S6K1 protects against age- and diet-induced obesity while enhancing insulin sensitivity. *Nature*, 431(7005):200–205, 2004. ISSN 0028-0836. doi: 10.1038/nature02979.

S. Vadia and P. A. Levin. Growth rate and cell size: A re-examination of the growth law. *Current Opinion in Microbiology*, 24:96–103, 2015. ISSN 18790364. doi: 10.1016/j.mib.2015.01.011. URL http://dx.doi.org/10.1016/j.mib.2015.01.011.

J. van Riggelen, A. Yetil, and D. W. Felsher. MYC as a regulator of ribosome biogenesis and protein synthesis. *Nature reviews. Cancer*, 10(APRII):301–309, 2010. ISSN 1474-175X. doi: 10.1038/nrc2819. URL http://dx.doi.org/10.1038/nrc2819.

A. Verdugo, P. K. Vinod, J. J. Tyson, and B. Novak. Molecular mechanisms creating bistable switches at cell cycle transitions. *Open biology*, 3(3):120179, 2013. ISSN 2046-2441. doi: 10.1098/rsob.120179. URL http://www.pubmedcentral.nih.gov/articlerender.fcgi?artid=3718337{&}tool=pmcentrez{&}rendertype=abstract.

E. Vergés, N. Colomina, E. Garí, C. Gallego, and M. Aldea. Cyclin Cln3 Is Retained at the ER and Released by the J Chaperone Ydj1 in Late G1 to Trigger Cell Cycle Entry. *Molecular Cell*, 26(5):649–662, jun 2007. ISSN 10972765. doi: 10.1016/j.molcel.2007.04.023. URL http://www.ncbi.nlm.nih.gov/pubmed/17560371.

W. J. Voorn and L. J. H. Koppes. Skew or third moment of bacterial generation times. *Archives of Microbiology*, 169(1):43–51, 1998. ISSN 03028933. doi: 10.1007/s002030050539.

M. Wallden, D. Fange, E. Gregorsson Lundius, Ö. Baltekin, and J. Elf. The synchronization of replication and division cycles in individual E. coli cells (in press). *Cell*, pages 729–739, 2016. ISSN 00928674. doi: 10.1016/j.cell.2016.06.052.

H. Wang, L. B. Carey, Y. Cai, H. Wijnen, and B. Futcher. Recruitment of Cln3 cyclin to promoters controls cell cycle entry via histone deacetylase and other targets. *PLoS Biology*, 7(9):e1000189, sep 2009. ISSN 15449173. doi: 10.1371/journal.pbio.1000189. URL http://dx.plos.org/10.1371/journal.pbio.1000189.

P. Wang, L. Robert, J. Pelletier, W. L. Dang, F. Taddei, A. Wright, and S. Jun. Robust growth of escherichia coli. *Current Biology*, 20(12):1099–1103, 2010. ISSN 09609822. doi: 10.1016/j.cub.2010.04.045. URL http://dx.doi.org/10.1016/j.cub.2010.04.045.

D. Weinkove, T. P. Neufeld, T. Twardzik, M. D. Waterfield, and S. J. Leevers. Regulation of imaginal disc cell size, cell number and organ size by Drosophila class I(A) phosphoinositide 3-kinase and its adaptor. *Current Biology*, 9(18):1019–1029, sep 1999. ISSN 09609822. doi: 10.1016/S0960-9822(99)80450-3. URL http://www.ncbi.nlm.nih.gov/pubmed/10508611.

E. Wood and P. Nurse. Pom1 and cell size homeostasis in fission yeast. *Cell cycle (Georgetown, Tex.)*, 12(19):3228–36, oct 2013. ISSN 1551-4005. doi: 10.4161/cc.26462. URL http://www.pubmedcentral.nih.gov/articlerender.fcgi?artid=3865018{&}tool=pmcentrez{&}rendertype=abstract.

F.-X. Yu, B. Zhao, and K.-L. Guan. Hippo Pathway in Organ Size Control, Tissue Homeostasis, and Cancer. *Cell*, 163(4):811–828, 2015. ISSN 00928674. doi: 10.1016/j.cell.2015.10.044. URL http://linkinghub.elsevier.com/retrieve/pii/S0092867415014002.

X. Yuan, J. Srividhya, T. De Luca, J.-H. E. Lee, and J. R. Pomerening. Uncovering the role of APC-Cdh1 in generating the dynamics of S-phase onset. *Molecular biology of the cell*, 25(4):441–56, 2014. ISSN 1939-4586. doi: 10.1091/mbc.E13-08-0480. URL http://www.ncbi.nlm.nih.gov/pubmed/24356446{%}5Cnhttp://www.pubmedcentral.nih.gov/articlerender.fcgi?artid=PMC3923637.

a. Zetterberg and O. Larsson. Kinetic analysis of regulatory events in G1 leading to proliferation or quiescence of Swiss 3T3 cells. *Proceedings of the National Academy of Sciences of the United States of America*, 82(16):5365–5369, 1985. ISSN 0027-8424. doi: 10.1073/pnas.82.16.5365.

Q. Zhang, F. Bassetti, M. Gherardi, and M. C. Lagomarsino. Cell-to-cell variability and robustness in S-phase duration from genome replication kinetics. *ArXiv*, q-bio.GN(January), 2017.

Y. Zhang and H. Xu. Translational regulation of mitochondrial biogenesis. *Biochemical Society Transactions*, 44(December):1717–1724, 2016. ISSN 0300-5127. doi: 10.1042/BST20160071C.

H. Zheng, P.-Y. Ho, M. Jiang, B. Tang, W. Liu, D. Li, X. Yu, N. E. Kleckner, A. Amir, and C. Liu. Interrogating the Escherichia coli cell cycle by cell dimension perturbations. *Proceedings of the National Academy of Sciences*, page 201617932, 2016. ISSN 0027-8424. doi: 10.1073/pnas.1617932114. URL http://www.pnas.org/lookup/doi/10.1073/pnas.1617932114.

E. Zlotek-Zlotkiewicz, S. Monnier, G. Cappello, M. Le Berre, and M. Piel. Optical volume and mass measurements show that mammalian cells swell during mitosis. *The Journal of Cell Biology*, 211 (4):765–774, 2015. ISSN 0021-9525. doi: 10.1083/jcb.201505056. URL http://www.jcb.org/cgi/doi/10.1083/jcb.201505056.

R. Zoncu. mTORC1 Senses Lysosomal Amino Acids Through an Inside-Out Mechanism That Requires the Vacuolar H + -ATPase Roberto Zoncu. *Science (New York, N.Y.)*, 334: 678–83, 2011. ISSN 0036-8075. doi: 10.1126/science.1207056. URL http://www.ncbi.nlm.nih.gov/pubmed/22053050{%}5Cnhttp://www.pubmedcentral.nih.gov/articlerender.fcgi?artid=PMC3211112{%}5Cnhttp://www.ncbi.nlm.nih.gov/pubmed/22053050{%}5Cnhttp://www.pubmedcentral.nih.gov/articlerender.fcgi?artid=PMC3211112.

APPENDICES

Appendix A

Appendix 1: Review

Exploring the function of cell shape and size during mitosis

Authors:

Clotilde Cadart[1,3], Ewa Zlotek-Zlotkiewicz[1,3], Mael Le Berre[1], Matthieu Piel[1,4], Helen Matthews[2,4],

Affiliations:

[1]Institut Curie/Institut Pierre-Gilles de Gennes Paris, France
[2]University College London, London, United Kingdom
[3]Co-first authors
[4]Co-corresponding authors

Published in:

Developmental Cell, 29, April 28, 2014

Appendix B

Appendix B: Protocol article

Fluorescence eXclusion Measurement of volume in live cells

Authors:

Clotilde Cadart[1], Ewa Zlotek-Zlotkiewicz[1], Larisa Venkova[1], Olivier Thouvenin[2], Victor Racine[3], Mael Le Berre[1], Sylvain Monnier[1], Matthieu Piel[1]

Affiliations:

[1]Institut Curie/Institut Pierre-Gilles de Gennes Paris, France
[2]Institut Langevin/ESPCI Paris Tech, Paris, France
[3]QuantaCell, Pessac, France

Published in:

Methods in Cell Biology, Cell polarity and Morphogenesis, Volume 139, 2017

Appendix C

Appendix C: résumé en français

Etude de l'homéostasie de taille chez les cellules de mammifères

Clotilde Cadart

Résumé du travail de thèse, effectué sous la direction de Matthieu Piel à l'Institut Curie

1. Introduction

1.1. La question de l'homéostasie de taille chez les cellules animales

Lors de l'observation d'un tissu, deux observations peuvent être faites : (i) les cellules d'un même type (exerçant une même fonction) ont une taille et une forme caractéristique (par exemple, les neurones peuvent faire 1 m de long alors que les érythrocytes ont un diamètre d'environ 6 µm) ; (ii) les cellules d'un même type dans le même tissu sont de taille remarquablement homogène (la distribution des tailles est étroite) (Ginzberg, Kafri, and Kirschner 2015). Dans les tissus cancéreux, l'homogénéité de taille des cellules est perdue (Ginzberg, Kafri, and Kirschner 2015). Les règles qui définissent la taille absolue d'une cellule (première observation) ou la distribution des tailles dans la population (deuxième observation) sont très peu connues. Dans le cas de cellules qui prolifèrent, la taille d'une cellule est le résultat de la vitesse à laquelle la cellule croît et la rapidité avec laquelle elle se divise. Etudier l'homéostasie de taille des cellules prolifératives revient donc à étudier comment la croissance et la progression dans le cycle cellulaire sont coordonnées. Cette question est d'une importance majeure car ces deux processus sont fortement dérégulés dans le cas du cancer.

L'homéostasie de taille a beaucoup été étudiée chez divers organismes unicellulaires modèles, tels que la bactérie et la levure. Ces cellules prolifèrent en permanence, tant que le milieu extérieur leur fournit suffisamment de nutriments. La question est en revanche plus compliquée pour les cellules venant d'organismes multicellulaires. En effet, dans ce cas, la croissance et la prolifération sont régulées, à l'échelle de l'organe et du corps entier, lors des processus développementaux ou à l'âge adulte, afin de maintenir une homéostasie tissulaire (Edgar 2006). L'importance de cette régulation extrinsèque de la croissance et de la prolifération a mené certains à douter de l'existence d'un mécanisme intrinsèque, à l'échelle de la cellule unique, permettant de coordonner activement la croissance et la prolifération (Lloyd 2013; Edgar 2006). Cependant, seule une approche rigoureuse, basée sur des mesures directes et dynamiques de la croissance et de la progression dans le cycle à l'échelle unique (Sveiczer, Novak, and Mitchison 2004) pourra envisager de (i) caractériser l'existence (ou non) d'un comportement homéostatique, (ii) tester la présence d'une coordination entre la croissance et la progression dans le cycle. De telles approches ont récemment permis d'importants progrès dans la caractérisation du processus homéostatique chez les bactéries (Kennard et al. 2016; Osella, Nugent, and Cosentino Lagomarsino 2014; Wallden et al. 2016; Taheri-Araghi et al. 2015; Campos et al. 2014) et la levure *S.* cerevisiae (Soifer et al. 2016) mais demeurent limitées par le défi technique que représente la mesure de la croissance chez les cellules animales. Nous développons chacun de ces trois enjeux dans la partie suivante.

1.2. Concepts importants pour l'étude de l'homéostasie de taille

1.2.1. Caractérisation du comportement homéostatique en termes de « sizer », « adder » et « timer »

A l'échelle phénoménologique, le processus homéostatique est déterminé par la relation entre le volume final et le volume initial de la cellule ($V_{mitosis} = \alpha V_{birth} + \beta$). Cette dernière relation permet de classifier le comportement en trois catégories. La première catégorie est appelée « sizer » et constitue le mécanisme contrôle de la taille le plus efficace où toutes les cellules se divisent une fois seulement qu'elles ont atteint une taille fixée : $V_{mitosis} = V_{Cst}$, dans ce cas, $\alpha = 0$ et $\beta = V_{Cst}$. Ce mécanisme est sans doute le plus connu car il a été montré il y a plusieurs décennies chez la levure *S. pombe* (Fantes and Nurse 1978). La seconde catégorie est appelée « adder » repose sur l'addition d'un volume constant ΔV_{Cst} à chaque cycle, indépendamment de la taille initiale de la cellule. Dans ce cas, $\alpha = 1$ et $\beta = \Delta V_{Cst}$. Par ce mécanisme, les grandes cellules grandissent moins, relativement à leur taille initiale que les petites cellules et les cellules convergent vers la taille moyenne dans la population génération après génération. Récemment, le « adder » est apparu comme un mécanisme très généralement observé, chez plusieurs types de bactéries (Campos et al. 2014; Taheri-Araghi et al. 2015; Deforet, Van Ditmarsch, and Xavier 2015; Soifer et al. 2016) et chez les cellules filles de *S. cerevisiae* (Soifer et al. 2016). Enfin, la dernière catégorie est appelée « timer » et repose sur le fait que toutes les cellules croissent pendant le même temps. Si les cellules croissent de manière linéaire, et ajoutent la même quantité de volume par unité de temps, un « timer » permet de de générer un « adder ». Néanmoins, si les cellules croissent de manière exponentielle, comme c'est le cas pour la plupart des cellules de bactérie (Osella, Nugent, and Cosentino Lagomarsino 2014; Iyer-Biswas et al. 2014; Wang et al. 2010), la levure *S. cerevisiae* (Di Talia et al. 2007; Grover et al. 2011) et certaines cellules animales (Tzur et al. 2009; Son et al. 2012b; Sung et al. 2013; Mir et al. 2011), le « timer » génère rapidement une divergence des tailles dans la population. En effet, si toutes les cellules doublent leur taille, les divergences de tailles par rapport à la moyenne sont rapidement amplifiées (Mitchison 2003). Dans le cas du « timer » combiné à une croissance exponentielle, $\alpha = 2$ et $\beta = 0$.

In fine, les termes de « adder », « timer », et « sizer » permettent seulement de caractériser le comportement homéostatique à l'échelle phénoménologique. La compréhension du mécanisme sous-jacent repose sur l'étude de la coordination de la croissance et du cycle.

1.2.2. Questions autour du rôle respectif de la régulation du cycle et de la croissance

L'hypothèse principale pour expliquer le contrôle de la taille repose sur une adaptation de la durée du cycle à la croissance. Ceci est important dans le cadre d'une croissance exponentielle et permet aux cellules plus petites, qui croissent plus lentement, de passer plus de temps dans le cycle pour gagner autant (adder) ou davantage (sizer) de taille que les grandes cellules. Les évidences soutenant cette hypothèse sont très nombreuse, chez les bactéries (Osella, Tans, and Cosentino Lagomarsino 2017) et chez les levures (Turner, Ewald, and Skotheim 2012). L'hypothèse alternative, où la croissance est activement adaptée à la taille (et non le cycle) a longtemps été négligée. Cependant, de récents résultats chez *S. cerevisiae* (Goranov et al. 2009) et chez les cellules animales (Son et al. 2012a; Kafri et al. 2013; Tzur et al. 2009) suggère que des modulations de la vitesse de croissance pourraient participer au processus homéostatique. La validation de ces hypothèses chez les cellules animales est néanmoins limitée pour l'instant par le manque de mesures directes de courbes de croissances.

De manière remarquable, le mécanisme moléculaire proposé pour expliquer l'adaptation de la durée du cycle à la taille des cellules repose presque toujours sur la titration d'un activateur d'une transition dans le cycle. Par exemple chez *S. cerevisiae*, il est proposé que Whi5, l'inhibiteur principal de la Cycline Cln3 est présent en quantité constantes durant la phase G1 : à mesure que la cellule croît en volume,

Cln3 est produite en quantité proportionnelle au volume, et Whi5 est dilué, jusqu'au moment où les quantités de Whi5 ne sont plus suffisantes pour inhiber Cln3, permettant ainsi à Cln3 de déclencher la transition dans le cycle suivant (Schmoller et al. 2015). A l'instar du mécanisme de titration proposé pour *S. cerevisiae*, la majorité des mécanismes permettant de « mesurer » la taille reposent en réalité sur une mesure du volume (Ho and Amir 2015; Soifer et al. 2016; Zheng et al. 2016; Si et al. 2016; Amir 2017; Delarue, Weissman, and Hallatschek 2016; Harris and Theriot 2016), suggérant ainsi l'importance de ce paramètre de taille. La mesure du volume est néanmoins très difficile à obtenir chez les cellules animales.

1.2.3. Aspects techniques

Contrairement aux bactéries ou aux levures, qui possèdent une paroi cellulaire rigide et ont donc des formes simples et constantes (sphère, bâtonnet …) tout au long du cycle, les cellules animales possèdent une membrane dont les contours fluctuent en permanence. Pour cette raison, alors que le volume est le principale paramètre de taille mesuré chez les bactéries et les levure grâce à une simple quantification des contours des cellules par imagerie à contraste de phase, ce paramètre a été très peu quantifié chez les cellules animales. La plupart des études se sont en effet attachées à mesurer divers paramètres liés à la masse des cellules (masse flottante, masse sèche, quantité de protéines) (Kafri et al. 2013; Son et al. 2012a; Godin et al. 2010; Sung et al. 2013; Mir et al. 2011). De plus, comme les cellules animales cyclent sur des temps longs (environ 20 heures), l'obtention de trajectoires complètes de croissance sur cellules uniques est très difficile. Deux études seulement ont rapporté ce type de mesure (Son et al. 2012a; Mir et al. 2011) et les travaux ont utilisé des méthodes indirectes, à l'échelle de la population (Conlon and Raff 2003; Echave, Conlon, and Lloyd 2007; Kafri et al. 2013; Tzur et al. 2009; Sung et al. 2013). Malgré l'importance de l'obtention de mesures directes et dynamiques sur cellules unique pour caractériser le processus homéostatique, ce type d'observation demeure très limité et il n'existe pour l'instant aucune mesure du volume des cellules à l'échelle individuelle sur des cycles complets.

2. Conclusion et objectifs de cette thèse

La manière dont les cellules animales maintiennent l'homéostasie de taille est très peu comprise à l'heure actuelle. L'existence même d'un mécanisme actif permettant la coordination de la croissance et de la progression dans le cycle est débattue (Lloyd 2013). De récents progrès techniques ont néanmoins permis d'établir que les cellules animales croissaient globalement de manière exponentielle (Son et al. 2012a; Sung et al. 2013; Tzur et al. 2009) et ainsi suggéré qu'un mécanisme de contrôle de la taille était nécessaire. Ces travaux ont également soulevé l'hypothèse que ce contrôle de la taille opérait via des modulations de la croissance (Kafri et al. 2013; Son et al. 2012a; Tzur et al. 2009) au lieu de ou en addition à des modulations de la durée du cycle, comme il avait été initialement supposé (Dolznig et al. 2004; Killander and Zetterberg 1965). Cependant, la validation de ces différentes hypothèses est limitée par la difficulté que représente la mesure de la croissance à l'échelle de la cellule individuelle sur des cycles complets et la plupart des résultats à ce jour, proviennent d'approches indirectes. C'est dans ce contexte que nous avons initié ce projet en projetant de : (i) développer une méthode de mesure directe et dynamique du volume des cellules sur des temps complets ; (ii) caractériser avec les données ainsi obtenues le comportement homéostatique des cellules animales et tester cette observation par différentes perturbations ; (iii) caractériser la contribution respective de la régulation de la croissance et du cycle dans le comportement homéostatique éventuellement identifié.

3. Résultats

3.1. Mesure directe et dynamique du volume à l'échelle de la cellule unique sur des cycles complets

A l'échelle phénoménologique, le processus homéostatique est décrit par la corrélation entre la taille initiale et la taille finale des cellules. Pour effectuer cette caractérisation il est donc nécessaire de mesurer la croissance de cellules à l'échelle individuelle et sur des cycles complets. Dans ce but, nous avons adapté une méthode de mesure du volume des cellules par exclusion de fluorescence (figure 1A) préalablement établie dans le laboratoire (Zlotek-Zlotkiewicz et al. 2015) à des expériences sur des temps longs (24-50 heures) permettant le suivi de cycles complets (figure 1B). Ces optimisations ont permis d'améliorer la précision de la mesure et la qualité de la croissance (figure 1 C-D) dans les chambres de mesure de volume (Cadart et al. 2017).

Grâce à cette méthode, nous avons obtenu le premier ensemble de mesure du volume des cellules animales sur des cycles complets. Ceci nous a permis de caractériser le processus homéostatique des cellules de mammifère.

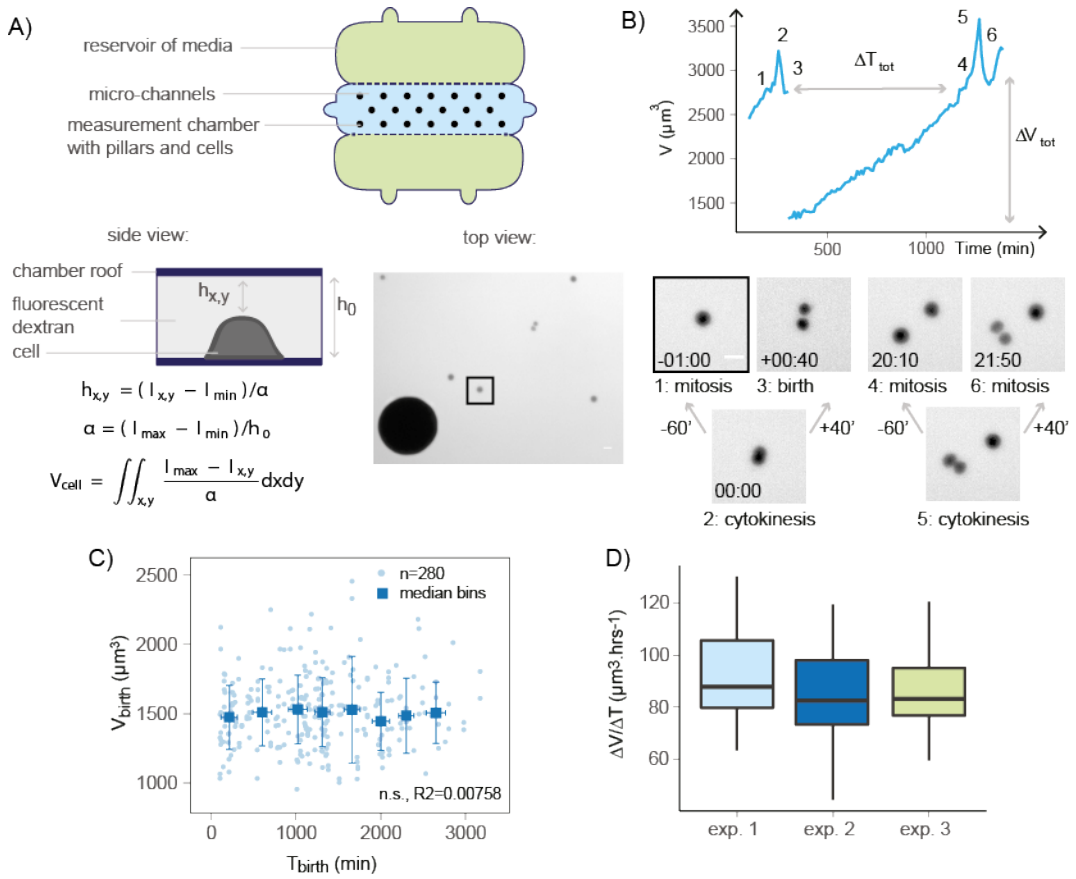

<u>Figure 1 : Mesure du volume sur cellule unique et sur des cycles complets par exclusion de fluorescence</u>. A) Description de la méthode de mesure du volume par exclusion de fluorescence. Haut : schéma de la chambre de mesure. Les cellules sont injectées dans une chambre de hauteur connue ($h_0 \approx 20\mu m$). L'homogénéité de la hauteur de la chambre est maintenue grâce à des piliers rapprochés qui soutiennent le toit de la chambre. Deux réservoirs de part et d'autre de la chambre contiennent du milieu et diffusent passivement des nutriments vers les cellules à travers des micro-canaux afin que le milieu contienne suffisamment de nutriments pour toute la durée de l'expérience.

Figure 1, suite légende. Bas : vue de profil de la chambre. Les cellules sont placées dans du milieu contenant une sonde fluorescente (dextran 10kDa-Alexa488 ou Alexa647) et cette sonde n'est pas internalisée par les cellules. L'intensité est maximale (I_{max}) quand aucun objet n'exclut la fluorescence et minimale (I_{min}) quand un objet tel que le pilier exclut la fluorescence de bas en haut de la chambre. Ainsi l'intensité de fluorescence en un point de la cellule $I_{x,y}$ est inversement proportionnelle à la hauteur de la cellule en ce point $h_{x,y}$ et le volume de la cellule est calculé en intégrant l'intensité de fluorescence sur toute la surface de la cellule. **B) Exemple d'une trajectoire unique de croissance sur un cycle complet**. Il est possible de définir 2 points remarquables, relativement à la cytocinèse : le volume à la mitose $V_{mitosis}$ est mesuré 60 minutes avant la cytocinèse et le volume à la naissance V_{birth} est défini 40 minutes après. Dans l'interval de temps ΔT_{tot} entre la naissance et la mitose, une cellule gagne un volume ΔV_{tot}. **C et D) Exemples de contrôles de la qualité de la croissance.** Pour chaque expérience, une série d'analyses permettant de vérifier la qualité de la croissance dans le système était effectuée. Par exemple, il était vérifié que le volume à la naissance était constant au cours de l'expérience (C) et que le taux de croissance moyen $\Delta V/\Delta T$ était constant d'une expérience à l'autre. Toutes les expériences présentées dans ce travail remplissent ces critères de qualités.

3.2. Le comportement homéostatique de la plupart des cellules animales est celui d'un «adder »

La relation entre le volume final et le volume initial permet de déterminer le processus homéostatique à l'échelle phénoménologique. Après avoir évalué cette relation pour différents types cellulaires (exemple en figure 2A), nous concluons que le comportement homéostatique est celui du « adder » pour tous les types cellulaires mesurés à l'exception de la lignée lymphoblastique Raji (figure 2B). Le « adder » est aussi observé chez les cellules L1210 étudiées dans un travail précédent (Son et al. 2012b).

Afin de tester la robustesse de cette observation, nous avons induit des divisions asymétriques par confinement dans des micro-canaux (figure 2C). Le confinement dans les canaux empêche l'arrondissement en mitose, ce qui induit des anomalies de positionnement du fuseau mitotique et génère des *in fine* des cellules filles de tailles inégales (Lancaster et al. 2013; Cadart et al. 2014). Comme prédit dans le cas d'un « adder », les différences de tailles entre cellules sœurs sont diminuées de moitié au cours du cycle suivant la division asymétrique de la cellule mère (figure 3D).

Ces résultats permettent donc d'établir pour la première fois que le comportement homéostatique des cellules animales est celui d'un « adder » à l'échelle phénoménologique.

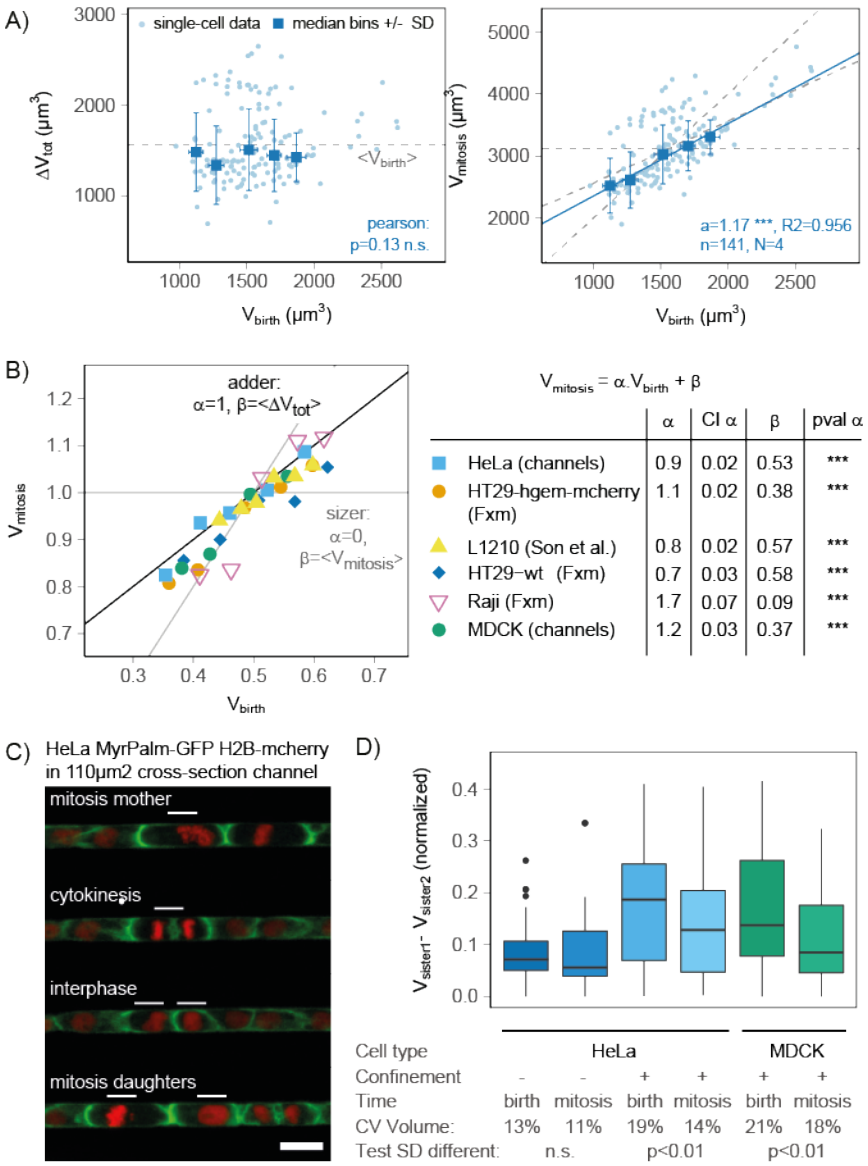

Figure 2 : A l'échelle phénoménologique, la plupart des cellules de mamifères se comportent comme un « adder ». A) Exemple de l'analyse du comportement homéostatique pour les cellules HT29. Pour chaque type cellulaire, le volume ajouté en fonction du volume à la naissance et la relation entre le volume en mitose et le volume à la naissance a été évaluée. **B) Résumé du comportement observé pour tous les types cellulaires analysés**. Graphe représentant le volume en mitose en fonction du volume à la naissance renormalisé pour pouvoir comparer tous les types cellulaires. A droite, le tableau résume les valeurs des coefficients α et β obtenus pour chaque type cellulaire ainsi que l'intervalle de confiance à 95% (CI) et la p value pour l'estimation de α. Nous rappelons que $\alpha \approx 1$ indique un comportement proche d'un « adder ». **C) Induction artificielle de divisions asymétriques par confinement dans des micro-canaux**. De bas en haut : (i) une cellule mère s'arrondit à l'entrée en mitose et (ii) se divise asymétriquement en une petite cellule fille et une grande cellule fille, (iii) en interphase, les cellules filles grandissent et (iv) finissent par se diviser *(HeLa MyrPalm-GFP (membrane)- H2B-mcherry (chromosomes) ; la barre d'échelle représente 20µm, l'aire de la section du canal est de 110 µm2)*. **D) Les divisions asymétriques sont réduites au cours du cycle suivant**. Comparaison de la différence de volume entre deux cellules sœurs (normalisée par la moyenne des deux volulmes) pour : (i) des cellules HeLa non confinées dans des canaux et (ii) des cellules HeLa ou MDCK confinées dans des canaux. Pour chaque paire d'observation (asymétrie à la naissance par rapport à l'asymétrie à la fin du cycle), un test comparant les variances (SD) est effectué. *(CV = coefficient de variation)*.

3.3. La durée de la phase G1 dépend du volume à la naissance mais cette adaptation est limitée par une durée minimale

L'hypothèse la plus directe pour expliquer l'observation d'un mécanisme de contrôle de la taille est celle d'une adaptation de la durée du cycle à la taille des cellules. Cette adaptation du temps permet aux petites cellules qui croissent plus lentement de croître de croître plus lentement afin d'ajouter la même quantité de volume (« adder ») ou d'atteindre la même taille finale (« sizer ») que les grandes cellules. Cette observation est communément admise chez les bactéries (Osella, Tans, and Cosentino Lagomarsino 2017), et les levures *S. pombe* et *S. cerevisiae* (Turner, Ewald, and Skotheim 2012). Chez les cellules animales en revanche, il n'existe pas de consensus à ce sujet. Afin de répondre à cette question, nous avons associé notre méthode de mesure du volume à une analyse de la progression dans le cycle grâce à l'expression de marqueurs fluorescents des phases du cycle. Ceci est en effet possible grâce aux sondes FUCCI (Sakaue-Sawano et al. 2008) où la protéine h-geminin qui n'est exprimée que en phase S-G2 est liée à la protéine fluorescente mCherry (figure 3A).

Cette technique nous permet de montrer que la durée de la phase G1 est très variable alors que celle des phases S-G2 l'est beaucoup moins et ressemble à un « timer » (figure 3C). La durée de la phase G1 est négativement corrélée avec le volume à la naissance (figures 3D-E) alors que la phase S-G2 n'est pas corrélée avec le volume en G1/S. De plus, le volume ajouté en G1 est négativement corrélé avec le volume initial (figure 3B) alors qu'il est positivement corrélé en S-G2 (figure 3B). Ces résultats suggèrent qu'un contrôle de la taille existe en G1 et repose sur l'adaptation de la durée de G1 au volume à la naissance. S-G2 en revanche, dont la durée est approximativement constante et où on observe une perte de contrôle de la taille est proche d'un « timer ». La combinaison de ces deux mécanismes génère un « adder » à l'échelle du cycle complet.

Cependant, l'adaptation de la durée de G1 au volume initiale atteint un plateau pour les cellules de grandes tailles. La durée de G1 semble en effet avoir un minimum, proche de 4 heures (figures 3D-E). En dépit de cette limite, les cellules de grande taille maintiennent un comportement homéostatique proche d'un « adder », ce qui est impossible si elles croissent de manière exponentielle (en effet, pour les cellules de grande taille qui cyclent dans le temps minimum de G1, G1 ressemble à un « timer » et la combinaison d'un « timer » avec une croissance exponentielle génère une perte du contrôle de la taille des cellules). Nous nous sommes donc demandé si toutes les cellules croissaient de manière exponentielle, indépendamment de leur taille.

3.4. Le taux de croissance sature et devient linéaire pour des cellules de taille anormalement grande

Pour répondre à cette question, nous avons artificiellement forcé des cellules HeLa à atteindre des tailles anormalement grandes. Ceci est possible en bloquant les cellules dans le cycle par un traitement à la roscovitine 20µM pendant 48 heures. Cette drogue bloque la progression dans le cycle (Meijer and Raymond 2003) mais pas la croissance, de sorte que les cellules atteignent des tailles jusqu'à 1.7 fois plus grande que leur taille normale (figure 4 A). Les cellules de taille anormalement grande montraient toutes une durée de la phase G1 qui n'était plus corrélée à leur volume initial et était proche de 4 heures. Ceci renforce l'observation faite chez les cellules HT29 (figure 3 D-E) qu'une durée minimale de G1 existe.

En revanche, même mes grandes cellules qui passaient une durée constante et minimum en G1 montraient un « adder » lors de cette phase (figure 4C). L'explication est que le taux de croissance sature pour des grands volumes et la croissance devient linéaire (figure 4 D).

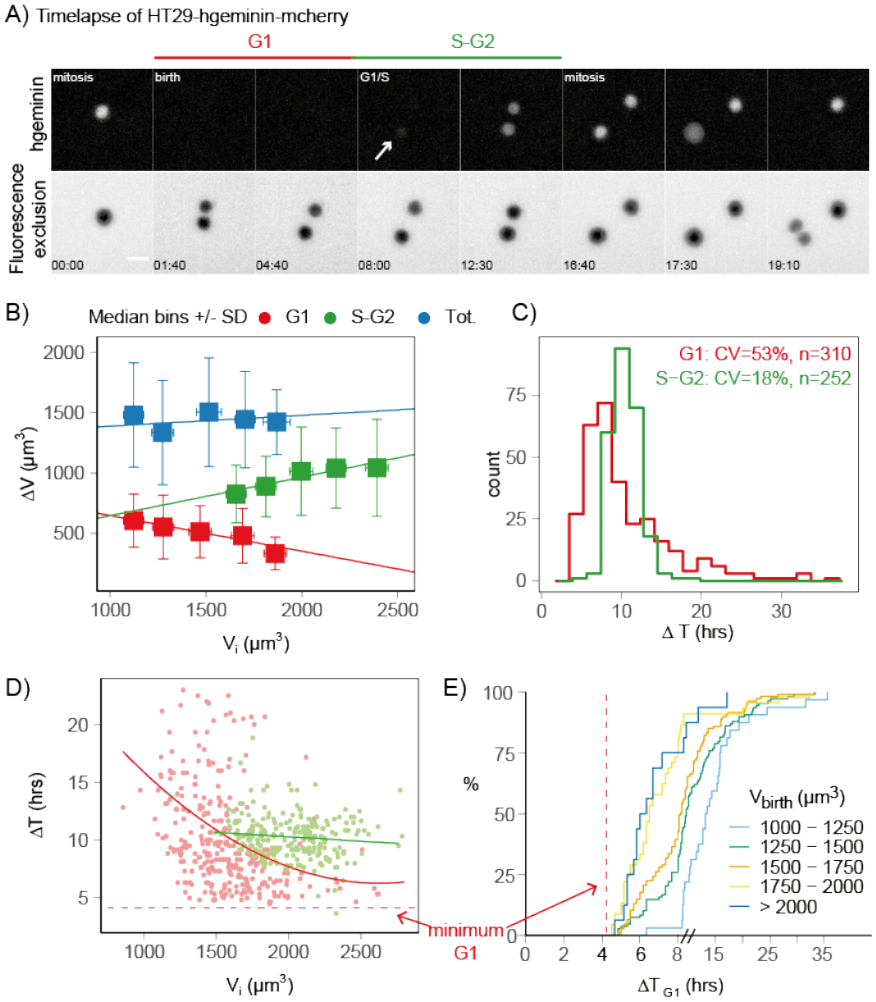

<u>Figure 3 : La durée de G1 est négativement corrélée avec le volume à la naissance</u> A) Photos d'une cellule HT29 au cours du cycle. L'expression de la protéine hgeminin-mcherry est phase-dépendente : son apparition marque l'entrée en phase S. Les photos du bas montrennt les cellules en exclusion de fluorescence dans la chambre de mesure du volume. **B) Le volume ajouté pour chaque phase** est (i) négativement corrélé avec le volume à la naissance en G1, indiquant un contrôle de la taille dans cette phase ; (ii) positivement corrélé avec le volume à la transition G1/S durant la phase S-G2, suggérant un « timer » et (iii) non corrélé, à l'échelle du cycle complet, avec le volume initial, comme dans un comportement de « adder ». **C) La durée de la phase G1 est très variable alors que la durée de la phase S-G2 l'est beaucoup moins. D) Durée de G1 et S-G2 en fonction du volume à l'entrée dans la phase**. G1 est négativement corrélée au volume à la naissance mais ceci est limité par un plateau qui représente un temps minimal de G1. S-G2 n'est pas significativement corrélée avec le volume en G1/S. **E) Fréquence cumulée de la durée de G1 pour différents groupes de volume à la naissance**. La probabilité de passer en phase S augmente avec la volume et le temps passé en G1. Elle est aussi nulle pour des temps inférieurs à 4 heures.

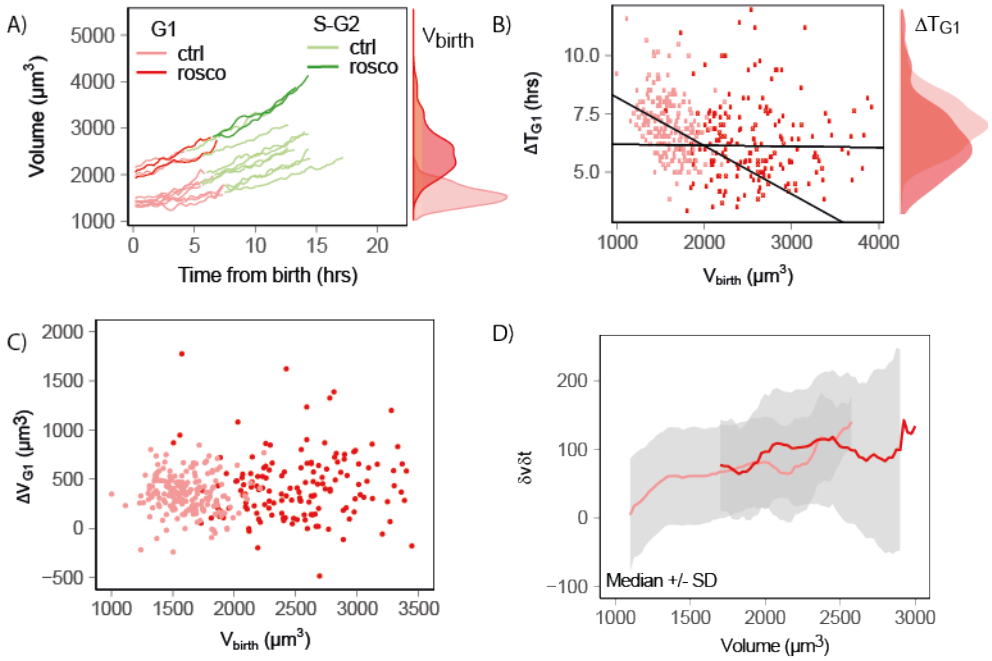

Figure 4 : Les cellules HeLa artificiellement forcées à atteindre de grandes tailles révèlent deux processus limites. A) Exemple de courbes de croissances pour des cellules contrôles et des cellules traitées à la roscovitine. Les grandes cellules de la condition contrôle montrent le même type de courbe de croissance que les cellules obtenues par traitement à la Roscovitine (20µM 48h). L'histogramme sur l'axe y montre que la distribution des volumes à la naissance est plus élevée *(1.7 fois en moyenne, test comparant les moyennes : p<0.0001)* que dans la condition contrôle. **B) La durée de G1 est inversement corrélée au volume à la naissance mais atteint un plateau pour les grandes tailles**. *(Régression linéaire robuste, roscovitine: n.s. n=184, N=3; control: a=-0.002±0.0004, R2=0.1, p<0.0001, n=214; N=2).* L'histogramme montre que les grandes cellules de la condition roscovitine cyclent dans des temps de G1 plus courts que les cellules de la condition contrôle. **C) Le volume ajouté en G1 est comparable dans les deux conditions et n'est pas corrélé au volume à la naissance**. *(regression linéaire non statistiquement significative pour les deux conditions : roscovitine: n=201 ; N=3; control: n=181; N=2).* **D) La vitesse de croissance $\delta v/\delta t$ atteint un plateau pour les large cellules traitées** (résultat préliminaire en cours de validation).

3.5. Proposition d'un cadre mathématique général permettant de comparer le comportement homéostatique de toutes les cellules, de la bactérie à la cellule animale

Afin de comparer les différentes combinaisons possibles de modulation de la croissance et de la durée du cycle et leur effet sur le comportement homéostatique, nous avons établi, en collaboration avec des théoriciens (Marco-Cosentino-Lagomarsino et Jacopo Grilli), un cadre mathématique général. Ce cadre définit trois paramètres liés par la relation :

$$\lambda = \theta \langle\alpha\rangle \langle\tau\rangle + \gamma \langle\alpha\rangle \langle\tau\rangle \quad \text{(Eq.1)}$$

Où α est le taux de croissance (supposée exponentielle à l'échelle d'un cycle complet) et τ la durée du cycle. Le premier terme, λ, caractérise le mécanisme homéostatique final : λ est la pente du célèbre « size-growth plot » (Di Talia et al. 2007) testant la relation entre la croissance définie ici sous une forme exponentielle ($\alpha\tau = \log(VF/Vi)$ et le log de la taille initiale). λ est égal à 1 dans le cas d'un « sizer », 0.5 dans le cas d'un « adder » et 0 dans le cas d'un « timer ». Le second terme θ, décrit la part de la correction de la taille qui est due à une adaptation du taux de croissance à la taille tandis que le

dernier terme, γ décrit la contribution des modulations du temps dans le processus homéostatique final (voir le manuscrit en cours pour plus de détails sur le modèle).

Grâce à ce cadre, il est possible de montrer que le « adder » est le comportement homéostatique le plus fréquemment observé, à la fois chez les bactéries et chez les cellules de mammifères (figures 5A-B). En revanche, alors que le « adder » résulte principalement d'une modulation de la taille chez les bactéries, différentes combinaisons de modulation de la croissance et du temps respectivement peuvent générer un « adder » chez les cellules de mammifères. Ainsi, les cellules HeLa et HT29 cultivées dans les chambres de mesure de volume montrent une importante modulation de la durée du cycle ($\gamma > 0$). Les très grandes cellules générées par traitement à la roscovitine montrent elles, un mécanisme qui repose essentiellement sur une modulation de la croissance et non de la durée du cycle. Il est à noter que cette modulation n'est pas à interpréter dans le sens d'un mécanisme actif mais dans le cadre d'une croissance qui est devenue linéaire et permet, passivement, de modérer les dispersions de tailles. Les cellules HeLa-MyrPalm-GFP et MDCK-MyrPalm-GFP qui montrent des évidences indirectes de croissance linéaire (résultats présentés dans le manuscrit en cours) elles aussi maintiennent un comportement homéostatique via une modulation apparente du taux de croissance ($\theta > 0$).

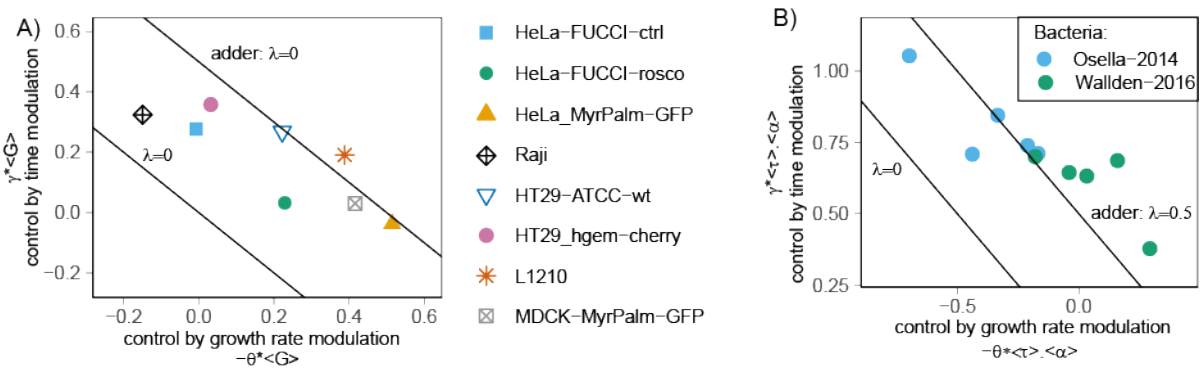

Figure 5 : Cadre mathématique général pour comparer le processus homéostatique chez les cellules de mammifères (A) et les bactéries (B) Les axes x et y quantifient, respectivement, les contributions des modulations de la croissance et du temps dans le comportement homéostatique final. Les données utilisées pour les bactéries proviennent de (Wallden et al. 2016; Osella, Nugent, and Cosentino Lagomarsino 2014).

4. Discussion

4.1. Identification de plusieurs règles contraignant la croissance ou la progression dans le cycle et participant à l'homéostasie de taille

Limitations du cycle. Nos résultats mettent en évidence plusieurs règles définissant la croissance ou la progression du cycle. Premièrement, les mesures sur les cellules HT29 et HeLa montrent pour la première fois de manière directe que la durée de la phase G1 est négativement corrélée au volume (figures 3D et 4B). Il est possible de faire l'hypothèse que cette adaptation du temps à la taille permet de générer une addition de volume qui est négativement corrélée au volume chez les HT29 ou similaire à un « adder » chez les HeLa (figures 3C et 4C). Cette observation avait déjà été faite de manière indirecte (Dolznig et al. 2004; Killander and Zetterberg 1965) et rappelle le mécanisme de contrôle de la taille chez *S. cerevisiae* (Johnston 1977; Hartwell and Unger 1977; Di Talia et al. 2007). Etant donné les similarités à l'échelle phénoménologique et moléculaire entre *S. cerevisiae* et les cellules animales

(Fisher 2016), le modèle récemment proposé pour expliquer l'adaptation de la durée de G1 au volume chez cette levure (Schmoller et al. 2015) constitue un intéressante piste de recherche future. Par ailleurs, les grandes cellules chez les HT29 et HeLa contrôles et les grandes cellules artificiellement induites par traitement à la roscovitine mettent en évidence une limite minimale à cette adaptation de temps avec une durée minimale de G1 de 4 heures (figures 3D-E et 4B). Il sera intéressant d'étudier la compatibilité de ce résultat avec la découverte récente que la dégradation du complexe APC-Cdh1 définissait une fenêtre de temps de minimale 4 heures avant la transition irréversible en phase S chez plusieurs types de cellules animales (Cappell et al. 2016).

Modulations de la croissance. Nos résultats identifient également une saturation du taux de croissance pour les cellules de très grande taille (figure 4D et résultats dans le manuscrit en préparation). Cette observation suggère une interprétation aux résultats précédemment décrits chez diverses cellules de mammifère qui montrait les grandes cellules croissaient moins vite que les petites en fin de phase G1 (Son et al. 2012a; Kafri et al. 2013). Nos résultats et les précédentes démonstration ne permettent pas, à notre avis, de suggérer l'existence d'un mécanisme actif qui permettrait d'adapter la croissance à la taille des cellules comme cela a été proposé (Kafri et al. 2013; Ginzberg 2015). Au vu des fluctuations observées dans les courbes de croissance, prouver cette hypothèse nécessite bien davantage d'observations. En revanche, il est possible d'imaginer qu'un mécanisme plus simple, qui reposerait sur des lois métaboliques ou physiques plus générales pourrait générer une modulation passive du taux de croissance telle que sa saturation pour de très grandes tailles. Il a par exemple été proposé que la métabolisme et la fonction mitochondriale atteignaient un maximum pour des tailles intermédiaires de cellules (Miettinen and Bjorklund 2016) et une manière intéressante de tester davantage cette hypothèse pourrait être de perturber la symétrie de ségrégation de différents sous-compartiments cellulaires tel que celui des mitochondries (Cadart et al. 2014).

4.2. Identification de plusieurs combinaison de modulations de la croissance et du cycle générant un « adder »

Les différents phénomènes limites observés permettent de définir trois modes de combinaison de croissance et progression dans le cycle principaux qui génèrent tous un « adder » phénoménologique : (i) les cellules qui croissent de manière exponentielle adaptent la durée de G1 (résultats sur les HT29 et HeLa contrôle) ; (ii) les cellules très grandes croissent en un temps minimal approximativement constant (« timer ») mais croissent linéairement, ce qui maintient l'observation du « adder » (résultats sur les grandes cellules HeLa) ; (iii) les cellules qui croissent lentement et de manière linéaire, possiblement à cause de leur confinement dans les micro-canaux allongent la durée de leur cycle et maintiennent également un « adder ». Ce dernier résultat est un argument de plus en faveur de l'existence d'un « adder » moléculaire puisqu'il suggère que, dans des conditions de croissance lente, les cellules sont capables d'étendre la durée de leur cycle pour maintenir une addition constante de volume similaire à celle ajoutée sans confinement (résultats dans le manuscrit en cours de préparation).

4.3. Généralité du « adder » et signification

L'observation la plus frappante dans notre travail et les précédents résultats publiés chez les bactéries et les levures est la généralité du « adder ». Plusieurs hypothèses sont actuellement débattues pour expliquer le « adder ». Certaines études argumentent en faveur d'un mécanisme unique permettant d'expliquer dans son ensemble, le comportement homéostatique de l'organisme considéré (Harris and

Theriot 2016; Ho and Amir 2015; Amir 2017; Soifer et al. 2016). D'autres études en revanche proposent que plusieurs processus, limitant soit la croissance, soit le cycle sont actifs séquentiellement au cours des phases successives du cycle (Adiciptaningrum et al., n.d.; Di Talia et al. 2007; Schmoller et al. 2015) ou en parallèle (Osella, Nugent, and Cosentino Lagomarsino 2014; Wallden et al. 2016) et résultent dans un comportement homéostatique effectif souvent, mais pas toujours (Kennard et al. 2016; Wallden et al. 2016; Delarue, Weissman, and Hallatschek 2016), proche du « adder ». Ces deux dernières hypothèses sont intéressantes car elles suggèrent une possible réconciliation avec les observations faites *in vivo* chez la drosophile, rapportant une certaine flexibilité de la taille des cellules en fonction des conditions environnementales ou une limite à l'adaptation de la durée du cycle à des taux de croissances très rapides (Edgar 2006) qui avaient mené certains à conclure qu'un mécanisme de contrôle de la taille n'existait pas chez les cellules animales (Lloyd 2013; Edgar 2006). En effet, nous résultats pointent vers un mécanisme homéostatique qui implique plusieurs processus, contrôlant la croissance ou le cycle et permet ainsi une réponse flexible selon les conditions de croissance (*i.e.* confinement, large cellules).

5. Conclusion

Notre travail permet un progrès significatif dans l'étude de l'homéostasie de taille des cellules animales. Il rapporte la première étude de courbes de croissance de cellules à l'échelle unique et sur des cycles complets et permet ainsi d'établir, pour la première fois, que le comportement homéostatique des cellules est celui d'un « adder ». Il montre également, de manière directe, que la durée de G1 est dépendante de la taille initiale, dans les limites d'un temps minimal de 4 heures en-dessous duquel l'adaptation n'est plus possible. Enfin, il suggère que des modulations de la croissance participent au processus homéostatique, au moins de manière passive. Comprendre si ces modulations sont le résultat d'un mécanisme actif ou de contraintes métaboliques et physiques plus générales est une importante voie de recherche pour progresser dans la compréhension de l'homéostasie de taille.

A mesure que nous évoluons vers une description de l'homéostasie comme mécanisme flexible qui implique plusieurs processus limitant la croissance et le cycle, une compréhension unifiée des règles homéostatiques, de la cellule unique au tissue sera sans doute possible

université PARIS-SACLAY
ÉCOLE DOCTORALE
Structure et dynamique des systèmes vivants (SDSV)

Etude de l'homéostasie de taille chez les cellules animales

Le mécanisme d'homéostasie de taille chez les cellules animales est très peu compris actuellement. Cette question est pourtant d'un intérêt majeur car le maintien de l'homéostasie de taille dans une population de cellules prolifératives doit se faire par une coordination entre la croissance et la division. Les études sur ce sujet ont jusqu'à présent été limitées par la difficulté de mesurer directement un paramètre de taille sur cellule individuelle. Dans cette thèse, nous développons deux méthodes permettant pour la première fois de mesurer directement le volume individuel des cellules animales sur des cycles complets. Nous montrons que plusieurs types cellulaires maintiennent l'homéostasie de taille via in mécanisme proche du "adder" où la quantité de volume ajouté à chaque cycle est indépendante du volume à la naissance. Ce comportement est le résultat d'une modulation de la durée de G1 en fonction du volume à la naissance. Afin de comparer le processus homéostatique observé chez les cellules animales avec celui, mieux connu, de plusieurs organismes unicellulaires (levure et bactérie), nous proposons un cadre mathématique. Ceci montre que le mécanisme du "adder" est le plus communément observé. En revanche, ce mécanisme repose uniquement sur une modulation de la durée du cycle chez les levures et les bactéries alors qu'il implique des modulations du cycle et de la croissance chez les cellules animales.

Mots clefs: taille cellulaire, cycle cellulaire, volume cellulaire, croissance cellulaire

Cell size homeostasis in animal cells

Despite decades of research, there is little consensus as to whether or not mammalian cells actively control their size. Moreover, it remains unclear how mammalian cell growth scales with cell size and varies across the cell division cycle. Answers to this question have been limited by the difficulty of directly measuring growth at the single cell level. Using two methods, we report the first direct measurement of single cell volumes over a complete cell division cycle in mammalian cells. Using a variety of cell lines, we show that mammalian cells in culture maintain size homeostasis by an adder mechanism, i.e. the volume added by cell growth across the cell cycle is independent of cell birth size. In normally cycling cells, this behaviour results from a change in the duration of G1, which depends on cell volume at birth. In order to compare our data to those from other systems, we propose a mathematical framework that can be used to characterise the full spectrum of size homeostasis mechanisms from bacteria to mammalian cells. This reveals that the adder mechanism is the most common type of size regulation, but shows that it can arise from various types of coupling between cell size, cell growth rate and cell cycle progression.

Keywords: size control, cell cycle, cell volume, cell growth

Université Paris-Saclay
Esspace Technologique - Immeuble Discovery
Route de l'Orme aux Merisiers RD128
91190 Saint-Aubin - France